PRACTICAL APPLICATIONS OF THE CONE PENETRATION TEST

A Manual On Interpretation Of Seismic Piezocone Test Data For Geotechnical Design

Geotechnical Research Group
Department of Civil Engineering
The University of British Columbia

TABLE OF CONTENTS

LIST OF SYMBOLS

α	Modulus factor or friction coefficient
a	Net area ratio
A_b	Area of pile base
A_f	Pore pressure ratio in triaxial test
A_N	Load transfer area behind the cone tip
A_T	Cross-sectional area at base of cone tip
B	Footing or foundation width
B_q	Pore pressure parameter $\dfrac{u_2 - u_1}{q_t - \sigma_{vo}}$
c_h	Coefficient of consolidation in horizontal direction
c_v	Coefficient of consolidation in vertical direction
C_Q	Correction factor for effective overburden stress level
C_c	Virgin compression index
C_s	Recompression index
CRR	Cyclic resistance ratio
CSR	Cyclic stress ratio
D	Grain size
D_r	Relative density
e	Void ratio
E	Young's modulus
E_u	Undrained Young's modulus, $E_u = 3\ G_{max}$ at small strains
E_{25}	Young’s modulus at 25% of peak strength
F or F_r	Normalized friction ratio = $\dfrac{f_s}{(q_t - \sigma_{vo})} x100\%$
f_p	Unit skin friction for pile
f_s	Friction sleeve stress
g	Acceleration due to gravity
G	Shear modulus
G_o, G_{max}	Maximum shear modulus at small strains
I_c	Material Index
I_R	Soil rigidity index or stiffness ratio = G/S_u for undrained conditions
I_{RD}	Relative Dilatancy Index
I_z	Strain influence factor
k	Hydraulic conductivity or constant
k_c	Bearing capacity factor
K_c	Correction factor based on grain characteristics
K_M	Correction factor for earthquake magnitude
K_o	Lateral earth pressure coefficient at rest
K_σ	Correction factor for effective overburden stress
L_2, L_1	Travel path lengths
LI	Liquidity index
LL	Liquid limit, %

m_v	Volumetric compressibility, $\frac{\Delta v/v}{\Delta\sigma'}$, in vertical direction
M	Drained constrained modulus = $1/m_v$
$N_{\Delta u}$	Pore pressure factor = $\Delta u/s_u$
M_t	Tangent (constrained) modulus
N	Standard penetration value, blows/ft
N_c	Cone factor without including overburden effect
NC	Normally consolidated
N_k	Cone factor when using q_c
N_{KT}	Cone factor when using q_t
OC	Overconsolidated
OCR	Overconsolidation ratio
Q_t	Normalized tip resistance $\frac{q_t - \sigma_{vo}}{\sigma_{vo} - u_o}$
p'_o	Mean normal effective stress
P_a	Reference stress
PI	Plasticity index, %
PL	Plastic limit, %
q_c	Measured cone bearing stress or tip resistance
q_e	Effective bearing stress or tip resistance
q_p	Unit end bearing for pile
q_t	Tip resistance after correction for pore pressure effects
q_{ult}	Ultimate bearing capacity
R	Radius of cone
R_b	Ultimate base capacity
R_f	Friction ratio = f_s/q_t x 100%
R_s	Ultimate shaft capacity
r_s	Unit shaft resistance
r_b	Unit base resistance
s_u	Undrained shear strength
S_t	Sensitivity (undisturbed strength ÷ remoulded strength)
t_1, t_2	Travel time
t_{50}	Time to 50% dissipation of pore pressure
T	Time factor
T*	Modified dimensionless Time Factor
T_{50}	Theoretical time factor for 50% consolidation
U, u	Pore water pressure
u_o	Equilibrium pore water pressure, in-situ
U_1, or u_1	Pore pressure measured on cone tip
U_2, or u_2	Pore pressure measured just behind shoulder of cone
U_3, or u_3	Pore pressure measured behind friction sleeve
V_s	Shear wave velocity
V_{s1}	normalized shear wave velocity
V_ρ	Compression wave velocity
w	Water content, M_w/M_s x 100%

β	Pile friction coefficient
Δ	Change in
Δp	Net footing pressure or pressure increase
Δu	$u-u_o$, excess pore pressure
ϕ'	Friction angle in terms of effective stress
ϕ'_{crit}	Effective friction angle at critical state
ϕ'_{cv}	Effective friction angle at constant volume
ϕ'_{ss}	Effective friction angle at steady state
ϕ'_{peak}	Peak friction angle
ρ	Settlement
ρ	Mass density
γ	Unit weight of soil
σ	Total normal stress
σ'	Effective normal stress = σ - u
σ_θ	Circumferential stress
σ'_{ho}	Effective horizontal stress
σ'_{mf}	Normal stress on failure plane
σ'_{mo}	Mean effective normal stress
σ_r	Radial stress
σ'_r	In-situ radial effective stress
σ_{vo}	Total overburden stress
σ'_{vo}	Effective overburden stress
τ	Shear stress
τ_f	Shear stress at failure
ψ	State parameter

LIST OF FIGURES

LIST OF TABLES

1 INTRODUCTION

The purpose of this manual is to provide guidance on the use and interpretation of the Seismic Piezocone Penetration Test (SCPTU) in site characterization and geotechnical design. This is the first major upgrade of the manual "Guidelines for use, interpretation and application of CPT and CPTU" first produced by the In Situ Testing Group of the University of British Columbia (Robertson and Campanella 1984). Since the original publication, there have been a number of minor revisions to the manual and the worked examples. The major role of Peter Robertson in the production of the early manuals, and the contributions of Alex Sy, Don Gillespie and Mike Davies are gratefully acknowledged. This upgrade of the manual was funded by a grant from the Highway and Transportation Institute of the Korea Highway Corporation as part of a research project entitled "Practical Applications of the Cone Penetration Test". The work was carried out in late 2004 and early 2005.

1.1 Scope

These guidelines are based on more than 20 years of field experience from equipment development to applications in engineering design at sites from the Beaufort Sea in the Canadian Arctic to tailings dams in Ontario, Alberta and British Columbia as well as more than 20 selected research sites in the Vancouver area. The use of SCPTU data in geotechnical design is complex and often project specific. However, design guidelines have been given (Chapter 9) to assist in their use. Relevant design examples and case histories have been given in a companion Worked Examples Manual which illustrates the application of the SCPTU data to geotechnical design.

The practice described is that followed in North America, which closely follows European methods. This manual is applicable to standard electronic cones with a 60 degree apex angle and a diameter of 35.7 mm (10 cm^2 cross-sectional area), although much of the manual is also applicable to the older mechanical cones of the same dimensions as well as 15 cm^2 (43.7 mm diameter) electronic cones. Application of these guidelines to interpretation of mechanical cone profiles should be done with due recognition of the differences between the two types of cones.

Summaries are provided at the end of each chapter on interpretation. These are intended to help the user, and should be used in conjunction with the main text.

The textbook "Cone Penetration Testing in Geotechnical Practice" by Lunne, T., Robertson, P.K. and Powell, J.J.M., Blackie Press, (1997) is an excellent reference text for this manual. It has very detailed and comprehensive chapters on Interpretation of CPTU and also on Direct Applications of the results.

1.2 Site Characterization

Geotechnical site characterization requires the determination of

1) Soil Stratigraphy
2) Hydrogeologic Parameters
3) Geotechnical design parameters
4) Geomechanical and biological characteristics of soil and pore fluid.

Typically all four are required for a Geoenvironmental Site Characterization but only the first three are required for most projects.

In conventional practice, only borehole drilling with occasional SPT and drive samples are used for site characterization. At best, a poor assessment is made of stratigraphy, no useful information is obtained for hydrogeologic parameters and geomechanical design parameters are based on a few somewhat unreliable SPT-N values at large depth intervals. The disturbed SPT samples would provide grain size and plasticity indices. A 30 m borehole with limited sampling would typically require one day of field time.

For about the same cost, an SCPTU investigation could provide a total penetration of more than 100 metres (the cone is pushed at about one metre per minute). That could be 4 soundings (or holes) to 30 m, with shear wave velocity measurements in one or more soundings. Near continuous stratigraphic data identifies soil types, their precise depths, compactness, variability, lensing, etc. Hydrogeologic parameters like groundwater table, the existence of any hydraulic gradients and estimates of permeability (hydraulic conductivity) are obtained. These are not obtained from drilling and sampling without considerable extra effort. Geomechanical parameters like compressibility, strength, liquefaction resistance are estimated and modulus determined from the seismic profile. Determination of the hydraulic parameters is often critical to site stability and this alone is worth piezocone testing. In addition, the measured shear wave velocities, provide a direct estimate of site stiffness important for seismic design.

1.2.1 Logging Methods

The CPTU is considered a “Logging Test” characterized by near continuous penetration data with depth, which is rapid, economical and repeatable and is primarily used for profiling. Its secondary use is for estimation of design parameters through empirical correlations.

1.2.2 Specific Test Methods

Specific in situ test methods measure a particular property at a point or zone, are specialized, often slow and expensive, used in critical areas defined by logging methods and should be suitable for fundamental analysis. Some specific test methods are soil or pore water sampling for specialized laboratory testing, in-situ tests like SPT, field vane shear test, pressuremeter test, etc. Within SCPTU, shear wave velocity measurements and dissipation tests to measure equilibrium pore pressure and gradient conducted during an SCPTU profile are considered specific tests.

1.2.3 Ideal Procedure for Conducting Subsurface Investigation

The following sequence is considered the ideal approach to conducting a subsurface investigation:

1) Develop a geological model of the site based on existing information. This allows an assessment of the applicability of SCPTU for site characterization.

2) Use a Logging Test Method (SCPTU) to define soil stratigraphy, hydraulic and seismic parameters and estimate geomechanical parameters.

3) Identify "Zones of Concern" for the particular project based on logging test (SCPTU) results.

4) Obtain additional information from specific test methods, which may comprise sampling and lab testing, or additional in situ tests such as field vane or pressuremeter tests to supplement and corroborate logging test results in zones of concern and to develop site-specific calibrations or correlations.

1.2.4 Cone Penetrometer as an INDEX TOOL

With as many as five independent measurements of soil response, the SCPTU can offer a reasonable assessment of the stress-strain-strength-flow characteristics of each soil layer. However, it must be remembered that the cone penetrometer is an INDEX tool. Except for shear wave velocity or elastic modulus and equilibrium pore pressure, which are directly measured, all other soil parameters are estimated from empirical correlations based on theoretical concepts. The best approach is to develop site-specific correlations for clays, e.g., measure representative undrained shear strength by field vane or lab tests and develop correlation parameters for your site or given clay layer. Unfortunately, this is not possible for sandy soils where undisturbed sampling is not possible, except by in situ freezing and correlations must be based on chamber calibration tests or other in-situ tests. The use of published global correlations is often problematic and these should be used with caution, since they vary with geomorphology, mineralogy, drainage, history and undefined measurement errors to name a few. Hence, their normal variation is very large.

1.3 General Description of CPTU

In a typical cone penetration test with pore pressure measurement or piezocone (CPTU), a cone (see Figure 1-1 for terminology) on the end of a series of rods is pushed into the ground at a constant rate of 2 cm/s and intermittent measurements are made at 2 to 5 cm depth intervals of the resistance to penetration of the cone tip, the frictional resistance on the outer surface of a sleeve or friction sleeve and of the pore pressure at the standard location, U_2.

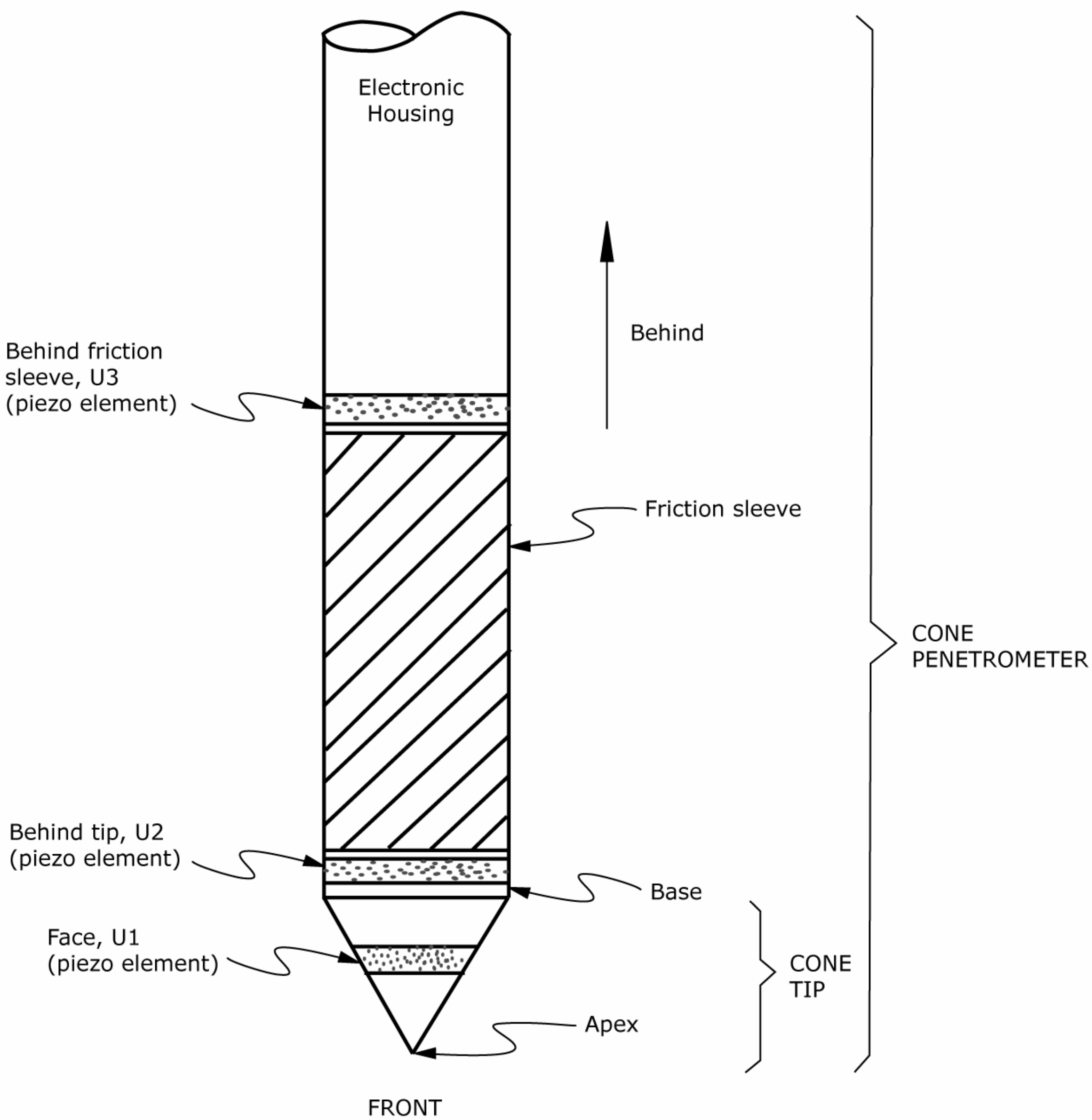

Figure 1-1 Terminology regarding the Cone Penetrometer

Probing with rods through weak soils to locate a firmer stratum has been practised since about 1917. The CPT was first introduced in a form recognizable today in the Netherlands in about 1934. The method has been referred to as the Static Penetration Test, Quasi-static Penetration Test, Dutch Sounding Test and Dutch Deep Sounding Test.

A cone with a 10 cm^2 base area cone tip with an apex angle of 60 degrees is accepted as standard and has been specified in the European and American Standards.

The friction sleeve, located above the conical tip, has a standard surface area of 150 cm^2. The porous filter of the piezo element is 5 mm thick.

In soft soils, cone penetration to depths in excess of 100 metres (330 feet) may be achieved provided verticality is maintained. Gravel layers and boulders, heavily cemented zones and dense sand layers can restrict the penetration severely and deflect and damage cones and rods, especially if overlying soils are very soft and allow rod buckling.

The version called a mechanical cone, which requires a double-rod system, offers the advantage of an initial low cost for equipment and simplicity of operation. However, it does have the disadvantage of a rather slow incremental procedure (usually every 20 cm), ineffectiveness in soft soils, a requirement for moving parts, labour intensive data handling and presentation, generally poor accuracy, shallow depth capability and no piezo measurements.

The types of mechanical cones generally used are those originally developed in Holland. In rather homogeneous competent soils, without sharp variations in cone resistance, mechanical cone data can be fully adequate, provided the equipment is properly maintained and the operator has the required experience. Nevertheless, the quality of the data remains much more operator dependent than with an electronic penetrometer. In soft soils, the accuracy of the results can sometimes be inadequate for a quantitative analysis of the soil properties. In highly stratified materials even a satisfactory qualitative interpretation may be impossible. The mechanical cone is still very popular today in developing countries.

The first electronic cone was introduced in 1948 and was vastly improved in 1971 (De Ruiter 1971) when strain gauged load cells were added. Cone development was driven by demands in the off-shore for the oil industry.

The electronic cone offers obvious advantages, such as a more rapid procedure, continuous recording, higher accuracy and repeatability, automatic data logging, reduction and plotting, and the possibility of incorporating additional sensors in the cone. However, the electronic cones have an initial high cost for equipment and require skilled operators with knowledge of electronics. They also require adequate back-up in technical facilities for calibration and maintenance.

The most significant advantage that electronic cones offer is their repeatability and accuracy (Schaap and Zuidberg 1982; Schmertmann 1975) and the nearly continuous data obtained. The most significant development in the CPT was the addition of pore pressure measurements (CPTU) in the mid-1970's. The introduction of pore pressure measurements has significantly improved the use and interpretation of the electronic cone (Torstensson 1975; Wissa et al. 1975) to evaluate geotechnical parameters, particularly in loose or soft, saturated deposits.

The main advantages of the CPTU over conventional CPT are:

- ability to distinguish between drained, partially drained and undrained penetration,
- ability to correct measured cone data to account for unbalanced water forces due to unequal end areas in cone design,
- ability to evaluate flow and consolidation characteristics,
- ability to assess equilibrium groundwater conditions including gradients,
- improved soil profiling and identification,
- improved evaluation of geotechnical parameters.

The primary purpose of the CPTU is for ***stratigraphic logging*** and ***preliminary evaluation*** of geotechnical parameters. Other in-situ test methods or borehole drilling with sampling and laboratory testing, may be better suited for use in critical areas that have been defined by the CPTU. The CPTU should be used to determine the locations and elevations at which other in-situ tests and/or sampling should be carried out.

Where the geology is uniform and well understood and where predictions based on CPTU results have been locally verified and correlated with structure performance, the CPTU can be used alone for design. However, even in these circumstances the CPTU may be accompanied by boreholes, sampling and testing for one or more of the following reasons:

1) to clarify identification of soil type
2) to verify local correlations
3) to assist where interpretation of CPTU data is difficult due to partial drainage conditions or problem soils
4) to assist where the effects of future changes in soil loading are not recorded by the CPTU. This is best done in a laboratory test on undisturbed samples.

2 EQUIPMENT

2.1 CPTU Equipment

A cone of 10 cm² base area with an apex angle of 60° is generally accepted as standard – e.g. the International Reference Test Procedure for Cone Penetration Test (CPT) by ISSMGE (International Society of Soil Mechanics and Geotechnical Engineering) and various national standards such as the American Standards (ASTM D5778-95(2000)). The IRTP is provided in Appendix A. The friction sleeve, located above the conical tip, has a standard area of 150 cm². The friction sleeve on electronic cones has the same diameter as the conical tip and push rods, i.e., 35.7 mm.

2.1.1 Tip and Friction Sleeve Load Cell Designs

Electronic penetrometers have built-in load cells that record end bearing force divided by 10 cm² base area to give tip or penetration stress, q_c, and friction sleeve force divided by 150 cm² to give sleeve stress, f_s. Bonded strain gauges are most commonly used for load cells, because of their simplicity, ruggedness, and zero stability, but inductive and vibrating wire types also exist (Sanglerat 1972). Load cells have also been developed that incorporate pressure transducers to record load (Torstensson 1982). In general, however, experience has shown that the use of the strain gauge provides a high precision for load cells. Full details on cone designs are given by Lunne et al. (1997). An extensive discussion of various types of load cells and transducers is given in Dunnicliff (1988).

In general, no single cone design will meet all requirements and needs. Flexibility in cone equipment and designs is important so that various cones can be employed depending on the soil conditions and project requirements. In general, a high capacity cone (tip load cell capacity of 10 tons) should be used to provide the preliminary soil profile and stratigraphy. There are three common types of load cell designs, the subtraction cone, the tension cone and the compression cone as shown in Figure 2-1. The subtraction cone uses two high capacity load cells, one for the tip and the second for the tip plus friction sleeve. Thus, the friction sleeve load is determined by subtracting the load cell readings. In the tension and compression cone the tip load is read by one load cell and the friction sleeve load by an independent second load cell in tension or compression. Since the capacity of the friction sleeve load cell is typically 1/10th the capacity of the tip load cell, a tension or compression cone can measure friction sleeve force much more accurately because of its higher sensitivity compared to the subtraction cone. The subtraction cone has two high capacity load cells, the loads on which are subtracted to obtain a very small value. The subtraction cone, however, is rarely damaged or overloaded and is more robust, while the tension cone is more prone to having the friction sleeve load cell overloaded.

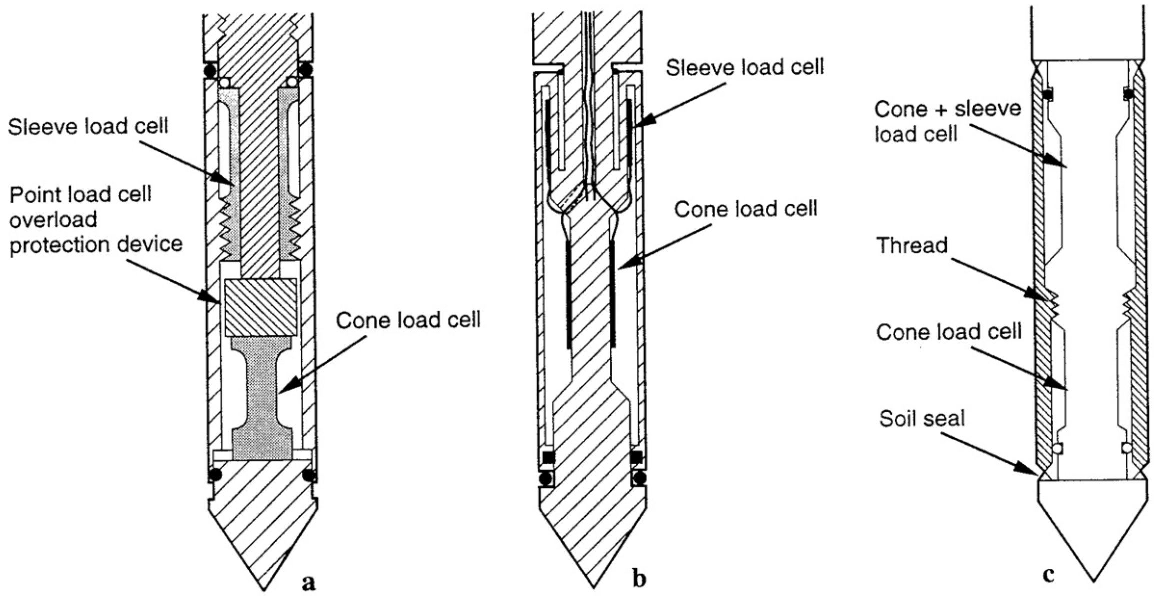

Figure 2-1 Cone Designs: (a)Tip & Sleeve in compression, (b)Tip in Compression and Sleeve in Tension, (c)Subtraction Cone (after Lunne et al, 1997)

If a soft layer is identified within a profile by a high capacity cone and requires more careful examination, a dual range cone or lower capacity tension cone could be used to do so. This flexibility in cone use requires careful design of the data acquisition system to obtain optimal sensitivity.

2.1.2 Pore Pressure Measurements

Measuring pore pressures during cone penetration requires careful consideration of probe design, choice and location of the porous element and probe saturation (see later sections and Campanella and Robertson 1988). The mechanical design of the cone must ensure that when the cone tip is stressed, no load is transferred to the pore pressure transducer, porous element or fluid volume. This problem can be checked by loading the tip of a fully assembled, saturated cone and observing the pore pressure response. If no mechanical load transfer occurs, no pore pressure response should be observed.

For a high frequency response, (i.e. fast response time), the design must have a small fluid filled cavity, low compressibility and viscosity of fluid, a high permeability of the porous filter and a large area to wall thickness ratio of the filter (Smits 1982). To measure penetration pore pressures rather than filter compression effects, the filter should be rigid. However, to maintain saturation, the filter should have a high air entry resistance, which requires a finely graded filter and/or high viscosity of the fluid. Clearly, not all of these requirements can be combined.

An essential requirement is to incorporate a small fluid cavity, a low compressibility of saturating fluid and a rigid or low compliance pressure transducer. A balance is required between a high permeability of the porous filter to maintain a fast response time and a low permeability to have a high air entry resistance to maintain saturation.

Figure 2-2 shows the essential elements of the most common designs. The design uses a small pressure transducer mounted within the cone and behind the tip to sense the water pressure. The design also has a minimal volume between the transducer and the external surface of the porous filter. This is important to minimize the response time of the measuring system.

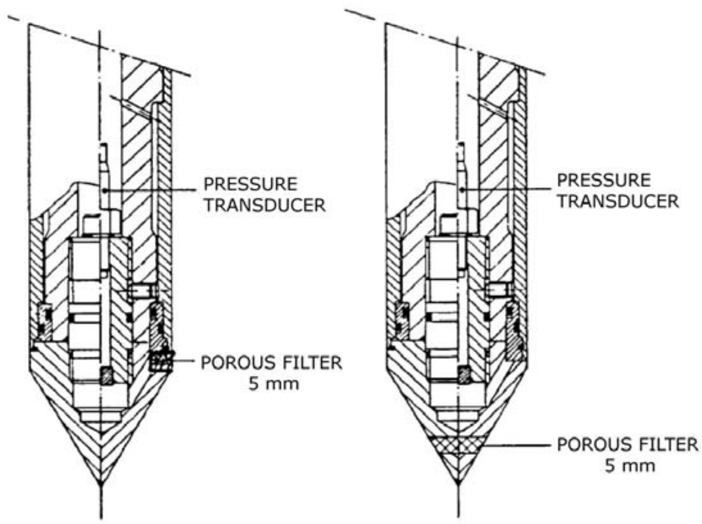

Figure 2-2 Hogentogler Piezocone Designs

The UBC and the Hogentogler design enables the filter or porous plastic element to be located either on the face of the conical tip at mid height or immediately behind it. This change in filter location can be made in the field (see Figure 3-3 which shows the UBC CPTU with tension friction cone). There are advantages and disadvantages for both filter locations. This will be discussed later.

The filter can be made from the following materials; porous plastic, ceramic, or sintered stainless steel. Its function is to allow rapid movements of the extremely small volumes of water needed to activate the pressure sensor while preventing soil ingress or blockage. Both machining and abrasion through dense sand tends to close off the openings into a stainless filter. A ceramic filter does not usually survive penetration through dense sands. Porous polypropylene, a tough hard plastic, survives well in dense sands and gravelly soils showing only minor wear.

During penetration into a dense layer with high cone tip resistance, the filter element can become compressed and generate high positive pore pressures. This will occur unless the filter element has a very low compressibility or if filter and soil are of sufficient permeability to rapidly dissipate the pore pressure due to filter element compression. Experience gained at UBC (Campanella and Robertson 1988) with a relatively compressible porous polypropylene plastic filter element **behind** the cone tip has shown no evidence of induced pore pressure due to filter squeeze. This is likely due to the low normal stresses behind the cone tip and the high permeability of the porous plastic element. However, problems may occur with face sensing filter elements in very stiff soils with permeabilities considerably lower than that of the porous element. In a UBC field comparison study between porous polypropylene (a hard plastic) and ceramic filters, only slight differences in penetration pore pressures were observed as shown in Figure 2-3. Filter squeeze is mainly critical for pore pressure measurements on the face of the cone tip during initial penetration into dense fine or silty sands and compact glaciated silts and clays.

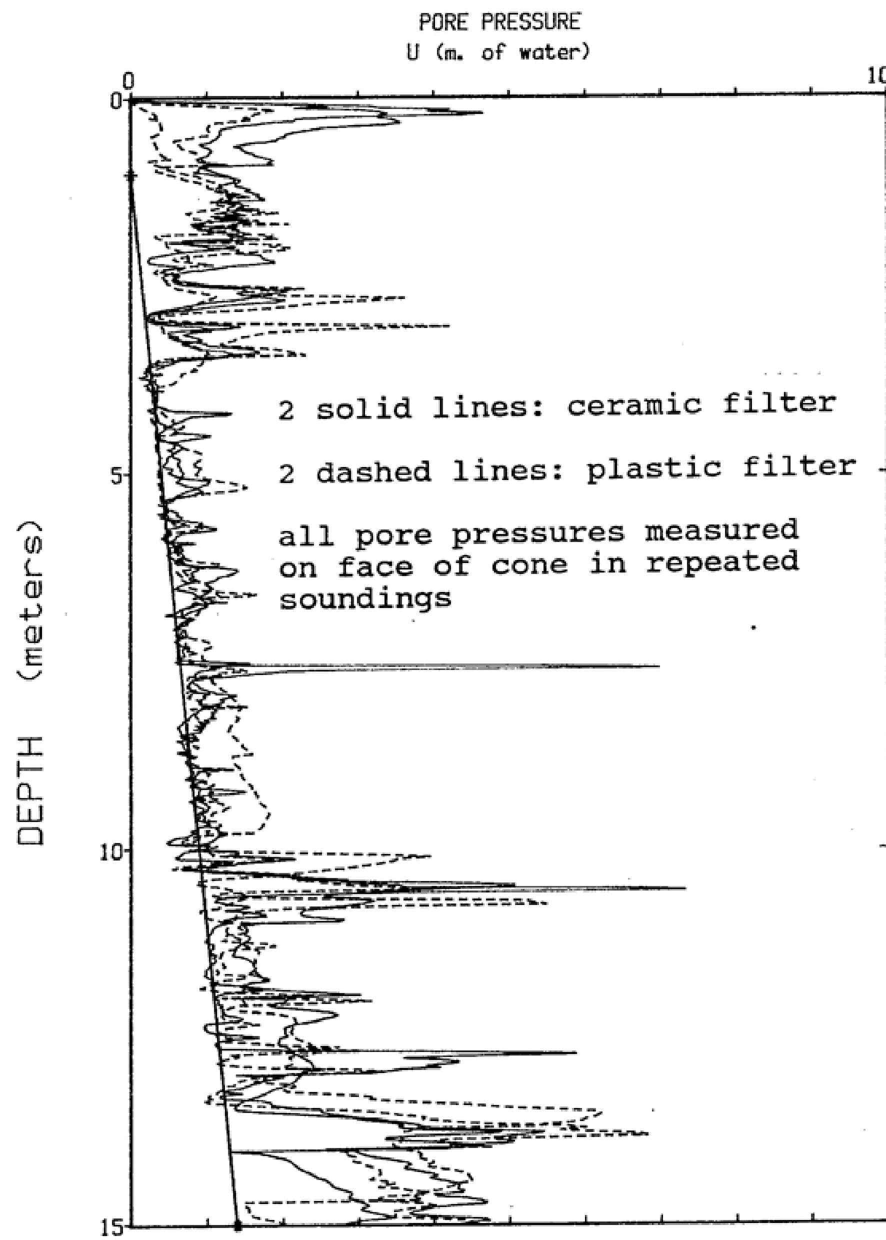

Figure 2-3 Face Pore Pressure comparison between Polypropylene and Ceramic Filters, two soundings each in dense silty sand (Gillespie 1990)

2.1.3 Recent Developments

The electronic penetrometer produces continuous data that requires relatively complex data collection and processing. The signals are usually transmitted via a cable prethreaded down the standard push rods.

Modern systems have evolved to include analog to digital (A/D) converters so that the amplified analog signals are directly converted to digital form for data logging (De Ruiter 1982). The digital data is ***incremental*** in nature, typically recording all channels every 1 to 5 cm in depth. Data is stored on a hard drive in a field computer running under MS DOS or Windows. Printers and displays are used in the field with the PC to calculate, print and plot data, such as tip stress, friction ratio, pore pressure, inclination and interpreted soil type during a cone sounding.

Current developments in cone technology include wireless cones, memocones in which data is stored in the cone downhole, wireless cones with sound and microwave transmission of live data, and all-digital cones with two-way live transmission of data.

The use of 15 cm^2 piezocones has become popular because of their robustness and greater depth capability when pushing with 10 cm^2 cone rods due to a reduction in rod friction. The larger 15 cm^2 cone gives essentially the same results as 10 cm^2 provided the friction sleeve has a surface area of 225 cm^2 to preserve geometric similitude, but many manufacturers ignore that requirement. If you use 15 cm^2 cones check the area of the friction sleeve. The larger cone has a lower sensitivity to the presence of thin layers than the smaller 10cm^2 cone. In that regard, mini-cones, of the order of 2 cm^2 (16 mm diameter) pushed to shallow depths of 15 m with continuous tubing have been developed to obtain better delineation of thin layers (Tumay and Kurup 2001).

Recent improvements in solid state electronics and microchip technology have made the current piezocones extremely stable and sensitive with capabilities exceeding published specifications. The decreased cost of electronic components has also made it possible to digitize the data in the cone and thus transmit a clean digitized signal. This enables a greater number of channels to be recorded with a minimum number of wires within the cable, thus making it possible to enhance the cone with additional sensors.

However, with increased numbers of channels, the data processing and presentation becomes more complex. The field or office computers require flexibility in software to enable a variety of calculations to be performed to produce profiles that correlate various parameters.

2.2 Additional sensors

New designs and the recent advances in electronic components have enabled the economic incorporation of a variety of additional sensors. A summary of available geotechnical and geoenvironmental sensors is presented in Tables 2-1 and 2-2. Some of the additional sensors are briefly discussed in the following sections. The additional sensors can significantly improve the use and application of CPT data to engineering design.

Sensor	Measurement	Applications	Reference
Inclinometer	Cone verticality	• Prevent damage of cone	Campanella et al. (1986b)
Resistivity	Mobility of ions in pore fluid using electrically isolated electrodes	• Porosity of sands • Fabric of sands • Conductivity = 1/Resistivity	Bellotti et al. (1994); Campanella and Weemees (1989)
Vibratory Module	Vibration of cone during push	• Assessment of soil liquefaction potential	Sasaki and Koga (1982); Sasaki et al. (1985); Mitchell (1988)
Accelerometer/ Geophone	Shear wave velocity	• Measurement of small strain properties of a soil • Site specific G_{max} • Particle velocity for damping ratio	Robertson et al. (1986)
Neutron/ Gamma Radiation	Moisture content	• Soil density • Moisture content • Correlation with liquefaction potential	Marton et al. (1988); Mitchell (1988); Sully and Echezuria (1988); Mimura et al. (1995)
Lateral Stress	Lateral stress on cone shaft	• Evaluation of in-situ states of stress	Mitchell (1988); Sully (1991)
Acoustic	Acoustic emissions	• Soil type • Soil compressibility • Soil fabric	Villet et al. (1981); Tringale and Mitchell (1982); Menge and Van Impe (1995)
Pressuremeter Module (Full displacement)	Radial deformation	• Shear strength • Horizontal stresses • Deformability	Houlsby and Withers (1988); Houlsby and Hitchman (1988); Ghionna et al. (1995)
Time Domain Reflectometry	Dielectric constant through pulsed electromagnetic wave	• Correlated with moisture content	Lightner and Purdy (1995)
Video	Video images of soil during penetration	• Grain size quantification • Soil stratigraphy	Hryciw and Raschke (1996); Raschke and Hryciw (1997)

Table 2-1 Review of Geotechnical Sensors Used in Piezocone Testing (Burns and Mayne 1998)

Sensor	Measurement	Applications	Reference
Resistivity	Mobility of ions in pore fluid using electrically isolated electrodes	• Salt water intrusion • Acid spills • Detection of water table in mine tailings	Horsnell (1988); Campanella and Weemees (1989); Strutynsky et al. (1991); Woeller et al. (1991a); Malone et al. (1992)
Temperature	Temperature of cone body	• Endothermic/ exothermic activity	Horsnell (1988); Mitchell (1988); Woeller et al. (1991b)
SCAPS	Laser-induced fluorescence of fuel contaminants; N2 laser at λ = 337 nm	• Fuel, oil, and lubricant contamination capable of fluorescing	Lieberman et al. (1991); Apitz et al. (1992a); Apitz et al. (1992b); Theriault et al. (1992); Lambson and Jacobs (1995)
Redox Potential	Reduction Oxidation Potential	• Monitoring of conditions during bio-remediation	Olie et al. (1992); Pluimgraaf et al. (1995)
pH	Hydrogen ion concentration	• Acid spills • Base spills	Brylawski (1994)
Dielectric Constant	Dielectric constant of soil/pore fluid mixture as a function of frequency	• NAPL contamination	Arulmoli (1994); Stienstra and van Deen (1994)
Raman Spectroscopy	Raman spectrograph to measure argon ion laser induced fluorescence	• NAPL contamination • Chlorinated hydrocarbons	Carrabba (1995) Bratton and Timian (1995)
ROST™	Laser-induced fluorescence of fuel contaminants; neodymium-doped yttrium aluminum garnet laser at λ = 280 - 300 nm	• Fuel, oil, and lubricant contamination capable of fluorescing	Naval Command (1995)
Gamma Radiation Probe	Detection of Uranium by-products using a NaI(Tl) crystal detector	• Identification of radioactive contaminants	Brodzinski (1995); Lightner and Purdy (1995)
Integrated Optoelectronics	Measurement of in situ chemical concentration by wave interference	• Ammonia • pH • BTEX	Hartman et al. (1988); Hartman (1990) This study

Table 2-2 Review of Geoenvironmental Sensors Used in Piezocone Testing (Burns and Mayne 1998)

2.2.1 Temperature

Measurement of soil temperature can be performed by incorporating a temperature sensor in the cone (Campanella and Robertson 1981; Marr 1981). Temperature measurements during penetrometer testing have been made in permafrost, under blast furnaces, beneath cooled storage tanks and along marine pipelines (De Ruiter 1982). These can furnish information about the environmental changes, whereas changes in temperature gradient with depth provide some insight in the heat conductivity of the soil. However, heat can be generated during penetration. In dry dense sand layers, temperature increases of several degrees Celsius (°C) have been observed. It has also been reported that pushing a CPT through deep medium dense sands above the water table in California resulted in enough generated heat to cause hard burns if the cone was touched after removal from ground. The temperature readings can also be used to adjust the calibration of the load cells due to temperature variations.

2.2.2 Inclination

Installation of an inclinometer in the cone greatly increases the reliability of the test, as it provides a record of the verticality of the rods during penetration. Details about the effect of inclination on measurements are given in Section 3.2.3.

2.2.3 Seismic

The seismic cone penetrometer was developed in the early 1980’s (Campanella and Robertson 1984; Robertson et al. 1986). It can significantly reduce the cost associated with most in-situ seismic methods. This device combines a CPTU with a miniature 28 Hz. seismometer built into the cone. The bearing, friction and pore pressure measurements can be used to log the stratigraphy of a site during penetration and the downhole seismic method (see Chapter 5 for details) can be performed at appropriate depths in the soil profile using the seismometer, to detect wave arrivals without significantly delaying the CPTU test.

2.2.4 Electrical Resistivity

The principle of electrical resistivity methods is based on the fact that sand grains consist of electrically non-conducting minerals, whereas the pore water is electrically conducting, especially if it contains dissolved salts. A resistivity probe used as a penetration cone was developed and has been in use by the Delft Soil Mechanics Laboratory since the late 1970’s (Kroezen 1981).

The University of British Columbia has developed a resistivity module for the CPTU for use in environmental studies of groundwater contamination (Campanella and Weemees 1990). The tool has been effective in studying acid mine drainage at mine tailings dams (Campanella and Davies 1997), salt water intrusion (Campanella 1999) and estimating density and degree of saturation (Daniel et al. 2002).

2.2.5 Other Sensors

The reader is referred to an excellent summary of additional sensors for the cone by (Burns and Mayne 1998). The references listed in the fourth column of Tables 2-2 and 2-3 are provided in the above publication.

2.3 Pushing equipment

2.3.1 On land

The rigs used for pushing the penetrometer consist basically of a hydraulic jacking system. They are usually specially built for this purpose, but sometimes the push of an anchored drill rig is used. The thrust capacity needed for cone testing commonly varies between 100 and 200 kN (10 and 20 tons). 50 kN and 20 kN (5 and 2 tons) capacity is also common for use in soft soils. 200 kN (20 tons) is about the maximum allowable thrust on the 35.7 mm diameter high tensile steel push cone rods. Exceeding that load often results in damage and/or buckling of the test rods, either in the rig or in softer upper layers of the soil. Experience shows that as long as the pushing thrust is below 100 kN (10 tons), it is rare that any damage occurs to the rods or cone. A thrust capacity of 100 kN (10 tons) will likely handle more than 95% of cone penetration testing to 30 m (100 feet) depth in most uncemented normally consolidated soils that do not contain large gravels and boulders.

Land based rigs are often mounted in heavy duty trucks that are ballasted to a total deadweight of around 150 kN (15 tons). Screw anchors are used to develop the extra reaction required for a thrust of 200 kN (20 tons). The power for the hydraulic rig is usually supplied from the truck engine. Sometimes all-terrain vehicles are used for work in marshy areas or soft fields.

The load of the hydraulic ram is transferred either by a thrust head on top of the test rods or by a clamping system that works by friction on the outside of the upper rod or by a notch cut into the rods. An automatic mechanical clamp saves time in the operation as the next rod can be screwed on while the rig is pushing down the previous one. The clamping system was first developed for offshore rigs, where it is indispensable. The standard cone rods have special tapered threads and are 1 metre (approximately 3.3 feet) in length. Rods are connected hand-tight and wrenches are rarely needed during disassembly. The enclosure of a truck provides ideal space for the installation of all electronic equipment for depth recording and read-out. In hot humid climates, the truck should be air conditioned for the comfort of personnel and preservation of electronics.

The penetrometer rig can also be placed on a light trailer equipped with earth anchors. A high production truck mounted rig can produce up to 250 metres (800 feet) of penetration testing in one day, as compared to about 120 metres (400 feet) for a trailer mounted rig, both under favourable site conditions. The most time consuming part of the trailer mounted operation is the setting of screw anchors which are usually required to provide additional reaction because of the lack of deadweight. An intermediate solution is to mount the rig on a heavy trailer or heavy duty pick-up truck frame which can be ballasted. CPT can also be performed using standard drill rigs but pushing capacity is often limited to about 5 tons or less without anchors. Use of a drill rig has the added advantage of improved cost and flexibility.

A friction reducer or expanded coupling is used at distances from 30 cm to 100 cm (1 foot to 3 feet) behind the cone tip. The purpose of the friction reducer is to expand the diameter of the hole to reduce soil contact against the cone rods and thus reduce rod friction behind the friction reducer at the expense of increased bearing and friction forces locally around the reducer. Also, experience suggests that the further back the friction reducer is from the tip, the better are chances of maintaining a vertically aligned hole but this is at the expense of increased friction force in front of the friction reducer.

It has been found that a 50 mm (2 inch) long, high strength steel tube of 1.75 inch O.D. slipped over the cone rod with ends welded and machined to a 30° chamfer works well in most soils.

Some cone operators use four steel blocks, about 5 to 10 mm square welded and evenly spaced around the standard cone rod. This technique tends to break up and slightly push the soil to reduce subsequent friction on the rod, but it does not appear to be as effective as a complete sleeve.

A 200 kN (20 ton) thrust will normally result in penetration depths of 50 to 60 metres (150 to 200 feet) in dense to medium dense sands and stiff clays. In weaker soils penetration to depths in excess of 100 metres may be achieved provided verticality is maintained. Gravel layers and boulders or heavily cemented zones can of course restrict the penetrations severely and deflect and damage cones and rods.

To reduce the pushing force required for cone penetration, a system was developed (Jefferies and Funegard 1983) where a natural or polymer drilling mud was pumped down the inside of the cone rods and injected into the soil at a steady flowrate of about 1 litre/min. (0.2 gallons/min.) from several injection ports located approximately 1.5 m (5 feet) behind the tip and immediately behind the friction reducer. The mud holds the soil off the cone rods thus minimizing friction. Trials have shown that the pushing force can be reduced by up to 50%. This has enabled CPT work to be performed using a standard drill rig with about 50 kN (5 ton) effective thrust. Mud pumping systems are commercially available for standard electronic cone systems to reduce pushing force requirements.

Standard Dutch Type cone rods of 20 ton capacity (high strength steel) are recommended for all cone soundings unless special requirements exist. The standard cone rods are the same diameter as the base of the tip and sleeve, measure 1 metre in length, have tapered threads and are assembled and dismantled by hand. Some operators prefer to use the locally available drill rods in longer lengths. Although it is more convenient and economical to use these, they do not have the capacity and buckling resistance. However, with reduced pushing forces of 5 - 10 tons as with drill rigs, the use of local drill rods can work well.

2.3.2 Over water

Modification of the standard techniques on land is necessary for cone testing over water and/or offshore. CPT work offshore can be divided into two main groups:

1) Shallow water (Depth < 30 m (100 feet) approx.)
2) Deep water (Depth > 30 m (100 feet) approx.)

For shallow-water CPT work, where the water depth is less than about 30 m (100 feet), equipment and procedures are similar to onshore CPT work. A ship or barge is often used as a platform and a dual casing used for lateral support of the cone rods. An anchored barge must have a heave compensation system to prevent cyclic loading during swells and wave action. If the water depth is shallow, a free-standing platform or jack-up barge resting on the seabed is very desirable and free of wave action.

A combination free standing platform (large heavy casing with inner cone rod casing founded on the seabed) and floating barge often provide the most economical solution in shallow waters. The free standing casing protrudes through the anchored barge with penetrometer mounted on the "stable" casing.

For deeper offshore CPT work special equipment is needed which can be divided into two categories:

1) Seabed bottom rigs and
2) Downhole penetrometres.

Full details of these can be found in (Lunne et al. 1997).

3 PROCEDURES

3.1 Calibration Procedures

3.1.1 General Comments

All calibrations should be done using reference type load cells (superior zero stability and linearity with little hysteresis) and a dead weight tester or pressure reference transducer. Calibrations should be done with all O-rings and dirt seals in place in the cone as they would be during penetration.

After all transducers in a new cone have been loaded to capacity approximately 20 times, the calibration procedure should be set up to measure and record all channels (i.e., cross-talk effects). For example, when the tip is loaded to reference values to establish the calibration curve of output versus load, each of the other measurement channels should be read and recorded at each tip load. By so doing mechanical load transfer error, which should be a minimum, can be evaluated for each channel.

3.1.2 Calibration

A detailed discussion on accuracy, calibration and performance of electronic cones is given by Lunne et al. (1997).

The two main errors related to the design of the load cells for CPT are:

1) Calibration error
2) Zero load error

An illustration of these terms is given in Figure 3-1, which is a graph of loading and unloading for a load cell.

Studies have shown that the major factor that contributes to changes in calibration error is soil ingress along the joints in the cone. However, this can be significantly reduced by regular inspections and maintenance. Also, the time between calibrations should be kept to a minimum. To assist in this latter part, a simple calibration loading device should be included in the field equipment to allow frequent field calibration checks. The calibration should evaluate repeatability, non-linearity and hysteresis effects to determine the best straight line fit for the data.

To reduce the hysteresis in the calibration curve, the cone should be loaded at least 20 times to its full capacity before performing the calibration.

The non-linearity of the calibration curve can be considerably reduced by using a calibration factor for the usual working range in the field. For example, if you typically

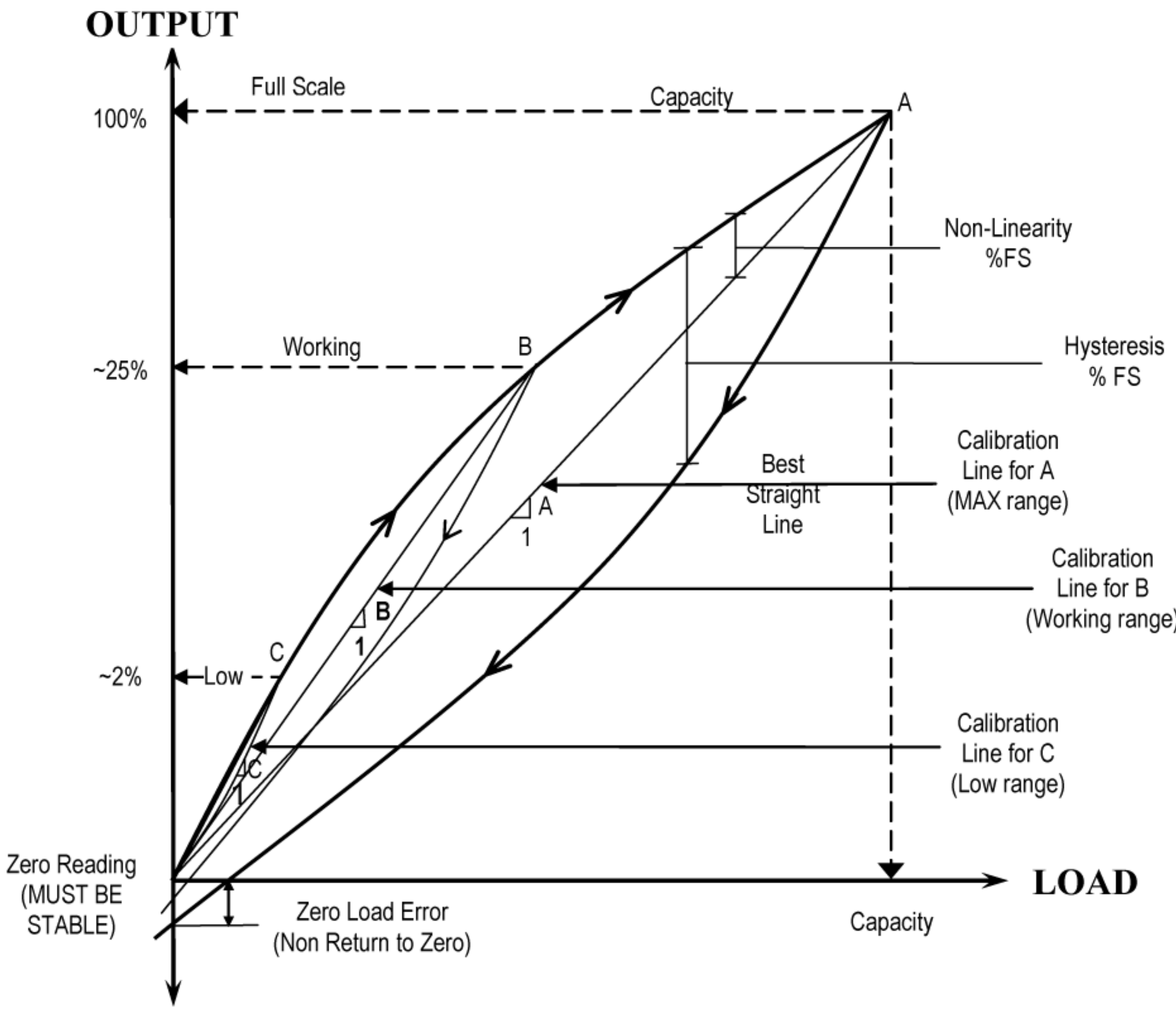

Figure 3-1 Typical Load Cell – Pressure Transducer Calibration Curve with Exaggerated Non-Linearity to Define Terms

have maximum tip stresses of about 400 bar (kg/cm^2 or t/ft^2) but most tip stresses are less than 200 bar, you could use the calibration factor for 0-200 bar, point B, on the calibration curve in Figure 3-1, even though the tip has a capacity of 1000 bar or more.

Testing in very soft normally consolidated soils where maximum tip stresses are of the order of 5 bar and less may require a calibration from 0-2 bar in order to obtain adequate sensitivity (point C in Figure 3-1).

In some cases, it may be possible to have a different calibration line for different load levels, e.g., slope C versus B in Figure 3-1. A 2 or 3-segment calibration curve technique is easily handled by a computer-based data acquisition system and reduces the error due to non-linearity.

For completeness, the effect of temperature on zero load output and on calibration factors should be determined by performing calibrations over a range in temperature which might correspond to field conditions. The effect of temperature variations can be minimized in the field by pushing the cone into the ground about 1 m and leaving it for about 1/2 hr. or more while setting up the data system. When the test is started, the cone is withdrawn to ground surface, zero outputs or baselines are recorded and the sounding is started. In this way, the cone is brought to ground temperature before starting the test. However, it might be easier to plunge the cone into a bucket of water which is near ground temperature for about 15-30 minutes immediately before a sounding.

The zero error can be reduced if proper care and procedures are followed in the field with recommended maintenance. Zero load error is variable and is determined for each sounding by recording the zero load reading ***just before penetration*** and immediately ***after the cone is withdrawn from the ground.*** The zero load error during calibration should be negligible (less than 0.05% F.S.).

The zero load conditions should always be displayed on the recorded data sheets to enable the engineer to check its variation. The zero load error should, in general, not exceed ½% to 1% of the full scale output. For measurements in soft soils, the error should be considerably less than ½% of full scale.

Load cells within penetrometers are generally compensated for temperature variations. With good temperature compensation, the output variation can be limited to about 0.05% of full scale output. However, procedures to reduce temperature variation should be used (as discussed in Section 4.1.3).

Unfortunately, few data are published concerning the accuracy of various cone designs. In general, however, strain gauge load cells have proven to provide better precision than vibrating wire and pressure transducer load cells. With careful design and maintenance, strain gauge load cells can have calibration errors less than 0.4% of full scale output. A study at NGI (Lunne et al. 1986) showed that high capacity load cell cones can give as repeatable and as accurate results as cones with lower load ranges provided the load cells are of a high quality and are carefully calibrated in various operating ranges and that attention is given to thermal zero shifts. The study at NGI also showed that the friction sleeve measurement was the least reliable for cones of different design, which is likely due to unequal end areas of the friction sleeve (see section 4.1.1).

Other factors that affect the accuracy of the measurements are related to the methods of calibration, data acquisition and processing.

The tolerance in machining the standard friction cone is such that the difference in diameter between the tip and the sleeve can be up to 0.25 mm (0.010 inches). This, combined with wear during usage often results in significant differences in diameter between the tip and sleeve. It has been found that variations in diameters between the tip and sleeve can result in significant differences in measured friction values.

This variation can be reduced by careful machining during construction and regular tolerance checks during the life of the cone. The O.D. of the cone tip should be identical or less than the O.D. of the friction sleeve by about 0.25 mm (0.010 inches). ASTM D3441 allows up to 0.024 in. (0.5 mm) less, which is not a sufficiently tight tolerance for research level testing.

If the output at zero load is measured before and after a test, the zero load error can be measured. In general, the zero load error is a reliable indication of the quality of a test and is the sum of a number of possible effects:

1) Output stability
2) Temperature induced apparent load
3) Soil ingress
4) Internal O-Ring friction (threshold)
5) Moisture ingress
6) Very short duration overload often causes a zero offset error
7) Deflection resulting in bending and local yielding.

3.1.3 Pore Pressure Calibration

The pore pressure calibration should be done with a pressure chamber as shown in Figure 3-2, which completely encloses the cone and is sealed at a point above the friction sleeve. Measurement of the tip stress and friction sleeve stress at applied pore pressures will allow direct determination of unequal end area effects and their correction factors as discussed in Section 4.1.1. The field data acquisition system should be set up as it would in the field to run a CPTU test. The valve in Figure 3-2 is open during the calibration. The calibration procedure is the same as that for the load cells discussed in the Section 3.1.2. When the pressure is at its maximum calibration value the pressure is maintained and the valve is closed and the fluid levels observed in the U-tube. The level should not change indicating that all the seals in the cone are working properly. This is an integrity test. If there is any movement of the fluid, the cone must be disassembled and all O-ring seals checked for cleanliness and lubricated with a light coating of silicone grease. The integrity test should be repeated until no leakage is observed.

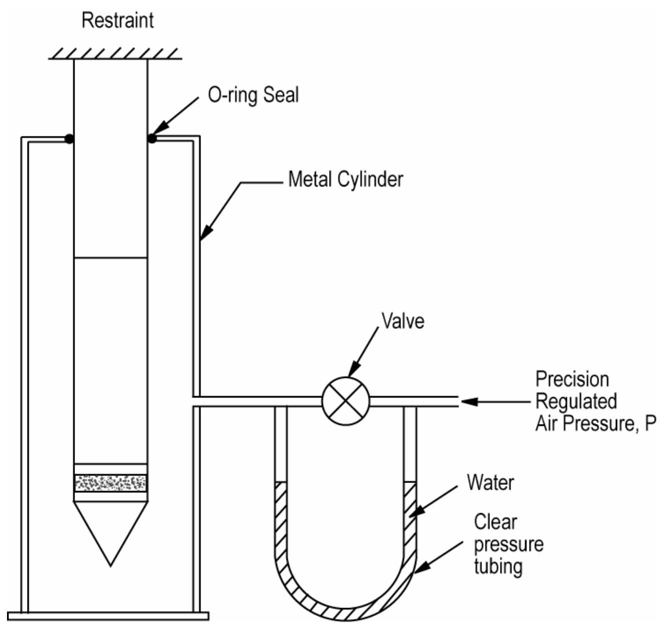

Figure 3-2 Simple CPTU Pressure Calibration Chamber

3.2 Test Procedures

3.2.1 General Comments

Efficient field operations with electronic cone testing requires skilled operators and adequate technical back-up facilities for calibration and maintenance of the equipment. The cones and the data acquisition systems including cables and connections need to be regularly checked or recalibrated. In the field, simple check calibrations and procedures are essential after connecting the equipment to ensure that all is functioning properly. These checks include measuring the variation of the output of the strain gauge load cells over their full operational range to check the calibration curve and the non-return at zero load. Checks and inspections of the equipment are also needed between each sounding or series of soundings.

The standard penetration speed for CPTU testing is 2 cm/sec ±0.5 cm/sec (see ASTM standard). It is important to obtain measurements of this speed to check that the speed control systems are functioning correctly. The use of a solid steel "dummy cone" of 15 cm^2 area (1.75 in. O.D. by 60° apex angle cone tip) is recommended to be pushed first in the upper zone (0 to 1 m or 3 ft) especially if gravel or random fill is suspected.

3.2.2 Saturation of Pore Pressure Measuring System

There are no major differences in field test operations between standard CPT testing and CPTU soundings, except those required for the preparation of the piezo-element. This preparation usually consists of the following operations:

1) Deairing of porous filter elements.
1) Deairing of the cone, especially with respect to the pressure chamber immediately adjacent to the pressure transducer.
2) Assembly of cone and filter.
3) Protection of system during handling, if required.

General preferred practice today is to carefully saturate the filter elements in the laboratory by placing them under a high vacuum with saturating fluid for approximately 5 to 24 hours. The practice at UBC has been to submerge the porous filter elements in warmed (40 to 60°C) glycerin in a small ultrasonic bath under a high vacuum (Use a two stage vacuum pump with a water trap). After several hours of vibration, the glycerin increases in temperature which reduces its viscosity, it boils under vacuum and this improves saturation. The filter elements are then placed in a small glycerin filled container ready for transportation into the field. Note that glycerin boils at 290°C (550°F) at atmospheric pressure which will damage porous plastic and is dangerously hot to handle.

Some reasons why glycerin is a preferred saturating fluid for pore pressure measurement in the CPTU are:

1) Glycerin's high viscosity (use 95% pure grade) maintains saturation in dry soils above the groundwater table.
2) Glycerin is miscible in water (oil is not and causes errors due to menisci stresses).
2) Glycerin is more incompressible than water.
3) Deaired glycerin absorbs air just like water.
4) Glycerin has a lower freezing point (-17°C) than water.
5) Glycerin is good for your skin, environmentally friendly, available at any drug store and inexpensive.

Some contractors still use oil or silicone as a saturating fluid, even though glycerin has superior properties as a saturating fluid.

The voids in the cone itself should be deaired by flushing with glycerin from a plastic syringe and hypodermic needle. It is suggested that all piezometer cone designs should be made such that flushing the void within the cone tip can be performed with a hypodermic. The cone can be held with tip pointing upward and fitted with a cut-off large plastic funnel sealing around the friction sleeve (see Figure 3-3). The entire tip is submerged in the saturating fluid during piezometer and tip assembly. Good results have been obtained when glycerin is used in the field to fill the void spaces in the pore pressure sensing cone system.

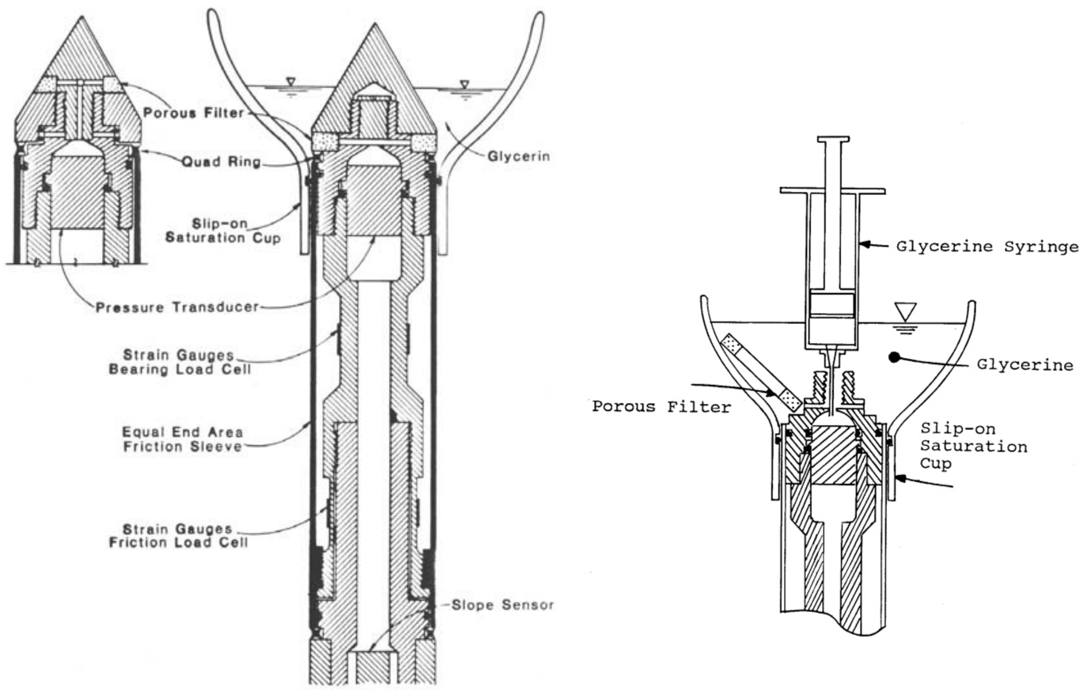

Figure 3-3 U.B.C. CPTU showing tip design to relocate porous filter (U1 or U2) and allow easy Saturation with Glycerin(Campanella et al, 1983)

Pore pressure response has been compared for saturated and air entrapped piezometer systems and an example is shown in Figure 3-4. Both the maximum pore pressure and dissipation times can be seriously affected by air entrapment. Notice that the saturated system is very responsive to stratification from 16.7 to 17.7 m and shows no lag in dissipation. It should be realized, however, that even a badly air entrapped system will record the correct equilibrium pore pressure as long as there is no further change in pore pressure with time.

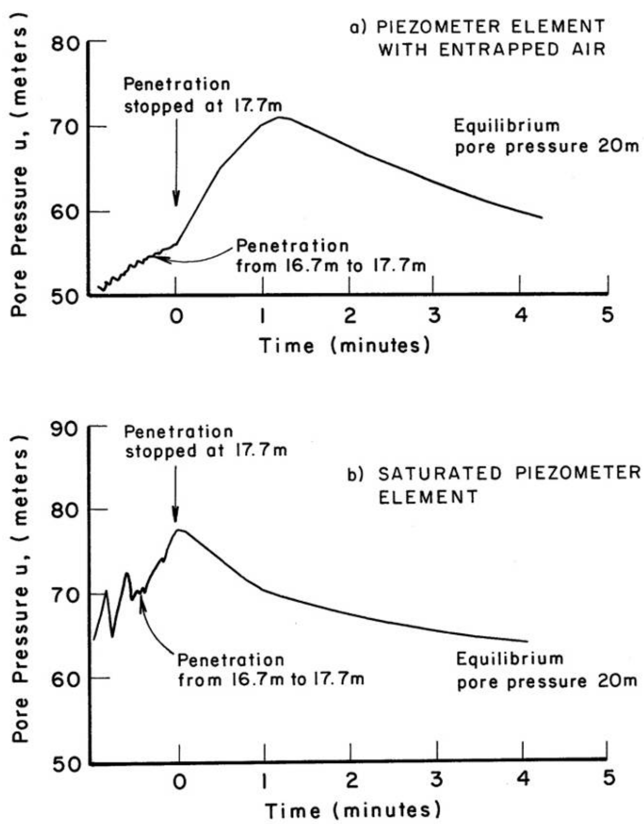

Figure 3-4 Effect of Entrapped Air on Pore Pressure Response in CPTU in Very Soft Silty Clay (Campanella and Robertson, 1981)

3.2.3 CPTU Test Procedure

The next step after cone preparation and assembly is the lowering of the string of cone rods. A thin protective rubber sleeve is sometimes placed over the cone. To avoid premature rupture of the rubber sleeve, a small hole is pushed with a "dummy cone" of a larger diameter (approx. 44 mm O.D.) than the piezocone. Sometimes a hand dug or a predrilled hole is made depending on circumstances and soil-stratigraphy. Predrilling is not always necessary if the filter element and saturating fluid develop a high air entry value to prevent loss of saturation as does glycerin. However, in some clay soils, suctions can be very large and predrilling may be necessary. The entire saturation procedure should be repeated after each sounding, including a change of the filter element. If undamaged, the filter elements may be reused after being resaturated in the ultrasonic vacuum bath. However, it is more efficient to dispose of porous plastic filters after each use.

The cone should be lowered through the guide/wiper sleeve to where the apex of the tip is at ground level or the reference starting level. The verticality of the cone rods should be checked in two directions with a quality level. The data system should be fully operational for at least 30 minutes. All the base lines or zero values for all data channels should be recorded. Then the data acquisition system is started and pushing begins at 2 cm/s. Cone rods are usually 1 m in length. While pushing, a helper cleans the rod threads with a wire brush and may spray a light lubricant on the threads. When the push is stopped, a length of rod is added and tightened hand-tight without rotating the system. The operator should check to be sure the rod shoulders are in full contact. If this is not done, rod breakage may occur at the threads.

3.2.4 CPTU Pore Pressure Dissipation Test Procedures

During a pause in the penetration, any excess pore pressures measured on the cone will start to dissipate and eventually stop at the equilibrium value for the given depth. The rate of dissipation depends upon the coefficient of consolidation which, in turn, depends on the compressibility and permeability of the soil.

A dissipation test can be performed easily at any depth by stopping penetration. In the dissipation test the rate of dissipation of excess pore pressure to a certain percentage of the equilibrium pore pressure, usually 50%, is measured.

If the cone rods are clamped at the surface, a stop in penetration should theoretically stop the movement of the cone rods. However, in practice, the cone will continue to move very slightly as the elastic strain energy in the rods causes the soil in front of the cone and around the rods to be displaced. The longer the cone rods or the deeper the penetration, the greater the tendency for the soil to creep, and the more significant this movement may be. This movement relaxes the total stresses in the soil around the conical tip and can influence the measured decay of pore pressure with time. It has been shown (Campanella et al. 1983) that this effect is only significant with the U1 element on the face of the cone tip (see Figure 3-5). It is standard procedure to completely release the load on the rod during pore pressure dissipation measurements for all piezometer locations.

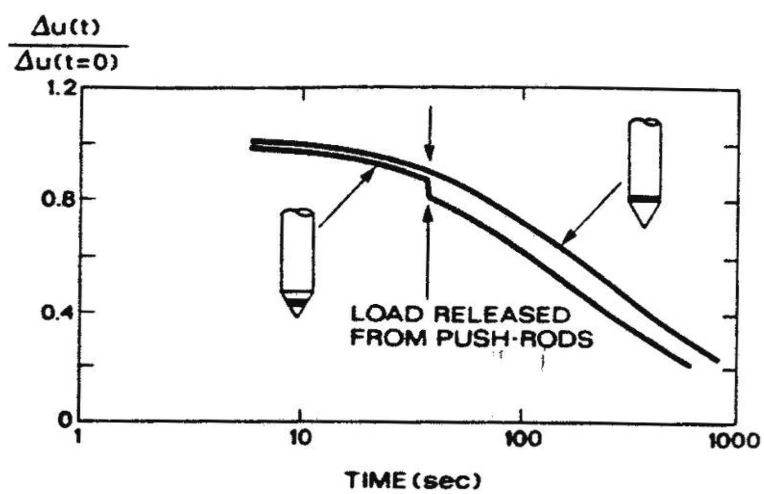

Figure 3-5 Effect of Load Release on Dissipation Response

Sometimes a fixed period of dissipation for all soil layers is used and sometimes dissipation is continued to a predetermined percentage of the initial excess pore pressure; for example, **50% or t_{50}.** It is desirable to obtain the **t_{50}** time at each rod break or every metre in depth, if possible.

Even in clayey soils, it only takes about 10 minutes to achieve t_{50} or a value that can be extrapolated to t_{50} using a square root time plot (see 6.2.1.5). Whenever the dissipation is rapid, as in sandy soils, it is valuable to obtain full dissipation and record the equilibrium pore pressure to evaluate the groundwater table.

3.3 Maintenance Requirements for Quality Assurance

The cone and friction sleeve should be checked for obvious damage or wear at the start of each sounding. Frequent checks should be made to ensure that the cone dimensions do not exceed the tolerances set out in various standards and guidelines (e.g. ASTM standards and the International Reference Test Procedures for CPT by ISSMGE.)

Before each test, the seals between different elements should be cleaned and inspected to ensure their integrity. After each sounding, it is good procedure to clean and inspect the cone and seals. Soil should be removed from all seals and the cone cleaned before and after each sounding.

Zero-load errors and calibration errors tend to change during testing. The zero load error should be checked by observing the zero-load output (or baselines) ***before*** and ***after*** each sounding, and recording the values on the data output.

The load measurement systems should be calibrated at intervals not exceeding three months, and more frequently when the equipment is in use continuously, and after every overhaul or repair. A one point calibration check is easily done in the field with a load cell and a hand operated hydraulic jack and frame.

To avoid disturbed ground, a CPT sounding should not be performed within a distance from a borehole less than 25 times the borehole diameter, or within one metre (3 feet) of a previously performed CPT.

3.3.1 Checks and Recalibration

Table 3-1 presents a suggested summary of maintenance requirements (checks and recalibrations). This summary can be used as a basis for setting up an ongoing maintenance program and check-list of procedures which should be established in conjunction with the manufacturer's Operator's Manual in order to maintain a high quality of cone data.

Item	Ref. to Section	FREQUENCY			
		At Start of CPTU Program*	At Start of CPTU Sounding	At End of CPTU Sounding	At 3-monthly Intervals
Verticality of thrust machine	2.2.2 3.2.3		■		
Straightness of push rods	4.1.5		■		■
Precision of measurements	3.1.2	■			■
Zero load error (taking baselines)	3.1.2 3.2.3 4.1.4		■	■	
Wear:					
- dimensions of cone, friction sleeve	3.1.2	■			■
roughness		■			■
Seals:					
- presence of soil particles	3.1.3	■	■		
- quality	3.3	■	■		
Calibration:					
- load cells and pressure transducers	3.1.2 3.1.3	■			■
- unequal end area	4.1.1				■
- temperature	2.2.1 4.1.3				■
* And regularly during a long testing program.					

Table 3-1 Summary of Checks and Recalibrations for CPT and CPTU Soundings

4 DATA PROCESSING

4.1 Factors Affecting CPTU Measurements

Because of the wide variety in cone designs, it is not possible within the scope of this manual to discuss in detail all the factors that affect the measured results. However, several significant aspects that pertain to almost all cone designs will be discussed. These include unequal end area effects, pore pressure response related to filter location, soil type and stress history. The reader is encouraged to investigate the details of the particular cone design being used before performing detailed interpretation of the data.

4.1.1 Unequal area effects

Water pressures can act on the exposed surfaces behind the cone tip and on the ends of the friction sleeve (see Figure 4-1). These water forces result in measured tip resistance (q_c) and sleeve friction (f_s) values that do not represent true total stress resistances of the soil. This error introduced in the measurement can be overcome by correcting the measured q_c for unequal pore pressure effects using the following relationship (Baligh et al. 1981; Campanella et al. 1982):

$$q_t = q_c + u(1 - a) \tag{4.1}$$

where:

q_t = corrected total tip resistance
u = pore pressure generated immediately behind the cone tip
a = net area ratio = A_N/A_T (see Figure 4-1)

Figure 4-1 shows the concept of net area ratio but this value must be determined from air chamber calibration (Figure 3-2) and cannot be measured reliably with callipers because of O-ring effects.

An example of the determination of the net area ratio using the output of a simple calibration vessel is shown in Figure 4-2. The calibration vessel is designed to contain the cone and to apply an all around air or water pressure with the valve open (Figure 3-2). When precision air pressures are applied, all cone channels should be recorded: tip, friction, pore pressure, etc. In this way, the pressure transducer will get calibrated, the “a” factor will be determined for the tip and the friction sleeve correction may be evaluated.

Many cones have values of net area ratio ranging from 0.90 to 0.60, but sometimes this ratio may be as low as 0.38 (see Figure 4-2). This correction for bearing area cannot be eliminated except with a unitized, jointless cone design.

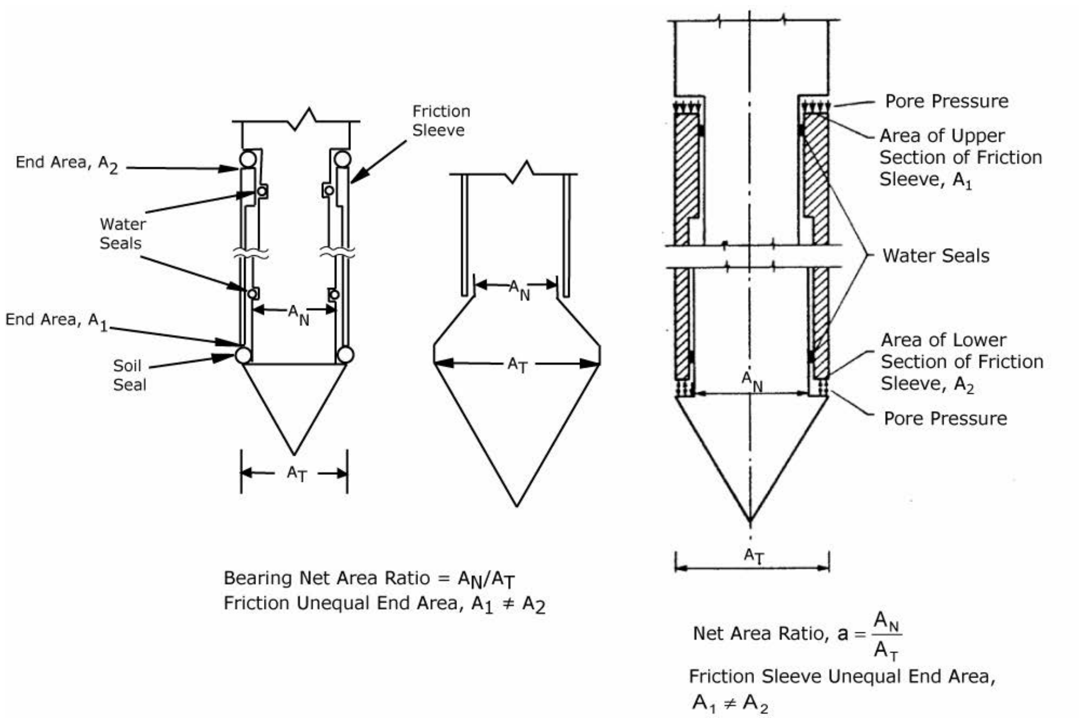

Figure 4-1 Influence of Unequal End Areas (After Campanella et al. 1982)

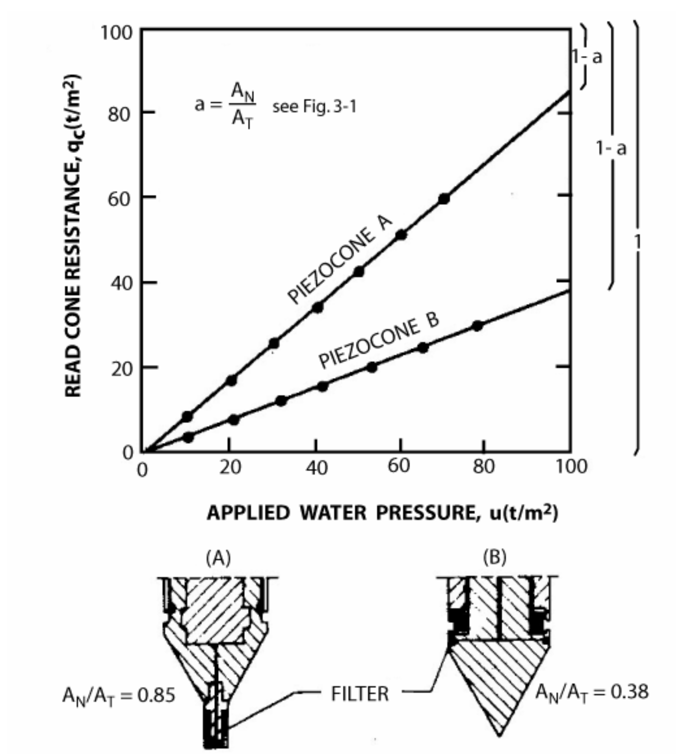

Figure 4-2 Determination of A_N/A_T for Two Types of CPTU Probes (After Battaglio and Maniscalco 1983)

This correction is especially significant in soft clays, where high-values of pore pressure and low cone resistance may lead to the physically incorrect situation of $u > q_c$. The use of an enlarged tip as shown in Figure 4-1 to increase sensitivity in very soft soils is not recommended because of the requirement for very large pore pressure corrections.

It should be noted that earlier correlations developed to obtain soil properties, such as undrained shear strength, s_u, from q_c measurements incorporated systematic errors, depending on cone design.

A similar correction is required for sleeve friction data. However, information is required of the pore pressures at both ends of the friction sleeve and it is usually assumed that the pore pressures are the same and equal to U_2. The importance of the sleeve friction correction can be significantly reduced and essentially eliminated using a cone design with an equal end area friction sleeve (see Figure 3-3, which shows such a design).

Several cone operators and researchers who use cones that record the pore pressure on the face of the cone tip have suggested correction factors to convert the measured pore pressures on the face to those that are assumed to exist immediately behind the tip. The assumed ratio of the pore pressure on the face to the pore pressure behind the tip is generally taken to be about 1.2 (i.e., the pore pressure on the face is assumed to be 20% larger than that immediately behind the tip). Measurements (Campanella et al. 1985; Jamiolkowski et al. 1985; Lunne et al. 1986) have shown that the ratio of 1.2 is generally only true for soft, normally consolidated clays. In stiff, overconsolidated, cemented or sensitive clays, the pore pressure on the face of the tip can be many times larger than that immediately behind the tip. Therefore, to correct the cone tip stress to q_t, the pore pressure ***must*** be measured behind the tip.

Soil ingress may change the net area ratios somewhat during field testing. Also, the distribution of pore pressure around the cone varies such that a simple net area ratio is not always correct, especially for a bulbous cone. But these problems tend to be rather minor since the corrections are usually most important in soft cohesive soils where the variation in pore pressures around the cone are generally small. The potential error due to these problems is significantly less than the error if no correction is applied.

A detailed discussion regarding cone design is given by Lunne et al. (1997).

4.1.2 Piezometer location, size, type and saturation

The measured pore pressures during piezometer cone testing (CPTU) depend very much on the piezometer element location (Campanella et al. 1982; Tavenas et al. 1982). In normally consolidated soft clays and silts, pore pressures measured on the face of the tip are generally 10-20 percent larger than those measured immediately behind the tip. In over-consolidated clays and silts and fine sands, pore pressures on the face of the tip tend to be large and positive whereas pore pressures measured immediately behind the tip may be considerably smaller and possibly negative.

The choice of pore pressure element location is very important with regard to data interpretation. The main locations currently used for measuring pore pressures are,

1) on the cone face, U_1
2) immediately behind the cone tip, U_2 (standard location) and
3) immediately behind the friction sleeve, U_3.

Figure 4-3 shows pore pressure profiles for U_1, U_2 and U_3 in a moderately sensitive normally consolidated clayey silt along with the equilibrium pore pressure, u_o. The penetration pore pressures are a result of changes in normal stress and shear strains. The U_1 values are dominated by the high normal stresses on the face, which are released at the shoulder. U_2 and U_3 values are mainly the response to shear strains or remoulding.

Data collected at several different sites with the pore pressure element located behind the tip and on the face of the tip is shown in Figure 4-4. Values of the ratio of measured to equilibrium pore pressure, u/u_o, are plotted against location along the cone. In normally consolidated insensitive clays and silts, pore pressures measured on the face are often approximately *three times larger than the equilibrium pore pressure (u_o)* and about 20% larger than pore pressures measured immediately behind the tip. As the overconsolidation ratio increases in clays and silts, the pore pressure on the face increases. This is due to the increased cone tip stress, which causes larger normal stresses on the face in overconsolidated soils. Also, overconsolidated soils tend to dilate or increase in volume when sheared which causes a decrease in pore pressure at U_2. In heavily over consolidated clays, like the London clay in Figure 4-4, U_2 values go below u_o and even negative. The apparent very high OCR for the Taranto clay is due to cementation and the high shear strains at U_2 and U_3 cause a collapse of soil structure and high pore pressures compared to the London clay.

The lower part of Figure 4-4 shows more granular soils. A fully drained soil like a coarse sand generates pore pressures equal to the equilibrium value. A silty fine sand is partially drained and will generate high face values (very large if a very dense sand as shown) and negative values behind the face because of the dilatancy of sands. It is of interest that while the loose and compact silt have similar face values, U_1, the U_2 values are very different and relate to the differing volume change characteristics of the two materials.

The penetration pore pressure during a CPTU sounding is complex and relates to location, soil type, stress history and structural properties. A convincing argument can be made to standardize the location behind the tip to provide a wide range of applications, yet maintain a practical location for protection and ease of saturation. The U_3 location is probably the best since it is away from the tip with the high pore pressure gradients around the shoulder and more closely represents a cylindrical boundary for analysis purposes. Unfortunately, the saturation procedures for the U_3 location are quite involved, making it less desirable for contractors and commercial applications. Hence, U_2 has been accepted as the STANDARD location and U_3 tends to be more valuable to researchers at the present. The face location, U_1, generally provides more useful information for overconsolidated soils.

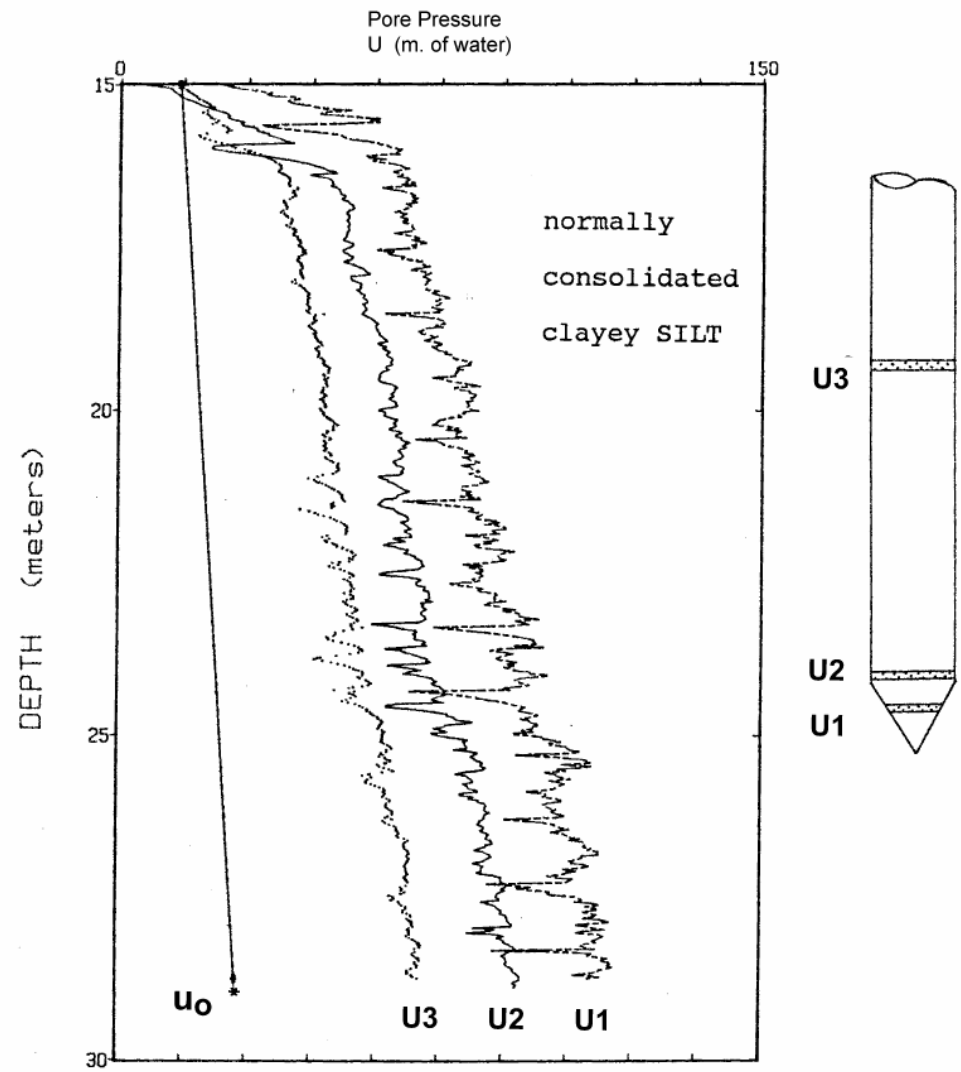

Figure 4-3 Measured U_1, U_2 and U_3 pore pressures in a Normally Consolidated Silt (McDonald Farm, Vancouver)

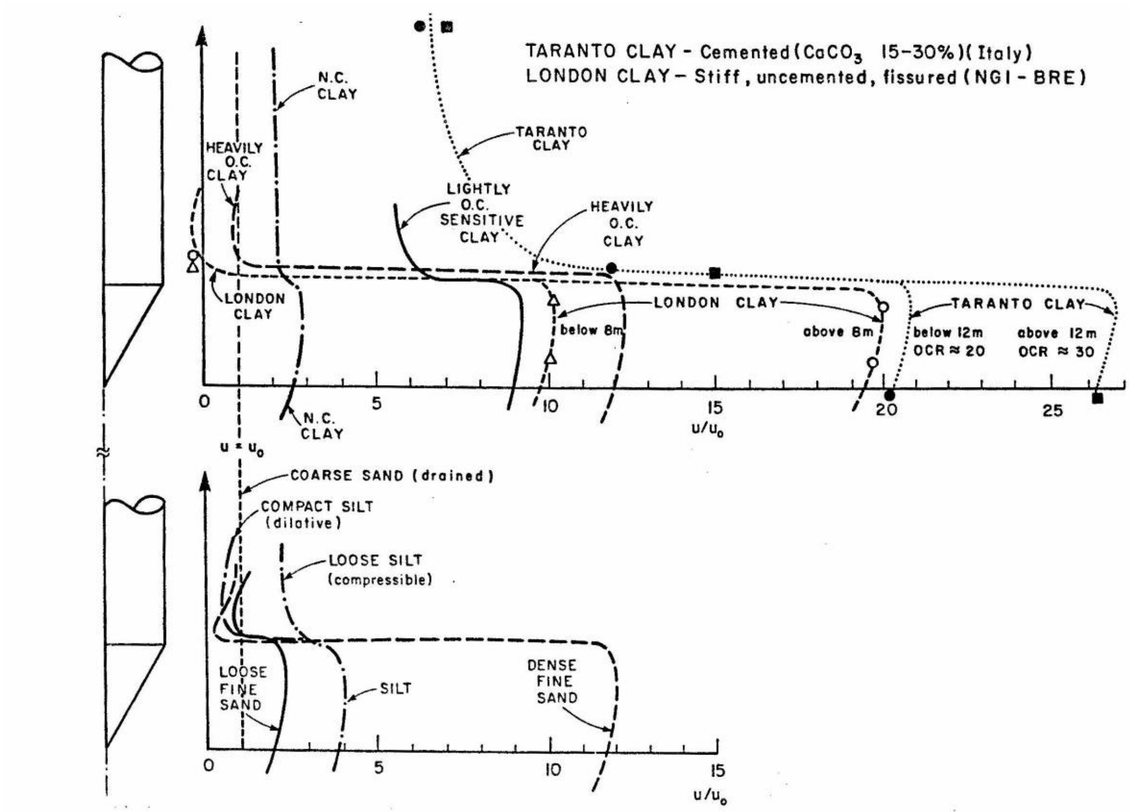

Figure 4-4 Conceptual Pore Pressure Distribution in Saturated Soil During CPT Based on Field Measurements (After Robertson et al. 1986a)

The following is a list of advantages of having the pore pressure element located immediately behind the cone tip at U_2:

1) Porous element is much less subject to damage and abrasion;
2) Measurements are less influenced by element compressibility;
3) Position is appropriate for correction due to unequal end areas;
4) Good stratigraphic detail is still possible.

In general, no single location can provide information for all applications of pore pressure interpretation. It is recommended that the overall cone design should be such that the porous element location can be changed in the field to allow soundings to be carried out at either the U_2 or, on occasion, the U_1 location to obtain specific pore pressure data. Alternatively, a cone could be used with piezometer elements both in the tip and behind the friction sleeve. However, saturation of the piezometer element behind the tip can become difficult unless the cone is designed carefully. All pore pressure measurements from cone testing must clearly identify the location and size of the sensing element.

The size of the porous element also influences the measured pore pressures, although little data is available to quantify the importance of this factor. If a porous element is located immediately at the shoulder of the cone tip, it is prone to damage and wear and is in an area of large stress gradients.

It has been observed that for thin pore pressure elements located immediately behind the tip, very small pore pressures (less than u_o) have been recorded. These pore pressures have often been smaller than those recorded with thicker elements located in the same position (see Figure 4-5) and this is due to the very high gradient of pore pressure around the shoulder. For this reason, the standard location for the U_2 pore pressure element is 2.5 mm behind the corner of the shoulder and the element should be 5 mm thick. It is believed that thin pore pressure elements can sometimes measure low pore pressures due to a shadow effect from a cone tip of slightly larger diameter. Thus, the O.D. of the cone tip should be identical or less than the O.D. of the porous element and friction sleeve by about 0.25 mm.

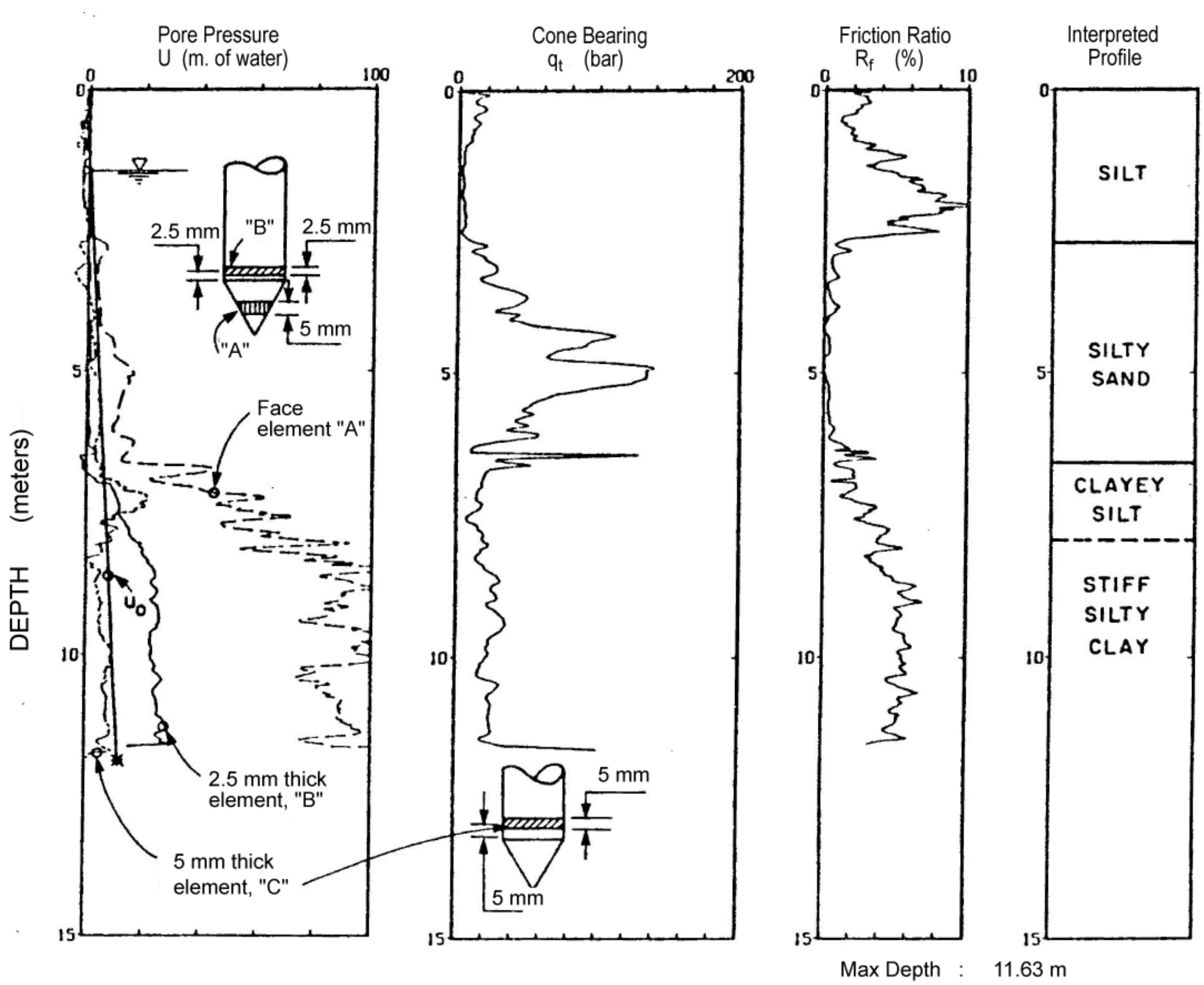

Figure 4-5 U_1 and U_2 Pore Pressure Response in an Overconsolidated Clay

Complete saturation of the piezometer element in CPTU is essential. Pore pressure response can be inaccurate and sluggish for poorly saturated piezocone systems. Both maximum pore pressures and dissipation times can be seriously affected by air entrapment. Response to penetration pore pressures can be significantly affected by entrapped air within the sensing element, especially in soft, low permeability soils.

Saturation of the piezometer element and cavity are especially important for shallow onshore soundings where equilibrium water pressure is small. Once significant penetration below the water table has been achieved, the resulting equilibrium water pressure is often sufficient to ensure saturation.

4.1.3 Temperature effects

The load cells and pressure transducers within the cone are often temperature sensitive and are almost always calibrated at room or air temperature. However, soil and groundwater are often considerably cooler than the calibration temperature and a shift in the zero can occur for both load cells and pressure transducers during penetration. For cone testing in dry sand, considerable heat can be generated during penetration. These changes in temperature have little consequence for cone testing in sand where measurements are usually large. However, the zero shift can be significant in very soft or loose soils. A zero shift due to temperature can make friction measurements very unreliable especially with subtraction type cones where the zero shift may be different for each load cell. Good temperature compensation can limit the variation to about 0.05% of full scale output over the normal expected temperature range.

Cones that use amplifiers within the cone can also suffer temperature shifts if the amplifiers are not temperature compensated. If the temperature of the cones is continuously monitored and temperature zero shift calibrations obtained, it is possible to correct all data as a function of temperature. These corrections are easily accommodated in a computer based acquisition system.

If temperature is not monitored, an alternate procedure is to allow the cone to reach equilibrium with the groundwater temperature before taking the initial zero readings (before penetration). Zero load readings should also be taken immediately after completion of penetration.

A temperature calibration should be performed on new cones. The cone should be connected to the data acquisition system as if to perform a full test. Base lines should be taken and the cone should be plunged into a deep bucket of ice water at about zero degrees Celsius. Periodic readings of all cone channels and the water temperature should be taken as the water warms to room temperature. Then warm water should be added to slowly increase the temperature up to usual maximum values. The zero readings versus temperature should be plotted for each channel and the average shift per degree temperature change should be determined. The results of this procedure should be kept for each cone.

4.1.4 Negative Friction Sleeve Measurements

Since it is physically not possible for the friction sleeve stress to be negative, measurements of negative friction are due to inaccuracies or errors caused by one or more of the following:

Negative zero load offset resulting from a temperature change

Side loading against the friction sleeve

Unequal end area of friction sleeve in soils with very high pore water pressure

1) Lack of accuracy of the load cell at very small readings (less than 0.05%).

Negative zero load offset due to a temperature change is most often the cause of negative frictions. Such temperature effects are dominant because of the very small value of friction but can be corrected if the temperature is monitored and the procedures given in Section 4.1.3 are followed.

Side loading against the friction sleeve can cause negative readings and this effect can be reduced with eight strain gauges placed symmetrically around the load cell to cancel out or reduce side load effects as is done in Hogentogler's current designs.

Unequal end area effects can be reduced and essentially eliminated with the modern designs which have equal end area friction sleeves.

Lack of accuracy is always a problem since a very small reading can either be plus or negative and these are often accompanied by very small bearing values. This gives rise to rather large 'negative' values of friction ratio which would go unnoticed if they were positive.

When negative friction values appear, it is important to isolate the cause and adjust your procedures. Negative frictions are rarely associated with tests in sands but often occur in very low tip stress clays, which generate high pore pressures. Data files containing negative frictions should be edited and adjusted after the cause is identified. If the measured zero base line after withdrawal shows a zero shift in friction then all readings should be adjusted by that amount.

Remember there is little engineering difference between a very small negative or very small positive friction value except that the negative value is very evident especially when plotted. The essential feature to realize is not the "negative" value but the "very small value" of friction, which is often less than the accuracy of the instrument. Modern cone designs and test procedures can virtually eliminate the occurrence of apparent negative friction sleeve measurements.

4.1.5 Inclination

Most electronic cones today have simple slope sensors incorporated in the design to enable a measure of the non-verticality of the sounding. This is particularly useful for very deep soundings where eventual tip inclinations in excess of 45° are not uncommon, especially in stratified soil. The maximum depth for which a slope sensor can be omitted depends on the acceptable error in recorded depth provided obstructions do not exist. However, for most CPT work the maximum depth without a slope sensor, for which negligible error in recorded depth can be assumed, is about 15 m (van de Graaf and Jekel 1982).

Deflection of soundings is also caused by bent cone rods and not establishing verticality at the start of the test. Straightness of cone rods is easily checked by rolling a rod on a flat surface or table or spinning the rod on one end. When setting up the pushing apparatus, check that the hydraulic rams are vertically oriented with an accurate level, which is at least 60 cm long. Before starting the initial cone push into the ground, again check the verticality of the cone rods with the level (see maintenance schedule, 3.3.1).

Experience suggests that once a cone tip is deflected, it continues along a path with a relatively consistent radius of curvature. The standard equipment tends to accept about 1° of deflection per metre length without noticeable damage. A sudden deflection in excess of 5° over one metre or less may cause damage to the cone and rods from bending, and penetration should be ceased. A maximum deflection of 12° is reason to abort a test, change location and try again.

4.1.6 Friction- tip resistance offset

The centre of the friction sleeve is approximately 10 cm (4 inches) behind the cone tip. To calculate the friction ratio (R_f), the average friction resistance (f_s) and tip resistance (q_c) are compared at the same depth. This usually involves an offset of the friction resistance by the physical distance of 10 cm (4 inches) from the apex of the tip which is taken as the reference depth of the sounding. However, the tip resistance is affected by the soil ahead of the tip, whereas the friction measurement is only affected by the soil in direct contact with the friction sleeve. Thus, the standard offset distance of 10 cm (4 inches) may not always produce realistic friction ratio plots, especially in heavily interbedded soils and in relatively stiff soils where the offset can be more than 10 cm. In general, however, the standard practice of a 10 cm friction-bearing offset usually provides adequate friction ratio plots.

4.2 Evaluation of CPTU Data

Before any data are plotted, they must first be reviewed in detail in a text editor or spread sheet program. The original data must first be duplicated and archived before any editing takes place. The data columns must be reviewed for abnormalities and corrected. This usually involves the first metre or so where preboring and backfilling with sand may have occurred, such as in locations over existing pavements or in fill areas. If the cone is lowered through an open or backfilled hole, it is convenient to give the tip stresses a value of 0.01 bar or 1 kPa and the friction stress of zero or 0.00 until native soil is reached. In the natural soil, it is important to identify and adjust any negative friction stress. The tip stress can never have a value of zero as that will lead to a value of infinity for friction ratio, which computers will not accept. Values at rod breaks should also be checked as it is not uncommon for a depth reading to be mis-recorded at these start-up points. The last few readings may also need checking. The final thing to do is to check that the recorded depth agrees with the measured depth from the rod count, since rods are precisely 1000 mm long.

In stiff soils, CPTU data are generally very reliable. However, in soft soils (q_t < 5 bar or 0.5 MPa) the cone resistance may be somewhat less reliable due to various factors (see Section 4.1). To evaluate the performance in soft soils, the zero load readings (baselines) before and after each sounding should be reviewed. The CPT data should be corrected based on the change in zero load readings. This can be important in very soft deposits where temperature variations can cause zero load readings to change significantly in relation to the measured values.

The pore pressure data should be reviewed to identify whether rapid response occurred in accordance with the detailed stratigraphy.

If dissipation tests have been performed, the response time and equilibrium pore pressures should be reviewed to assess the level of saturation of the piezocone system and compare groundwater table depth. For example, if the groundwater table depth keeps changing a little at each rod break, this an indication that a vertical gradient may be present and hydrostatic conditions do not exist.

4.3 Presentation of Data

The recommended graphical presentation of CPTU data should include all measured parameters as demonstrated in Figure 4-6. A useful method of data presentation is as follows (from left to right using SI units of MPa and metres in Figure 4-6):

1) Measured pore pressure, U_2 vs. depth with hydrostatic pore pressure line, u_o

2) Measured sleeve friction stress, f_s vs. depth
(where f_s = friction sleeve force divided by surface area of sleeve, 150 cm^2.)

3) Total cone resistance, q_t vs. depth
(where q_t = corrected tip force divided by bearing area of 10 cm^2)

4) Friction Ratio, $\frac{f_s}{q_t}$ x l00% vs. depth.

5) Differential Pore Pressure Ratio, $\frac{u_2 - u_o}{q_t}$ or $\frac{\Delta u}{q_t}$

6) Box for soil stratum identification as some indication of the interpreted profile is also desirable.

Details and interpretation of the above terms are given in later sections.

Figure 4-7 shows a CPTU profile in very soft organic soil in which more sensitive scales have been used to bring out the important features of the organic soil. Also, note that stress units are in bar where 1 bar = 100 kPa ~ 1 kg/cm^2 ~ 1 US Ton/ft^2. This is a very convenient unit which allows easy conversion to kilogram force system and US systems of units. The pore water pressure units used here are metres of water pressure head, which allows an easy relation to depth.

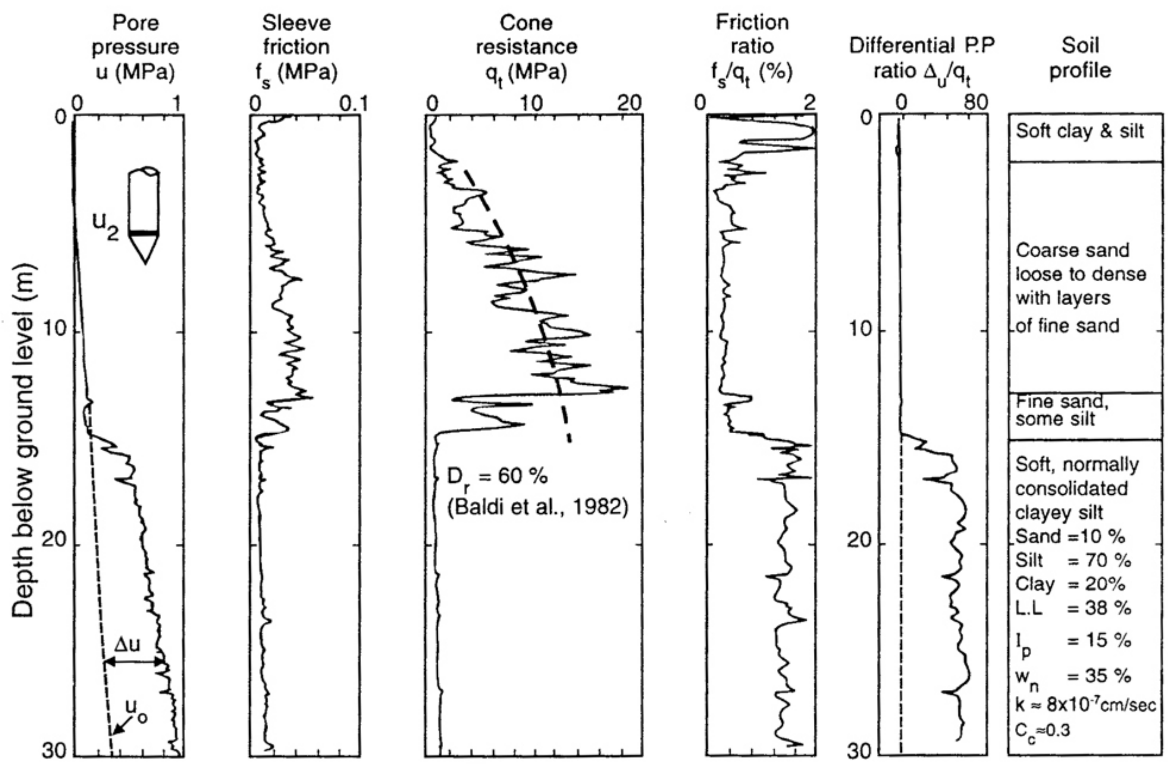

Figure 4-6 Recommended arrangements for presentation of data (Campanella and Robertson 1982)

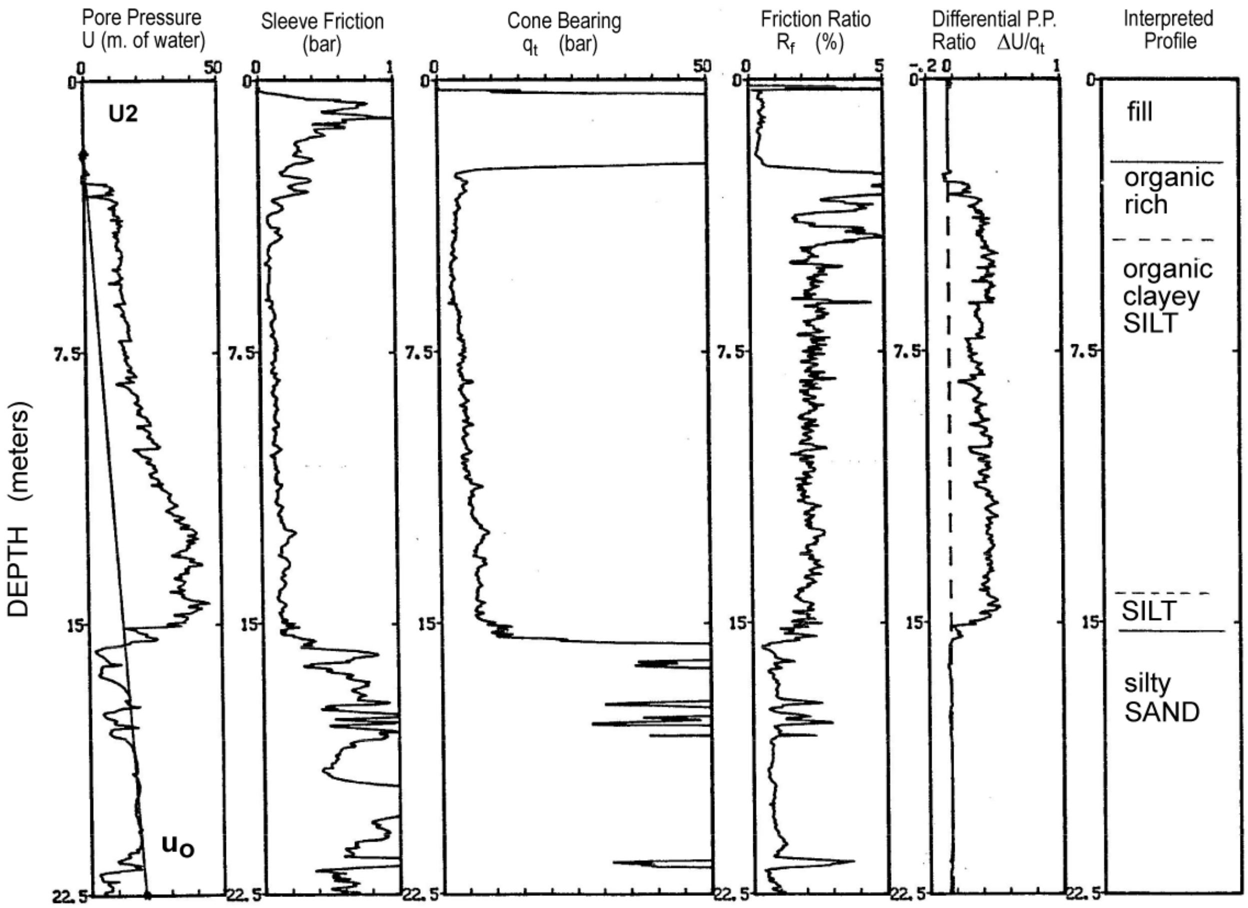

Figure 4-7 CPTU Profile at Pile Research Site, Richmond, BC with UBC preferred units (Gillespie 1990)

5 SEISMIC CONE TESTING

5.1 Introduction

The Seismic Cone was born in the early 1980's and was first tried by a seismologist at the Long Beach office of then ERTEC. The addition of a miniature seismic sensor (usually a geophone but may be an accelerometer) rigidly attached inside the barrel of a standard electronic piezocone (CPTU) is termed a seismic piezocone (SCPTU) (Campanella and Robertson, 1984, Campanella et al, 1986). The exceptional coupling between cone and soil provides a very clear and well-defined seismic trace when seismic waves pass by a cone in the ground. The seismic sensor allows the measurement of the arrival of vertically propagating waves during a pause in the usual piezocone test, thus allowing the determination of the velocity of travelling body waves. Besides the advantage of retaining all of the information available with the standard piezocone, a further attraction of downhole seismic cone test is its very much lower cost when compared with standard borehole downhole or crosshole geophysical seismic methods.

There are two types of seismic body waves and seismic sensors react to both pressure or compression waves (P waves) and shear waves (S waves). The P wave always arrives first. In soils below the ground water table, the P wave typically travels around 1500 m/s or many times faster than the S wave, so separation of the two body waves is easily seen. However, above the water table the difference is very small and separation of P and S waves may be very difficult, requiring specialized techniques (Campanella and Stewart, 1992). The most significant difference between P and S waves is that S waves are easily reversible. Therefore, using a source that is reversible can enable the identification of S waves, thus allowing the determination of the average shear wave velocity, V_s. Furthermore, a well-designed shear source minimizes the amplitude of P waves relative to S waves. Typical values of V_p and V_s to a depth of 40 m and recognizing that these values vary with overburden stress are given in Table 5-1 below.

Material	V_s (m/s)	Material	V_p (m/s)
V_s in water	0	V_p in water	1482
V_s in saturated soils	<50 - 400	V_p in saturated soils	1500 – 1900
V_s in unsaturated soils	<50 - 200	V_p in unsaturated soils	<100 – 600
V_s in lightly cemented soils	250 - 700	V_p in air	343
V_s in saturated Peat/organic soils	<15 - 50	V_p in gassy soils below GWT	800 - <1500

Table 5-1 Typical Wave Velocities in top 40 m

Using elastic theory one relates the maximum shear modulus, G_o; shear velocity, V_s; total mass density, ρ; total unit weight, γ; unit gravity, g as:

$$G_o = \rho V_s^2 = (\gamma / g) V_s^2 \tag{5.1}$$

Shear waves travel through the skeletal structure of the formation at very small strains (shear waves can not travel through the porewater in the soil). Shear modulus is a fundamental soil property, which relates shear deformation to shear loading of the skeletal structure.

As most soils are strain softening at large enough strains, shear modulus typically decreases with increasing shear strain. However, the shear modulus is almost always constant for a given soil at a given normal stress at shear strains less than 10^{-4}% and is generally referred to as the elastic or initial shear modulus, G_o at these low strains. Shear strains are less than 10^{-4}% in the seismic cone test.

5.2 Methodology

During a pause in cone penetration, usually at the time a push rod is added, a vertically propagating shear wave can be created at the surface and the measurement made of the travel time to the seismic sensor in the cone. By repeating this measurement at another depth, one can determine the interval time and so calculate the average shear wave velocity over the depth interval. A repetition of this procedure with cone advancement yields a vertical profile of vertically propagating shear wave velocity (See Figure 5-1).

5.3 Equipment

An extensive discussion of equipment, sources and receivers for the SCPTU can be found in Campanella and Stewart (1992). Only the essential aspects will be presented below.

5.3.1 Miniature seismometer

The seismometer can be either a geophone (velocity proportional to output) or accelerometer (acceleration proportional to output), which must be small enough to fit inside the cone barrel. Most commercially available seismic cones use a geophone, which typically has a natural frequency of less than 28 Hz and has a high signal to noise ratio. See Campanella and Stewart (1992) for a more detailed discussion of seismometers. The seismometer must be mounted firmly in the cone barrel with the active axis of its moving mass in the horizontal direction and the axis alignment indicated on the outside of the cone body.

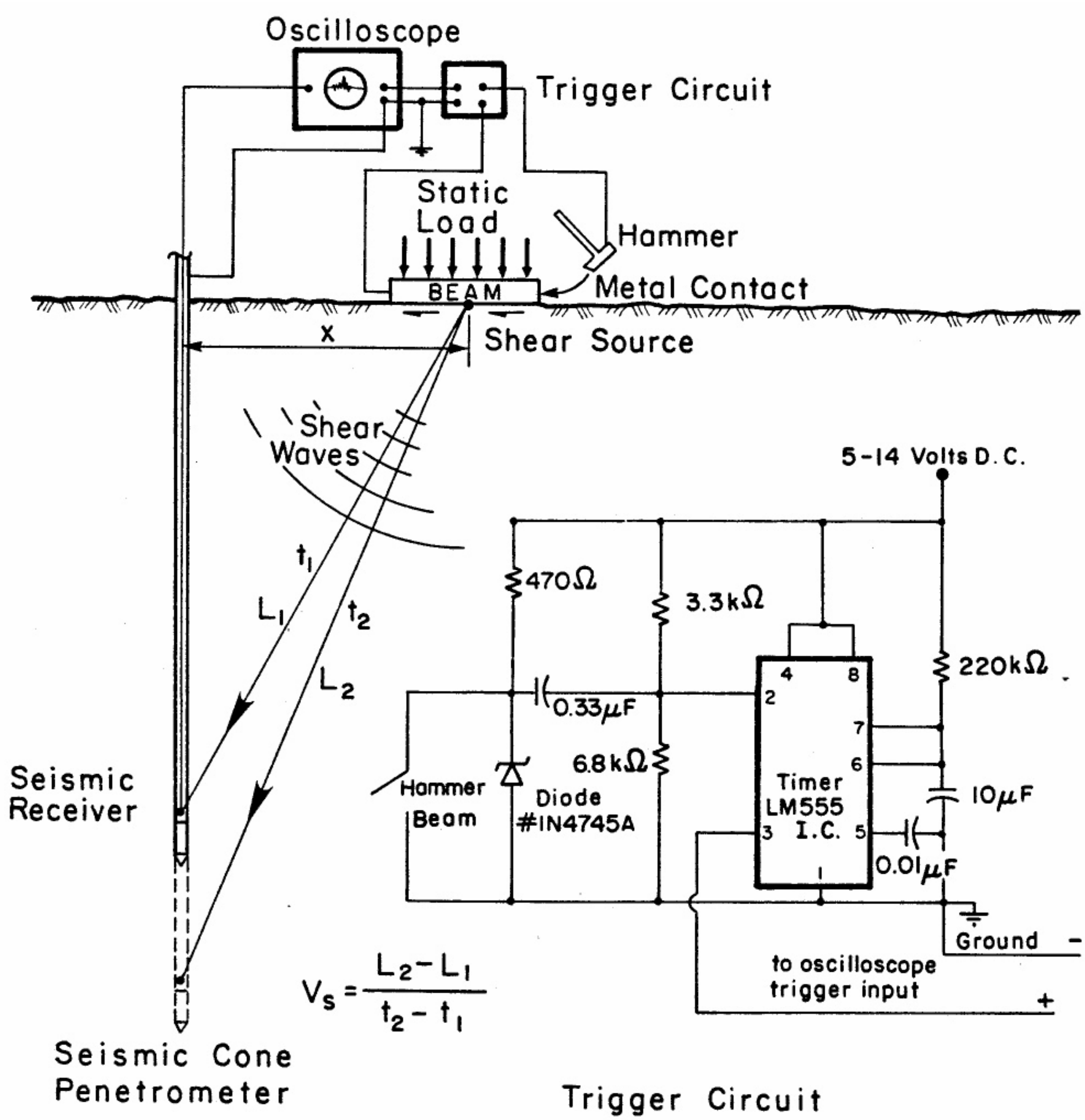

Figure 5-1 Typical Layout of Downhole SCPTU with Trigger Circuit (Campanella and Stewart 1992)

5.3.2 Shear Beam

The beam can be continuous (2.4 m long and 150 mm wide) or two shorter beams, one under each jack or wheel of the cone pushing apparatus. The beam can be steel or wood encased at the ends and bottom with a minimum 25 mm thick steel. The strike plates or anvils at the ends are welded to the bottom plate and the bottom plate should have cleats welded to it to prevent sliding when struck. The shear beam is placed on the ground and loaded by the levelling jacks of the cone pushing equipment or the axle load from vehicle wheels. The most important aspect of transmitting energy to the ground is to have the beam as heavily loaded as possible. The shear beam should not move when struck by the sledgehammer, otherwise energy is dissipated and does not travel into the ground.

5.3.3 Hammer(s)

A heavy hammer with head mass between 5 and 15 kg and a fixed axis of swing is used to strike the plate or anvil on the end of the shear beam in a direction parallel to the long axis of the shear beam and the active axis of the seismometer. Two fixed axis swing hammers, which strike each end of the beam in the specified directions, will significantly speed up the operation. A typical setup is shown in Figures 5-2 and 5-3 for a drill rig adaptation and for a cone truck, respectively. Of course, many operators just use sledgehammers swung by hand. While this method works, it adds variability to the procedure and is less efficient and is stressful for the workers.

5.3.4 Data recording equipment

The recording equipment can be a digital oscilloscope, a laptop with installed A/D board and oscilloscope software, a commercial data acquisition system such as a seismograph or a purpose built seismic cone data system. The data recording equipment must be able to record at intervals of 50 μs (microsecond) per data point or faster, to ensure high enough resolution to determine the wave velocity with adequate accuracy. The start of logging requires an automatic trigger. Commercial data recording equipment usually includes amplifiers and signal filters to help enhance recorded signals. The effect of these processes on the recorded signals must be considered before their use. For example, filtering can cause phase shift of signals and amplification is usually limited to a frequency range. In either case, the signals may not be directly comparable.

5.3.5 Trigger

A trigger device is used to start the logging of the signals received by the seismometer upon the impact of the heavy hammer on the shear beam. The trigger is required to be very fast (e.g. 10 microsecond rise time) and repeatable. A contact trigger is recommended. When the hammer hits the shear beam, the electrical contact activates the trigger circuit. A typical metal contact trigger circuit is shown in Figure 5-1, which provides a very fast rise time and has proven to be very repeatable and reliable. A seismometer mounted on the beam or the hammer may be used as a trigger provided it is fast enough, and repeatability and delay time is checked.

5.3.6 Multiple Seismometers

The use of 2 sets of seismometers set a fixed distance apart in order to obtain true interval time without the need for perfect triggering was found to be unnecessary. UBC have spent several years studying this procedure and found that pseudo interval velocities from a single seismometer always agreed with true interval velocities from a set of seismometers 1 m apart in the cone rod (Rice, 1984). This verified that the contact closure trigger (Figure 5-1) was indeed very repeatable as well as very fast and the additional complication of a second set of seismometers was not needed. The fast direct contact trigger was found to be superior to a seismic trigger.

Also, in UBC's experience it was not possible to make use of the seismic data from a vertically oriented seismometer in the cone (Laing 1985). There was always far too much noise, reflections and what looked like ringing from waves going up and down the steel rod. UBC gave up on the vertical seismometer, especially when it was realized that the horizontal seismometer also responds to P-wave arrival and can be used to get compression wave velocity in soils above the water table and to identify gassy soils below the water table.

5.3.7 Cone Orientation

Orientation of axis of strike and seismometer in the cone must remain parallel to each other for maximum signal output. It is recommended that the rods should be marked on the front face with a felt pen at the top of each rod after it is tightened. This helps the operator to be more careful and to check for rotation. If rotation should inadvertently occur, it can easily be corrected. The rod can be incrementally turned (using a wrench), shear beam hit and amplitude noted until a maximum amplitude is obtained.

It has been observed that axis rotation within plus and minus 45 degrees gives signals of acceptable amplitude, but greater rotation causes rapid decreases in signal until there is no signal at 90 degrees. This means that installing two orthogonal horizontal seismometers within the cone will always provide acceptable signals regardless of rotational position. Of course, the use of two seismometers is initially more costly and requires more time to run the test and to process the data. Therefore, it is not recommended unless maintaining orientation is a major difficulty for a given project.

Figure 5-2 Seismic Swing Hammer Shear Wave Source adapted to Mobile Drill Rig

Figure 5-3 Seismic Swing Hammer Shear Source on a Cone Truck

5.4 Test Procedure

The seismic cone is advanced at 2 cm/s as a fully operative cone penetrometer and is stopped (typically at a rod break or at 1 m intervals) to record pore pressure dissipation. At this time, the seismic procedure is also carried out and the depth to the seismometer and horizontal offset distance, x, from cone to the centre of the shear beam are recorded. Typically, this procedure is carried out at depths greater than about 2-3 m in order to minimize the interference of surface wave affects.

The procedure begins when the trigger is armed and the hammer strikes the shear beam activating the time-based recording of self-generated voltage from the geophone, which is displayed on the recording equipment. For quality assurance, it is recommended that the trigger be reset and the procedure repeated until a consistent and reproducible trace is obtained. The voltage-time traces should lie one over the other. If this is not the case, the procedure should be repeated until measured responses are identical.

The trigger is reset and the shear beam is then struck by the hammer on the opposite end of the shear beam on the other side of vehicle. This will cause initial particle motion in the opposite direction and create a mirror image to the one from the opposite side, as shown in Figure 5-4. The procedure is again repeated until identical traces are obtained.

The above procedure is carried out typically at each 1 m depth or where the seismic test is required.

5.5 Analysis

The seismic traces at a given depth are plotted together, the shear wave is identified (usually clearly seen as a mirror image in time) and an arrival time is picked.

With reversed image traces, the first major cross-over can be taken as the “reference” arrival as shown in Figure 5-4, or one trace may be used and an arrival pick made visually by an experienced operator. Alternatively, a cross-correlation procedure may be used to find the interval travel time using the wave traces from strikes on the same side at successive depths as shown in Figure 5-5 (Campanella and Stewart 1992). This technique is more involved, but eliminates the arbitrary visual pick of arrival time and is necessary if symmetry of reverse wave traces is lacking.

As depth increases, the signal to noise ratio decreases. At large depths, it may be necessary to increase the signal/noise ratio (depending on the amplification, resolution and accuracy of the data recording equipment). Using multiple hits of source events (from 4 to 10) and either averaging or adding the measured signals will reduce most of the random noise and increase the signal/noise ratio.

The average downhole shear wave velocity is calculated over the depth interval between arrival time measurements. The calculation of the average shear wave velocity over the given depth interval in units of m/s is given by the straight ray path equation:

$$V_s = \frac{L_2 - L_1}{t_2 - t_1} \tag{5.2}$$

where:

L_2 = calculated length, m of the straight travel path distance from source to receiver at greater depth (use horizontal offset, x, and vertical depth).

L_1 = calculated length, m of the straight travel path distance from source to receiver at shallower depth.

t_2 = shear wave “reference” travel time, s, from source to receiver at greater depth.

t_1 = shear wave “reference” travel time, s, from source to receiver at shallower depth.

$t_2 - t_1$ = interval travel time.

The data are easily recorded and V_s tabulated in a spreadsheet. The V_s values are plotted as a step graph versus depth to indicate that V_s is an average value over the depth interval.

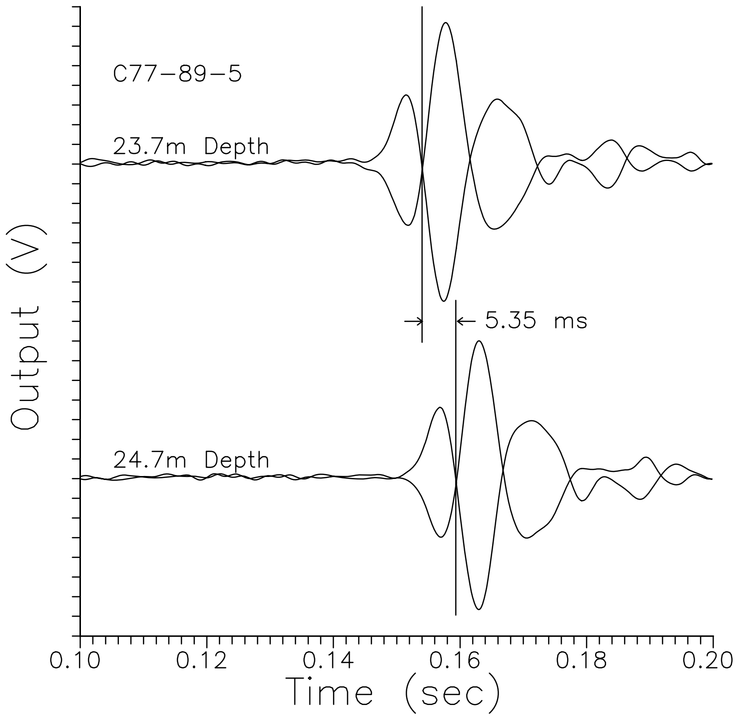

Figure 5-4 Cross-over method for time interval (Campanella and Stewart 1992)

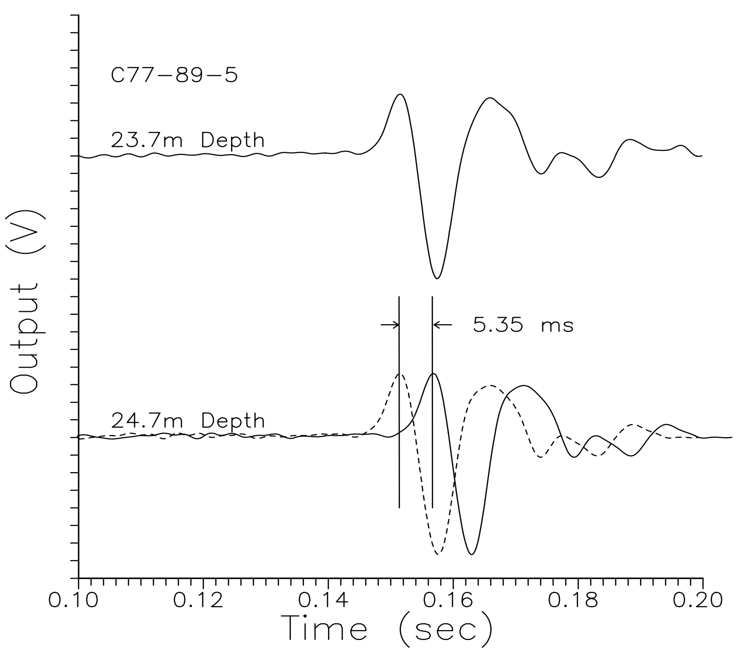

Figure 5-5 Cross-correlation method for time interval (Campanella and Stewart 1992)

5.6 Buffalo Gun – An Alternate Shear Source

The Buffalo gun was developed by the Geologic Survey Canada (Pullan and MacAulay 1987) as an inexpensive and simple way to generate a point P-source as opposed to using seismic caps. A sketch of the design is shown in Figure 5-6. The tool is made up of 19 mm (¾ inch) iron pipe pieces and is easily assembled. Also required is a 25 mm (1 inch) wood coring drill bit, which is welded to the extension rod of a posthole hand auger. This hand auger drill works nicely to make holes up to 1 metre deep. The steel drop rod should be covered with plastic shrink-wrap tubing to just fit and slide inside the pipe. The drop rod is machined with a point to work as a firing pin and an electrical wire is attached to the other end for connection to one side of the trigger circuit. The other side of the trigger wire can be attached anywhere on the gun handle. A flange plate is also needed to slide on the pipe to cover the hole when the gun is fired.

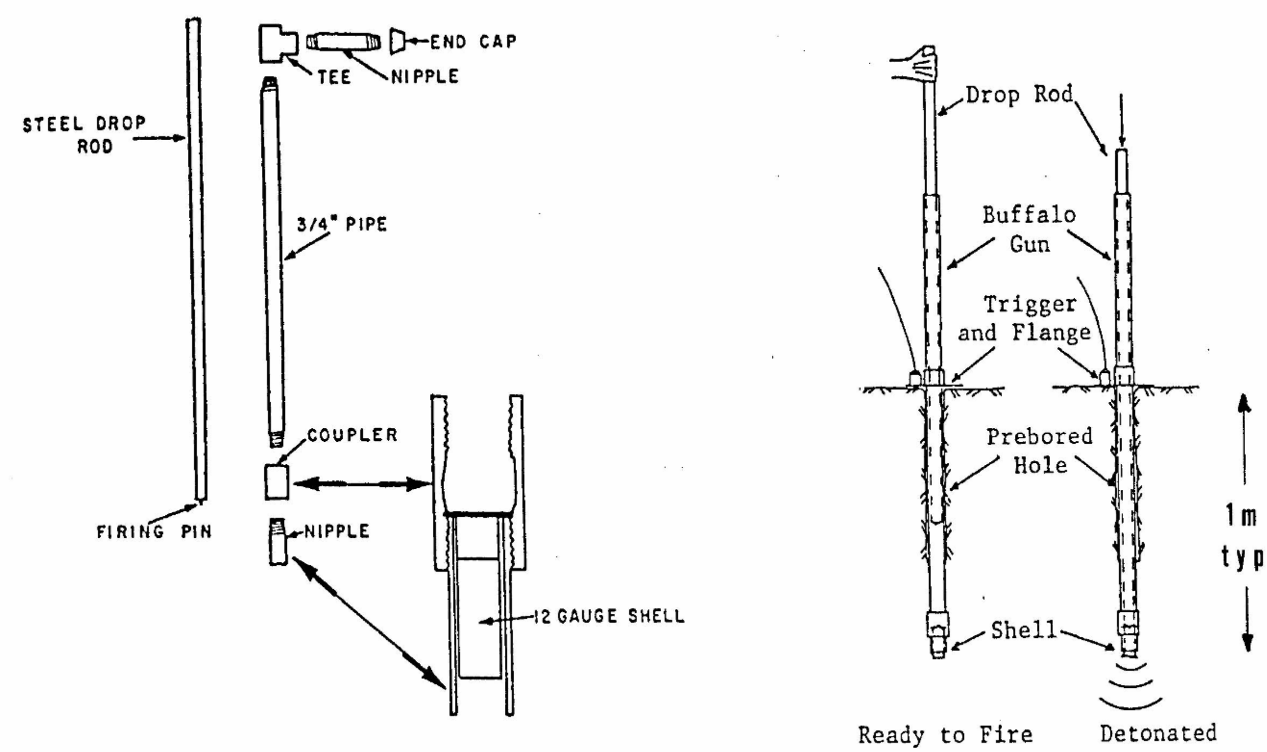

a) Schematic of Buffalo Gun (from Pullan and MacAulay, 1984)

b) Operation of Buffalo Gun

Figure 5-6 Buffalo Gun Design and Operation (Gillespie 1990)

To deploy the Buffalo gun, a hole should be drilled about ¾ m deep and should be filled with water, which acts to enhance the transmission of energy to the soil when the gun is fired. UBC uses a 12-gauge magnum shell with BB shot. The shell is attached using the coupling to hold it in place. The gun barrel is inserted into the water-charged hole and the cover flange is clamped in place. The drop rod is lowered halfway down the barrel, the trigger is armed and the rod is dropped to fire the shell. The shell fires with a soft thud sound. The operator should keep a foot on the flange plate to contain any water back splash and any recoil, if any. The hole can be reused from 4-10 times, depending how large the bulb gets at the bottom of the hole.

Typical traces from an accelerometer sensor in the SCPTU are shown as Figure 5-7. Note how clearly both the P-wave and S-wave show up in this saturated soil. With the use of a cross-correlation procedure both the P-wave and S-wave profile can be determined. You would have to window a cycle of the P-wave and zero out the rest of the trace on both sides of the window before performing a cross-correlation. To analyze the S-waves, the windowing procedure should be repeated a second time with the S-waves.

Comparisons of S-wave velocity profiles for Buffalo gun and shear beam (hitting both sides for the cross-over method and hitting one side for cross-correlation methods) yields essentially the same results (Campanella and Stewart, 1992).

5.7 Conclusion

The capability of the CPTU can be enhanced by the inclusion of seismic sensors just above the cone. These are used to determine arrival times of body waves that can be interpreted to give shear and compression wave velocities, V_s and V_p, of the soil. Reliable measurements require careful selection of equipment, close control of the test procedure and careful analysis of the results. Examples of the use of V_s in cone interpretation are given in Chapters 7 and 9.

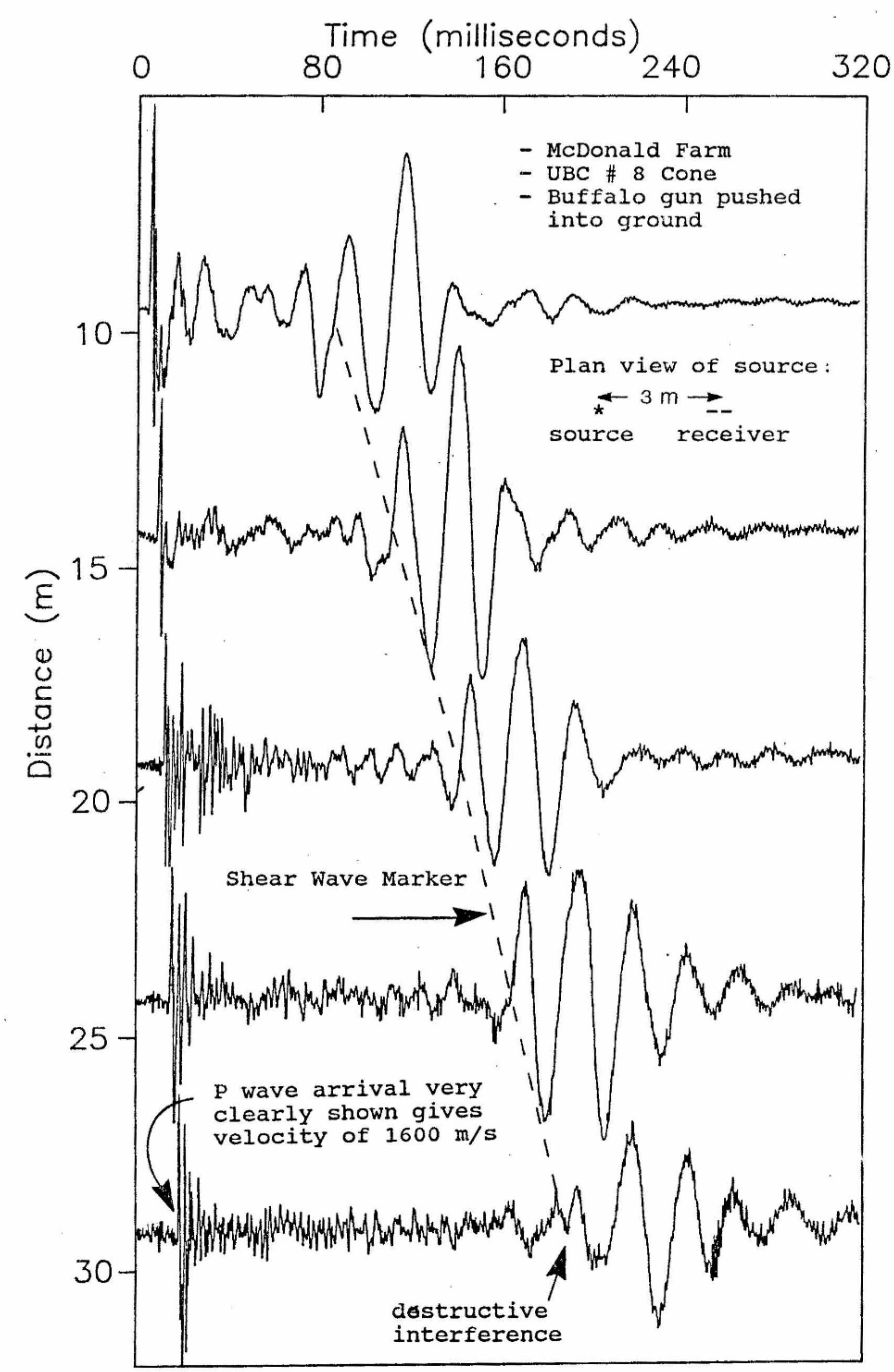

Figure 5-7 SCPTU Seismic Response Profile to Buffalo Gun Source (Gillespie 1990)

6 STRATIGRAPHIC LOGGING

6.1 Factors affecting interpretation

Before analyzing any electric cone data, it is important to realize and account for the potential errors that each element of data may contain. Significant aspects that pertain to cone designs will be discussed. The reader is encouraged to investigate the details of the particular cone design before performing detailed interpretation of the data.

The reader should also be aware of the significant ways in which soil conditions can influence the measured cone data and thus the interpretation.

6.1.1 Equipment design

Section 4.1 outlined the significant factors regarding cone design that influence the measured parameters and therefore the subsequent interpretation. The three major areas of cone design that influence interpretation are:

1) Unequal area effects
2) Piezometer location, size and saturation
3) Accuracy of measurements, especially zero stability

It is strongly recommended that cones be calibrated for all around pressure effects and q_c should always be corrected to q_t, which is usually automatically done in modern CPTU data acquisition systems. The errors associated with equipment design are usually only significant for penetration in soft, normally consolidated, fine grained soils. Test results in sand are little influenced by the above factors.

6.1.2 Soil conditions

6.1.2.1 In-situ stress

Theoretical models and calibration chamber test studies have shown that the in situ radial effective stress, σ'_r, has a dominant effect on the cone resistance, q_t, and the friction sleeve stress. Therefore, the soil's stress (geologic) history is of great importance in CPT interpretation. Unfortunately, there is often only qualitative data available concerning geologic history and the techniques for measuring in-situ radial stresses are not very well developed or reliable, especially for sands.

We know that excavation will reduce σ'_r in horizontally adjacent soils. Even an open borehole, if closer than about 25 hole diameters may significantly reduce σ'_r. Both static and vibratory roller compaction or the use of compaction (or displacement) piles can greatly increase σ'_r. Vibroflotation and dynamic compaction can also significantly increase σ'_r. The engineer must consider, at least qualitatively, such effects when evaluating CPT data for design. For example, an increase in friction ratio is often measured after in-situ densification due to an increase in σ'_r.

Subsequent sections will show that the relative density correlations for sand are significantly influenced by changes in horizontal stresses. However, the correlations of friction angle, (ϕ), appear to be much less influenced by changes in σ'_r.

6.1.2.2 Compressibility

The compressibility of sand can significantly influence q_t and f_s. Highly compressible carbonate and very angular sands tend to have much lower q_t and higher friction ratios than incompressible quartz rounded sands. Some carbonate sands have friction ratios as high as 3%, whereas, typical incompressible quartz sands have friction ratios of about 0.5%. The compressibility of sand during cone penetration is also influenced by grain crushing.

Subsequent sections will show that variations of sand compressibility have a significant influence on correlations with relative density but a smaller influence on correlations with friction angle.

6.1.2.3 Cementation and Aging

Cementation between particles reduces compressibility and increases strength, thereby increasing q_t. Cementation is always a possibility in-situ and is more likely in older soil deposits, mine tailings, carbonate sands and residual sands. Subsequent sections will show that recent correlations between sear modulus, G_o, and q_t have provided a clear means of separating soils that are uncemented from those that are cemented.

The effect of aging is very similar to cementation and each can be detected in a clay by determining the OCR. An apparent overconsolidation of the order of OCR equal to 1.1 to 1.4 is often the result of aging. Unfortunately, a slight amount of cementation due to chemical, biological or physicochemical effects would have the same effect and in fact often happens as part of the aging process.

6.1.2.4 Particle Size

When the particle size of a soil penetrated becomes a significant fraction of the cone diameter, then q_c can increase abruptly because of the decreased compressibility due to having to displace these particles as rigid units. This effect tends to produce sharp peaks in the q_t profile when encountering gravel sized particles. Intersecting very large particles can abruptly stop penetration or cause a sudden deflection. Penetration through gravelly soils often produces a distinct sound up the cone rods.

6.1.2.5 Rate of penetration

Rate effects are generally due to pore pressure effects. However, rate effects can also be caused to some extent by creep and particle crushing. In general, however, the pore pressure effects predominate and are of most interest, especially when using the piezometer cone.

The recommended constant rate of penetration for an electronic static cone sounding is 2 cm/sec. The ASTM D5778 Standard allows a penetration rate of 2-4 ft/min (10-20 mm/s) ±25%. Traditionally cone penetration in sands has been considered to be drained and penetration in clays undrained. However, for mixed soils such as silty sands to clayey silts, the drainage condition during penetration is not well defined. The drainage condition can be approximated from the soil behaviour type classification or by measuring the rate of dissipation of excess pore pressure in a CPTU test (t_{50} relates to drainage as shown in Section 6.3.4 on estimating permeability, k).

Figure 6-1 shows the effect of rate of penetration in the clayey silt at the UBC Research Site, McDonald Farm, in a soil with a k ~ 10^{-6} cm/s at a depth of 20 m. The rate had to be decreased more than 10 fold from 2 to 0.1 cm/s before there was some drainage during penetration. As the penetration rate was decreased another 10 fold, the pore pressure was less with a marked increase in friction due to an increase in effective lateral stress. However, the bearing or tip stress only increased slightly, in part because the tip stress is a total stress which also includes the pore pressure. Thus, as the pore pressure decreases it causes the measured tip resistance to decrease, but that is offset by an increase in effective stress in the soil, which causes a strength increase resulting in a tip resistance increase. The net effect is practically nil or only a slight increase in total tip stress. To illustrate this behaviour, the effective bearing is also plotted. Note that all measured values were corrected for base line temperature shift as well as pore pressure unequal end area effects. The results also suggest that for this normally consolidated clayey silt the penetration rate would have to be about 0.01 cm/s or 200 times slower than the standard 2 cm/s to obtained a drained penetration where the pore pressure equals the equilibrium value.

6.1.2.6 Soil Layer Interface and Layer Thickness

Theoretical cavity expansion models and chamber test studies have shown that the cone penetration resistance, q_c, is influenced by an interface ahead and behind the tip. The distance over which the cone tip senses an interface increases with increasing soil stiffness. Thus, the cone tip can respond fully (i.e., q_c to reach full value within the layer) in thin soft layers better than in thin stiff layers. Therefore, care should be taken when interpreting cone bearing in a thin sand layer located within a soft clay deposit.

For example, chamber studies (Schmertmann 1978; Treadwell 1975) show that the tip senses an interface between 5 to 10 cone diameters ahead and behind as depicted in the sketch of boundary effects in Figure 6-2. The distance over which the cone tip senses an interface increases with increasing soil stiffness. For interbedded deposits, the thinnest stiff layer to which the cone can respond ***fully*** (i.e. q_c to reach full value within the layer) is about 10 to 20 diameters. For the standard 10 cm² electric cone, the minimum stiff layer thickness to ensure full tip resistance is therefore between 0.35 and

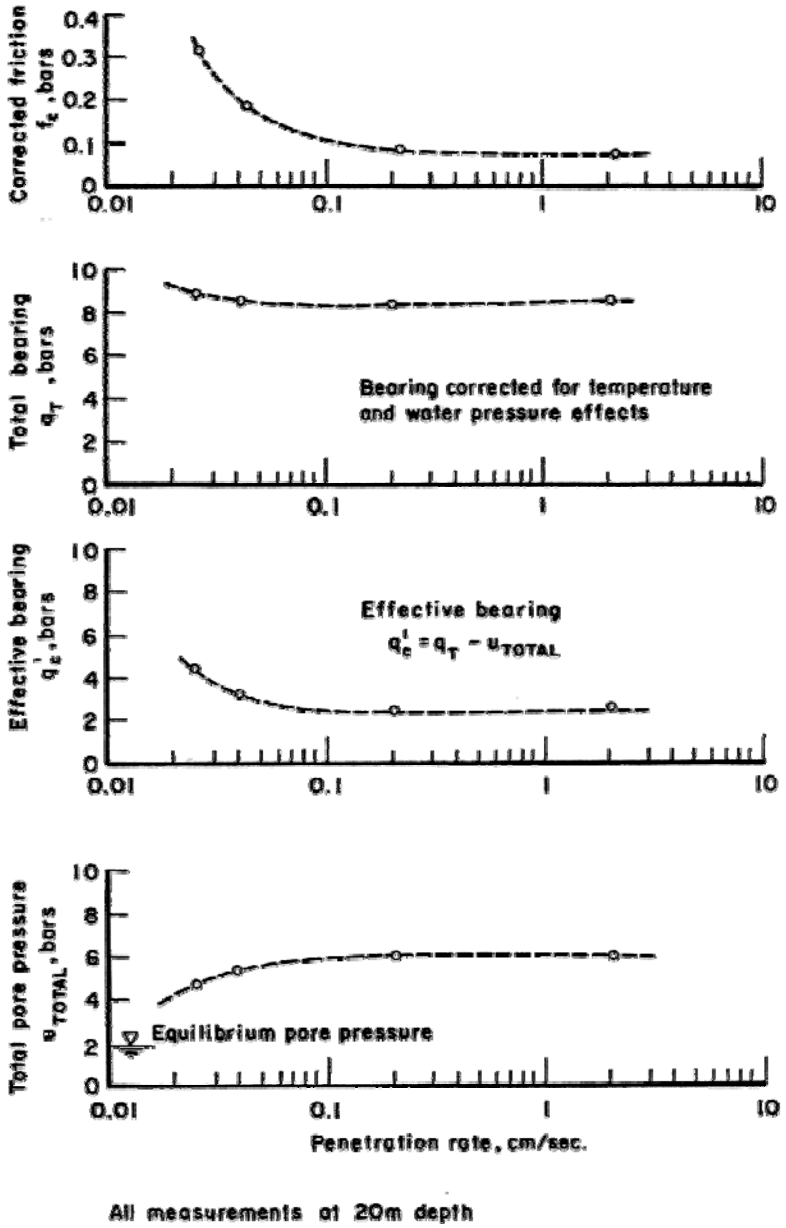

Figure 6-1 Effect of CPTU Penetration rate (Campanella et al, 1982)

0.7 m (14 to 28 inches). The tip will however, respond fully for soft layers considerably thinner than 0.35 m in thickness. Since the cone tip is advanced continuously, the tip resistance will sense much thinner stiff layers, but not fully. This has significant implications when interpreting cone tip stress, for example, for relative density determination in sand. If a sand layer is less than about 0.7 m thick and located between, say, two soft clay deposits, the cone penetration resistance may not reach its full value within the sand because of the close proximity of the adjacent interfaces. Thus, the relative density in the sand may be severely underestimated.

The natural variability of many sand deposits produces q_c profiles with many sharp peaks and troughs. A comparison of CPT data in sands from 10 cm² and 15 cm² cones shows that the 15 cm² data will not reproduce the stiff peaks but will reproduce the soft troughs. A 15 cm² cone may require a minimum thickness of 0.9 m (Figure 6-2) for a full response. This effect of layering can also cause scale effects when using cones of a larger diameter (i.e., 15 cm² cone area). Since the relative layer thickness for full response of q_c is smaller for softer layers, the average q_c profile tends to be slightly lower for the 15 cm² cone in sands. Generally speaking, however, in moderately uniform soil, the results of a 15 cm² cone are essentially the same as those for the standard 10 cm² cone.

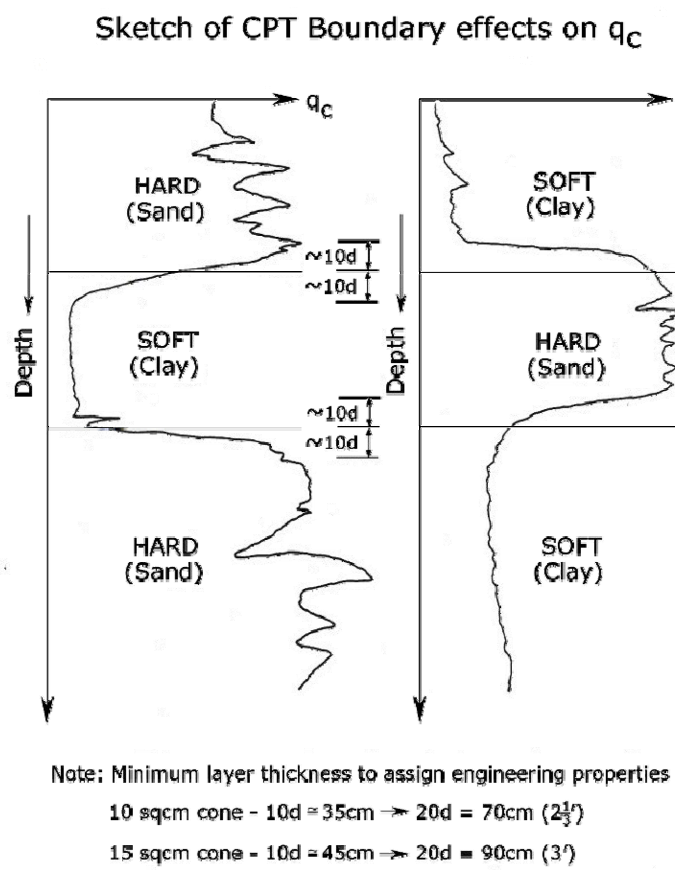

Figure 6-2 Sketch of Soil Boundary Effects on q_c Measurements

The continuous monitoring of pore pressures during cone penetration can significantly improve the identification of soil stratigraphy (Campanella et al. 1983). The pore pressure develops in response to the soil type being penetrated in the immediate area of the pore pressure sensing element. To aid in the identification of very thin silt or sand layers within clay deposits, some researchers (Torstensson 1982) have proposed and successfully used thin (2.5 mm) pore pressure elements located immediately behind the cone tip. For a pore pressure sensing element behind the tip, sands give very low or negative pore pressures while clays are very high. Dilative silts also give low or negative pore pressures while contractive silts give high positive pore pressures.

The frequency response of a fully saturated piezometer cone is usually fast enough to observe changes in pore pressure with a period of 0.25 seconds or less. This corresponds to layer thickness of about 0.2 inches (5 mm) or less at the standard penetration rate of 2 cm/sec. Whether or not such thin layers are observed in practice depends on the response of the soil to the advancing cone and the depth interval of data recording. Additional discussion of pore pressure response to thin layers can be found in section 6.2.1.4.

6.1.2.7 Drainage Effects

Soil theories and therefore interpretation of CPTU data are well developed for fully drained penetration in sands as well as fully undrained penetration in clays and these will be discussed in section 7. It should be realized that partially drained penetration in, say, sandy silts makes it very difficult, if not impossible, to interpret any meaningful or useful parameters for these soils.

6.2 Soil classification and interpretation of stratigraphy

6.2.1 Visual classification

6.2.1.1 Introduction

After the CPTU data are recorded and carefully scrutinized and edited where necessary according to section 4.2, the profiles should be plotted as indicated in section 4.3. It is now best to visually evaluate and classify the soils, looking for trends, layer interfaces and distinctive soil types realizing that there are no uniform or homogeneous layers in nature. Uniform soil layers only exist in textbooks for simplifying analyses. The visual or qualitative interpretation of the profiles will be explained in the next few sections and should be done before any computerized interpretation is attempted. The increase in tip stress with depth for a given soil is due to corresponding increases in overburden stress.

6.2.1.2 Evaluating tip stress profiles

The best explanation of the process for evaluating tip stress profiles was given by John Schmertmann in 1978 and is shown here as Figure 6-3.

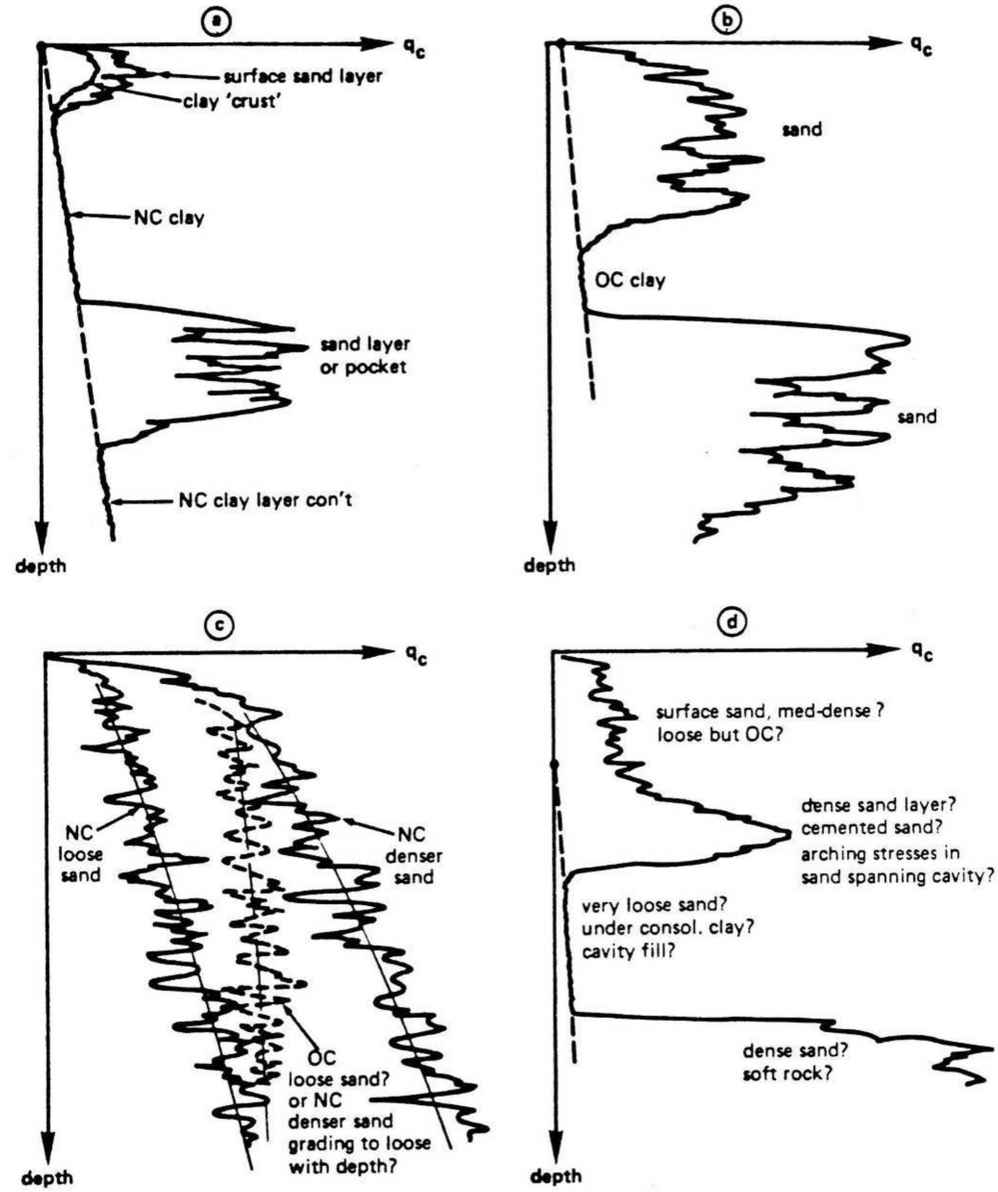

Figure 6-3 Simplified examples of q_c (or q_t) Profiles showing Likely and Possible Interpretations for Soil Types and Conditions (Schmertmann, 1978)

Normally consolidated, (NC), saturated clays always show a linearly increasing tip stress with depth which is zero when extrapolated to zero depth as shown in Figure 6-3(a). On the other hand, overconsolidated clays (OC), always have a positive tip stress at zero depth (see b) and the larger the overconsolidation ratio, (OCR), the larger is the zero depth intercept. An underconsolidated clay, i.e. still consolidating, is indicated by a negative tip stress intercept at zero depth (see d). It is extremely important to identify a normally consolidated clay layer when it exists as such information can be used in later interpretation of undrained shear strength. The overconsolidated clay crust is as indicated in Figure 6-3(a)

Typically penetration stress in sand is more variable than in clays and sand values are orders of magnitude larger than clays at the same depth as shown in Figure 6-3(a). This helps you to quickly separate clays from sands visually. Clays, however, will also exhibit similar variability when stratified with coarser soil lenses and thin layering. The variability in sands can be due to variations in gradation and density, especially in deltaic deposits.

Figure 6-3(c) illustrates the effect of density on a normally consolidated sand, where the left hand curve is for a uniform loose sand and the right hand curve is for the same sand but in a uniform very dense condition. The dashed curve in Figure 6-3(c) illustrates a possible overconsolidated loose sand where the OCR is decreasing with depth or this could also be a normally consolidated dense sand at shallow depth which becomes loose with depth. Of course, the third and most plausible situation is for a shallow dense sand which grades into a finer and silty sand with depth. Obviously the condition of a sand is more difficult to interpret than a clay and some of that difficulty is illustrated in Figure 6-3(d).

6.2.1.3 Evaluating Friction Ratio Profiles

Another important parameter to interpret is friction ratio (FR or R_f) or friction sleeve stress divided by tip stress expressed as a percentage, i.e. (f_s/q_t)x100%. This parameter has a typical maximum value of about 8% and sometimes higher in organic soils. Although it might seem more logical to use other sleeve friction parameters, tradition has prevented any changes. The FR for a clean sand is around 0.5% and increases as soil grains becomes finer. A silty clay has a FR of the order of 3-4%. Remember, however, that a sand has a friction sleeve stress which is more than an order of magnitude higher than that of a silty clay.

The first work on soil classification using CPT data was done by Schmertmann (1978) and then by Douglas and Olsen (1981) based on extensive data collected from areas in California, Oklahoma, Utah, Arizona and Nevada. The complexities of the chart by Douglas and Olsen (1981) make it difficult to use and it was adapted by Robertson and Campanella, 1983a, to include UBC experience to produce the simpler but somewhat less comprehensive classification chart shown in Figure 6-4.

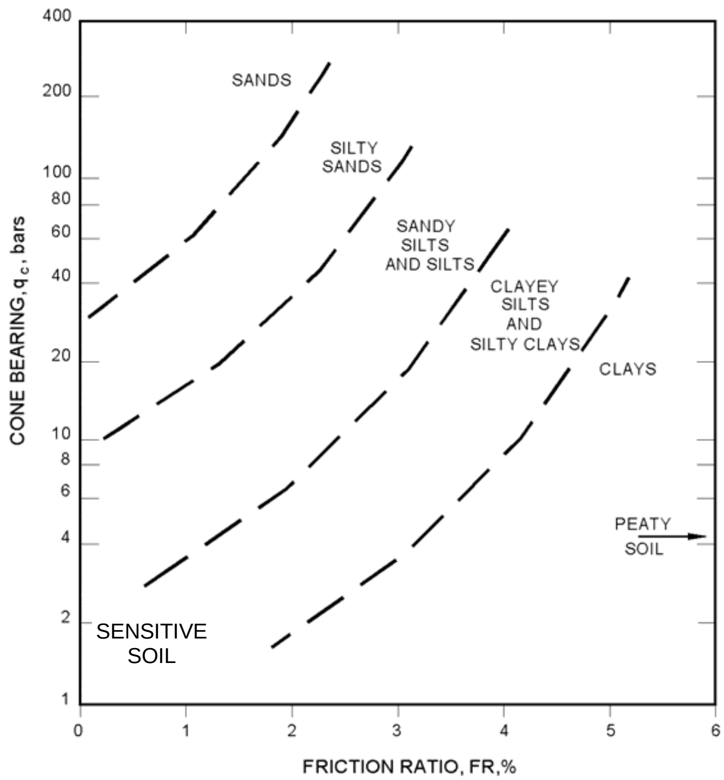

Figure 6-4 Simplified Chart of Tip Stress versus Friction Ratio (Robertson and Campanella, 1983a)

The value q_c is now considered to be q_t. Of course, from the discussion of Figure 6-4, it should be realized that a plotted point in Figure 6-4 is not fixed by grain size and will vary according to relative density, in-situ stress, aging, cementation, soil fabric and sensitivity. For that reason the chart was referred to as the SOIL BEHAVIOUR TYPE CLASSIFICATION CHART.

6.2.1.4 Evaluating Penetration Pore Pressure Profiles

With the development of the piezocone in the early 1980's, a third independent parameter was added to the cone test. It was observed that when penetrating sands below the groundwater table, the measured pore water pressure, U2, was very close to the equilibrium pore pressure and often below it. In any event, when the penetration was stopped to add a rod, the pore pressure immediately became equal to the equilibrium value. With increasing fines, the pore pressures during penetration were above the equilibrium value and, as soils became plastic, the generated pore pressures became very large indeed.

A typical CPTU profile was previously shown as Figure 4-7 and will be shown here again as Figure 6-5 for a discussion of visual classification.

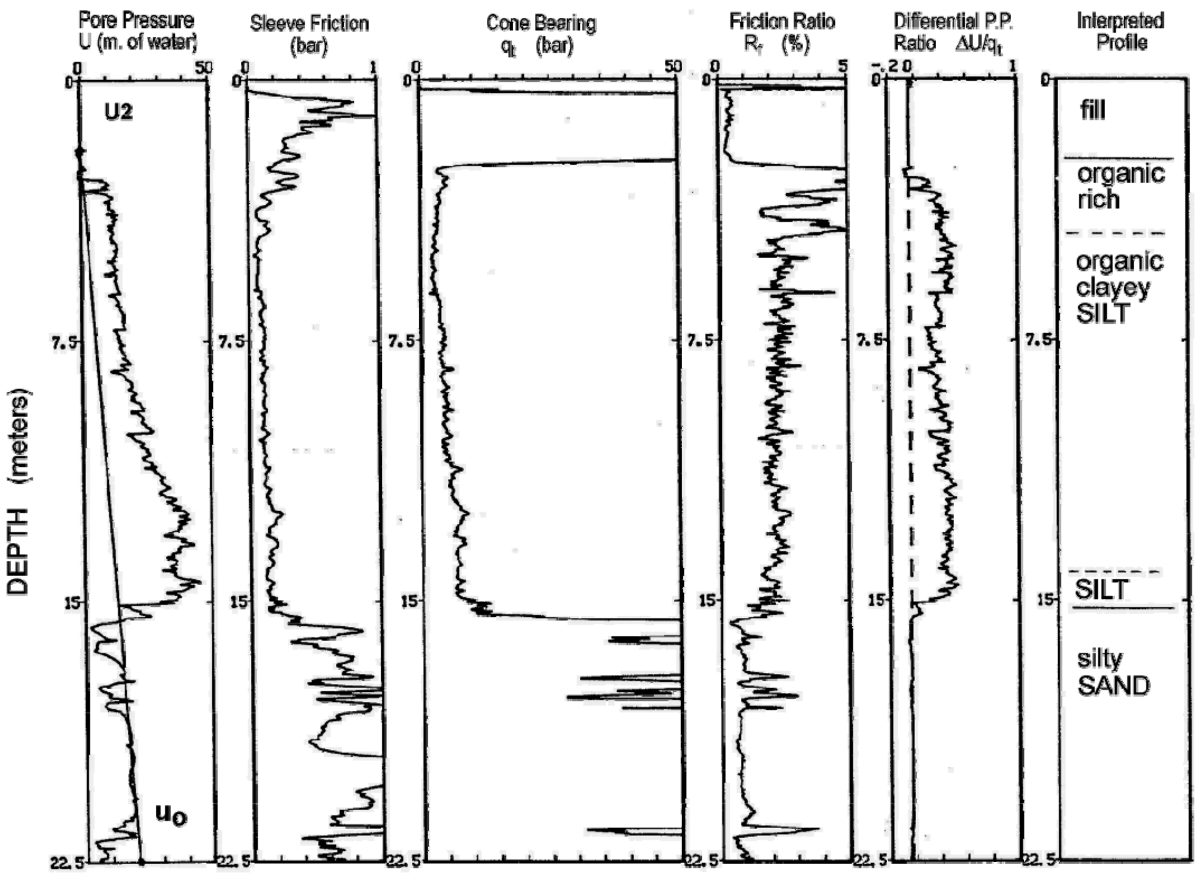

Figure 6-5 CPTU Profile at Test Fill-Richmond, BC

The pore pressure, U_2, is plotted in units of metres of water pressure and is referenced to the line of equilibrium pore pressure, which is hydrostatic in this case. The groundwater table, GWT, is 2.5 m below ground level. The fully drained sand from 18 to 21 m helps to position the equilibrium line. The differential pore pressure ratio plot, $(U_2\text{-}U_o)/q_t$, clearly identifies the mostly undrained organic clayey silt as well as the mostly drained silty sand. Note that the tip stress in the clayey silt is around 5 bar or 0.5 MPa and is mostly normally consolidated except for the upper organic rich zone which is in the zone of groundwater fluctuations and is likely somewhat desiccated. The FR also identifies the layers and supports the classification by the pore pressure. In addition, the FR clearly shows the clayey silt layers in the silty sand at depths of about 17.5 and 21 m. The FR is up to 5% in the upper organic rich layer, 2% in the clay silt layer and a little less than 1% in the silty sand layer. The clay silt and silty sand plot near or at the upper boundaries of their zones in Figure 6-4.

The usual progression of site investigation using the cone penetration test (CPTU) is to perform the CPTU soundings, perform a visual classification of soils and boundaries, develop detailed site profiles with the soil behaviour type charts (Figure

6-4), and then selectively sample and test to provide any additional information regarding ambiguous classifications. With local experience this latter step is often not necessary. In this case, Figure 6-5 might be recommended to obtain undisturbed samples from the clay silt layer for consolidation testing.

6.2.1.5 Evaluation of Pore Pressure Dissipation

As previously explained, the rate of pore pressure dissipation (PPD) relates to soil permeability or hydraulic conductivity and can be characterized by the time for 50% dissipation or t_{50}, which is the time it takes for the pore pressure to reach half way to the equilibrium pore pressure. This value can be directly measured at pauses in penetration to add a cone rod. Often t_{50} can be obtained if insufficient time was allowed by plotting pore pressure versus square root of time, which is approximately linear to 50% dissipation and can be linearly extended to obtain t_{50}. An approximate relationship between t_{50}, k and soil gradation was developed by Parez and Fauriel (1988). Their relationship is shown as Figure 6-6 and the relationship follows:

$$k(\mathrm{cm/s}) \approx \left(\frac{1}{251 \times t_{50}(\mathrm{sec})}\right)^{1.25} \qquad (6.1)$$

Although this relationship is only approximate, it gives a quick idea of soil type and the comparison of several t_{50} values with depth gives an excellent measure of relative gradational changes.

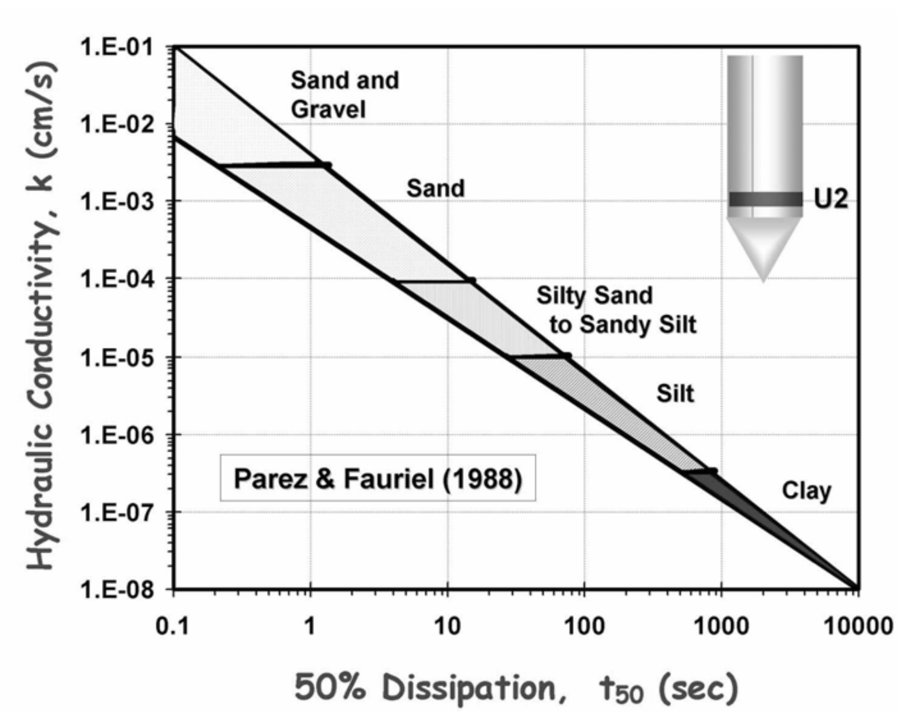

Figure 6-6 Soil Type related to t_{50} and k (Parez and Fauriel, 1988)

Figure 6-7 gives an excellent example of detailed stratigraphic and t_{50} logging. The figure shows the deepest 35 m of this sounding to 69 m. The vertical scale has been enlarged compared to the horizontal, which has the effect of sharply identifying the interfaces between soil types. The soil profile boundaries were identified using both the plot of differential pore pressure ratio and bearing (tip) stress. The t_{50} times were identified to the right and carefully located according to the recorded cone penetration depth. t_{50} values of 100 seconds and greater line up with the silt layers, those from 20 to 40 seconds line up with the silty sand and values below 15 are in the sand layer. These values agree fairly well with Figure 6-7 except at the smallest values less than 10 seconds. However, equipment limitations in the early 1980's resulted in data being recorded only every 5 seconds with as much as a 5 second wait before the first data point was taken. Field tests later determined that the thin sand layers at depth were likely interconnected and effectively acted to drain the silt layers.

6.2.1.6 Delineation of thin layers

The results in Figure 6-8 demonstrate the effectiveness of the pore pressure sensor to very quickly respond to changing soil type. The upper part of the figure shows the CPTU profile in alternating sand and silt layers from 52 to 78 m depth while the lower part shows a 10-minute time plot of measured U2 pore pressure from 72.6 to 76.6 m including dissipations. In the early 1980's, CPTU data was recorded in analogue form on a strip chart pen recorder. The pens moved proportionately with transducer voltage and the paper moved at a constant rate of say 1 cm/min. The lower part of Figure 6-8 is a reproduction of the strip chart plotter. The solid line denotes data recorded during penetration and the dashed line represents periods of dissipation when a cone rod was added. Values below the static pore pressure are indicative of dilation in sand and high values are in the silt. At 72.6 m, the U_2 sensor starts in sand, but quickly penetrates a silt layer. A very thin coarser lens causes a sharp drop in U_2 before it again rises. The penetration stops and the pore pressure dissipates to about 14 bar but quickly rises again to 24 bar when penetration commences. At about 74.0 m, the U_2 sensor encounters a sand layer and the pore pressure plunges from 24 to 4 bar. After pushing about 0.4 m in the sand the push is stopped to add a rod. The approximate position of the cone during the dissipation is shown in the detail. The pore pressure rises then dissipates. The rapid rise is due to the fact that the tip has just started to penetrate a silt layer and the high pore pressure there spreads into the sand momentarily until the sand dissipates the pore pressure toward the static value. When penetration is started again, the pore pressure again rises as the tip penetrates the silt, goes through a sand lens and stops at a point where it is about to leave the silt and again penetrate the sand layer. With such a plot, one can estimate the thickness of the penetrated layers. The tip stress measurement does not show this level of sensitivity at identifying boundaries because the tip senses soil in front as well as behind to distances of a cone diameter and more. Since data are no longer collected on analogue strip chart recorders, it would be necessary to digitize data at very short depth intervals to generate a similar plot. For example, if you wanted to identify features that are 10 cm in thickness it would be necessary to take data at 1-2 mm intervals. To identify shear failure zones, it would be necessary to take data at least every 1 mm of depth. While possible, such a high resolution in depth may not be practical.

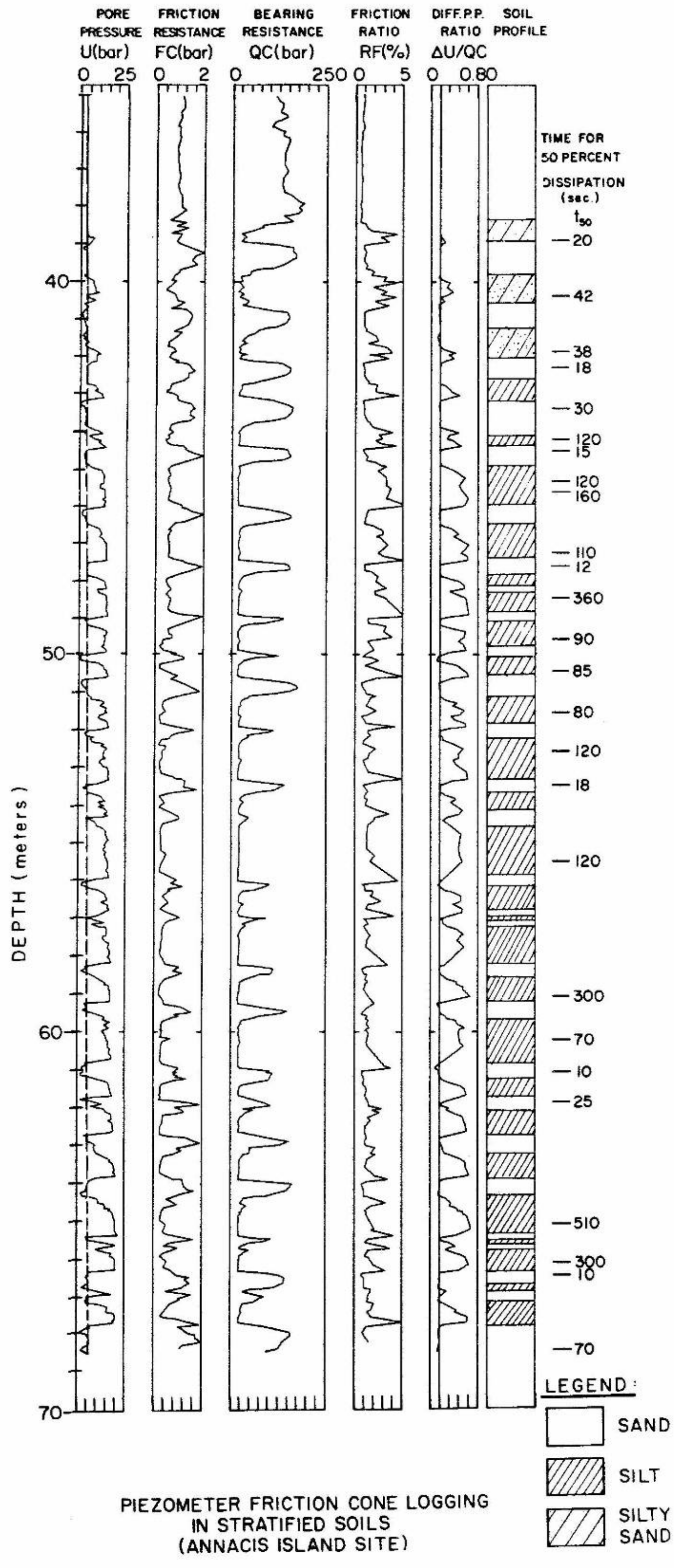

Figure 6-7 Example of stratigraphic logging using CPTU Profile and t_{50} Logging at Annacis Island, BC (Gillespie 1981)

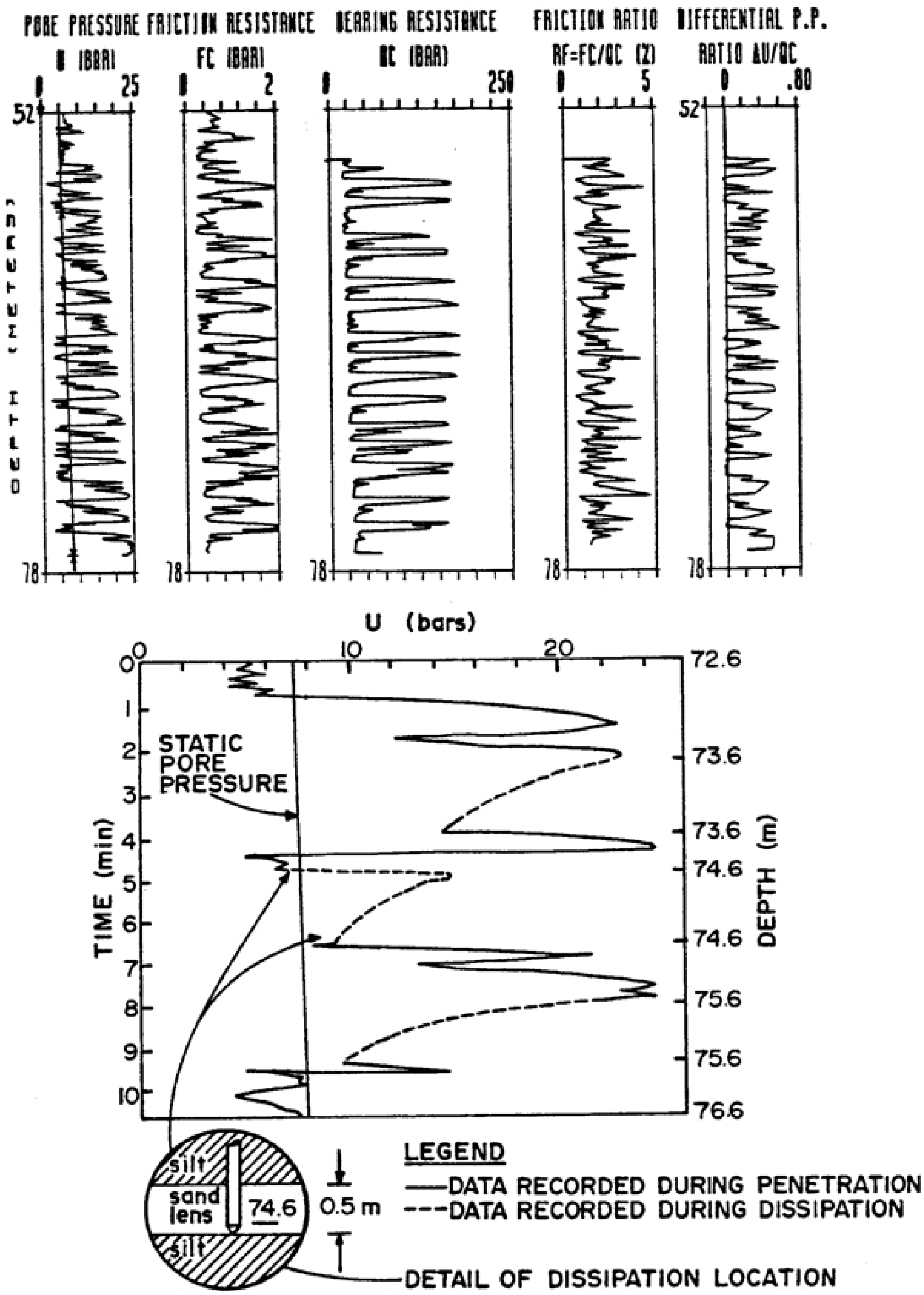

Figure 6-8 Layer Delineation and Detail Logging using the Rapid Pore Pressure Response to Soil Type (Gillespie 1981)

6.2.1.7 Stratigraphic Logging – Visual Example at its Best

Figure 6-9 shows an exceptional example of stratigraphic logging. CPTU penetration extended to a depth of 74m. Equilibrium pore pressure (full dissipation) was determined each time the pore pressure sensor stopped in a sand layer and the values are plotted as opposing arrows in the U2 profile. The equilibrium values indicated a hydrostatic condition and GWT at a depth of 0.5 m below ground. The friction sleeve stress, f_s, is plotted next, then bearing resistance (tip stress), q_t, friction ratio, FR, differential pore pressure ratio, $(U2-u_o)/q_t$, soil profile description and finally all the measured t_{50} values.

It is immediately apparent that there are 5 major soil layers. Below the 1 m thick sand fill, there is an organic silt layer extending to 15 m with tip stresses less than 5 bar. The upper 4-5 m is very young and fibrous, indicated by the very high friction ratio values of 6-10%. The values in the lower organic silt are 2-4%.

Below the very soft organic silt lies a 13 m thick sand layer which was thought to be uniform and competent as a result of boring logs. The bearing profile shows it is anything but uniform with two distinct silt layers in that zone, which can be clearly seen in the differential pore pressure ratio profile where the sand has a value of zero. The sand has a friction ratio of about 0.5%. Since piles were to be embedded in the sand layer to support approach spans to the main Fraser River Bridge, CPTU was subsequently required at each pile bent prior to driving and the results were used for the pile capacity design.

From 28 to 74 m the soil is markedly stratified. However, from the q_t profile one can identify three zones of distinctly different depositional characteristics. The first layer is mainly a silt interbedded with very thin lenses and layers of sand. The next layer is interbedded sand and silt and the deepest layer is made up of distinct alternating layers of sand and silt. This level of detail could not be picked up during drilling and logging (using mud rotary), but was well identified by the CPTU log which was subsequently verified by taking continuous undisturbed Shelby tube samples to 80 m depth.

It could also be concluded that the entire site was normally consolidated and at equilibrium under the existing overburden stresses. This conclusion was made because a linear line can be drawn as the lower bound q_t values with depth and that line has zero tip stress at zero depth. This lower bound line represents the strength of the weakest component or the silt fraction. This allowed a fairly good determination of the undrained shear strength profile with depth. Such determination will be discussed in chapter 7.

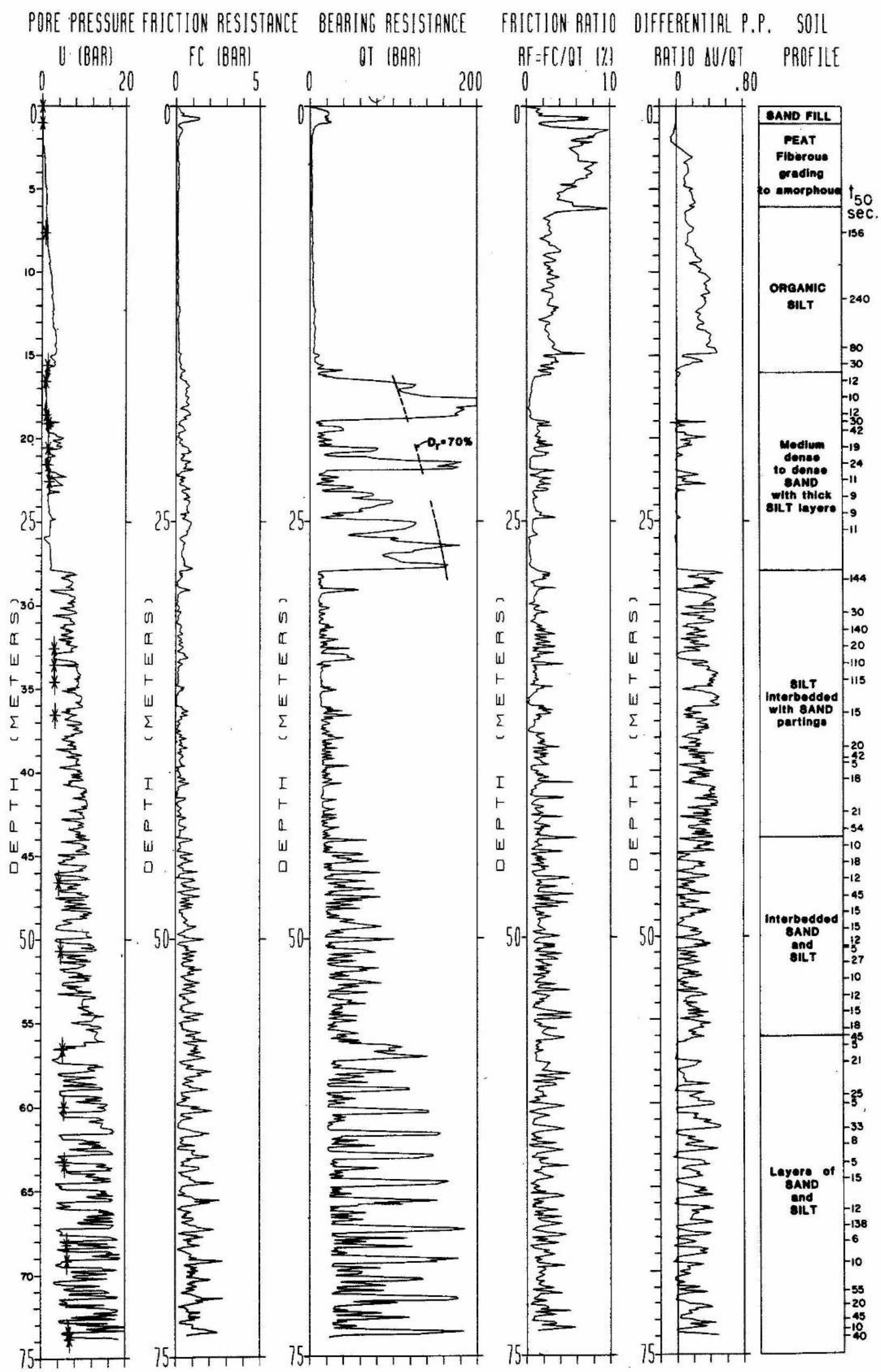

Figure 6-9 CPTU Stratigraphic Logging - Pile Research Site (Campanella et al, 1983)

The log of t_{50} values with depth proved to be very valuable, since most of the values were quite small and many were 5-10 seconds. Only a few in the upper silt layer (28-35 m) were from 100-150 sec. This all suggested that drainage and subsequent consolidation of the silt would be fairly rapid as long as all the sand layers were interconnected, which was likely. Subsequently banks of 1 m diameter steel pipe piles were used to support the main towers of the bridge. Tower settlement was monitored and all settlement had stopped 6 months after construction.

The friction sleeve stress is plotted in the profile as one of the three independent variables but little use is made of it except that it is used to calculate friction ratio, which is used extensively in interpretation.

All of the data in Figure 6-9 were collected in one day over about a 10 hour period by a crew of three. Unfortunately, at that time in 1982, all data was collected on a multi-pen strip chart recorder. It subsequently took several weeks to a month to scale the results off the chart, reduce the data and replot the results in the form shown in Figure 6-9. With current computer based data recording, analysis and plotting systems, the final results could be plotted in a day. Unfortunately, the computer does not speed up the field testing.

6.2.2 Computerized Classification

6.2.2.1 Introduction

With the development of the personal computer in the 80's users of the CPT and CPT data wanted a form of automatic classification and interpretation. Visual interpretation was very effective as seen for Figure 6-9 and UBC was concerned that layer boundary effects could lead to misleading interpretation in an automated system, which calculated parameters sequentially without regard for layering. Also, averaging over several depth readings could add to misinterpretation if data is not carefully scrutinized.

6.2.2.2 UBC Behaviour Type Classification Chart

In the mid-1980's, UBC developed a computerized chart called 'Soil Behaviour Type Classification' or SBT meaning that the classification is based on observed behaviour rather than grain size. The first thing required was the extension of the boundary curves in Figure 6-4 to the axes and the number of zones was increased and given numbers as shown in the upper part of Figure 6-10 using q_t and R_f.

Figure 6-10 shows 12 zones, where 7 and higher tends to be sandy and 5 and lower tends to be clayey. In the sand range, increasing density increases q_t and may decrease R_f. Increasing OCR (increased K_o which increases lateral stress) will increase both the cone resistance and friction ratio. For fine grained soils, an increase in liquidity index (LI) will produce a decrease in both q_t and R_f. Thus, sensitive soils (high S_t) tend to have very low friction ratios and zone 1 was created. Organic soils like peat exhibit very high R_f and very low q_t values and, hence, zone 2 was created. Increasing compressibility (increasing void ratio, e) produces a

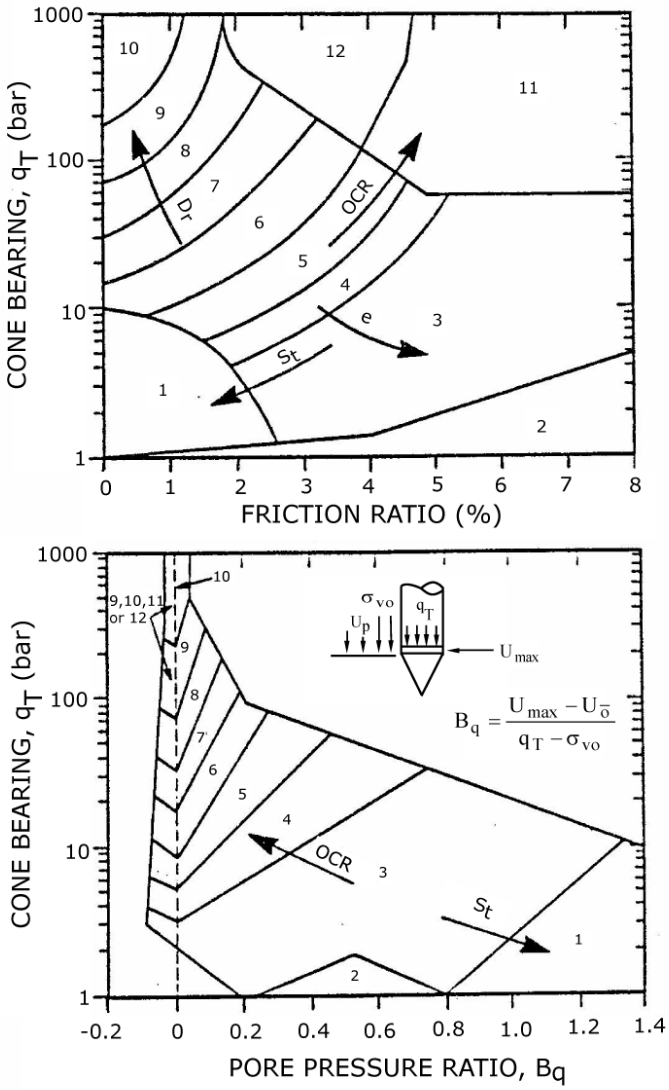

Notes:

1. Expect some overlap in zones.
2. Local correlations preferable.
3. Based mainly on data obtained from depth < 30 m.
4. Review available dissipations of u to guide overlap in charts.

Zone	Soil Behaviour Type	q_T/N	t_{50} (minutes)
1)	sensitive fine grained	2	10-500
2)	organic material	1	2-20
3)	clay	1	10-100
4)	silty clay to clay	1.5	5-10
5)	clayey silt to silty clay	2	2-5
6)	sandy silt to clayey silt	2.5	1-2
7)	silty sand to sandy silt	3	.5-1
8)	sand to silty sand	4	0-.5
9)	sand	5	drained
10)	gravelly sand to sand	6	drained
11)	very stiff fine grained (*)	1	unknown
12)	sand to clayey sand (*)	2	unknown

(*) overconsolidated or cemented

Figure 6-10 Traditional Soil Behaviour Type Interpretation Chart (Adapted from Robertson and Campanella 1983a)

decrease in cone resistance with an increase in friction ratio. Thus, carbonate sands or sands with high mica content tend to have high friction ratios, and may fall in the sandy silts region.

With the measurement of pore pressure, u_2, it became apparent that a similar soil behaviour type classification existed for pore pressure. Several classification charts were proposed based on q_t and pore pressure (Baligh et al. 1980; Jones and Rust 1982; Senneset and Janbu 1984). The chart by Senneset and Janbu (1984) uses the pore pressure parameter ratio, B_q, defined as;

$$B_q = \frac{\Delta u}{q_t - \sigma_{vo}} \tag{6.2}$$

where

Δu	= excess pore pressure measured behind the tip, u_2-u_o
q_t	= cone resistance corrected for pore pressure effects,
σ_{vo}	= total overburden stress.

The original chart by Senneset and Janbu (1984) used q_c. However, it is generally agreed that the chart and B_q should use the corrected cone bearing, q_t. The correction is usually only significant in soft, fine grained soils where q_c can be small and Δu can be very large. Normalized parameters will be discussed in the next section.

Note that negative pore pressures are shown to exist for all 12 zones. The B_q chart has proven to be very useful for saturated soils and as an independent parameter usually agrees with the classification by R_f. Therefore, it is recommended that all three pieces of data (q_c, u, and f_s) in the form of q_t, B_q and R_f be used to define soil behaviour type.

The importance of cone design and the effect that water pressures have on the measured tip stress and friction due to unequal end areas have been discussed (section 4.1.2). Thus, cones of slightly different design will likely give slightly different tip stress, friction and friction ratios. With proper calibration and measurement, the effects of unequal end areas can be corrected. The data originally used to compile the classification charts (Figure 6-10) used tip stress and friction values that had generally not been corrected for pore pressure effects, since, in general, pore pressure measurements were not made at that time. Recent data indicates that there is little difference between corrected and uncorrected friction ratios for most soil types except for those soils that classify in the lower portion of the charts (Figure 6-10). These soils usually generate large positive pore pressures during penetration and have very low measured bearing (q_t <10 bar) and small friction values where corrections become very significant. Where CPT is done without pore pressure measurement or for above the groundwater table, the chart in the upper part of Figure 6-10 can be used directly to provide a reasonable estimate of soil type.

Also shown in Figure 6-10 is UBC's experience with correlation of the standard penetration test (SPT) to the CPT, which is shown as the ratio of q_t (bars) divided by SPT N-value for each of the zones. Experience with pore pressure dissipation data is also shown as a t_{50} time range in minutes for each of the zones.

It is important to realize that the classification charts are entirely based on field observations and are therefore empirically based and must be treated accordingly. It is interesting that although the charts were developed in the early 1980's they have not been adjusted and have proven to give excellent results on a worldwide basis. The only criticism has been that the mid-zones from 5 to 7 tend to classify the soil as 'finer' than actually exists. Any CPTU based classification system should always be used with caution and should ***always be adjusted to reflect local experience***.

The charts in Fig 6-10 are global in nature and should only be used as a ***guide*** to define soil behaviour type based on CPTU data. Occasionally soils will fall within different zones on each chart, in these cases judgment is required to correctly classify the soil behaviour type. Often the rate at which the excess pore pressures dissipate during a pause in the cone penetration will aid in the classification. For example, a soil may have the following CPTU parameters; q_t = 10 bar, R_f = 4%, B_q = 0.1. It would classify as a clay on the R_f chart and as a clayey silt to silty clay on the B_q chart. However, if the rate of pore pressure dissipation were very slow (t_{50} > 10 min.) this would add confidence to the classification of a clay. If the dissipation were rapid (t_{50} < 2 min.) the soil is more likely to be a clayey silt or possibly a clayey sand.

6.2.2.3 Normalized Behaviour Type Classification Chart

A problem associated with existing CPT classification charts is that soils can gradually change in their apparent classification as cone penetration increases in depth. This is due to the fact that q_t, u and f_S all tend to increase with increasing overburden pressure. For example, in a thick deposit of normally consolidated clay, the cone bearing will increase linearly with depth resulting in an apparent change in CPT classification. Existing classification charts are based predominantly on data obtained from CPT profiles extending to a depth of less than 30 m (100 ft). Therefore, for CPT data obtained at depths significantly greater than 30 m, some error can be expected when using the standard global CPTU classification charts in Figure 6-10.

Attempts have been made to account for this by normalizing the cone data with the effective overburden stress, σ'_{vo} (Douglas et al. 1985; Olsen 1984; Robertson and Campanella 1985).

Normalization of CPTU data would avoid some of the problems associated with variations in q_t with soil strength. At present, a very loose clean sand may be classified as a sandy silt to silty sand because of the low q_t.

Robertson, 1990, proposed a soil behaviour type classification chart based on normalized cone tip resistance and normalized friction ratio for integration with a B_q chart. Figure 6-11 shows the classification charts proposed. The tip stress normalization is given as

$$Q_t = \frac{(q_t - \sigma_{vo})}{(\sigma_{vo} - u_o)} \tag{6.2}$$

and pore pressure normalization was previously given as

$$B_q = \frac{(u - u_o)}{(q_t - \sigma_{vo})} \tag{6.3}$$

In addition, friction ratio values (ratio of the sleeve friction to the tip resistance) should be stress normalized as:

$$F_r = \frac{f_s}{(q_t - \sigma_{vo})} \times 100\% \tag{6.4}$$

It should be realized, however, that non-normalized friction ratio values are almost always numerically equivalent (to significant digits) to normalized values due to the fact that the overburden stress is usually very small compared to the tip stress. This means that the only significant difference between the charts in Figs 6-10 and 6-11 is the normalized tip stress, Q_t.

As per non-normalized values, F_r from equation 6-4 is most commonly quoted as a percentage for convenience. F_r is also denoted by F.

Note that the ability to partially assess stress history becomes a bonus when using these charts. Unfortunately, other researchers have suggested that this normally consolidated zone may not be as located and should be checked by other means. Also, note that the zones defined in Figure 6-11 are different from those in Figure 6-10. The normalized charts have shown their effectiveness for deep deposits in excess of 30 m (Robertson 1990).

It is often important to realize that the classification charts are generalized global charts that provide a guide to soil behaviour type. The charts cannot be expected to provide accurate prediction of soil type for all soil conditions. However, in specific geological areas, the charts can be adjusted for local experience to provide excellent local correlations.

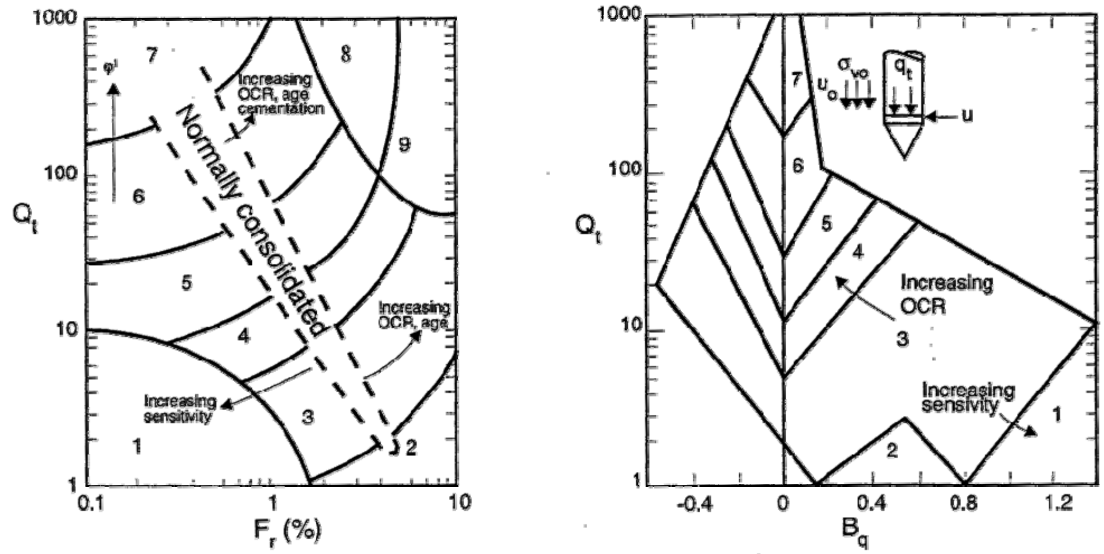

$$Q_t = \frac{q_t - \sigma_{vo}}{\sigma'_{vo}} \qquad B_q = \frac{u_2 - u_o}{q_t - \sigma_{vo}} \qquad F_r = \frac{f_s}{q_t - \sigma_{vo}} \times 100\%$$

Zone	Soil behaviour type	Zone	Soil behaviour type	Zone	Soil behaviour type
1.	Sensitive, fine grained;	4.	Silt mixtures clayey silt to silty clay	7.	Gravelly sand to sand;
2.	Organic soils-peats;	5.	Sand mixtures; silty sand to sand silty	8.	Very stiff sand to clayey sand
3.	Clays-clay to silty clay;	6.	Sands: clean sands to silty sands	9.	Very stiff fine grained

Figure 6-11 Soil Behaviour Type Classification Chart Using Normalized Parameters (After Robertson 1990)

6.2.2.4 Unified and Normalized Soil Behaviour Type Classification Chart

Jefferies and Davies (1991) modified the Robertson (1990) charts and proposed the concept of incorporating tip stress, pore pressure and friction sleeve stress data directly into one chart through the $Q(1\text{-}B_q)$ grouping. This expands the interpretation range in finer soils while leaving the interpretation in sands unchanged (B_q=0 for sands); a characteristic felt important for mine tailings work. Their proposed chart is shown in Figure 6-12. Note that the boundaries of soil behaviour type are defined by a material index, I_c, proposed by Jefferies and Davies (1991), given by

$$I_c = \sqrt{\left\{3 - \log_{10}\left[Q(1 - B_q)\right]\right\}^2 + \left[1.5 + 1.3(\log_{10} F)\right]^2} \qquad (6.5)$$

In Equation 6-5, $Q(1 - B_q)$ is dimensionless and F is in its usual percentage format.

As shown on Figure 6-12, the mapping is used to obtain a plot with concentric circles, and the centre of the circles is log(Q) = 3, log(F) = - 1.5. The logarithms used are base 10. Within this proposed classification of soil behaviour types, values of I_c and the corresponding behaviour type are summarized in Table 6.1. Here there are 5 zones defined by I_c; a sand zone, a sand mixture zone, a silt mixture zone, a clay zone and an organic soil zone. A sensitive soil zone 1 is not defined by I_c and is in the lower left of the chart as before. For this chart, the drained sand zone is where I_c<1.8 and the undrained zone is defined where I_c>2.76.

MATERIAL INDEX I_c	ZONE	SOIL BEHAVIOUR TYPE
I_c < 1.80	6	Clean Sand to Silty Sand
1.80 < I_c < 2.40	5	Sand Mixtures - Silty Sand to Sandy Silt
2.40 < I_c < 2.76	4	Silt Mixture - Clayey Silt to Silty Clay
2.76 < I_c < 3.22	3	Clays - Clay to Silty Clay
3.22 < I_c	2	Organic Soils - Peats
Q(1-Bq) < 10 & F < 1%	1	Sensitive Fine Grained Soils

Table 6-1 Soil Behaviour Type from Material Index I_c

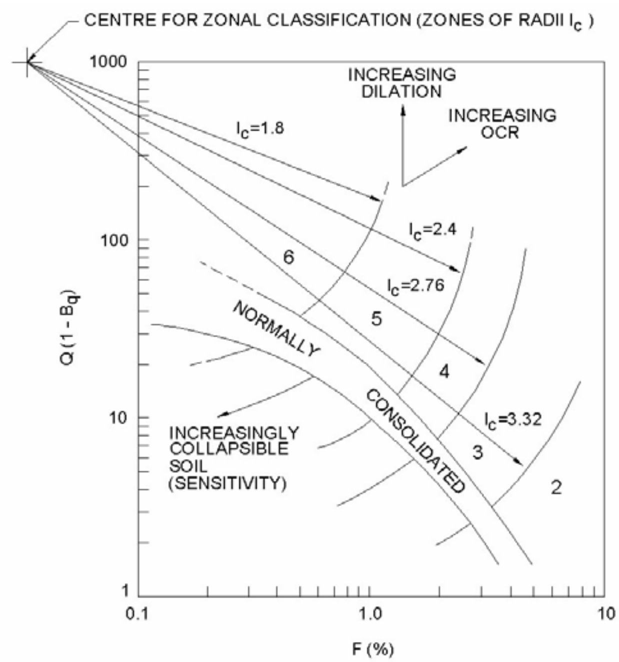

ZONE	SOIL BEHAVIOR TYPE (after Jefferies and Davies, 1991)
6	CLEAN SAND TO SILTY SAND
5	SAND MIXTURES - SILTY SAND TO SANDY SILT
4	SILT MIXTURES - CLAYEY SILT TO SILTY CLAY
3	CLAYS - CLAY TO SILTY CLAY
2	ORGANIC SOILS - PEAT

Figure 6-12 Unified Soil Behaviour Type Normalized Classification Chart (after Jefferies and Davies, 1991)

Comparison of Figs. 6-11 and 6-12 shows that the zones used by Jefferies and Davies have the same names as those by Robertson, but the boundaries are different as is the normally consolidated zone, which resulted from their expanded database. Later Robertson and Wride (1998) used the same I_c concept proposed by Jefferies and Davies (1991), but defined it in terms of only Q and F (no pore pressure). The Robertson and Wride (1998) I_c is given by the expression:

$$I_c = \sqrt{\{3.47 - \log Q\}^2 + \{\log F_r + 1.22\}^2} \qquad (6.6)$$

where $Q = \dfrac{q_t - \sigma_{vo}}{(\sigma_{vo} - u_o)^n}$

F_r is given by Equation 6.4 and is a percentage

n = stress exponent

Olsen and Malone (1988) noted that exponent n should vary from n = 0.5 in sands to 1.0 m in clays.

Consequently, Robertson (2004) recommended that n be defined as follows:

If	$I_c < 1.64$,	n = 0.5
If	$I_c > 3.30$,	n = 1.0
If	$1.64 < I_c < 3.30$,	$n = (I_c - 1.64)0.3 + 0.5$
If	$\sigma'_{vo} > 300$ kPa,	n = 1.0

He indicated that the engineer should iterate until $\Delta n < 0.01$.

The Jefferies and Davies (1993) approach gives the advantage of including drainage effects and is simpler. The reader is referred to Jefferies and Davies (1991) and Robertson (1991b) for a discussion of the merits of the different definitions of I_c.

6.2.2.5 Fines Content

Robertson and Wride (1998) and Davies (1999) suggested relationships between Material Index and fines content. Davies (1999) developed a database of I_c (Eq. 6.5) and grain size shown here as Figure 6-13. The database was composed of CANLEX BC lower mainland Delta data and mine tailings data. As can be seen, the data form a fairly good straight line relationship. Evaluation of fines content in a CPTU profile is not determined to make use of the actual size of grains, but to give relative grain size changes and to identify interface boundaries as well as to identify marker layers or elevations when comparing adjacent profiles.

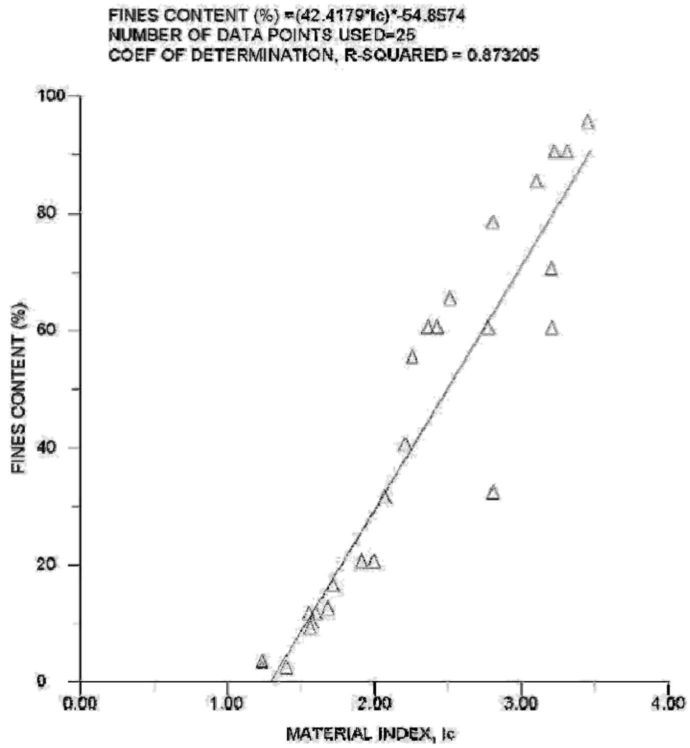

Figure 6-13 Fines Content Database against Material Index (Davies, 1999)

6.2.2.6 Proposed State Parameter from Unified Soil Behaviour Classification

The state parameter is simply defined as the difference between the current void ratio (e) and the critical void ratio (e_c) at the same stress level. The critical void ratio is that reached after large shear strain at the given stress. At critical state, the soil is assumed to shear at constant shear stress and constant volume. If the current void ratio is lower (more dense) than the critical value, then the soil will dilate (expand) when sheared and the state parameter (void ratio difference) is negative in sign. If the current void ratio is higher than critical (looser) the soil will collapse when sheared and the state parameter is positive. Plewes et al., 1992 presented an initial relationship between piezocone parameters and in-situ state which include material compressibility, a parameter neglected in the original Been and Jefferies (1985) work. Plewes et al. (1992) developed the chart shown in Figure 6-14 for estimating material state from piezocone data. It is based upon the equation:

$$\psi = \frac{\ell n\left[\dfrac{Q\left(1-B_q\right)}{\left(3.6+10.2/F\right)}\right]}{\left(1.33F-11.9\right)} \tag{6.7}$$

Figure 6-14 shows the state parameter equation plotted on the unified soil behaviour type classification. Davies (1999) showed that when this approach is used as a screening tool for liquefaction, several tailings sites where liquefaction slumps occurred plotted near and below the $\psi = 0$ line.

Davies (1999) used data from the CANLEX project in Canada where 6 sites (2 natural deltaic and 4 mine tailings deposits) were extensively characterized for liquefaction, which included the "perfect" undisturbed sampling method of in-situ freezing and coring (Robertson and Wride, 1997). The samples were laboratory tested to determine the state parameter. Multiple CPTU tests were also carried out at the sites. A comparison of the measured state parameter to the estimated value using Eq. 6.7 is given in Figure 6-15. The agreement is encouraging.

The use of the state parameter as a screening tool for liquefaction, whether static or seismically triggered, is very useful to indicate where additional studies are needed. Any value of state parameter, which is more than –0.1 is of concern and any positive values should be investigated as a potential failure zone.

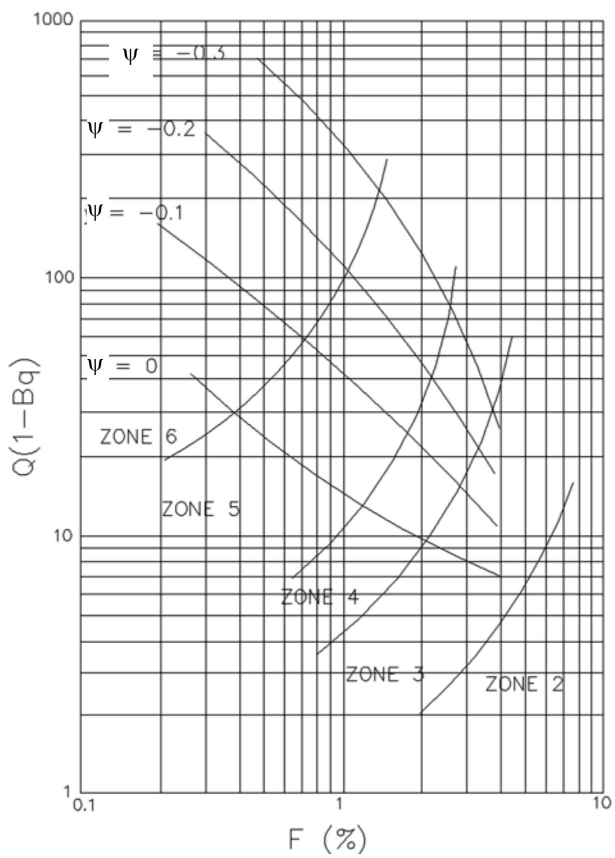

Figure 6-14 CPTU State Parameter on Unified Soil Behaviour Type Classification (Plewes et al. 1992)

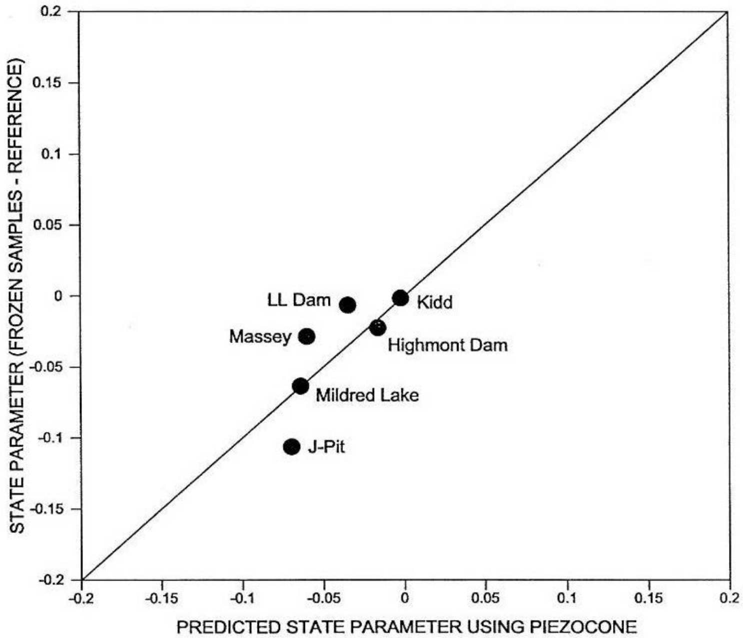

Figure 6-15 CPTU Predicted State Parameter Compared to CANLEX Measured Values (Davies, 1999)

6.2.2.7 CPT-SPT Correlations

A method for estimating equivalent Standard Penetration Test (SPT) N-values from CPT data was presented by Robertson et al. (1983), which identified the importance of variations in soil grain size and the need to calibrate and correct SPT N-values. This requires the measurement of penetration energy during driving. Using an extensive worldwide database, they showed a relationship between the ratio of tip stress divided by blow count versus mean grain size. The mean grain size was related to soil behaviour type zone number and an average correlation ratio of q_t/N was recommended as indicated in Figure 6-10. This empirical correlation, which varies from 1 for clay to 6 for gravel, has proven to be very useful. Because of the high degree of variability and uncertainty in measuring SPT blow counts, even with energy calibration, it is more reliable to perform CPTU profiling and convert q_t to N when N-values are needed for design.

About 10 years later, Jefferies and Davies (1993) developed a revised CPT-SPT relationship based on material index, I_c, instead of soil gradation. They used the Robertson et al (1983) database, but added additional data from literature and their own extensive database from many mine tailings investigations. The resulting relationship is given as:

$$\frac{q_t(\text{MPa})}{N_{60}(\text{blows per 300mm})} = 0.85\left(1 - \frac{I_c}{4.75}\right) \tag{6.8}$$

Davies (1999) observed excellent agreement between predicted and measured N-values in materials ranging from fine sands to cemented (brittle) old tailings to coarse dense sands at the CANLEX Mildred lake program. Measured N-values ranged from 5-70.

Both of these CPT-SPT correlation methods are programmed into the Freeware UBC CPTINT program, to be discussed in Chapter 8.

6.3 Interpretation of ground water regime

6.3.1 Introduction

The CPTU probe is a piezometer and therefore reads the pore water pressure at the location of the saturated sensing element. However, a moving piezometer records pore pressures created by the penetration and responds as described in section 4.1.2.

The sensor is pressed into the soil and is automatically sealed as there is no leakage along the cone surface. Saturation is important and easily obtained if the procedures described in section 3.2.2 are followed and glycerin is used in the porous filter and the pressure cavity. Occasionally the pore pressure will go below the equilibrium and even negative, especially in a shallow saturated dense sand where the pore pressure may reduce to –1 atmosphere (approximately –10 m of water, -100 kPa or –10 bar) and appear to cavitate. However, cavitation does not necessarily mean there is air in the system and saturation can be maintained especially when penetrating below the groundwater table. A rapid response in pore pressure changes when going from sand to clay is indicative of a saturated system.

6.3.2 Equilibrium Pore Pressure – Groundwater Table

The groundwater table (GWT) is technically the depth in the ground where the equilibrium pore pressure is zero or 1 atmosphere. However, the location of the GWT is only really useful when a hydrostatic condition is determined to exist. When the cone is penetrating through sandy or stratified soils, the procedure is to obtain a full dissipation to measure the equilibrium pore pressure whenever possible. For example, when penetration is stopped and it is observed that the pore pressure is rapidly dissipating, it is recommended that the operation pause for 5 minutes or more to get an equilibrium value. A minimum of three full dissipations at widely different depths are required to determine if a hydrostatic condition exists. The more full dissipations that are obtained, the more reliable is the determination. Each full dissipation should have a pressure such that the water rises to the same elevation (or GWT), to verify that a hydrostatic condition exists. Figure 6-9 is a good example of this procedure. If those conditions are not met, then a vertical seepage gradient condition exists.

If the entire CPTU profile is through clayey soils, it may not be practical to obtain a full dissipation. The best time to try to obtain full dissipation is during a lunch break.

If knowledge of the ground water condition at a clay site is critical (e.g., to establish if consolidation is completed or for slope stability analyses), the best recommendation is to install field piezometers at strategic locations.

Often when penetrating saturated sand layers, the drainage is so fast that full drainage is achieved or very close to it and it is possible to draw a hydrostatic pore pressure line on the depth profile of u_2 pore pressure as shown in Figures 4-6 and 4-7.

6.3.3 Hydraulic Gradients

Hydraulic gradients are a common occurrence, especially near aquifers, in river valleys and even in relatively flat terrain. The gradients are often small and less than 0.1 and indicate a flow or seepage in the upward direction if in a regional discharge area like a valley or downwards in a regional recharge area. To establish a vertical gradient, at least two full dissipations at two depths are needed in a CPTU sounding. To establish a horizontal gradient, two adjacent CPTU soundings are needed where at least one full dissipation is established at the same elevation in each sounding.

Figure 6-16 demonstrates a fast pore pressure dissipation. Notice that the pore pressure (units of metres of water) is plotted against square root of time, rather than the usual log of time, which does not have a value of zero time. The plot on the left shows that at a depth of 1.925 metres, the equilibrium pore pressure was 1.00 metre of water, or a piezometric level of 0.925 m below ground. The graph on the right shows the full dissipation at 8.00 m depth. If a hydrostatic condition existed the piezometric level would stay constant and the equilibrium pore pressure would be 7.075 m. Instead the measured pore water pressure was 8.35 m, which puts the piezometric level 0.35 m above ground. Thus the potential energy is higher at depth and the water is flowing upward.

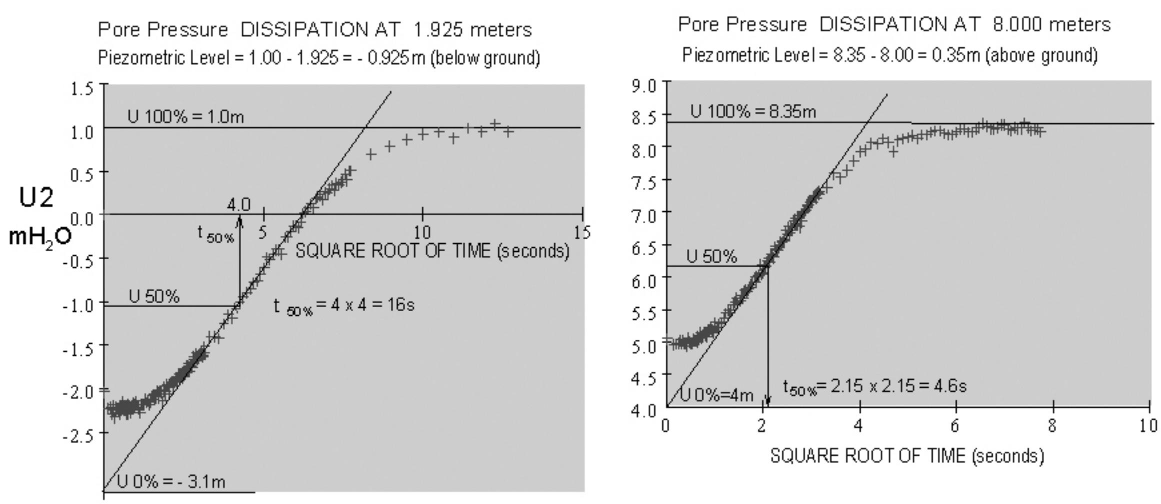

Upward Gradient = [0.35-(-0.925)] / (8.000-1.925) = 0.21 m/m

$c_h = T_{50}\, r^2 / t_{50}$ & $K = c_h\, \gamma_w / M$ let $M = \alpha q_t$ and $T_{50} \sim 75$(sand) for a = 4 (NC) and r = filter radius where $T_{50} \sim 75$ is determined from site specific correlation to measured K In-situ

Figure 6-16 Rapid Pore Pressure Dissipation in Outwash Sandy Gravel Aquifer showing Gradient Determination

The hydraulic gradient would be the total energy loss divided by the distance over that loss in the direction of flow. In this case the head loss was 0.35-(-0.925)=1.275 m and the distance (8.000-1.925)=6.075 m. The gradient is 1.275/6.075=0.21 m/m.

This example clearly demonstrates the usefulness of using units of metres of water head instead of the usual pressure units like kPa for the pore water pressure. To complete the gradient study, it would be required to determine if there is any head loss in the horizontal direction, which requires equilibrium pore pressure measurements at the same elevation but horizontally spaced. The quantity of flow would be dictated by both the gradient and the hydraulic conductivity (permeability) in the direction of flow.

6.3.4 Pore Pressure Dissipation to Measure t_{50} and Estimate Permeability

As previously explained in section 6.2.1.5 it is desirable to record the t_{50} time for dissipation each time penetration is paused. However, there is often insufficient time to reach 50% dissipation. Also, a consistent and easy procedure should be developed to obtain t_{50}, the problem being that it is not always easy to determine the starting pore pressure at zero time. It has been observed that the CPTU dissipation behaviour versus time generally follows a parabolic response up to approximately 60% dissipation, which is analogous to consolidation theory. A parabolic time response means a linear response with respect to square root of time.

Figures 6-16 and 6-17 are examples of various PPD in square root time, which demonstrate the difficulty in getting a zero time value for pore pressure. When penetration is stopped, the load is released from the push rods, which causes a pore pressure change. Also, during penetration the pore pressure on the face, u_1, could be very much more than behind the tip, u_2 or u_3, as shown in Figure 4-4. When pushing is stopped and load released, there is an immediate equalization of pore pressure around the tip. This could happen before and during the early seconds of dissipation. Thus we see in many instances where pore pressures rise before they fall and dissipate to the equilibrium value as demonstrated in the many plots in Figure 6-17. Or in the case for Figure 6-16 where pore pressure is depressed due to dilation and pore pressures rise during dissipation.

The procedure is to draw the best straight line through the initial dissipation and extrapolate the line to t=0 to obtain the initial pore pressure. The equilibrium value can usually be estimated for the depth at the site from other measurements like hydrostatic conditions and full dissipation at other depths. The pore pressure value midway between the starting and finishing value identifies the point on the best straight line fit to indicate the square root time value, which is then squared to get the time for t_{50}.

The lower right figure in Figure 6-17 shows how one can use the best straight line fit to also extrapolate the data to greater time to get t_{50} when there are insufficient data.

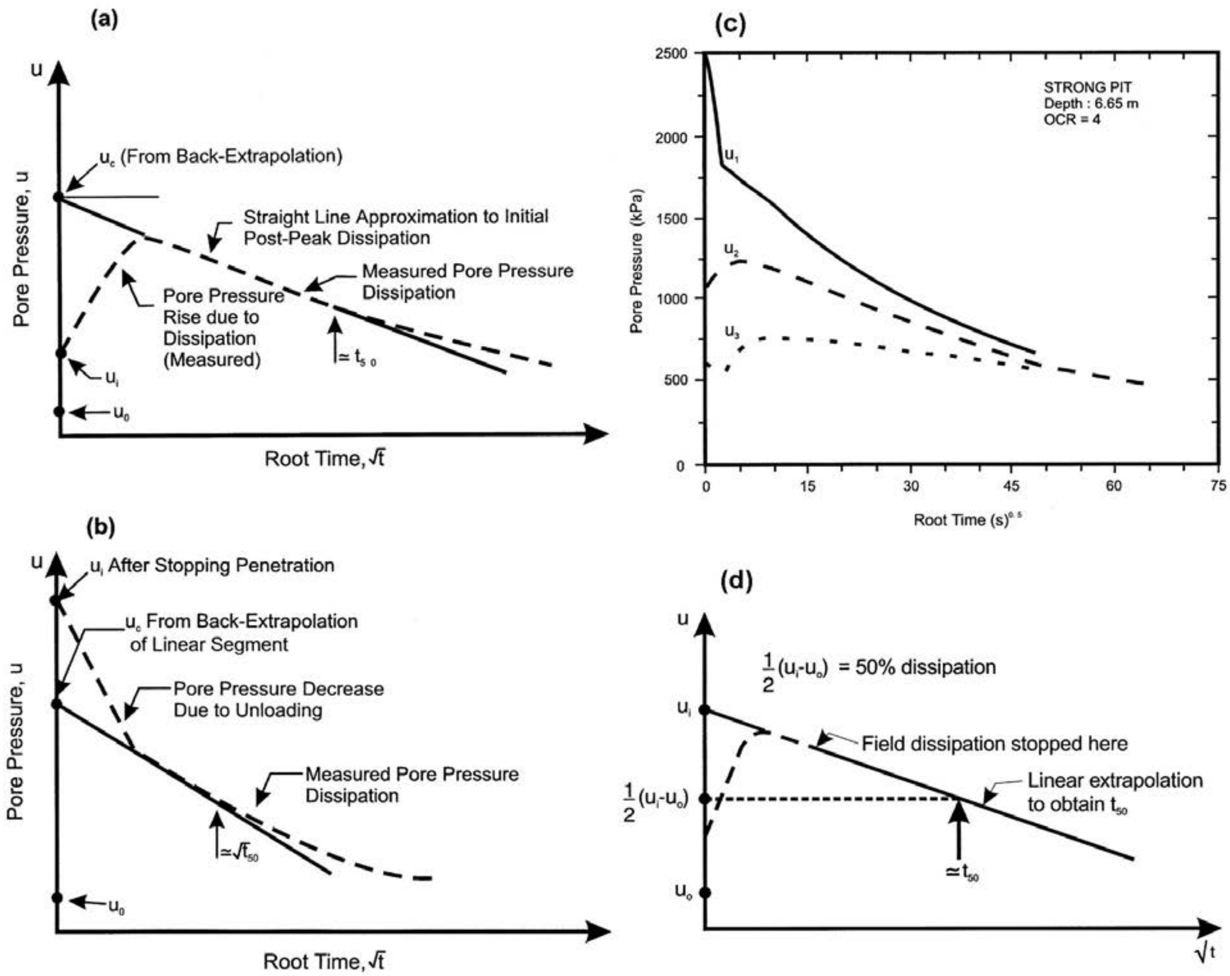

Figure 6-17 Interpreting Pore Pressure Dissipation Using Square Root of Time Plot (Sully et al. 1999)

Figure 6-16 shows the need for fast dissipation data recording in coarse and gravelly sand deposits. Here the measured t_{50} times were 16 sec and 4.5 sec. The typical data system collects PPD data every 5 seconds and would not capture the t_{50} time for these soils.

The lower part of Figure 6-16 shows the analytical procedure to calculate hydraulic conductivity (some use permeability), k, which requires both the coefficient of consolidation and the modulus or stiffness of the soil. The horizontal coefficient of consolidation, c_h, is calculated knowing t_{50}, the filter radius, r, and the time factor, T_{50}. The modulus, M, can be estimated from the average tip stress. The estimate of both c_h and M are complicated and require judgement (often require site specific correlation) and will be discussed in a later section under estimating soil properties. A very approximate approach makes use of the global correlation in Figure 6-6, which gives k values from 5-20 x 10^{-5} cm/sec.

6.4 Conclusion

This chapter has presented the recommended approach to evaluation and interpretation of CPTU data. We have illustrated how site stratigraphy, soil behaviour type and groundwater conditions can be interpreted from the CPTU data. The interpretation is greatly improved by an understanding of the geology and the factors likely to affect the data and considerable judgement is required in order to arrive at a consistent interpretation. Soil classification can be based on global classification charts but it is emphasized that these should be calibrated by local experience. When used with appropriate care and attention, the CPTU provides an extremely detailed understanding of the soil and groundwater conditions at a site.

7 ESTIMATION OF SOIL PROPERTIES

7.1 Introduction

Field exploration has two main objectives:

1. Stratigraphic Logging and Material Classification
2. Determination of the characteristic engineering behaviour of the ground.

The use of CPTU and SCPTU data for stratigraphic logging and material classification and as an aid to determination of the ground water conditions at the site has been covered in Chapter 6. Once the materials have been identified, estimates of characteristic behaviour can be made. This should be based on an understanding of the principles and limitations of engineering geology, in situ testing, sampling and laboratory testing.

The estimation of properties may be based on one or all of the following:

- Previous experience in materials with similar classification properties and of similar geological origin and history
- Site specific in situ testing
- Site specific laboratory testing
- Prototype testing, e.g. footing or pile load tests.

This chapter will deal with the interpretation of CPTU data to estimate initial stress state, stress history and material properties for use in engineering design

Seismic CPTU data can be interpreted to identify characteristics of soil behaviour using two basic approaches:

- Use of correlations between measured CPTU parameters and soil behaviour obtained by other test methods such as laboratory tests, in situ vane shear tests, calibration chamber tests where CPTU tests are run in samples under carefully controlled conditions, or back-analysis of prototype load tests or of full scale foundation performance.

- Use of analytical models to calculate soil properties from the measured CPTU parameters.

Numerical analysis techniques and constitutive models of soil behaviour are now sufficiently developed that reasonably good agreement can be obtained between numerical predictions of cone parameters and the results of chamber tests (Ahmadi

2000) (Salgado et al. 1998; Yu 2004). The primary advantage of this progress is that we now understand the many factors that contribute to the measured tip resistance, friction and pore pressure. However, chamber tests have only been carried out in a small number of soils (primarily dry cohesionless) and the chamber test samples cannot model the range of effects that affect the in situ properties such as ageing and cementation and structure. Background on chamber testing can be found in Lunne et al. (1997) and (Huang and Hsu 2004). Calibration chamber tests have been run mainly in sands because of the difficulty of obtaining undisturbed samples for independent measures of soil properties. Consequently, interpretation should be based on all the available information about the soils at a site and not only on CPTU data.

As soils are complex materials, it is necessary to simplify or idealize the material behaviour while preserving the essential characteristics. The most common idealizations used in soil mechanics for soil modelling are the following:

- Homogeneous or uniform soil – which never exists in nature;
- Equivalent elastic: most common in estimates of deformation;
- Elastic – perfectly plastic: used when considering the undrained behaviour of clays;
- Frictional-plastic in which failure is typically assumed to be represented by the Mohr-Coulomb failure criterion: used for analysis of failure in terms of effective stress.

It is also possible to carry out numerical analysis of complex geotechnical problems using finite element modelling. Such modelling can be carried out using a variety of soil models ranging from the simple models above to advanced plasticity models. A useful discussion of the merits and pitfalls of numerical modelling is provided in Potts (2003).

Derivation of design parameters from site exploration data for input to a particular design method or approach should be done with clear recognition of the idealizations that have been adopted to model material behaviour. The differences in scale, stress and strain level, and stress and strain rates between the in situ test and the full-scale design condition should be specifically addressed. Leroueil and Hight (2003) provide a comprehensive review of the current understanding of soil behaviour.

7.2 Background to correlations

Correlations between in situ cone parameters and the properties of fine-grained soils can be developed from laboratory testing on undisturbed samples. The limitations and advantages of undisturbed sampling are well-understood. However, it is very difficult to obtain undisturbed samples of sands and gravels. Hence correlations must be obtained by comparison between laboratory testing on reconstituted samples and cone parameters obtained in penetration tests in large calibration chambers (Holden, 1971).

The interaction between cone and soil can be understood by consideration of Figure 7-1 which depicts a large calibration chamber. The cavity is created by the cone. The soil close to the cone experiences shear failure and very large strains. This is the Plastic Zone. Physically, penetration of the cone requires creation of a cavity with a volume equivalent to that of the cone. During drained penetration, the soil in the plastic zone may expand or contract. During undrained penetration, no volume change occurs in the plastic zone. Under free-field conditions, for which the elastic zone is incompressible, the deformation of the elastic zone must accommodate the volume of the cone plus any volume change occurring in the plastic zone. Consequently, the tip resistance is a function of both the soil response at failure in the plastic zone and the deformation properties of the soil in the elastic zone.

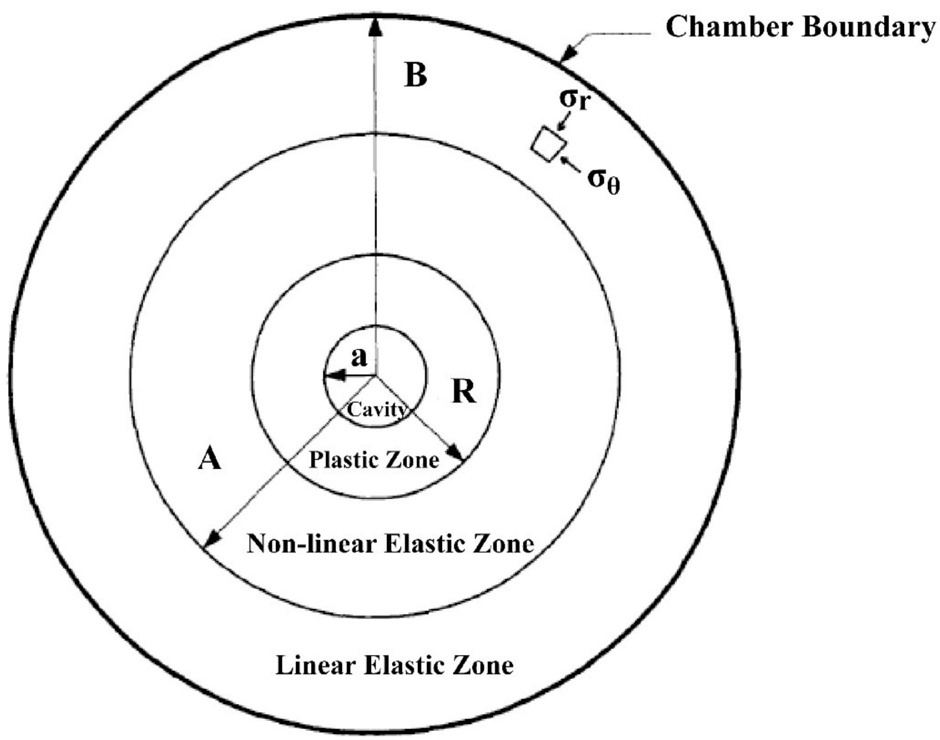

Figure 7-1 Expanded cavity in calibration chamber sample and plastic, nonlinear elastic, and elastic zones around it (Salgado et al. 1998)

This can be shown to be the case theoretically using cavity expansion concepts (e.g. Vesic 1972).

The comprehensive calibration chamber test work by Baldi et al (1986) and work by Mitchell and Keaveny (1986) showed that the cavity expansion theory appeared to model the measured response extremely well. Since 1986, many more attempts have been made to match analysis to measurements in calibration chambers using increasingly complex soil models.

The most recent efforts at modelling of cone penetration (Salgado et al. 1998; Yu 2004) can still only obtain agreement between measured and predicted tip resistances of ± 30% for chamber test data. This uncertainty means that properties cannot be obtained analytically from CPT data and has led to the adoption of empirical correlations based on chamber testing for estimating properties of sands from cone tip resistance. It has been recognized that chamber test results are affected by chamber boundary effects. Parkin and Lunne (1982) concluded that boundary conditions do not have a significant effect on cone resistance in loose sands but that the effects are considerable for dense sands. Correction factors were introduced for the effect of chamber size and boundary conditions on correlations. However, in re-evaluation of chamber boundary effects, Salgado et al. (1998) found that earlier correction factors were too low. They concluded that for chamber tests in dense (D_r =90%) Ticino sand, a typical moderately compressible silica sand, the ratio of chamber to field resistance would be between 0.5 and 0.9. They recommended that earlier correlations developed from chamber tests should be corrected if they are intended for use in field applications. Consequently, most correlations available in the literature may be unconservative in dilatant sands. For unaged loose sands, the overprediction will be much smaller but could still be 20%.

In addition to the above, Lunne et al. (1997) note that no method exists that can rationally be used to take into account the effect of ageing and cementation.

Most calibration chamber work has been carried out in dry sands and penetration is drained. Chamber testing in clay is difficult for two main reasons:

1. It takes a very long time to prepare large samples of saturated clay due to the time required for drainage.

2. Undrained penetration at constant volume results in very large chamber boundary effects which cause unnaturally high pore pressures and tip stresses.

Consequently, most correlations for fine-grained soils have been developed from field data correlated to laboratory tests on undisturbed samples.

7.3 Estimation of initial state

In order to characterize the engineering behaviour of the soil, the following parameters are critically important:

- In situ effective stresses and initial density or void ratio;
- Overconsolidation ratio or stress history to allow definition of yield stresses (also referred to as preconsolidation pressure in 1-D compression).

An understanding of site geology will aid greatly in the interpretation of CPTU data which should not be interpreted in isolation from the geological model.

A preliminary assessment of the in situ state of the soil can be made from its position on the classification chart (Figures 6-10, 6-11, 6-12) and from the ratio of G_o/q_t as discussed in section 7.3.1.3. Where penetration is undrained, the pore pressure response during penetration can be indicative of the degree of overconsolidation as is discussed in section 7.3.2.

7.3.1 Initial state of sands – estimating density, lateral stress, and stress history

7.3.1.1 Density

The in situ state of sands is usually assessed by estimating the Relative Density (D_r) from penetration resistance data. Although the stress-strain and strength behaviour of cohesionless soils is too complex to be represented solely by D_r, it is still a useful index of soil behaviour and so some discussion is given here on relating cone penetration resistance to soil D_r. Density must be considered in conjunction with confining stress.

Research in the 1970's and 80's in large calibration chambers (see Lunne et al. 1997 for a history of chamber testing) provided numerous correlations of cone resistance (q_t) with soil relative density (D_r). Most of these works showed that no single unique relationship exists between D_r, in-situ effective stress and cone resistance for all sands. This is not surprising since other factors such as soil compressibility also influence cone resistance.

A review of the numerous calibration chamber tests performed on a variety of different sands shows a significant range of D_r versus q_t relationships. However, all the chamber test results show that the curves are all similar in shape and most show that the cone resistance can be more uniquely related to D_r for any given sand, if correlated by the in-situ initial horizontal effective stress (σ'_{ho}) or mean stress, σ'_{mo} or p'_o. If σ'_{ho} or σ'_{mo} is used, the relationship can be expected to apply to both normally and overconsolidated sand. Figure 7-2 shows a comparison between the curves proposed by Schmertmann (1976b), Villet and Mitchell, (1981) and Baldi et al (1981) for two levels of D_r. All the curves have been corrected for chamber size using correction factors available at the time. Details of the sands used in the calibration chamber studies are given in Table 7-1.

The calibration test data (Figure 7-2) shows the importance of sand compressibility. The curves by Schmertmann (1976b) represent the results of tests on Hilton Mines sand, which is a relatively compressible quartz, feldspar, and mica mixture with angular grains. The curves by Villet and Mitchell (1981) represent results on Monterey Sand which is a relatively incompressible quartz sand with subrounded particles. Schmertmann (1976b) also performed tests on Ottawa sand, which is also an incompressible quartz sand with rounded particles, and obtained curves almost

Reference	Sand Name	Mineralogy	Shape	Gradation		Porosity	
				D_{60}	D_{10}	n_{max}	n_{min}
Baldi et al. (1981; 1982)	Ticino	Mainly quartz, 5%* mica	Subangular to angular	0.65	0.40	0.50	0.41
Villet & Mitchell (1981)	Monterey	Mainly quartz, some feldspar	Subrounded to subangular	0.40	0.25	0.45	0.36
Schmertmann (1976b)	Ottawa #90	Quartz	Rounded	0.24	0.13	0.44	0.33
Schmertmann (1976b)	Hilton mines	Quartz + mica + feldspar	Angular	0.30	0.15	0.44	0.30
Parkin et al. (1980)	Hokksund	35% quartz, 45% feldspar, 10%* mica	Rounded to subangular	0.5	0.27	0.48	0.36
Veismanis (1974)	Edgar	Mainly quartz	Subangular	0.5	0.29	0.48	0.35
Veismanis (1974)	Ottawa	Quartz	Subangular	0.54	0.45	0.42	0.32
Holden (1971)	South Oakleigh	Quartz	Subangular	0.19	0.12	0.47	0.35
Holden (1971)	South Oakleigh	Quartz	Subangular	0.37	0.17	0.43	0.29
Chapman & Donald (1981)	Franktson	Mainly quartz	Rounded to subangular	0.37	0.18	----	----

** Percent mica by volume*

Table 7-1 Properties of Sand Tested in Calibration Chamber Studies (After Robertson and Campanella 1983a)

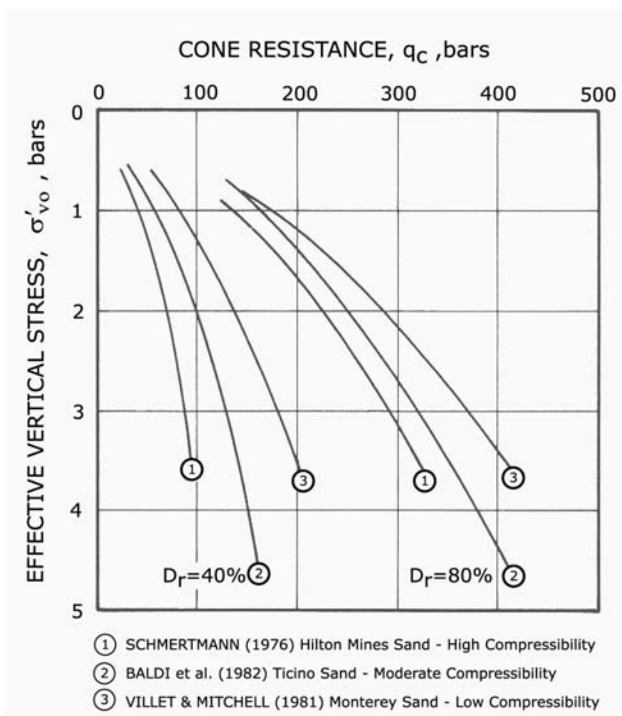

Figure 7-2 Comparison of Different Relative Density Relationships (After Robertson and Campanella 1983a)

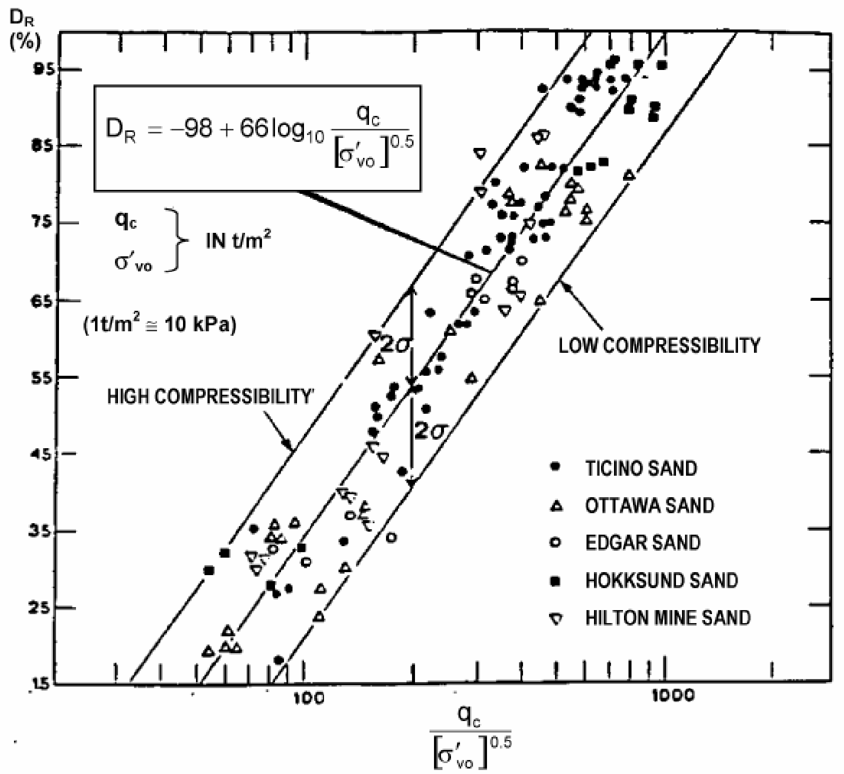

Figure 7-3 Influence of Compressibility on N.C. uncemented, unaged, predominantly quartz sands (After Jamiolkowski et al. 1985)

identical to those of Villet and Mitchell (1981). Thus, it appears that sands with a low compressibility have a D_r - q_t relationship similar to that shown by Villet and Mitchell (1981) and sands with a high compressibility have a relationship similar to that shown by Schmertmann (1976b). The sand used by Baldi et al (1986) (Ticino Sand) was a quartz, feldspar, mica mixture with subangular particles. The Ticino Sand appears to have a moderate compressibility somewhere between the two extremes of Hilton Mines and Monterey Sand. Figure 7-3 illustrates the range of D_r - q_t relationships for most of the sands tested in calibration chambers. (Note: D_R is used in some of the figures in place of D_r and q_c is used instead of q_t).

A large portion of CPT work is often carried out in siliceous sands where the grain minerals are predominately quartz and feldspar. These are sands similar to those tested in most of the calibration chamber work. Research has shown that there is relatively little variation in the compressibility for most such sands, although this depends on the angularity of the grains (Joustra and de Gijt 1982). Angular quartz sands tend to be more compressible than rounded quartz sands. If an estimate of D_r is required for a predominantly quartz sand of moderate compressibility, the writers recommend that the relation for Ticino sand be used.

The original relationship obtained for Ticino sand was published by Baldi (1986) and is given by the following expression

$$D_r = \frac{1}{C_2} \ln \left[\frac{q_t}{C_o (\sigma'_{vo})^{c_1}} \right] \tag{7.1}$$

where C_o = 157, C_1 = 0.55 and C_2 = 2.41 and q_t is in MPa.

This has been widely used in practice for interpretation of cone testing in young, normally consolidated, uncemented sands similar in compressibility to Ticino sand.

Jamiolkowski et al. (1988, 2001) re-evaluated these data incorporating revised chamber size correction factors and obtained the revised expression

$$D_r = \frac{1}{C_2} \ln \left[\frac{q_t / p_a}{C_o (\sigma'_{vo} / p_a)^{c_1}} \right] \tag{7.2}$$

where C_o = 17.74, C_1 = 0.55 and C_2 = 2.9. In this case, q_t and σ'_{vo} are normalized using p_a which is atmospheric pressure in the same units at q_t and $\sigma'_{vo.}$ The revised correlation results in a looser D_r for a given q_t and stress level with the effect being larger for denser sand.

Alternatively, the relationship may be expressed in terms of mean stress, σ'_{mo} as follows.

$$D_r = \frac{1}{C_2} \ln \left[\frac{q_t / p_a}{C_o (\sigma'_{mo} / p_a)^{c_1}} \right] \tag{7.3}$$

where C_o=23.19, C_1=0.56 and C_2=2.97 and $\sigma'_{mo} = \frac{1}{3} \sigma'_{vo} (1 + 2K_o)$.

This expression may be used for NC and OC sands. Figure 7-4 shows the updated correlation between relative density (D_r), vertical effective stress (σ'_{vo}) and cone resistance (q_t). The relationship is for normally consolidated uncemented and unaged sand. Figure 7-5 shows the relationship obtained for Ticino sand (Jamiolkowski et al. 2001) plotted in terms of mean stress instead of (σ'_{vo}). If the geological model for the site indicates OC or aged sands, then the relationship in Figure 7-5 should be used to estimate D_r. Figure 7-5 returns the same D_r as is obtained from Figure 7-4 if the mean stress is calculated assuming K_o=0.45.

It is suggested that Figures 7-4 and 7-5 should be used only as a guide to in-situ D_r, but can be expected to provide reasonable estimates for young, clean, normally consolidated, moderately compressible quartz sands. As most natural sands have been aged to some extent, a conservative approach to determining D_r would be to assume K_o=1 and use the OC chart for a first estimate of D_r. Some engineers have suggested that the D_r values obtained from charts like Figures 7-4 and 7-5 should be referred to as ***"Equivalent"*** D_r values when applied to natural sands.

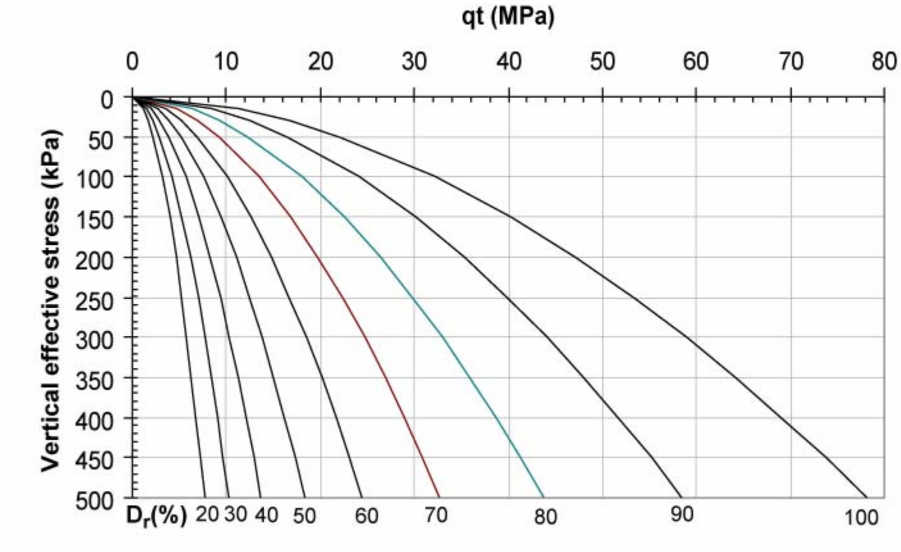

$$D_r = \frac{1}{C_2} \ln\left[\frac{q_t/p_a}{C_o(\sigma'_{vo}/p_a)^{c_1}}\right] x100\%$$

C_0=17.74
C_1=0.55
C_2=2.9

Figure 7-4 D_r correlation for N.C. moderately compressible, uncemented, unaged quartz sands (after Jamiolkowski et al., 2001)

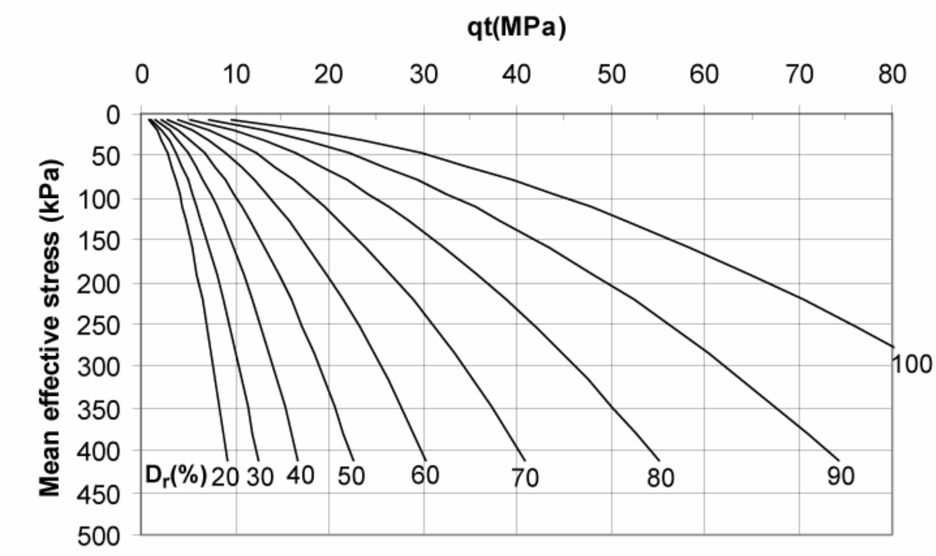

$$D_r = \frac{1}{C_2} \ln\left[\frac{q_t/p_a}{C_o(\sigma'/p_a)^{c_1}}\right] \times 100\%$$

C_0=23.19
C_1=0.56
C_2=2.97

Figure 7-5 D_r correlation for N.C. and O.C. moderately compressible, uncemented, unaged quartz sands (after Jamiolkowski, 2001)

In an attempt to avoid some of the limitations of the D_r concept, Been and Jefferies (1985) introduced the concept of State Parameter for use in the interpretation of CPTU data. The State Parameter is defined as the void ratio difference between the in situ void ratio and the void ratio at critical state e_{cs}, as shown in Figure 7-6. At any stress level, dense sands have a more negative State Parameter than loose sands. Loose sands may have a positive state parameter. A more negative state parameter indicates the soil will dilate more strongly towards failure than a soil that has a state parameter just less than zero. Soils with a positive state parameter will contract to failure. In undrained loading, soils with a positive state parameter will generate positive excess pore pressure during shear and will liquefy more easily than soils with a more negative ψ. The latter will generate negative excess pore pressures during shear and are less easily liquefied.

Been, Jefferies and their co-workers developed a unified approach to the interpretation of state from CPTU data and proposed that ψ can be related to other physical parameters like strength. The method also requires an estimate of sand compressibility and of in situ horizontal stress. Figure 6-14 is an example of how state parameter may be used in soil classification.

7.3.1.2 Assessment of compressibility

Given the importance of compressibility when interpreting CPTU data in sand, it would be useful to have a means of identifying sands of unusual compressibility. Many compressible carbonate sands have friction ratios as high as 3 % (Joustra and de Gijt 1982) whereas, typical incompressible quartz sands have friction ratios of about 0.5 %. Thus, the presence of compressible sands may be identified using the friction ratio, i.e. the position on the classification chart.

Figure 7-3 can be used as a guide to adjust the D_r correlations for sands that may be more or less compressible. A visual classification of the grain characteristics would significantly improve the choice of D_r correlation. The compressibility of sands tends to increase with increasing uniformity in grading, with increasing angularity of grains, with increasing mica content and with increasing carbonate content. Care should be exercised in interbedded deposits where the cone resistance may not have reached the full value within a layer.

More recent work in problem soils such as residual and cemented soils has led to a recognition that the combination of q_t and V_s measurements can also prove useful for this purpose. The chart shown in Figure 7-7 (Robertson et al. 1995) can be used in addition to the traditional classification charts in Figures 6-10, 11 and 12 as a first step to the identification of compressible soils. If a soil classifies as a clean sand in the traditional classification charts but falls in the “sand mixtures” classification or lower in Figure 7-7, then it may be an unusual sand. Schnaid et al. (2004) recently presented Figure 7-8 which they recommended for use in identifying soils of unusual compressibility. q_{c_1} is defined as follows:

$$\frac{(q_t/p_a)}{(\sigma'_v/p_a)^{0.5}} = \frac{q_t}{(\sigma'_{vo})^{0.5}} \tag{7.4}$$

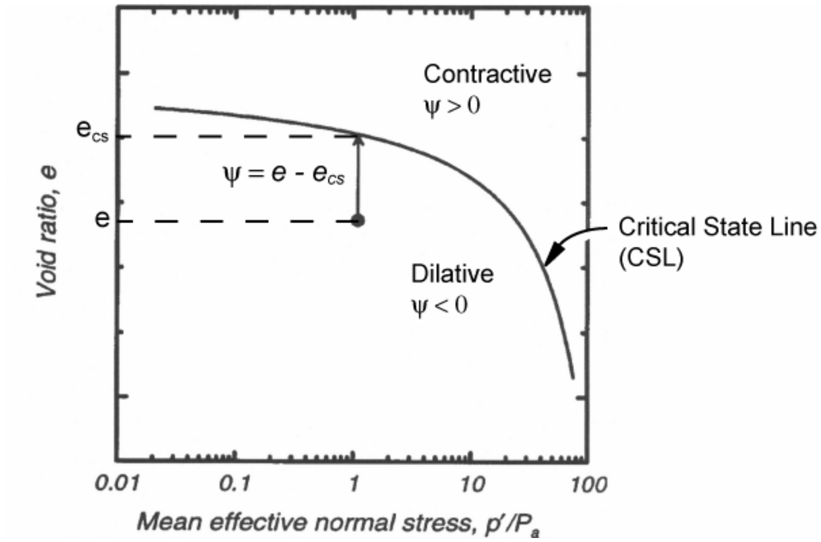

Figure 7-6 Critical state line and state parameter from Bolton's (1986) IRD relation (adapted from Boulanger 2003)

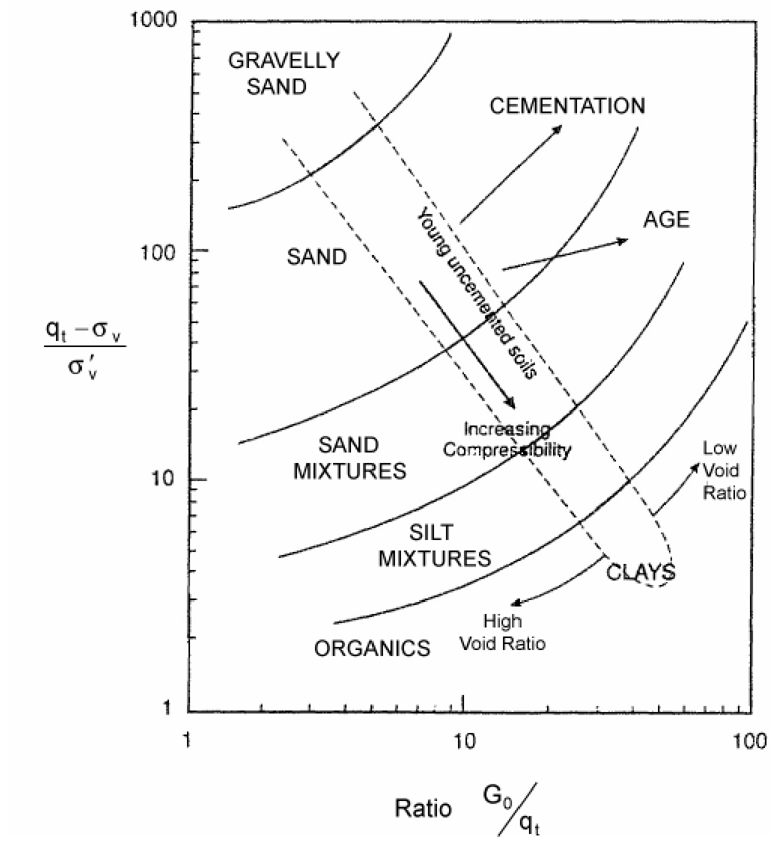

Figure 7-7 Proposed Soil behaviour type chart based on normalized CPT penetration resistance and the ratio of small strain shear modulus with penetration resistance (G_o/q_t) (Robertson et al. 1995)

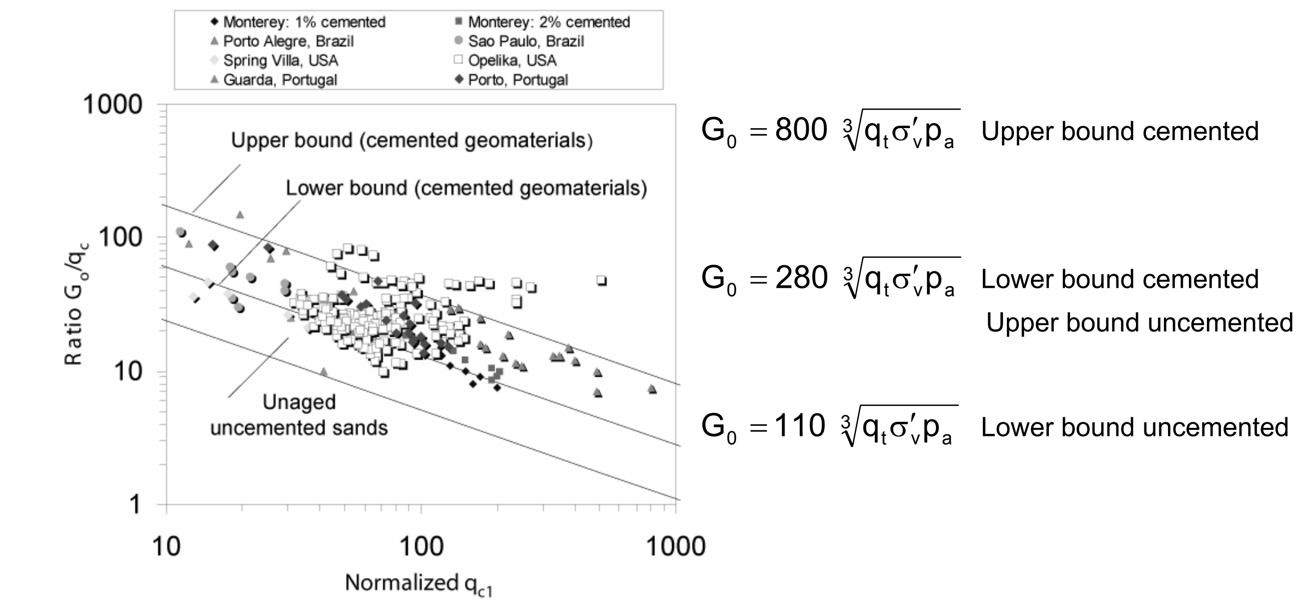

Figure 7-8 Relationship between G_o and q_c for residual soils (Schnaid et al. 2004)

7.3.1.3 Initial Stress and Stress History — Drained Penetration

When attempting to distinguish the stress history from cone penetration data during drained penetration, an indication of high horizontal stresses, i.e. high OCR, can sometimes be obtained from the D_r correlation. If Figure 7-4 is used with the vertical effective stress, σ'_{vo}, it is possible to predict relative densities in excess of 100% (D_r > l00%). This is usually a sign of high horizontal stresses or cementation.

Sometimes, the presence of high horizontal stresses can produce high friction sleeve values, f_s. However, to quantify the stress level, it is necessary to know the friction sleeve value of the same sand under normally consolidated conditions. Thus, it is impossible to distinguish between a dense normally consolidated sand and a loose overconsolidated sand. As noted in the previous section, Figures 7-7 or 7-8 can also be used to screen for cemented soils.

Mayne (2001) presented the results of an analysis of a large number of chamber tests from which he derived the following correlation for K_o:

$$K_o = 1.33 q_t^{0.22} \left(\sigma'_{vo}\right)^{-0.31} OCR^{0.27} \tag{7.5}$$

where q_t is in MP_a and σ'_{vo} is in kPa.

This approach produced the correlation between predicted and measured lateral effective stress shown in Figure 7-9. There is considerable scatter. Mayne noted that this correlation applies only to unaged sands. For mechanical overconsolidation, Mayne and Kulhawy (1982) adopted the relationship:

$$K_{o(OC)} = K_{o(NC)} (OCR)^{\sin\phi'} \tag{7.6}$$

where $(K_o)_{NC}$=1-sinϕ'. By combining relationships 7.5 and 7.6, Mayne (2001) derived the expression:

$$OCR = \left[\frac{1.33}{K_{0NC}} \frac{{q_T}^{0.22}}{({\sigma_{vo}}')^{0.31}} \right]^{1/(\sin\phi' - 0.27)} \tag{7.7}$$

where q_t' is in MPa and σ'_{vo} in kPa.

Despite the apparent scatter, Figure 7-11 (Mayne 2001) shows the predictions obtained with this expression for a site in Sweden – Stockholm sand (Dahlberg 1974) known to have experienced mechanical unloading. The agreement is good. The reader is cautioned that this applies only to conditions of mechanical unloading.

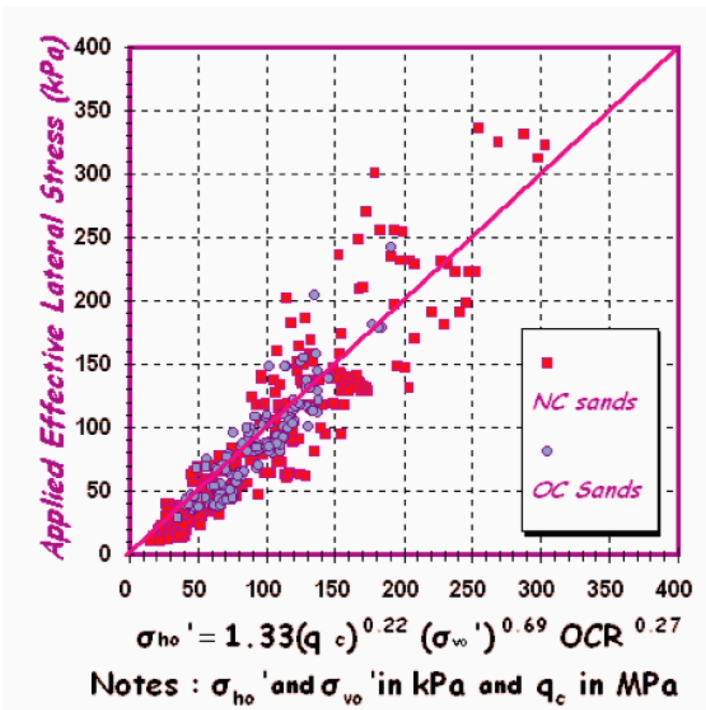

Figure 7-9 CPT calibration chamber relationship for evaluating lateral stresses in unaged clean quartz sands (Mayne, 2001)

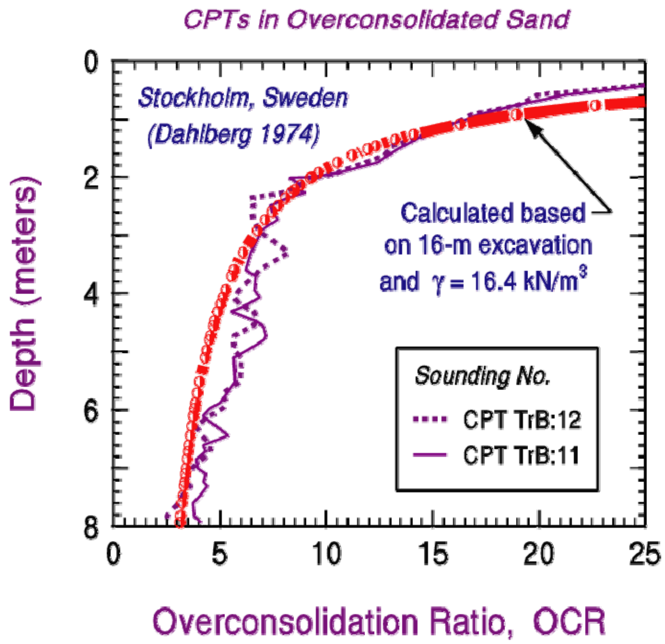

$$OCR = \left[\frac{1.33}{K_{0NC}} \frac{q_T^{0.22}}{(\sigma'_{vo})^{0.31}}\right]^{1/(\sin\phi' - 0.27)}$$

Figure 7-10 CPT-evaluated profile of OCR in Stockholm sand deposit (data reported by Dahlberg, 1974) (Mayne, 2001)

Attempts have also been made to use both q_t and the shear wave velocity to determine OCR and lateral stress as both are different functions of stress and D_r (Eslaamizaad and Robertson 1996b). While initial results are encouraging, assessment of lateral stress and stress history in sands is still difficult and requires additional research.

7.3.2 Initial stress and stress history — undrained penetration.

7.3.2.1 Qualitative methods

In fine-grained soils, the stress history of the soil can be estimated qualitatively from the shape of the tip resistance profile or, in saturated soils, from the pore pressure response. This was explained in Section 6.2. Correlations are also available that allow quantitative estimates of σ'_p or OCR where:

$$OCR = \frac{\sigma'_p}{\sigma'_{vo}} \tag{7.8}$$

The shape of the tip resistance profile can give an approximate indication of stress history. For normally consolidated clay deposits with hydrostatic groundwater conditions, the tip resistance increases linearly with depth and has zero tip stress at zero depth. For most young clays where overconsolidation has been caused by erosion or desiccation, the OCR will decrease with depth until the deposit, at depth, is approximately normally consolidated. In these cases, the tip resistance would be approximately constant or even decrease with depth until the depth where the deposit is normally consolidated, and will then increase linearly with depth. For aged clays where the OCR is constant with depth, the tip resistance increases with depth but has a positive tip stress at zero depth. An example of this kind of profile is shown in Figure 6-3a and b.

Baligh et al. (1980) suggested that the pore pressure measured during undrained cone penetration may reflect the stress history of a deposit and the OCR and this has led to many attempts to derive correlations between pore pressure parameters and OCR.

7.3.2.2 Methods based on correlations

Wroth (1984) pointed out that only the shear induced excess pore pressure reveals the nature of the soil behaviour and depends on stress history. Unfortunately, because of the complex nature of cone penetration, it is not possible to isolate the shear induced pore pressures. However, the pore pressures measured immediately behind the cone tip (u_2) appear to be mostly influenced by shear stresses, although changes in normal stresses complicate any quantitative interpretation.

A review of published correlations shows that no unique relationship exists between the normalized pore pressure ratios at one location and OCR, because pore pressures measured at any one location are influenced by clay sensitivity, preconsolidation mechanism, soil type and local heterogeneity (Battaglio et al. 1986; Robertson 1986; Robertson et al. 1986).

Since the shear induced pore pressures cannot be isolated with measurements at any one location on the cone, Campanella et al. (1985) suggested that the difference between pore pressures measured on the face and somewhere behind the tip may correlate better with OCR, as was subsequently shown by Sully et al. (1988).

At present, any empirical relationship should be used to obtain only quantitative information on the variation of OCR within the *same* relatively homogeneous deposit.

<u>Approach based on net tip resistance</u>

Demers and Leroueil (2002) carried out an investigation of 9 methods available in the literature for estimating preconsolidation pressure (or yield stress) and OCR from CPTU data. Based on a database of 31 sensitive clays from Quebec, Canada, they found that the relationship that worked best for determination of σ'_p was based on the net tip resistance, (q_t-σ_v). They derived a linear relationship for Quebec clays:

$$\sigma'_P = \frac{(q_t - \sigma_{vo})}{3.4} = 0.29(q_t - \sigma_{vo}) \tag{7.9}$$

Chen and Mayne (1996) also found a linear relationship between net tip stress and σ'_r as shown in Figure 7-11. They considered both intact and fissured clays and appeared to note an effect of plasticity. For intact clays, Chen and Mayne derived

$$\sigma'_p = 0.305(q_t - \sigma_{vo}) \tag{7.10}$$

Based on the above, an initial estimate of σ'_p may be obtained from the relationship

$$\sigma'_P = 0.3(q_t - \sigma_{vo}). \tag{7.11}$$

It follows that OCR may then be estimated using the expression:

$$OCR = \frac{\sigma'_P}{\sigma'_{vo}} = 0.3\frac{(q_t - \sigma_{vo})}{\sigma'_{vo}}. \tag{7.12}$$

Lunne et al. (1997) recommend the use of:

$$OCR = kQ_t = k\frac{(q_t - \sigma_v)}{\sigma'_v} \tag{7.13}$$

with k varying from 0.2 to 0.5 but recommend an average value of 0.3 with higher values appropriate in aged, heavily overconsolidated clays.

The findings of Demers and Leroueil (2002) and Chen and Mayne (1996) indicate that OCR may be estimated for many clays using Equation 7.13. However, these profiles should not be used for final design and site specific correlations should be developed based on oedometer tests on high quality samples.

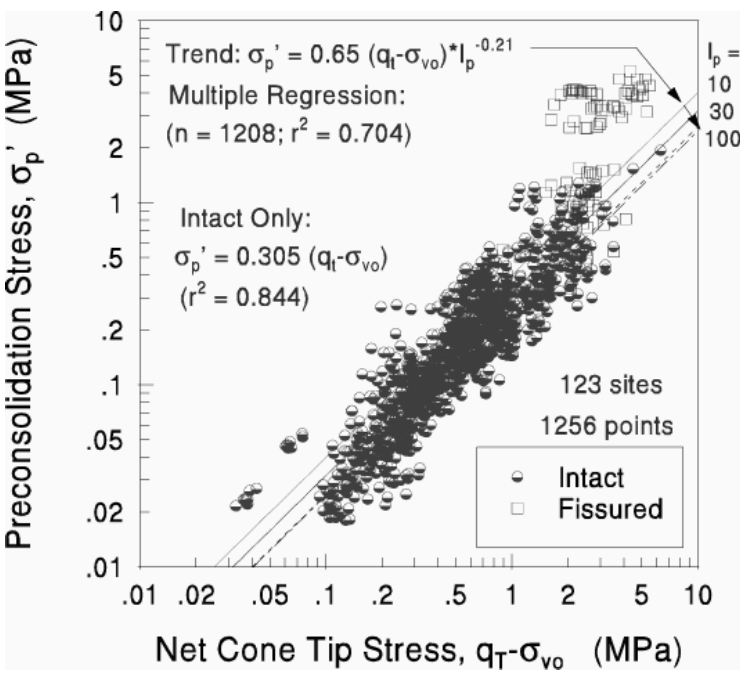

Figure 7-11 Empirical trend for σ'_p and net tip stress in clays (After Chen and Mayne, 1996)

Approach based on undrained strength ratio

OCR may also be estimated using a method based on the undrained shear strength ratio, s_u/σ'_{vo}, using values of shear strength interpreted from the q_t profile in combination with the SHANSEP expression (Ladd and Foott 1974):

$$OCR = \left(\frac{s_u / \sigma'_v}{S}\right)^{1/m} \tag{7.14}$$

S is the undrained strength ratio for normally consolidated soils which must be chosen carefully as it varies depending on the type of test used to determine undrained strength. Figure 7-12 shows how plasticity index (PI) affects the variation of $\left(\frac{s_u}{\sigma'_{vo}}\right)_{NC}$ with mode of shear in common laboratory tests.

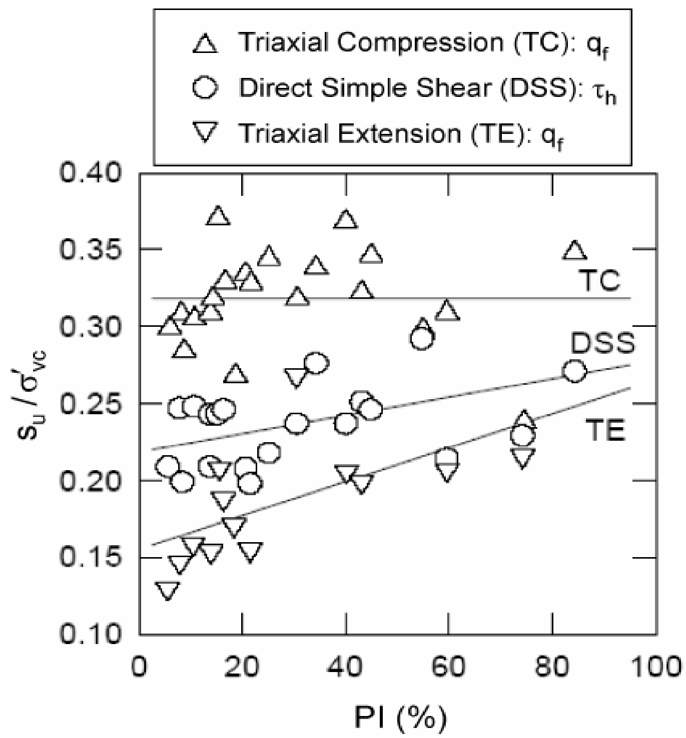

Figure 7-12 Undrained Strength Anisotropy from CK_0U Tests on Normally Consolidated Clays and Silts (data from Lefebvre et al. 1983; Vaid and Campanella 1974; and various MIT and NGI Reports) (Ladd 1991)

For undrained strengths measured by field vane shear, $s_{u(FV)}$, Chandler (1988) found that m=0.95. The OCR was given by the expression:

$$OCR = \left(\frac{s_{u(FV)} / \sigma'_v}{S_{FV}}\right)^{1.05} \tag{7.15}$$

where S_{FV} is the field vane undrained strength ratio measured at OCR=1.0. S_{FV} was obtained from Bjerrum's (1973) relationship for "Young" clays shown in Figure 7-13 (Ladd and DeGroot 2003).

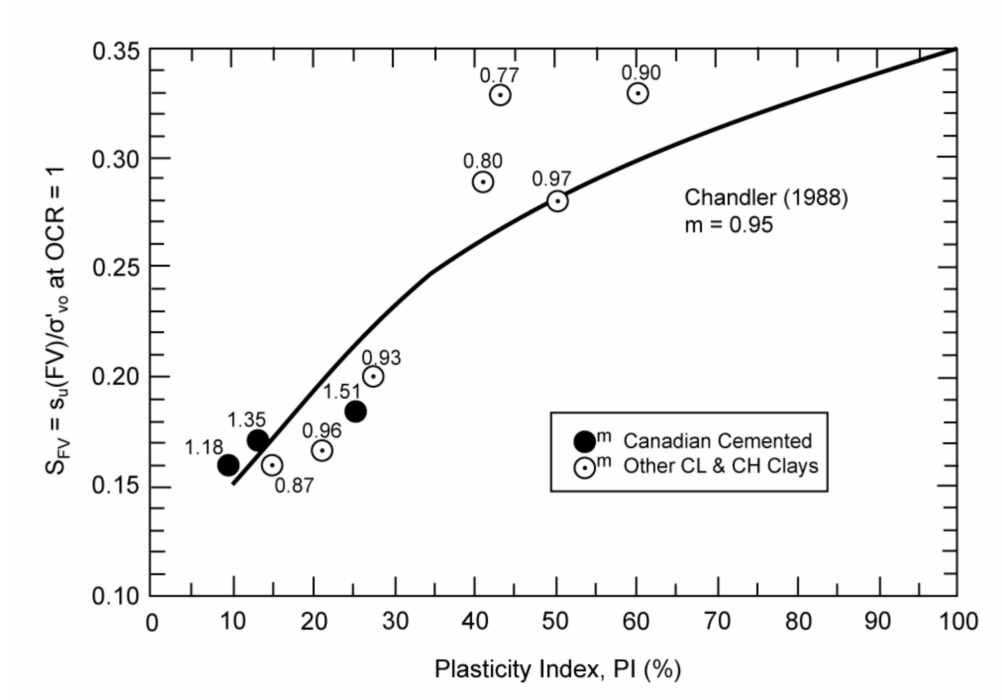

Figure 7-13 Field vane undrained strength ratio at OCR = 1 vs. plasticity index for homogeneous clays (no shells or sand) [data points from Lacasse et al. 1978 and Jamiolkowski et al. 1985] (Ladd and deGroot, 2003)

Ladd and de Groot (2003) found that Equation 7.15 worked well except in strongly structured clays and that σ'_p could be found with good accuracy when field vane test results were used. Successful use of the technique requires a good correlation between q_t and $(s_u)_{FV}$ — see Section 7.4.2.

The recommended approach is the following:

i) estimate $(s_u)_{FV}$ from q_t or Δu (see 7.4.2);

ii) estimate vertical effective stress, σ'_{vo}, from soil profile;

iii) compute s_u/σ'_{vo};

iv) estimate S_{FV} from the curve in Figure 7-13. A knowledge of the plasticity index (PI) is required.

v) estimate OCR from equation 7.15.

Chandler indicated that this approach based on $(S_u)_{FV}$ would give the OCR within ±25%. He excluded the use of this approach in cemented, sensitive, strongly structured, organic or otherwise unusual clays.

An earlier version of this approach was proposed by Schmertmann (1975) based on s_u determined from direct simple shear and triaxial tests. He used m=0.8 in equation 7.14 as shown in Figure 7-14. This is the approach programmed into the FREEWARE program CPTINT described in Chapter 8. If no plasticity information is available, OCR can be determined using Figure 7-14. Schmertmann (1978) cautioned that this approach to estimating OCR could lead to large error. Local calibration is required.

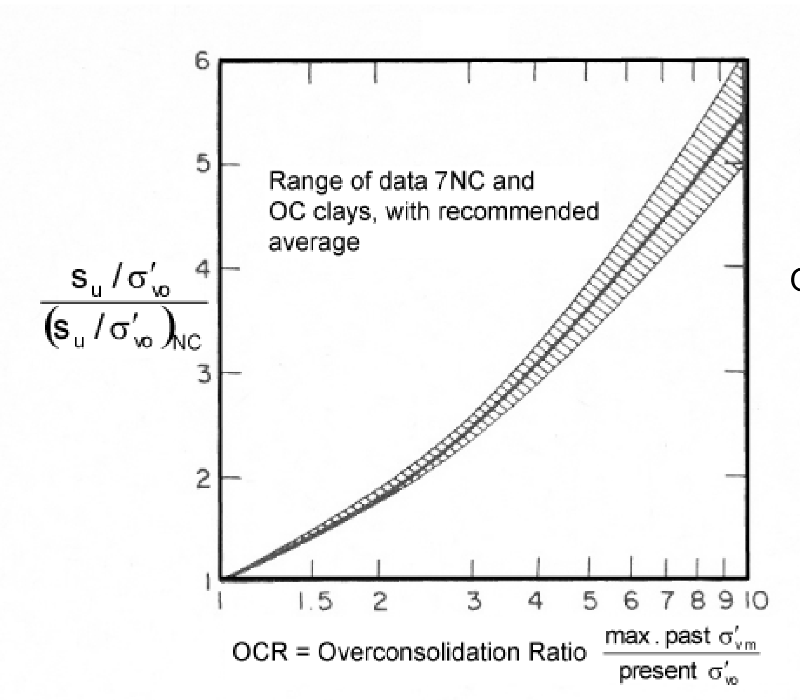

$$OCR = \left[\frac{(s_u / \sigma'_v)}{(s_u / \sigma'_v)_{NC}} \right]^{1.25}$$

Figure 7-14 Normalized s_u/σ'_{vo} ratio and Plasticity Index, for normally consolidated clays

Experience in the low plasticity clayey silts in the Vancouver area indicates that reasonable estimates of σ'_p and OCR can be obtained using Figure 7-14 with $(s_u)_{FV}$ data and an S_{FV} = 0.25.

Once OCR is estimated, the following expression may be used to estimate K_o:

$$K_o = (1 - \sin\phi'_{tc}) OCR^{\sin\phi'_{tc}} \tag{7.16}$$

where ϕ'_{tc} is the triaxial compression ϕ' value (Kulhawy and Mayne 1990).

7.4 Estimation of mechanical properties

7.4.1 Strength—Drained Soil

7.4.1.1 Bearing capacity approach

Many theories and empirical or semi-empirical correlations for the interpretation of drained shear strength of sand from cone resistance have been published. The theories can be divided into two categories; namely those based on bearing capacity theory (Durgunoglu and Mitchell 1975; Janbu and Senneset 1974) and those based on cavity expansion theory (Vesic 1972).

Work by Vesic (1963) showed that ***no unique relationship*** exists between friction angle for sands and cone resistance, since soil compressibility influences the cone resistance. The curvature of the Mohr-Coulomb failure envelope for granular soils also affects tip resistance.

A common correlation used to determine an estimate of the peak friction angle that would be measured in a drained triaxial compression test was given by Robertson and Campanella (1983a)

They analysed chamber test data as shown in Figure 7-15. Details of the sands used in the studies were given in Table 7-1. They concluded that the limited scatter in the results illustrated the limited influence of soil compressibility on interpreted shear strength. Also shown in Figure 7-15 are the theoretical relationships proposed by Janbu and Senneset (1974) and Durgunoglu and Mitchell (1975). The Durgunoglu and Mitchell method includes the effect of in-situ horizontal stresses. The difference between the normally consolidated state, where K_o=1-sinϕ, and the overconsolidated state (OCR $\approx$ 6), where K_o = 1.0, is less than 2 degrees, as shown on Figure 7-15. Robertson and Campanella proposed an average empirical relationship which was used to derive Figure 7-16.

The relationship shown in Figure 7-16 can be expected to provide reasonable estimates of peak friction angle for normally consolidated, uncemented, moderately incompressible, predominantly quartz sands, similar to those used in the chamber studies. For highly compressible sands, the chart would tend to predict conservatively low friction angles (see Figure 7-16). Durgunoglu and Mitchell's theory shows that there is little change in predicted friction angle for relatively large changes in stress history. It is important to note that the friction angle predicted from Figure 7-16 is related to the in-situ initial horizontal stress level before cone penetration.

It is recommended that, for sands that fall within zones 7, 8, 9 and 10 in Figure 6-10, the peak friction angle can be estimated using Figure 7-16. In overconsolidated sands, Figure 7-16 may slightly overestimate the friction angle by up to about +2° (see Figure 7-15). Care should be exercised in interbedded deposits where the cone resistance may not have reached the full value within a layer.

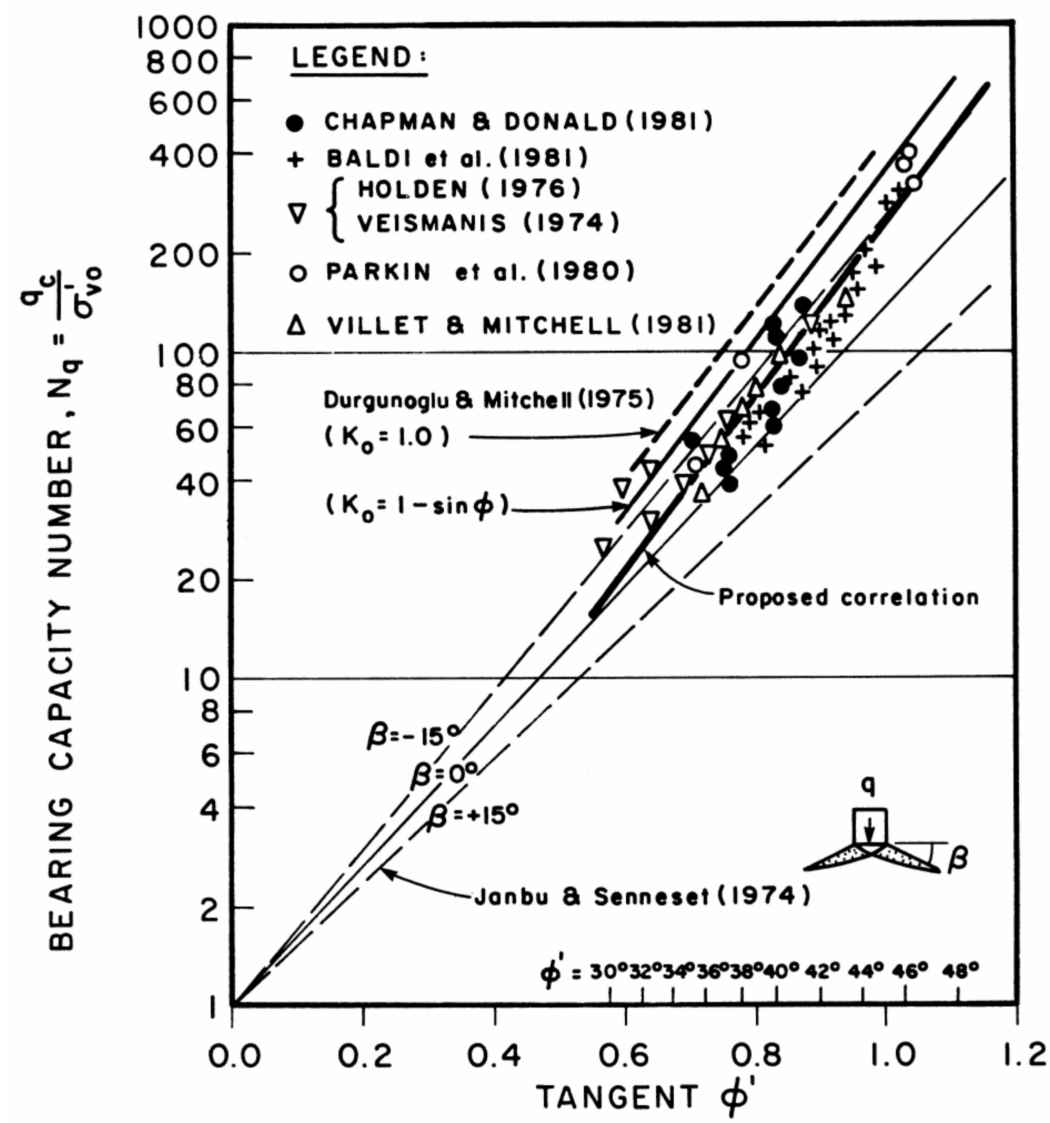

Figure 7-15 Relationship between Bearing Capacity Number and Friction Angle from large Calibration Chamber Tests (After Robertson and Campanella 1983a)

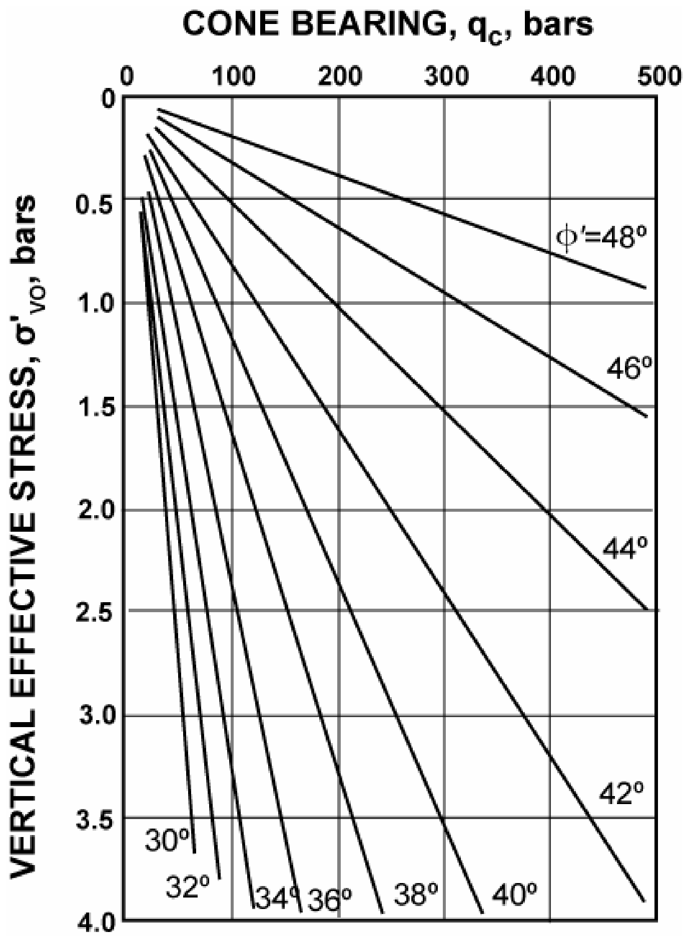

Figure 7-16 Proposed Correlation between Cone Bearing and Peak Friction Angle for Uncemented Quartz Sands (After Robertson and Campanella, 1983a)

7.4.1.2 Alternative approaches

Been and Jefferies (1985) proposed the use of State Parameter approach (see section 7.3.1.2) to determine the shear strength of sand. This method incorporates the determination of the Steady State Line (SSL) on disturbed samples of sand and the measurement of the in situ horizontal effective stress (σ'_{ho}). The incorporation of the slope of the SSL attempts to account for variations in sand compressibility. For sands with dominant silica content, the state parameter approach gives similar answers to those obtained using Figure 7-16.

A related approach has been developed based on the work of Bolton (1986). It uses the idea that increased mean normal stress suppresses the tendency for dilation. Where dilation is prevented, the friction angle of the sand at failure is ϕ_{cv},, representing shear at constant volume (CV). ϕ_{cv} depends primarily on the mineralogy of the soil. ϕ_{cv} has also appeared in the literature as ϕ_{ss} for the friction angle at Steady State (SS) or ϕ_{crit} for the angle at Critical State. For this discussion, it is assumed that $\phi'_{ss} = \phi'_{crit} = \phi'_{cv}$. Table 7-2 provides a list of values of ϕ_{cv} for a number of typical sands discussed in the literature.

SAND	MINERALOGY		Q	ϕ_{cs}	REFERENCE
TICINO	SILICEOUS (**)		10.8	34.6	
TOYOURA	QUARTZ		9.8	32.0	Jamiolkowski et al., 1988
HOKKSUND	SILICEOUS		9.2	34.0	
MOL	QUARTZ		10.0	31.6	Yoon, 1991
OTTAWA	QUARTZ	FINES 0%	9.8	30.0	Salgado et al. 1997 Salgado et al. 2000
		FINES 5%	10.9	32.3	
		FINES 10%	10.8	32.9	
		FINES 15%	10.0	33.1	
		FINES 20%	9.9	33.5	
ANTWERPIAN	QUARTZ & GLAUCONITE		7.8 to 8.3	31.5	Yoon, 1991
KENYA	CALCAREOUS		9.5	40.2	Jamiolkowski et al., 1988
QUIOU	CALCAREOUS		7.5	41.7	

(*) inferred from TX compression tests

(**) i.e.: containing a comparable amount of quartz and feldspar grains

Table 7-2 Q and $\phi_{cv} = \phi_{cs}$ values for different uniform sands (*) (Adapted from Jamiolkowski et al. 2001)

According to this approach, the peak friction angle is greater than ϕ_{cs} by an amount that depends on the amount of dilation required to allow the particles to move past each other during shear. Bolton (1986) proposed an empirical procedure to estimate the dilatancy potential of a sand. He showed that it could be captured by the Relative Dilatancy Index, I_{RD}, given by the expression:

$$I_{RD} = D_r\left(Q - \ln\frac{100}{p_a}p'\right) - 1 \qquad (7.17)$$

where D_r is the relative density, p' is the mean normal stress and p_a is atmospheric pressure in the same units as p'. Q is a parameter related to the mineralogy of the soil as shown in Table 7-2. The difference between the peak friction angle and the angle at general shear failure, $\phi'_{max}-\phi'_{cs}$ was found to be a function of I_{RD}. For different values of I_{RD}, zero dilation occurs at a specific value of mean normal stress as shown in Figure 7-17. The value of p' at zero dilation decreases as I_{RD} diminishes, i.e. as the soil gets looser. Using this approach, the peak friction angle of a sand can be estimated using the equation:

$$\phi'_{peak} - \phi_{cs} = 3\,I_{RD} \text{ for triaxial conditions} \qquad (7.18)$$

$$\phi'_{peak} - \phi_{cs} = 5\,I_{RD} \text{ for plane strain}$$

once D_r has been interpreted from q_t data. Again an estimate of K_o is required to allow estimation of mean normal stress. The values of Q and ϕ_{cs} must be chosen based on a knowledge of the sand mineralogy. Using this approach, the engineer can choose a friction angle appropriate to the stress levels applied in his or her design problem.

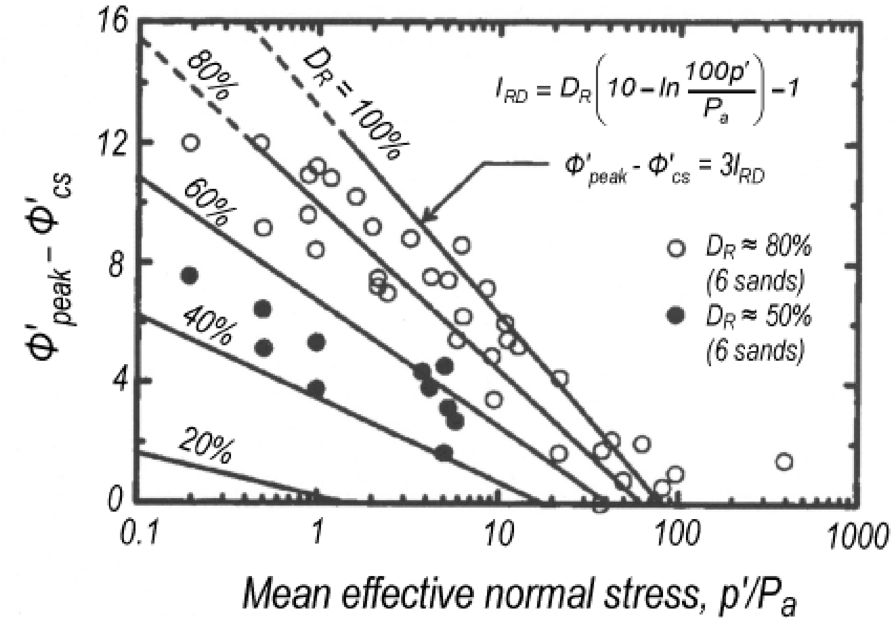

Figure 7-17 Use of relative dilatancy index (I_{RD}) to predict dilatancy angle in drained triaxial compression tests (after Bolton 1986) (Boulanger 2003)

Jamiolkowski et al. (2001) have derived charts based on an adaptation of the Bolton (1986) theory to illustrate how peak friction angle varies with sand type and stress level. They also illustrate how this approach can be used for selecting appropriate design parameters. The figures illustrate the effects on estimated peak friction angle with variation in sand type.

7.4.1.3 Conclusion on shear strength of sands

All approaches have their merits but have been verified only through comparison with chamber test data. Jamiolkowski et al. (1988) noted that due to the effects of aging, it is likely that any correlations based on chamber test data will lead to an overestimate of D_r and this would lead to an overestimate of properties derived from D_r. This cannot be overcome. It is recommended that a first estimate of peak friction angle may be obtained from Figure 7-16. The friction angle may also be calculated based on the interpreted D_r and the method of Bolton (1986), and the two values compared. This will require an assumption about K_o and ϕ_{cs}. G/q_t should also be checked to ensure that the sand is not unusual.

The choice of design value of friction angle should be based on a good understanding of the stress levels and modes of shearing in the design case. The peak triaxial value at in situ stress is rarely appropriate for use in foundation design.

7.4.2 Shear Strength—Undrained Penetration

7.4.2.1 Undrained Shear Strength

7.4.2.1.1 Peak Strength

One of the earliest applications of the cone penetration test was in the evaluation of undrained shear strength (s_u) of clays. Analytical solutions to the problem of cone penetration generally derive an equation of the form:

$$q_t = N_c s_u + \sigma_o \tag{7.19}$$

where N_c is a theoretical cone factor, and σ_o is the in situ total stress. An advantage of such an approach to the problem is that an understanding is gained of the factors affecting cone penetration. Yu and Mitchell (1998) reviewed these analytical methods and concluded that cavity expansion theories gave the closest overall agreement between predicted and measured q_t. For undrained penetration, the cone factor N_c is a function of the rigidity index, G/s_u, showing the effect of soil stiffness as well as strength on the penetration resistance. However, as real soil is always different from the idealization used in the models, it is necessary to resort to empirical correlations to obtain a relationship between in situ undrained shear strength and q_t.

As the undrained shear strength of clay is not a unique parameter and depends significantly on the mode of shearing, the rate of strain and the orientation of the failure planes, it is important to define a reference shear strength. In normally consolidated soils, q_t is often correlated with the field vane shear strength, $(s_u)_{FV}$. When the reference value of shear strength is based on laboratory testing, the value of cone factor obtained will depend on the degree of sample disturbance experienced by the soil during and after sampling and on the type of laboratory test carried out.

Estimates of s_u from q_t are made using the following equation:

$$s_u = \frac{q_t - \sigma_{vo}}{N_{kt}} \tag{7.20}$$

where

σ_{vo} is the in-situ total overburden pressure

N_{kt} is an empirical cone factor.

Early attempts at correlations did not necessarily include the correction for pore pressure effects from q_c to q_t and correlations were made to a variety of reference shear strengths. This resulted in a large range of cone factors being reported. It is now common to make preliminary estimates of $(s_u)_{FV}$ using an N_{kt} factor of 15. For sensitive clays, N_{kt} should be reduced to around 10 or less, depending on sensitivity. Powell and Quaterman (1988) noted that it is more difficult to establish similar correlations in stiff over-consolidated clays because of the important effects of fabric and fissures on the response of the clay.

Some investigators (Campanella and Robertson 1982; Lunne et al. 1985; Robertson et al. 1986; Senneset et al. 1982) have suggested the use of "effective" cone resistance, q_e, to derive correlations to s_u where q_e is defined as follows:

$$q_e = q_c - u_2 \tag{7.21}$$

and u_2 = total pore pressure measured immediately behind the cone tip. Mayne (1991) developed a relationship based on cavity expansion theory and critical state soil mechanics between s_u and q_e which has been recently modified by Trevor and Mayne (Trevor and Mayne 2004). The method appears to capture the general trends of variations in s_u with depth compared to field vane values.

One major drawback of this approach is the reliability to which q_e can be determined. In soft normally consolidated clays, the total pore pressure, u_2, generated immediately behind the tip during cone penetration is often approximately 90 percent or more of the measured cone resistance, q_c. Even when q_c is corrected to q_t, the difference between q_t and u_2 is often very small. Thus, q_e is often an extremely small quantity and is sensitive to small errors in q_t measurements.

Using excess pore pressure to estimate s_u - Several relationships have been proposed between excess pore pressure (Δu) and s_u based on theoretical or semi-theoretical approaches using cavity expansion theory (Battaglio et al. 1981; Campanella et al. 1985; Massarsch and Broms 1981; Randolph and Wroth 1979; Vesic 1972) using:

$$s_u = \frac{\Delta u}{N_{\Delta u}} \tag{7.22}$$

where $N_{\Delta u}$ can vary between 2 and 20 (on a global basis).

These methods have the advantage of increased accuracy in the measurement of Δu, especially in soft clays, where Δu can be very large. In soft clays, the cone resistance can be very small and typically the cone tip load cell may be required to record loads less than 1% of rated capacity with an associated inaccuracy of up to 50% of the measured values. However, in soft clays, the pore pressures generated can be very large and the pressure transducer may record pressures up to 80% of its rated capacity with an associated accuracy of better than 1% of the measured value. Therefore, estimates of s_u in soft clays will inherently be more accurate using pore pressure data, as opposed to the tip resistance.

The cone resistance and the excess pore pressures generated during cone penetration into fine grained soils will be dependent on the stress history, sensitivity and rigidity index. Low values of stiffness ratio generally apply to highly plastic clays (plasticity index, PI > 80) which tend to generate low pore pressures. High values of stiffness ratio generally apply to low plastic clays and silts (PI $\leq$ 15) which tend to generate high pore pressures. The excess pore pressures also tend to increase with increasing soil sensitivity and decrease with increasing overconsolidation ratio (stress history). A semi-empirical solution was proposed by Massarch and Broms (1981) based on cavity expansion theories which included the effects of overconsolidation and sensitivity by using Skempton's pore pressure parameter at failure (A_f). Campanella et al. (1985) presented the charts in Figure 7-18. An estimate of the rigidity index and A_f is required to use the charts. Massarsch and Broms (1981) developed their method based on values of G at 50% of failure stress and undrained shear strength in triaxial tests and so this is the value that should be used in Figure 7-18.

If pore pressures are measured immediately behind the cone tip, the measured values may not have reached the true cylindrical cavity expansion value. Therefore s_u estimated from the chart with the pore pressures behind the tip may be slightly overestimated. Also because of the tendency for low or negative pore pressures measured behind the tip in insensitive, overconsolidated clays, the chart in Figure 7-18 is not recommended for highly overconsolidated clays ($-0.5 < A_f < 0$). There has been some research work suggesting that $N_{\Delta u}$ is related to the B_q parameter but while this appears to hold on a site specific basis, no global correlation has been identified. Lunne et al. (1997) recommend using a value of $N_{\Delta u}$ of between 7 and 10 using $\Delta u = u_2 - u_o$.

Conclusion on shear strength from undrained penetration - For standard cone testing it is recommended that Equation 7.20 be used with an N_{kt} value of 15 for preliminary assessment of s_u, if no data are available for s_u. For sensitive clays, the N_{kt} value should be reduced to around 10 or less depending on the degree of sensitivity. The overburden pressure can be taken as the total vertical stress. With local experience, individual correlations for N_{kt} should be determined for specific clays. **It is also recommended that N_{kt} be defined for a specific method of evaluating s_u, such as by the field vane test, since s_u is not a unique soil parameter.**

For very soft soils, $N_{\Delta u}$ **may prove useful. If possible, always make a direct measurement of s_u (field vane or even U-U, etc.) and determine $N_{\Delta u}$ for specific clay layers at a given site to determine s_u profiles from CPTU data.**

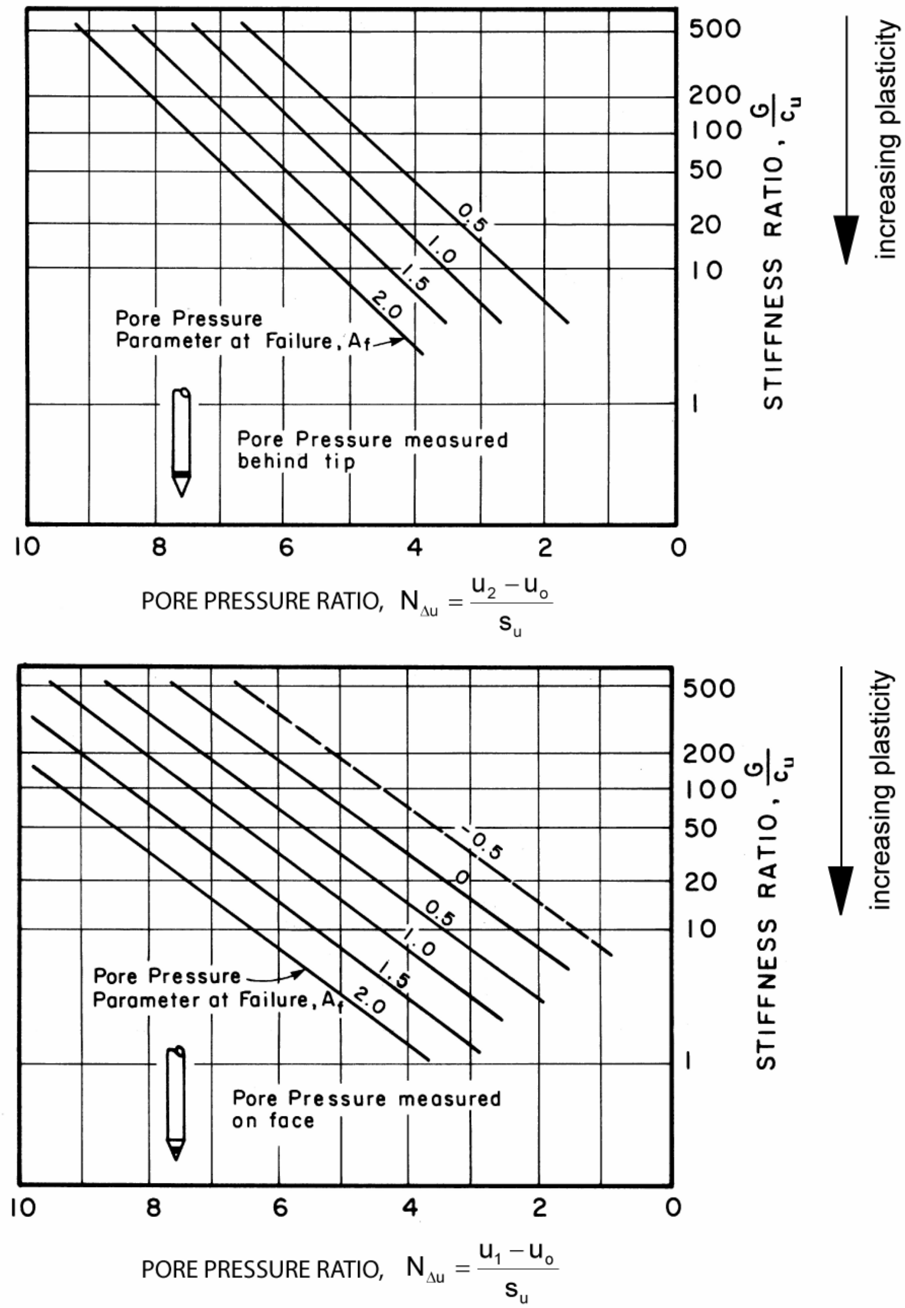

Saturated Clays	Approximate A_f Range
Very sensitive to quick	1.5 - 3.0
Normally consolidated	0.7 - 1.3
Lightly overconsolidated	0.3 - 0.7
Highly overconsolidated	-0.5 - 0

Figure 7-18 Proposed Charts to Obtain s_u from Excess Pore Pressure, Δu, Measured during CPTU (adapted from Campanella et al. 1985)

7.4.2.1.2 Remoulded Strength/Sensitivity

The sensitivity (S_t) of a clay, which is the ratio of undisturbed strength to totally remoulded strength, can be estimated from the friction ratio (R_f%) using,

$$S_t = \frac{N_s}{R_f\,\%} \tag{7.23}$$

Schmertmann (1978) suggested a value of N_s = 15 for mechanical CPT data. Robertson and Campanella (1983b) initially suggested N_s=10 for electronic CPT data. Lunne et al. (1997) recommend using N_s=7.5. Local correlations should be developed.

It has been recognized for many years that the sleeve friction stress, f_s is approximately equal to the remoulded undrained shear strength, s_{ur}. Data from the Vancouver area has shown that the friction sleeve stress is generally close to the remoulded strength. However, the friction sleeve values are very small and the variations in results are probably due to the inherent difficulty of measuring small sleeve frictions. The observation that soils with a high sensitivity have very low sleeve friction values is also reflected in the R_f classification charts (Figure 6-10).

7.4.2.2 Drained Shear Strength

Senneset et al (1982) and Keaveny and Mitchell (1986) have suggested methods to determine the drained effective stress shear strength parameters (c', ϕ'), from the cone penetration resistance and the measured total pore pressures. However, these methods, as with any method for determining effective stress parameters from undrained cone penetration data, can be subject to serious problems. Any method of analysis must make assumptions as to the distribution of total stresses and pore pressures around the cone. Unfortunately, the distribution of stresses and pore pressures around a cone is extremely complex in all soils and has not adequately been modelled or measured to date except perhaps in soft normally consolidated clays. Also, an important problem, which was not identified by Senneset et al, (1982) is the location of the porous element, since different locations give different measured total pore pressures.

The authors believe that the present state of interpretation and analyses of CPT data has not yet reached a stage to allow reliable estimates of drained shear strength parameters from undrained cone penetration data.

7.4.3 Stiffness

7.4.3.1 General

As already discussed, the cone penetration resistance is a complex function of both strength and deformation properties. Hence, no generally applicable analytical solution exists for cone resistance as a function of stiffness. Instead, many empirical correlations between cone resistance and deformation modulus have been established. The modulus is commonly obtained by multiplying the cone tip resistance by a factor α, i.e.

$$\text{Soil stiffness} = \alpha q_t. \tag{7.24}$$

The value of α selected varies depending on the design condition being analyzed and on the assumptions of the calculation method being used. This has led to a large number of correlations appearing in the literature (e.g. Lunne et al. 1997).

These correlations are to a variety of moduli (Young's modulus, shear modulus, constrained modulus, etc.) at a range of stress and strain levels. It should be noted that the following comments apply to soil modulus in general as shear (G), Young's (E) and Constrained Moduli (M) are linked by linear elasticity theory through Poisson's Ratio as follows:

$$G = \frac{E_u}{2(1+\nu_u)} = \frac{E'}{2(1+\nu')} \tag{7.25}$$

$$M = \frac{(1-\nu')E'}{(1+\nu')(1-2\nu')}$$

where ν_u is the Poisson's ratio during constant volume deformation, ν' is Poisson's Ratio during drained deformation.

The 1-D compressibility, m_v, is just the inverse of the constrained modulus, M. Values of E can be interpreted from G using appropriate values of ν. For undrained deformation, ν_u=0.5. In drained deformation, Poisson's ratio typically varies from 0.1 to 0.25.

Some of the confusion concerning the use of CPT for interpretation of deformation modulus can be overcome if the following points are considered.

a) Soil is not linear elastic and modulus varies with both stress and strain level.

b) Modulus is often derived from or applied to non one-dimensional loading conditions.

c) Different theoretical methods were applied when obtaining correlations.

It is now understood that soil behaviour is only truly elastic at very small strains but it is still common to characterize the variation of soil stiffness with strain as shown in Figure 7-19. The stiffness of the soil is represented by the secant (or tangent) to the stress-strain curve at the appropriate mobilized shear strain, γ, or shear stress ratio τ/τ_f. In undrained shear, τ_f=s_u The shear stress ratio can also be considered as the inverse of a safety factor. The result of this approach is shown in Figure 7-20 which shows the degradation in modulus with increased strain. This is an "equivalent" elastic modulus as both elastic and plastic strains occur when the soil is strained beyond small strains. The determination of an appropriate modulus thus requires:

- an estimate of G_o and
- an estimate of how the equivalent G reduces with strain level or mobilized shear stress level.

G_o is assumed to be appropriate up to a threshold shear strain level. This threshold strain level varies with soil type and stress history. It is often taken as about 0.0001% in sands and 0.01 to 0.001% in clays. Beyond the threshold strain, G/G_o reduces with strain level. Atkinson (2000) noted that the degree of non-linearity varies consistently with the nature of the soil grains and with the current state of the soil. Hyperbolic G/G_o vs γ relationships have been derived mainly based on resonant column testing on reconstituted samples (Hardin and Drnevich 1972; Seed and Idriss 1970; Vucetic and Dobry 1991). Fahey (1998) suggested that an alternative approach to modulus degradation with strain level is to assume that G varies with shear stress ratio, τ/τ_f, according to the expression:

$$G=G_o[1-(\tau/\tau_f)^g] \tag{7.26}$$

where g is an empirical fitting parameter. Mayne (2001) suggested that $g=0.3 \pm 0.1$ was appropriate for many soils.

Figure 7-21 shows the relationship in Equation 7.26 plotted for g=0.3. In the past, it has been common practice to estimate stiffness at mobilized shear stress ratios of 25% and 50% of failure, i.e. τ/τ_f = 0.25 and 0.5. From Figure 7-19, G_{25} and G_{50} will occur at G/G_o of about 0.33 and 0.19, respectively. Young's moduli may be obtained by Equation 7.25 using appropriate Poisson's Ratios.

It is clear that in order to select an appropriate design parameter, it is important for the engineer to understand the nature of the modulus required for the design problem under consideration, and for the design method being used.

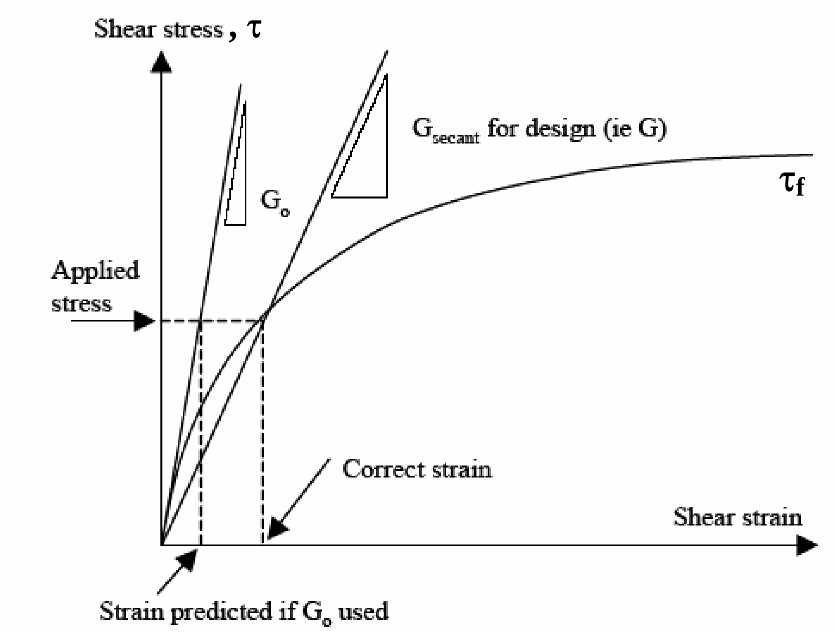

Figure 7-19 Illustration of non-linear stiffness of soil, and definition of initial tangent shear modulus (or small strain shear modulus) G_o, and secant shear modulus G (Fahey et al. 2003)

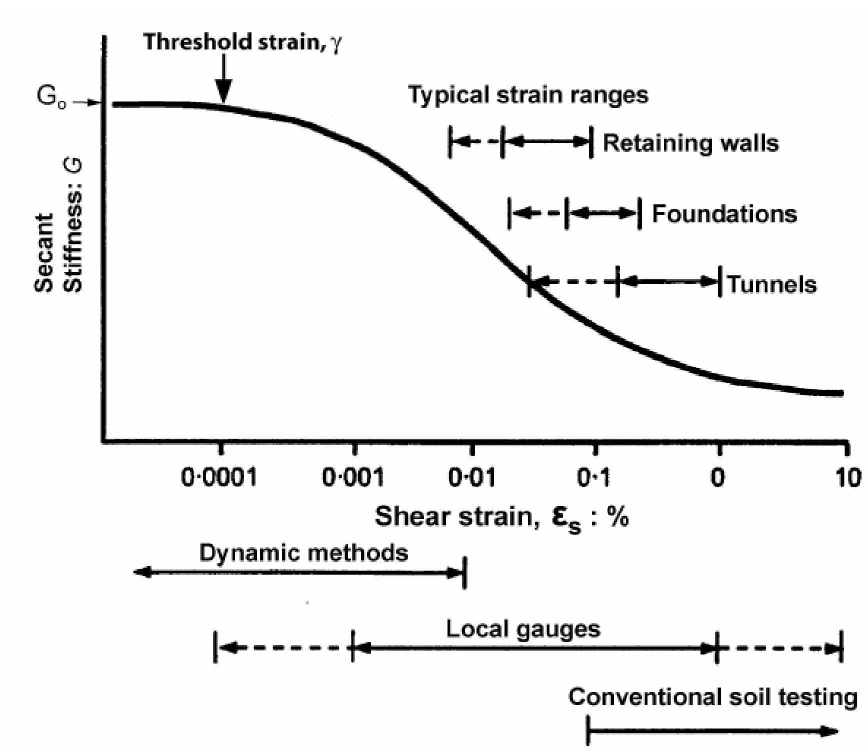

Figure 7-20 Characteristic stiffness-strain behaviour of soil with typical strain ranges for laboratory tests and structures (After Atkinson and Sallfors 1991; Mair 1993)

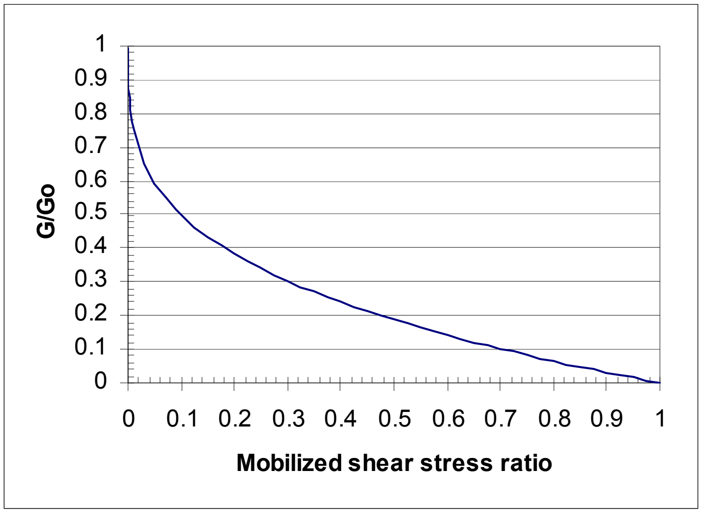

Figure 7-21 Variation of G/G_o using Equation 7.26 with g=0.3

7.4.3.2 Stiffness of Sands

Where shear wave velocities are measured, G_o can be found directly from V_s using the expression:

$$G_o=\rho V_s^2 \tag{7.27}$$

Where ρ is the mass density of the sand. Where V_s measurements are not available, a correlation between q_t and G_o such as Figure 7-22 may be used to estimate G_o. It is for uncemented, unaged, predominantly quartz sands.

Correlations between penetration resistance and non-linear deformation moduli at strains larger than the threshold exist but Jamiolkowski et al. (1989) noted that they were unreliable. Many of the available correlations (e.g. Lunne et al. 1997), refer to an estimate of the stiffness that would be observed in a triaxial test in the laboratory at a particular stress or strain level. Typical correlations for Ticino sand between secant Young's Modulus in triaxial tests at an axial strain level of 0.1% and q_t are presented in Figure 7-23. Similar correlations to E_{25}/q_t and E_{50}/q_t can be obtained using the procedures discussed in Section 7.4.3.1. There is a large effect of age, stress level, and density on the interpreted modulus and the selection of a design value of stiffness depends on the specifics of the design problem and of the design method being used. This is addressed further in Chapter 9.

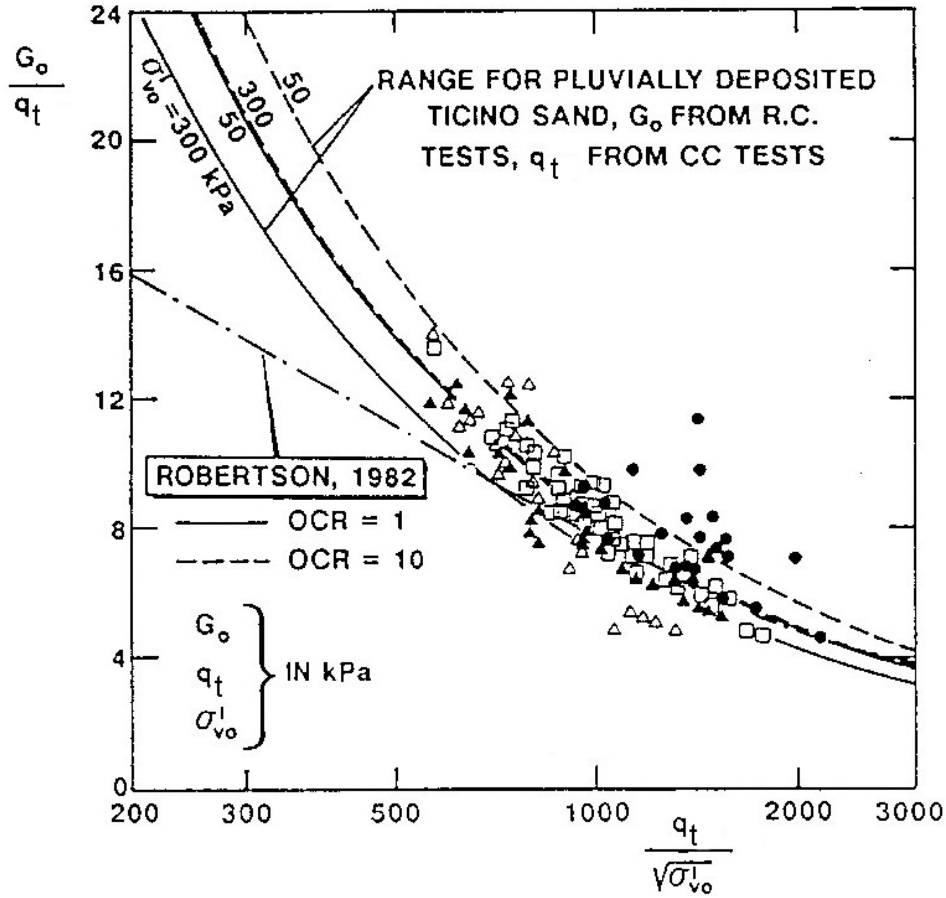

	SITE	SOIL	G_o SOURCE	BOREHOLE
△	VIADANA	MEDIUM SAND	CROSS-HOLE	4017
▲	VIADANA	MEDIUM SAND	SEISMIC CONE	4017
□	S. PROSPERO	MEDIUM SAND	SEISMIC CONE	16 17
●	GIOIA TAURO	SAND WITH GRAVEL	CROSS-HOLE	209 219

DEPTH BELOW G.L. CONSIDERED: 5.5 TO 43.5 m

Figure 7-22 q_t versus G_o correlation uncemented predominantly quartz sands (Bellotti et al. 1989)

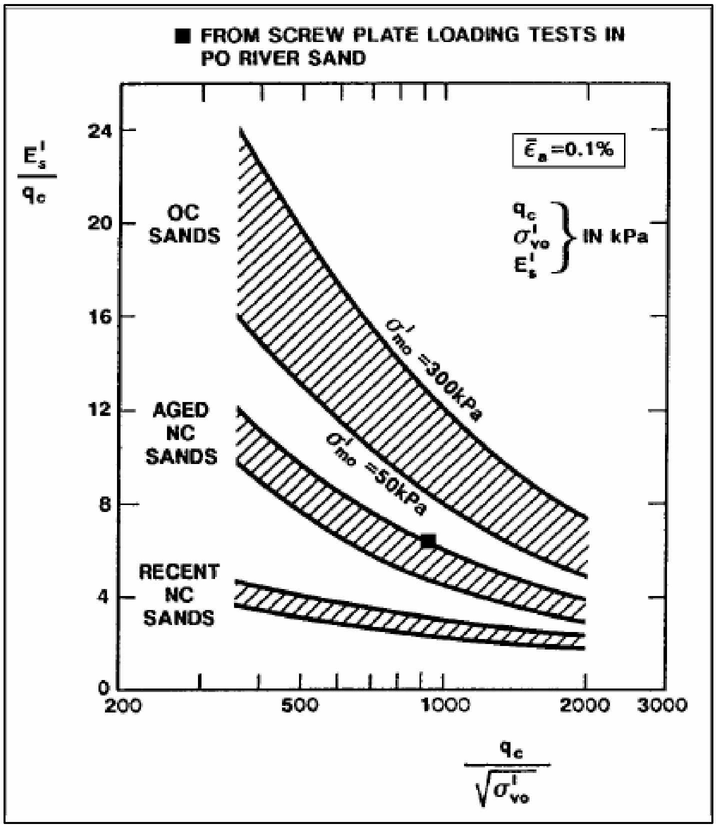

Note $G' = \frac{E'}{2(1+v')}$

Figure 7-23 Ratio of 'working strain' stiffness E'_s to q_c versus $q_c/\sqrt{\sigma'_v}$ for sands with different stress histories (Baldi et al. 1989)

7.4.3.3 Undrained deformation in Clays

Where shear wave velocities are measured, G_o can be found directly from V_s using the expression:

$$G_o=\rho V_s^2 \tag{7.28}$$

where ρ is the bulk density of the soil.

If V_s is not available, empirical correlations may be used to estimate G_o. Massarsch (2004) showed that G_o varies widely in fine-grained soils. He presented an empirical correlation for normally consolidated clays, based on field and laboratory data, between normalized G_o versus water content. G_o was normalized to the square root of s_u. He found that normalized G_o is much higher in silty clays and silts than in clays and that as the water content increases above about 40-50%, normalized G_o drops rapidly. It is thus difficult to estimate G_o empirically.

Figure 7-23 shows a correlation presented by Robertson and Campanella (1995) between G_o/q_t and OCR for a wide range of plasticity. The correlation also suggests a very wide range of normalized q_t with low plasticity soils having much greater normalized stiffness than high plasticity soils. Leroueil et al. (2002) found that G_o was approximated by the expression

$$G_o = 40(q_t - \sigma_{vo}) \tag{7.29}$$

for a high plasticity soft clay which is in reasonable agreement with Figure 7-24. Therefore, it is recommended that a first approximation to G_o may be obtained from Figure 7-24.

Again, the method outlined in Section 7.4.3.1. may be used to estimate values of moduli at intermediate shear strains or at higher levels of mobilized shear stress.

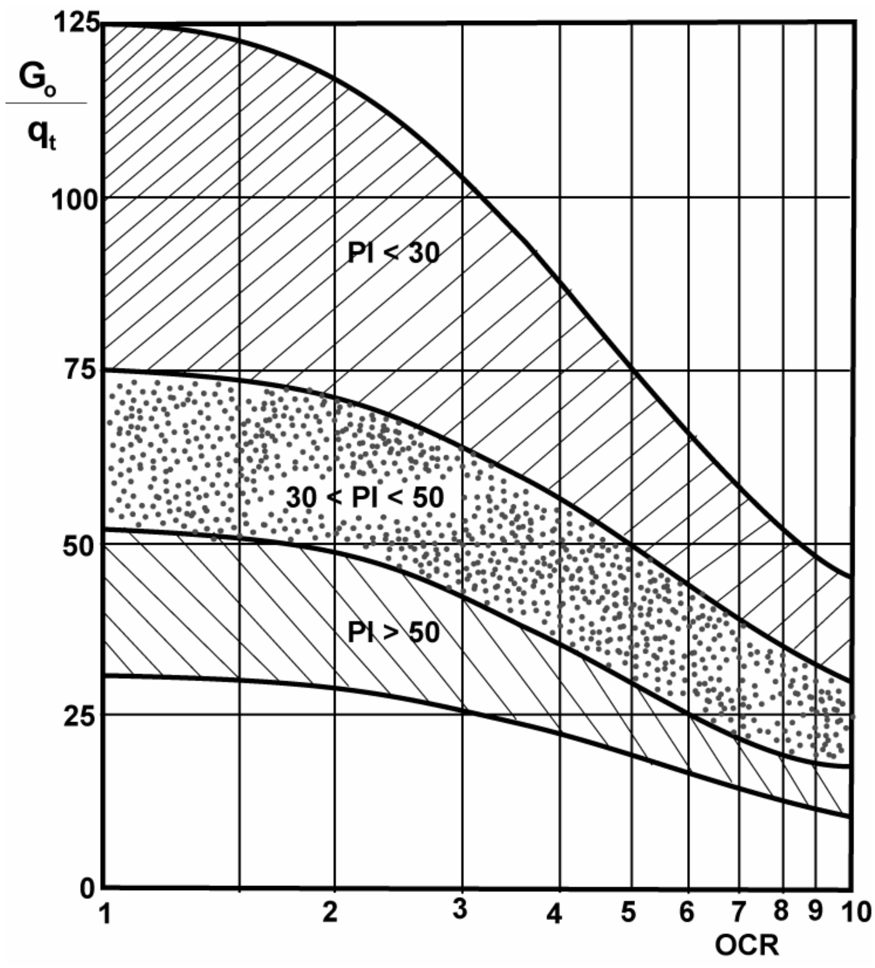

Figure 7-24 Tentative correlation for estimating dynamic shear moduli (G_o) in clay soils (Robertson and Campanella 1989)

7.4.3.4 Drained Deformation in Clays

The estimation of drained deformation parameters from q_t observed during undrained penetration is liable to result in serious errors. Nevertheless, correlations do exist in the literature to 1-D Constrained Modulus, M. These are usually in the format

$$M=\frac{1}{m_v}=\alpha q_t \tag{7.30}$$

Typical values are shown in Table 7-3 e.g. Mitchell and Gardner (1975). More recently, Kulhawy and Mayne (1990) argued that many of the previous parameters were developed from data obtained with a variety of mechanical and electric cones and suggested that the following relationship was applicable to modern cones:

$$M=8.25(q_t-\sigma_{vo}) \tag{7.31}$$

This relationship was based on data from 12 sites. This is a secant value of M applicable to calculation of consolidation settlement.

Schmertmann developed a method that related the s_u/σ'_{vo} ratio to the overconsolidation ratio (OCR) and then to the one dimensional compression index of the soil, C_c, as shown on Table 7-4.

$M=\frac{1}{m_v}=\alpha q_t$		
$q_t < 7$ bar $7 < q_t < 20$ bar $q_t > 20$ bar	$3 < \alpha < 8$ $2 < \alpha < 5$ $1 < \alpha < 2.5$	Clay of low plasticity (CL)
$q_t > 20$ bar $q_t < 20$ bar	$3 < \alpha < 6$ $1 < \alpha < 3$	Silts of low plasticity (ML)
$q_t < 20$ bar	$2 < \alpha < 6$	Highly plastic silts & clays (MH, CH)
$q_t < 12$ bar	$2 < \alpha < 8$	Organic silts (OL)
$q_t < 7$ bar: $50 < w < 100$ $100 < w < 200$ $w > 200$	 $1.5 < \alpha < 4$ $1 < \alpha < 1.5$ $0.4 < \alpha < 1$	Peat & organic clay (P_t, OH)

Table 7-3 Estimation of Constrained Modulus, M, for Clays (Adapted from Sanglerat, 1972) (After Mitchell and Gardner 1975)

s_u / σ'_{vo}	approx. OCR	$C_c / (1 + e_1)$
0 – 0.1	less than 1	greater than 0.4 (still consolidating)
0.1 – 0.25	1	0.4
0.26 – 0.50	1 to 1.5 (assume 1)	0.3
0.51 – 1.00	3	0.15
1 – 4	6	0.10
over 4	greater than 6	0.05

Table 7-4 Estimation of Compression Index, C_c, from s_u / σ'_{vo} ratio(After Schmertmann 1978)

The coefficient of volume change (m_v) and the compression index (C_c) are related by:

$$m_v = \frac{0.435 C_c}{(1 + e_o)\sigma_{va}} \tag{7.32}$$

where e_o = initial void ratio,

σ_{va} = average of initial and final stresses.

These methods provide only a guide to estimating soil compressibility. The values by Schmertmann in Table 7-4 appear to give very conservative estimates of C_c and appear to be too large by a factor of about 2. Increasing sensitivity can significantly increase the compressibility of a clay at stresses higher than the preconsolidation stress. Additional data from Atterberg limit tests (PI) and/or undisturbed sampling and oedometer tests are required for more reliable estimates.

The estimation of drained parameters such as the one dimensional compression index, C_c, or compressibility, m_v, from an undrained test is liable to serious error, especially when based on general empirical correlations. Conceptually, total stress undrained measurements from a cone cannot yield parameters for drained conditions without the addition of pore pressure measurements. The predictions of volume change based on q_t using either Table 4-3 or Table 4-4 may be in error by ±100%. However, with local experience individual correlations can be developed for specific soil types.

7.4.4 Consolidation Characteristics

The use of dissipation tests to help in classification of soil behaviour type and interpretation of the ground water regime was described in section 6.3. A dissipation test consists of stopping cone penetration and monitoring the decay of excess pore pressures (Δu) with time. The decay of excess pore pressure with time is a familiar problem in soil mechanics and is conventionally analyzed using the theory of consolidation. For one dimensional consolidation, the coefficient of consolidation c, is related to the compressibility, m_v, or constrained modulus, M, and permeability (k) of the soil through the relationship:

$$c = k\frac{M}{\gamma_w} \text{ and } m_v = \frac{1}{M} \tag{7.33}$$

This relationship is based on many simplifying assumptions but has found wide application in geotechnical engineering. Pore pressure dissipation around a cone has been analyzed by a number of researchers using a variety of approaches and assumptions. Lunne et al. (1997) present a useful summary of the various solutions available.

Analysis of dissipation curves is carried out by matching field pore pressure dissipation curves to dissipation curves derived from theory. Baligh and Levadoux (1986) recommended the following procedure for evaluating c_h, the coefficient of consolidation in the horizontal direction:

a) Plot the normalized excess pore pressure with log time.

b) Compare the measured dissipation curve with the theoretical curves

c) If the curves are similar in shape, compute c_h from:

$$c_h = \frac{r^2 T}{t} \tag{7.34}$$

where:

T = theoretical time factor for given tip geometry and porous element location

t = time to reach given value of $\Delta u(t)/\Delta u_{initial}$

r = average radius of cone filter sensing pore pressures.

They noted that

1. Consolidation is taking place predominantly in the recompression mode, especially for dissipation less than 50%.

2. The initial distribution of excess pore pressures around the cone has a significant influence on the dissipation process.

Provided the assumptions of the theory are representative of the real soil behaviour, an approximate value of the coefficient of consolidation in the horizontal direction (c_h) can be obtained. Figure 7-25 shows a summary of early solutions for pore pressure dissipation.

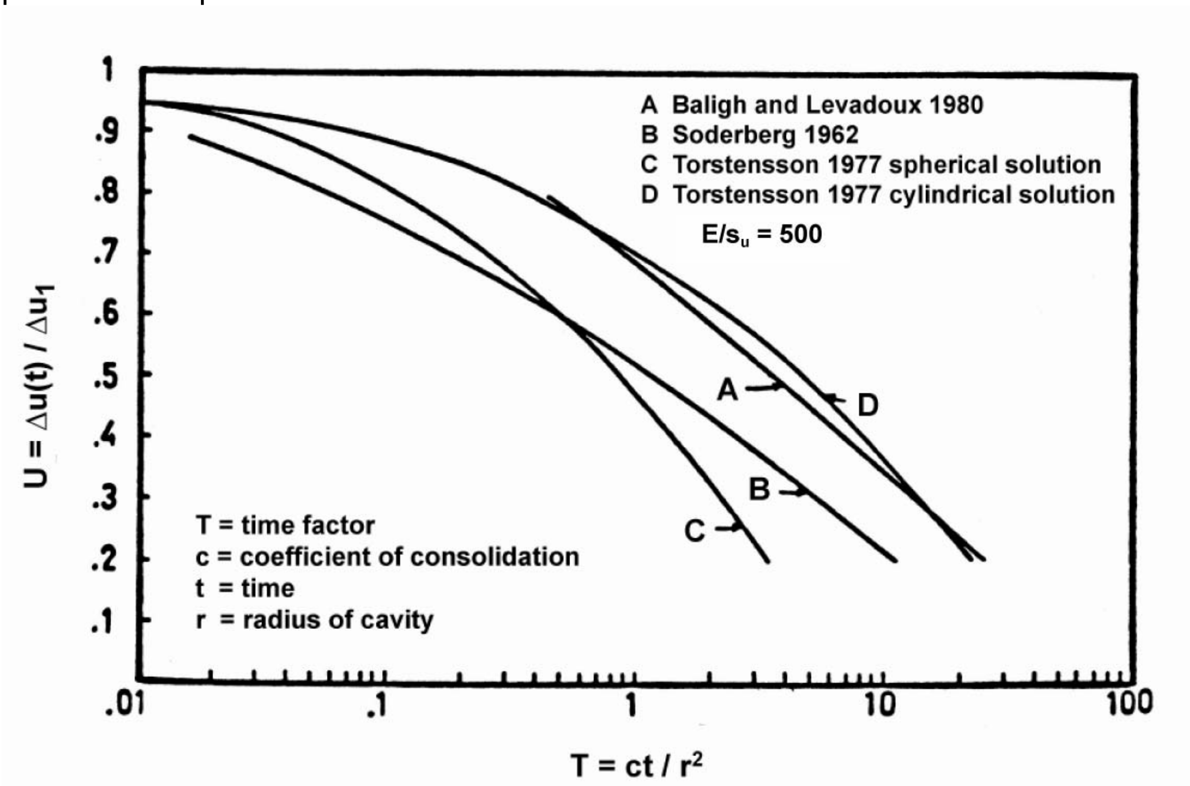

Figure 7-25 Summary of Existing Solutions for Pore Pressure Dissipation (Adapted from Gillespie and Campanella 1981)

Teh and Houlsby (1991) improved on the Baligh and Levadoux solution. Their solution allows prediction of dissipation curves at any point along the cone shaft and includes the effect of soil stiffness through the rigidity index, $I_r = G/s_u$. They derived a modified dimensionless time factor, T*, defined as:

$$T^* = \frac{c_h t}{r^2 \sqrt{I_r}} \tag{7.35}$$

from which c_h can be obtained.

Robertson et al. (1992a) reviewed a large amount of field data and concluded that the Teh and Houlsby solution should provide reasonable estimates of c_h with the least scatter occurring for the u_2 position. Using T^*_{50} values of 0.245 and 0.118 for the u_2 and u_1 positions, respectively, they proposed the chart shown in Figure 7-26 for finding c_h from t_{50}, where t_{50} is the time at which 50% of the excess pore pressure has dissipated. The recommended procedure to measure t_{50} is given in Section 6.3.4.

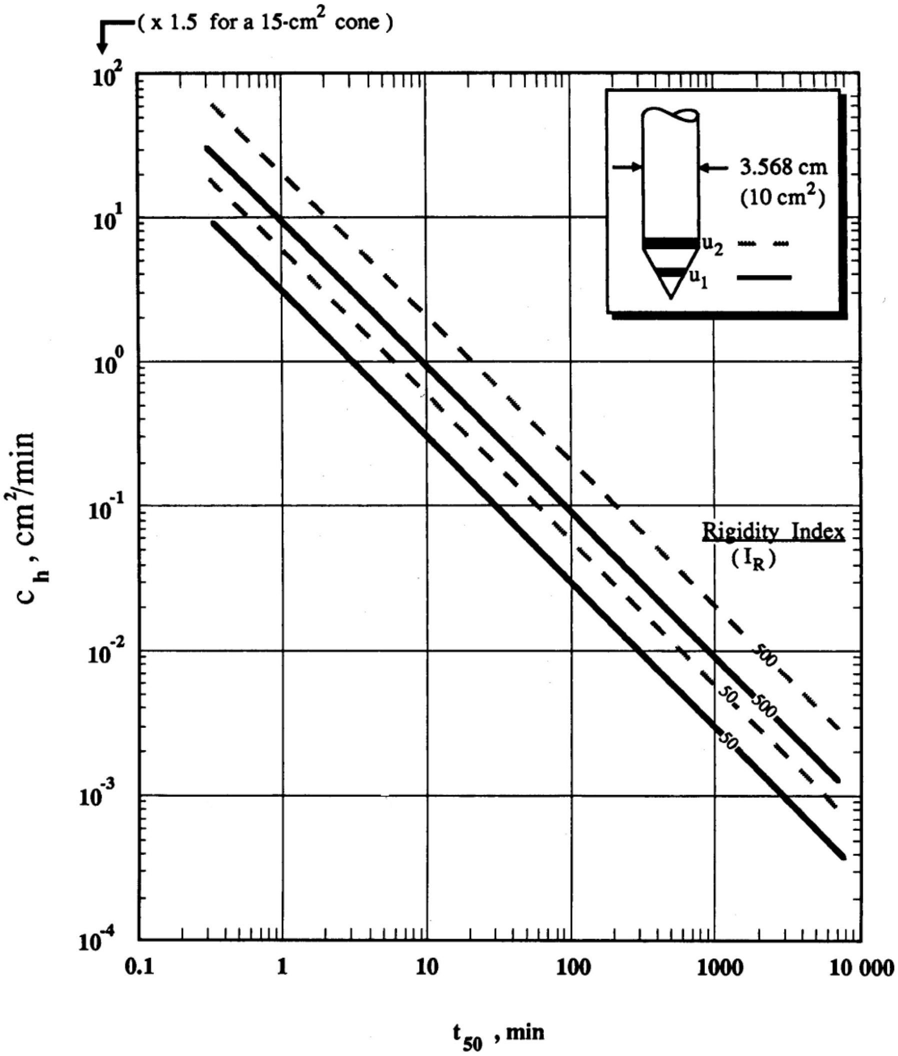

Figure 7-26 Chart for evaluation of c_h from t_{50} for 10 and 15 cm^2 piezocone (based on theoretical solution by Teh and Houlsby, 1991) (Robertson et al. 1992a)

According to Baligh and Levadoux (1986), errors in the measurement of the initial and equilibrium pore pressures have the least effect on c_h for U_t=0.5. Similar charts could be derived for other degrees of consolidation using the relevant values of T*.

A disadvantage of the chart approach is that the measured and theoretical dissipation curves are not compared in detail to see how closely the field curves represent the theoretical ones. Danziger et al. (1997) presented an interesting case history for a Brazilian soft clay in which they carried out detailed curve matching before using the Teh and Houlsby solution to estimate c_h. They obtained good results compared to c_h values from very carefully conducted laboratory tests. The advantage of the chart is that it provides a straightforward and consistent approach to determining c_h.

In overconsolidated clayey soils, the pore pressure gradient around the cone can be extremely large. This gradient of pore pressure often results in dissipations recorded behind the tip that initially increase before decreasing to the final equilibrium value. This type of response is believed to be due to the redistribution of excess pore pressures around the cone before the primarily radial drainage, although poor saturation of the cone can also cause this response.

Where an initial redistribution of excess pore pressure is apparent, the methods outlined in Section 6.3.4 can be used to help in estimation of t_{50}.

Figure 7-26 requires an estimate of I_R. Danziger et al. (1997) found that good results were obtained when I_R was determined using G_{50} from quick triaxial tests on tube samples or from interpretation of tip resistance using the methods outlined in Sections 7.4.2 and 7.4.3.

The value of c_h determined for $\Delta u(t)/\Delta u = 0.5$ (i.e., 50% consolidation), may be used in problems involving horizontal flow in the over-consolidated range. To obtain c_h in the normally consolidated range, use

$$c_h(\text{N.C.}) = \frac{RR}{CR} \cdot c_h(\text{CPTU}) \tag{7.36}$$

where:

RR = recompression ratio = $C_s/1+e_o$

CR = virgin compression ratio = $C_c/1+e_o$

If no data are available, take $\frac{RR}{CR} \simeq 0.15$ (Jamiolkowski et al. 1983).

At present, because of the difficulties in predicting the initial distribution of excess pore pressures around a cone in stiff, over-consolidated clays (OCR > 4), the theoretical solutions for estimating c_h from dissipation tests for u_2 are limited to normally to lightly overconsolidated clays (OCR < 4). U_1 is not similarly affected.

In spite of the above limitations, the dissipation test provides a useful means of evaluating ***approximate*** consolidation properties, soil macrofabric and related drainage paths of natural clay deposits. The test also appears to provide very important information for the design of vertical drains (Battaglio et al. 1981; Robertson et al. 1986).

A crude estimate of permeability can be made from the t_{50} values (Figure 6-6).

A more reliable estimate of permeability for fine grained soils can be made from the consolidation and compressibility characteristics. Since:

$$k_v = c_v m_v \gamma_w \tag{7.37}$$

$$k_h = c_h m_h \gamma_w \tag{7.38}$$

where k_v and k_h are the coefficient of permeability in the vertical and horizontal directions, respectively. Results of limited past experience suggests that soil compressibility can be regarded as approximately isotropic, $m_v = m_h$ (Ladd et al. 1977; Mitchell et al. 1978) for the purposes of estimating permeability.

Since an estimate of m_v can be made, then estimates of vertical permeability can be obtained. Estimates of m_v can be made using Table 7-3 or using an α factor based on local experience.

If it is assumed that soil compressibility is isotropic, then:

$$c_v = c_h \times \frac{k_v}{k_h} = \frac{c_h}{r_k} \tag{7.39}$$

where $r_k = k_h/k_v$. An estimate of r_k can be obtained from Table 7-5, after Baligh and Levadoux (1980). Evidence of the soil heterogeneity can be obtained from examination of the q_t, R_f and dynamic pore pressure records.

	Nature of Clay	$r_k=k_h/k_v$
1.	No evidence of layering	1.2 ± 0.2
2.	Slight layering, e.g., sedimentary clays with occasional silt dustings to random lenses	2 to 5
3.	Varved clays in north-eastern U.S.	10 ± 5

Table 7-5 Anisotropic Permeability of Clays (After Baligh and Levadoux 1980)

7.5 Problem Soils

Correct interpretation of CPT or CPTU data requires some knowledge that the penetration is predominantly drained or undrained. Problem soils are often soils where penetration is taking place under partially drained conditions, such as fine sands and silts and some organic soils.

One of the major advantages of CPTU data is the ability to distinguish between drained, partially drained and undrained penetration. The dissipation of excess pore pressures during a pause in penetration can provide valuable additional information regarding drainage conditions. If the excess pore pressures dissipate fully in a time from about 30 seconds to 3 minutes for a standard 10 cm² cone, the penetration process was most likely partially drained and quantitative interpretation is very difficult. Other factors, such as stratigraphy and poor saturation of the sensing element can also influence the pore pressure response.

If CPTU data are not available, Figure 6-10 can be used to estimate drainage conditions during penetration. Soils that fall within zones 7, 8, 9, 10 and 12 tend to have drained penetration. Soils that fall within zones 1, 2, 3, 4 and 5 tend to have undrained penetration. Caution should be used when soils fall in or close to zones 6 and 11, since penetration may be partially drained and quantitative interpretation is very difficult.

Fibrous organic soils can sometimes be difficult to interpret. The shear strength is often controlled by the fibrous nature of the soil mass. Often instability is generated in thin layers of soft organic (non-fibrous) clays or silts that exist immediately above or below the fibrous deposit. Therefore, the CPT data should be studied carefully to look for the possibility of such soft layers, since often they will control stability.

Gravelly soils also present a problem for interpretation of CPT data. Appreciable gravel content can make penetration with a cone impossible. Small gravel content can allow cone penetration but can cause large spikes in the q_c and f_s profile. These spikes cannot be interpreted to give realistic geotechnical parameters, such as D_r, ϕ or E. Caution should be exercised when interpreting CPT data in gravelly soils. Additional data, such as shear wave velocity, can be useful to evaluate the extent of gravel content.

7.6 Groundwater Conditions

While it has been common practice to use the height of water in a borehole to estimate the piezometric level, the groundwater conditions are rarely hydrostatic. The use of CPTU data to interpret the ground water regime is described in Section 6.3. Often there is a slight upward or downward gradient of water pressures resulting from overall regional groundwater conditions. The equilibrium piezometric pressures recorded during stops in penetration are needed for evaluating consolidation conditions or unusual hydraulic gradients. Identifying the actual groundwater conditions can be extremely valuable for investigations of slopes, embankments, tailings disposal and tidal areas. Note that effective vertical stress calculations must include gradient effects on pore pressure.

The time required to reach full equilibrium pore pressure during a stop in penetration will depend mainly on the soil permeability. For many investigations, it is sufficient to take equilibrium measurements at the end of the profile before pulling the rods and during rod breaks in any sand layers or purposely stopping in a coarser layer to obtain a rapid dissipation to an equilibrium pore pressure.

A poorly saturated piezometer element and cavity will not affect the accuracy of the measured equilibrium pore pressure, but will lengthen the time it takes to reach equilibrium.

8 UBC FREEWARE CPTINT VERSION 5.2

8.1 Introduction

Before any data are interpreted with the aid of a computer program, they must first be thoroughly scrutinized and edited where necessary, as per section 4.2. Then the data must be plotted (section 4.3) and visually interpreted (section 6.2.1) so the operator can become familiar with the general characteristics of the site and profiles including groundwater regime (section 6.3). The data may now be entered into a computerized interpretation program.

The in-situ testing group of the Civil Engineering Department at UBC has been developing interpretation software for CPTU data since the mid 1980's. Many versions had evolved with the last major update to version 5.2 completed in October 1998. In March 2002, the last minor fixes were made to CPTINT 5.2. Since software support was no longer available in the department, it was decided to halt software development and make CPTINT 5.2 available as Freeware to the Geotechnical community, as is, and without support. There is no graphics in this program. The program has been tested and runs in all Windows operating systems, which have support for DOS.

CPTINT was written in C++ as an MSDOS program by Thomas Wong with a user friendly, menu driven interface where the operator has full control over the interpretation parameters and correlations used in the program. The main objective of the program was to automate the lookup of interpretation relationships as published by various researchers after they had been tested and evaluated to be useful.

The main program comes with several important information files and example data files. The file 'readme.doc' should be read first and contains initial distribution information such as a list of files, instructions on how to set up the program, file definitions, helpful hints and list of update changes from version 4.00 to 5.20.

A table file, 'cptcptbl.doc', lists all the equations and references used in the program and the file 'cptint.doc' is the user manual, which explains program operations. These files may be read in 'word' or from inside the program.

8.2 Program

CPTINT is a user-friendly, MENU driven program for CPT and CPTU Interpretation which can search, view, define and save both input and output file formats in units which can be specified for each parameter (English, metric or SI). More than 35 different correlation parameters, including: interpretation for soil classification type by friction and pore pressure ratios; relative density and internal friction by 3 methods; SPT N and N_1; cyclic stress ratio to cause liquefaction and applied by earthquake; dynamic shear modulus; constrained modulus and Young's modulus over various depth intervals with a choice of units can be calculated in the SAND Parameter Menu. The CLAY Parameter Menu allows the interpretation for: undrained shear strength by one of 5 methods; OCR; and moduli.

Other features include: an enhanced level-ground empirical liquefaction analysis including use of either R_f or B_q zone for basis of interpretation in a separate LIQUEFACTION menu and input of user-defined values of unit weight, SPT N, water pressure, Q_t, R_f or B_q Zone, and CSR(EQ) with Depth. Zone 6 (silty-sand) may be switched from undrained to drained analysis and the user may specify an above ground water table. Version 5.2 added an average vertical hydraulic gradient specified by the user. A material index, I_c, according to Jefferies & Davies (1993), which uses Normalized Q, F and B_q in one relationship was added. I_c is used to calculate an alternative SPT N_{60} value and to estimate the Fines Content (%). A State parameter (void ratio units) calculation according to Davies, 1999, was added which incorporates all measured normalized parameters Q, F and B_q. An alternative determination of OCR in clays was added which uses penetration pore pressure differences, U_1-U_2 or U_1-U_3. All units are user-definable and the output file is compatible for direct input into a Spreadsheet, GRAPHER or other plotting program.

8.2.1 DATA - Input definition files and units

When the program is started, a screen comes up as in Figure 8-1 and asks for the operator’s name, which will be stored with the data output file.

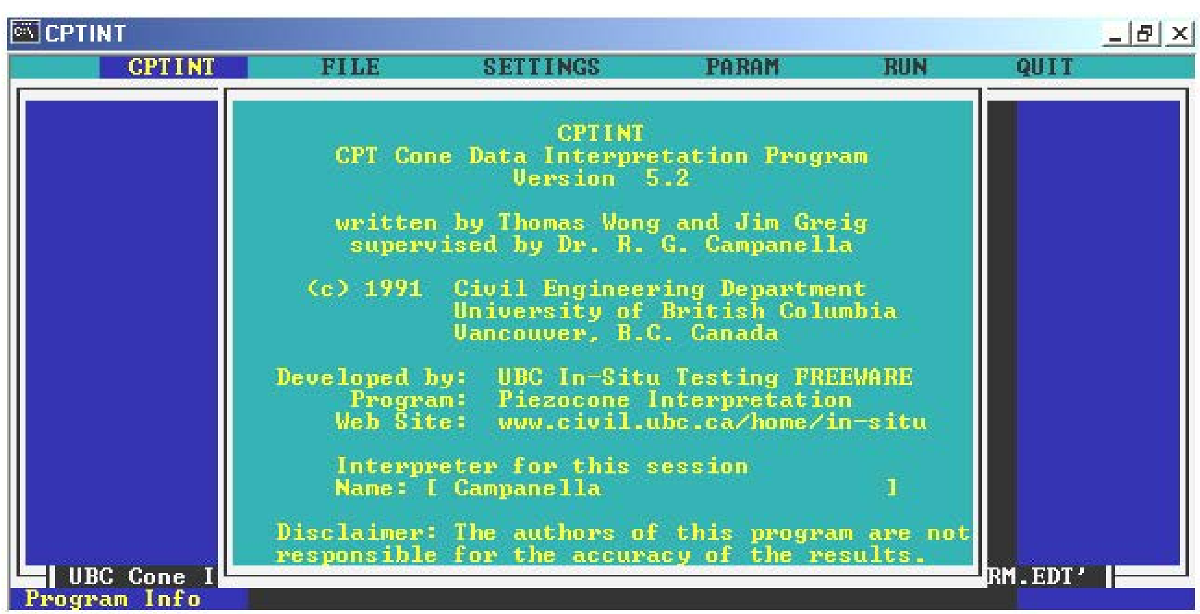

Figure 8-1 Opening Screen in CPTINT 5.2 requesting users Name

Once you enter your name and press ‘Enter’, the frame in Figure 8-2 comes up asking for the location and name of the data file to be interpreted. Type in f:*.* and the subdirectories in drive ‘f’ are displayed. Moving the cursor and hitting ‘Enter’ will allow you to move through the menu system.

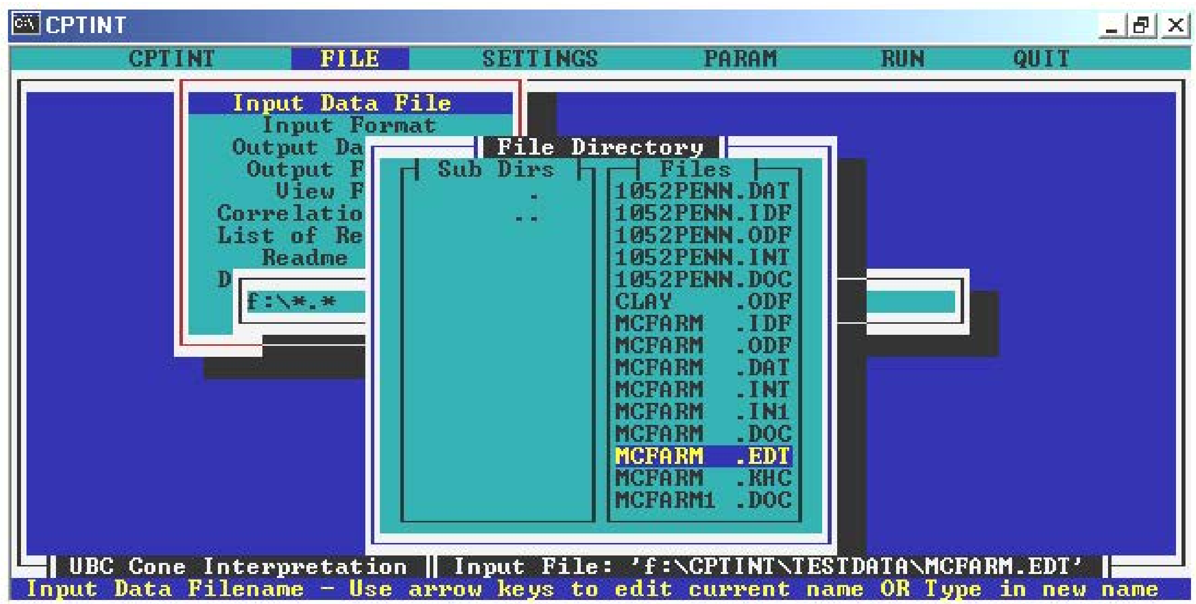

Figure 8-2 Pull Down Menu for input data file ‘f:\CPTINT\TESTDATA\MCFARM.EDT’

The general layout of the program Menu system is shown in Figure 8-2. There is no mouse control in the program and arrow, page-up and page-down keys control the cursor movement. Press ‘Enter’ to enact. Press ‘Esc’ to go back one entry and cancel your choice. There are 6 menu headings: CPTINT, FILE, SETTINGS, PARAM, RUN AND QUIT. Input Data File, Input Format, Output Data File Name, Output Data Format, View File, etc. appear under FILE. Note that the bottom line in the program window always indicates the operation of the current cursor location.

To enter the file name, type in the full path and name of the data file to be interpreted and press ‘Enter’. Alternatively, move the cursor through the subdirectories until the file is located and highlighted. Press ‘Enter’ and the file will be activated and appear at the bottom of the program. In Figure 8-2, it appears as MCFARM.EDT. This is the edited data file for McDonald’s Farm, Vancouver Airport, after it was fully scrutinized, evaluated, edited and visually interpreted as explained in the introduction, 8.1.

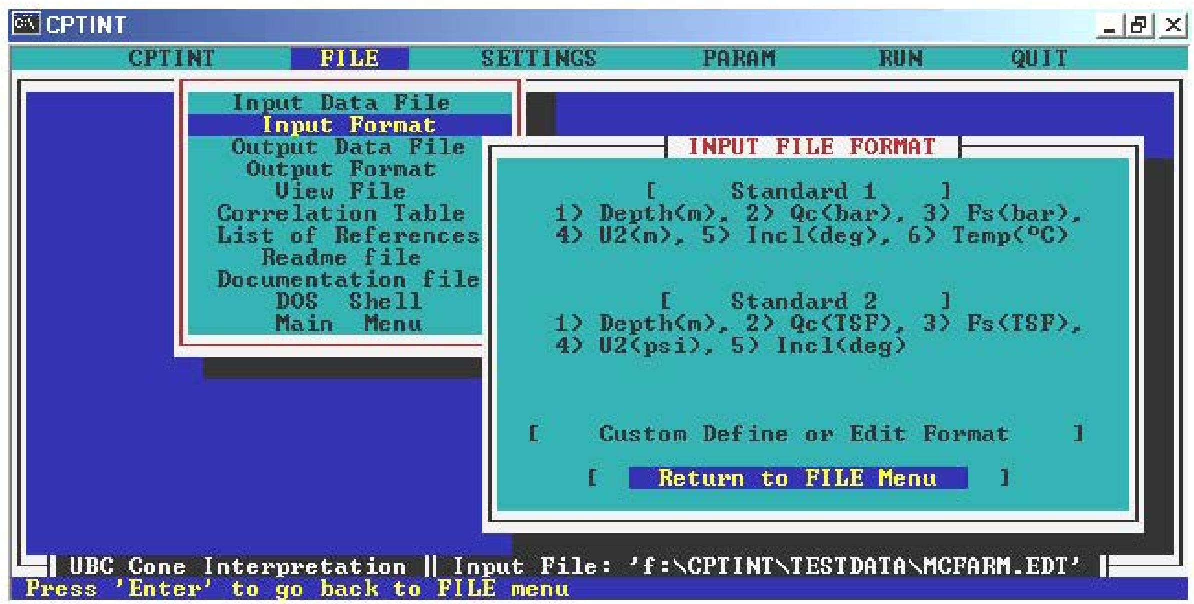

Figure 8-3 Input File Format Menu

After the file name is entered, the input file format must be specified. The data is always in columns. Here the format may be Standard 1, 2 or Custom/Edit Format as the cursor moves down. Any number of parameters and units may be defined in the Custom menu and saved as a standard and also as a NAME.IDF file or input definition format for this data file. Always move the cursor to 'Return to File Menu' and press 'Enter' to activate your choices. Doing anything else, like pressing 'Esc', will cancel your choices.

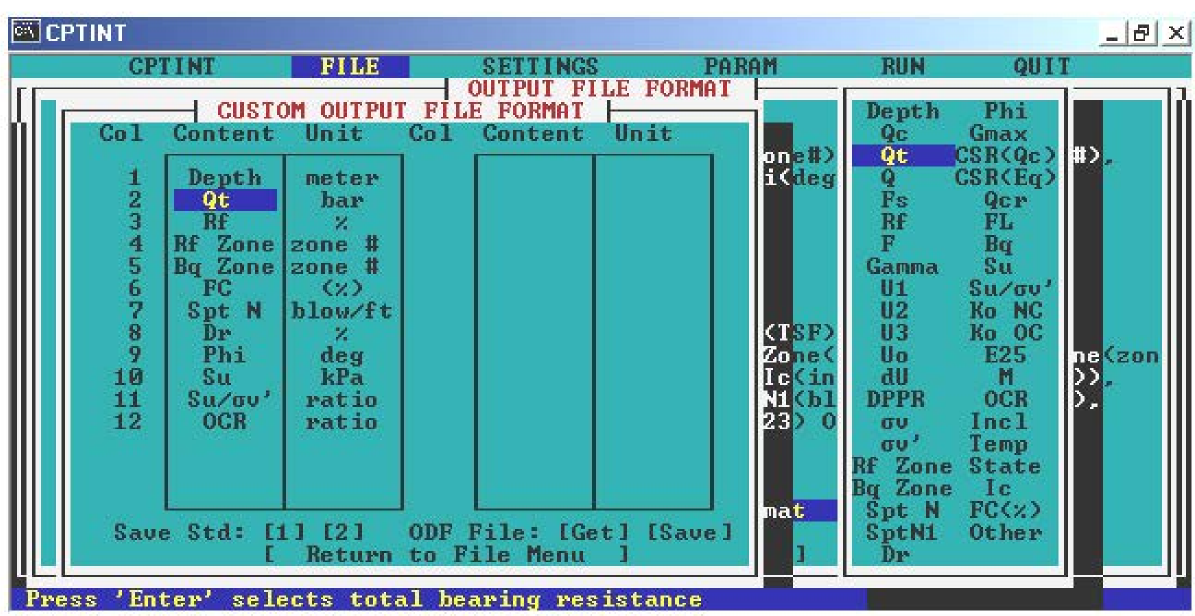

Figure 8-4 OUTPUT FILE FORMAT PARAMETERS and UNITS

8.2.2 DATA – Output Definition Files and Units

The operation of the Output File Format menu is similar to the Input File Format. Figure 8-4 shows the choice of a rather large number of parameters and a range of units just to demonstrate the wide variety of choices possible. The wide choice of 41 different parameters is to the right. A customized output file format list may be saved as a standard and as a NAME.ODF or output definition file for future use.

The SETTINGS menu allows one to set the Video mode, colour attributes and printer output settings, all of which are rarely changed. The printer output was originally set for a matrix printer and is no longer used, so output is always sent to a file.

8.2.3 PARAMETER MENU

The PARAM pull-down menu is shown in Figure 8-5. The PARAM menu requires you to input the tip stress correction factor, 'a', for pore pressure when q_c is input, the water table depth in metres below ground (or negative value of metres above ground for submerged soil), a vertical flow gradient if not hydrostatic, a valid zone number for interpretation (sand or clay) based on R_f or B_q, unit weight of soil to the first depth and method to calculate SPT N (either R&C or J&D). The CLAY Parameter menu is shown and identifies the operator's choice of α (75) for calculation of G_{max}, method to calculate S_u shown as N_{kt} with choice of N_{kt} as 9.5 (not shown), α (4.00) to calculate constrained modulus, and the method to calculate OCR shown as S_u/EOS where $(Su/EOS)_{NC}$ was specified as 0.25 (not shown).

Figure 8-5 PARAM Pull Down Menu showing CLAY Parameters

The pull-down menu for Sand Parameters is shown in Figure 8-6. The first item allows you to decide if you want to identify zone 6 for drained parameters.

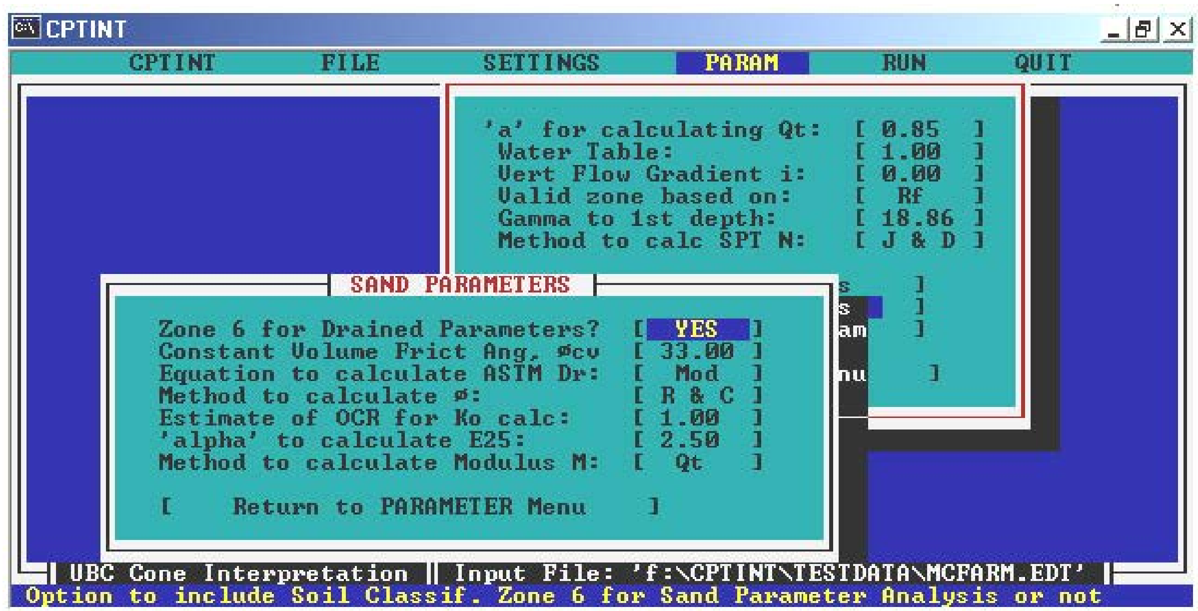

Figure 8-6 PARAM PULL DOWN MENU showing SAND PARAMETER CHOICES

The first choice should be 'NO' to conform with the classification behaviour type until there is reason to decide otherwise. Next, the operator types in the choice for the constant volume friction angle, typically from about 31 to 34 degrees. The choice for Moderate or High compressibility D_r relationship or for the average D_r for ALL sands is next. The choice is shown as Moderate. The D_r correlation options provided in the program do not include the updated one presented in Figures 7-4 and 7-5. The method to calculate Friction Angle allows the choice of R & C, D &M and 3 by Janbu. The choice made is R & C. The estimate of OCR for this sand is chosen as 1.00. The α to calculate E_{25} is chosen as 2.5 and finally the method to calculate Constrained Modulus is either the αq_t method (chosen here with α at 4.00, not shown) or the Baldi method.

The pull down menu for Liquefaction Parameters is shown as Figure 8-7. If liquefaction and seismic design is not an issue for this site then this menu can be by-passed. Here, the first choice is if there is to be an SPT correction of 7 applied to silty sand and the answer is NO. The design earthquake magnitude is typed in here as 7.5 and the next line has the peak ground acceleration for design entered as 0.3. The next line uses Seed's r_d vs. depth and the last line asks for the FL (factor of safety) to be used if Q_{cr} is calculated. Note that this value of 1.00 is high lighted and the meaning is shown on the bottom line. Q_{cr} in this case is the value of cone tip stress, q_t, needed to just have a factory of safety of 1 against liquefaction for the identified earthquake characteristics above at each depth or depth interval specified in the program.

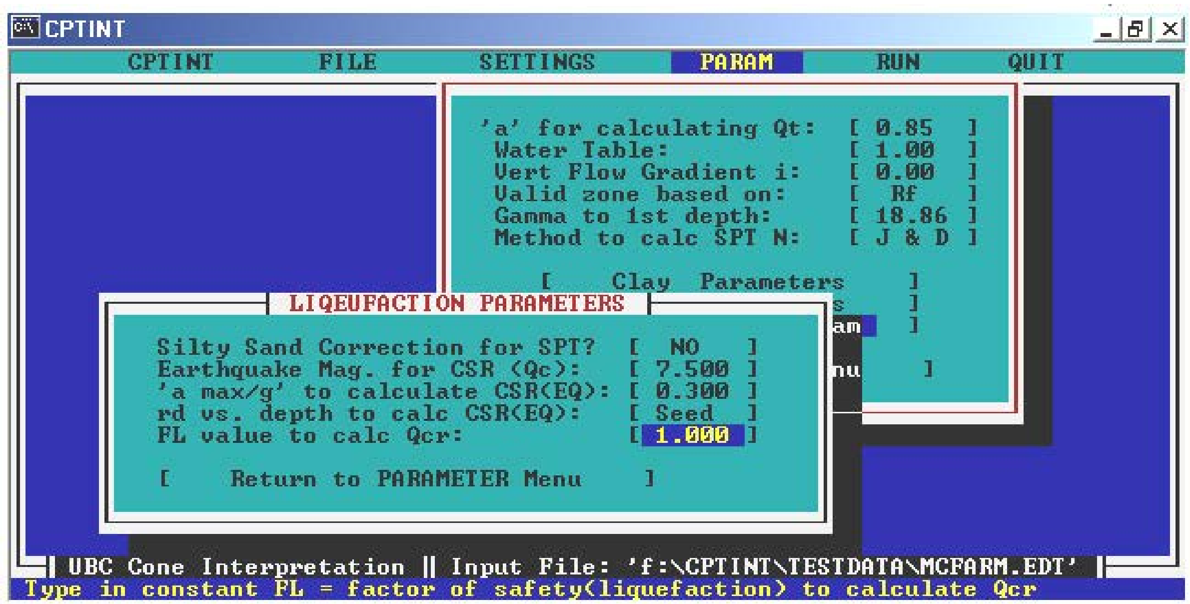

Figure 8-7 PARAM PULL DOWN MENU Showing LIQUEFACTION PARAMETER Choices

8.2.4 RUN MENU – Depth Averaging

The RUN MENU with depth averaging is shown in Figure 8-8. Here, the operator can choose the starting and finishing depth for analysis as well as indicate what type of depth averaging is desired. Depth averaging of 0.00 means that interpretation analysis will be applied to each recorded depth. This is always the best choice to identify layering and other stratigraphic details. Averaging can obscure results unless it is performed in a fairly uniform layer. Averaging will always remove details, especially at layering interfaces and at lenses, and should be used with extreme caution. There are many choices here for averaging, mostly based on requests from previous users. It is always convenient to use a start depth, which is half the averaging interval. In the case shown here, depth averaging was 0.5 m from a starting depth of 0.25 m, in order to have the values reported at even 0.5 m intervals. The averaged values are given the depth at the mid-point of the average.

It is also possible to have missing data identified as zeros or simply ignored. The results can be sent to a printer or file. However, since the program was set up for a dot matrix printer, it will not properly print in Windows. Therefore output to a file, which you can import into Word and format to fit your needs. This is covered in the readme file hints. Move the cursor over 'Begin Execution' and press 'Enter' and the output will be rapidly created.

Figure 8-8 RUN MENU Showing Depth Averaging Interval Chosen

8.2.5 Program Output

The output text file created by the program is shown in Table 8-1 for McDonald's Farm, Vancouver Airport. The headers in the table have information relating to the field site, the program interpreter, and all the program choices. These choices can easily be adjusted and added to in subsequent outputs. The header is never separated from the data output.

Eleven output parameters were chosen for this example. Sand (drained) parameters are only applied to soil behaviour zones >5 and clay (undrained) are applied to zones <6. The value 9E9 is used to identify parameters, which are 'out of range' and cannot be determined. The user can easily change these with search/replace command in a text editor. Also, this output file can be entered into Excel or other spreadsheet for plotting if required.

Table 8-1 Typical CPTINT 5.2 Output of tabular results

```
"
"Output file from CPTINT - Version 5.2
"======================================
"INPUT FILE: f:\CPTINT\TESTDATA\MCFARM.EDT
"------------------------------------------
"
"Developed by: UBC In-Situ Testing FREEWARE
"     Program: Piezocone Interpretation
"    Web Site: www.civil.ubc.ca/home/in-situ
"
"Interpreter Name: Campanella
"
"File Number:    2            Date: 84-05-24 GWT=1m
"Operator:   MCDONALD FARM    On Site Location: OLD AREA Dmax=25
"Cone Type: UBC6STDppU2       Comment: CPTU COURSE
"
"SUMMARY SHEET
"-------------
"'a' for calculating Qt:                 0.850
"Value for Water Table (in m):           1.000
"Valid Zone Classification based on:     Rf
"Missing unit weight to start depth:     18.860
"Method for calculating Su:              Nkt
"Value of the constant Nkt:              9.000
"Method used to calculate OCR:           Su/EOS
"(Su/EOS) for normal consolidation:      0.250
"Define Zone 6 for Sand Parameters?      YES
"Sand Compressibility for calc Dr:       Moderate
"Method for Friction Angle:              Robertson & Campanella
"Vertical Flow Gradient, i (- up):       +0.000
"CPT to SPT N60 Conversion:              Jeffries & Davies
"
"Soil Behavior Type Zone Numbers
"For Rf Zone & Bq Zone Classification
"-------------------------------------
"Zone #1=Sensitive fine grained     Zone #7 =Sand with some Silt
"Zone #2=Organic material           Zone #8 =Fine sand
"Zone #3=Clay                       Zone #9 =Sand
"Zone #4=Silty clay                 Zone #10=Gravelly sand
"Zone #5=Clayey silt                Zone #11=Very stiff fine grained *
"Zone #6=Silty sand                 Zone #12=Sand to clayey sand *
"   * Overconsolidated and/or cemented
"
"NOTE:
"-----
"For soil classification, Rf values > 8 are assumed to be 8.
"
"( Note: 9E9 means Out Of Range )
"
```

(Table 8-1 continued)

"---| INPUT FILE: f:\CPTINT\TESTDATA\MCFARM.EDT |--

" Depth " (meter)	Qt(avg) (bars)	Rf (%)	Rf Zone (zone #)	Bq Zone (zone #)	FC (%)	Spt N (blow/ft)	Dr (%)	Phi (degree)	Su (kPa)	Su/EOS (ratio)	OCR (ratio)
0.500	8.437	4.534	3	6	54.541	2	9E9	9E9	92.654	9.430	93.484
1.000	3.925	4.114	3	4	67.045	1	9E9	9E9	41.474	2.154	14.761
1.500	8.919	1.469	5	6	40.320	1	9E9	9E9	95.909	4.033	32.332
2.000	11.366	1.038	6	6	33.120	2	11	37	9E9	9E9	9E9
2.500	18.493	0.757	6	6	23.301	3	27	39	9E9	9E9	9E9
3.000	21.360	0.847	6	7	25.270	4	29	39	9E9	9E9	9E9
3.500	49.216	0.401	8	8	3.021	8	59	41	9E9	9E9	9E9
4.000	50.781	0.339	8	8	1.277	8	58	41	9E9	9E9	9E9
4.500	27.739	0.674	7	7	22.372	5	32	37	9E9	9E9	9E9
5.000	79.484	0.288	8	9	0.000	12	71	43	9E9	9E9	9E9
5.500	79.472	0.365	8	9	0.088	12	69	43	9E9	9E9	9E9
6.000	37.110	0.605	7	8	19.914	6	38	39	9E9	9E9	9E9
6.500	82.591	0.341	8	9	0.323	13	68	41	9E9	9E9	9E9
7.000	111.089	0.296	9	9	0.000	17	78	43	9E9	9E9	9E9
7.500	119.339	0.283	9	9	0.000	18	79	43	9E9	9E9	9E9
8.000	87.212	0.421	8	9	5.715	14	66	41	9E9	9E9	9E9
8.500	89.131	0.304	9	9	0.893	14	65	41	9E9	9E9	9E9
9.000	81.689	0.359	8	9	5.518	13	61	41	9E9	9E9	9E9
9.500	119.079	0.337	9	9	0.000	19	74	41	9E9	9E9	9E9
10.000	146.678	0.318	9	9	0.000	23	82	43	9E9	9E9	9E9
10.500	43.284	1.179	7	8	36.446	9	33	37	9E9	9E9	9E9
11.000	80.245	0.396	8	9	9.939	13	56	39	9E9	9E9	9E9
11.500	120.628	0.373	9	9	3.818	20	71	41	9E9	9E9	9E9
12.000	115.330	0.301	9	9	1.616	18	69	41	9E9	9E9	9E9
12.500	164.515	0.326	9	9	0.000	26	81	43	9E9	9E9	9E9
13.000	203.777	0.268	9	9	0.000	31	89	43	9E9	9E9	9E9
13.500	44.044	0.946	7	7	35.999	9	29	35	9E9	9E9	9E9
14.000	86.112	0.569	8	9	17.947	15	54	39	9E9	9E9	9E9
14.500	52.654	0.599	8	8	26.604	10	34	35	9E9	9E9	9E9
15.000	26.214	0.975	7	7	45.974	6	7	31	9E9	9E9	9E9
15.500	9.459	1.485	5	4	77.062	3	9E9	9E9	71.696	0.453	2.100
16.000	8.410	1.908	5	3	86.717	3	9E9	9E9	58.995	0.362	1.589
16.500	7.442	1.565	5	3	92.063	3	9E9	9E9	47.191	0.282	1.162
17.000	8.029	1.769	5	3	89.382	3	9E9	9E9	52.666	0.306	1.289
17.500	7.032	1.536	5	3	98.531	3	9E9	9E9	40.544	0.230	0.900
18.000	6.955	1.718	5	3	100.000	3	9E9	9E9	38.637	0.213	0.821
18.500	7.140	1.646	5	3	100.000	3	9E9	9E9	39.648	0.214	0.822
19.000	7.230	1.577	5	3	100.000	3	9E9	9E9	39.601	0.208	0.796
19.500	7.683	1.607	5	3	100.000	4	9E9	9E9	43.580	0.224	0.872
20.000	7.669	1.728	5	3	100.000	4	9E9	9E9	42.376	0.213	0.818
20.500	9.492	1.801	5	3	90.102	3	9E9	9E9	61.590	0.302	1.269
21.000	8.459	1.501	5	3	97.825	4	9E9	9E9	49.056	0.236	0.929
21.500	8.191	1.483	5	3	100.000	4	9E9	9E9	45.034	0.212	0.813
22.000	8.613	1.602	5	3	100.000	4	9E9	9E9	48.679	0.224	0.872
22.500	9.184	1.530	5	3	97.014	4	9E9	9E9	53.975	0.243	0.967
23.000	9.683	1.585	5	3	95.411	4	9E9	9E9	58.469	0.258	1.042
23.500	9.889	1.492	5	3	96.152	4	9E9	9E9	59.711	0.259	1.044
24.000	9.693	1.429	5	3	99.091	4	9E9	9E9	56.483	0.240	0.950
24.500	9.782	1.446	5	3	99.637	4	9E9	9E9	56.432	0.235	0.927
25.000	10.883	1.737	5	3	96.604	5	9E9	9E9	67.612	0.277	1.135

9 APPLICATIONS OF CPTU AND SEISMIC CPTU DATA TO ENGINEERING DESIGN

9.1 Introduction

There are two main methods for applying cone data to geotechnical design:

1) Indirect methods where soil design parameters (e.g. ϕ', D_r, s_u and E) are first evaluated from interpretation of cone data and then are used in conventional design procedures.

2) Direct use of cone data for design, e.g. calculation of pile capacity directly from factored cone resistance based on empirical rules and experience based on performance.

Much of the early use of cone data for geotechnical design was through direct application to pile design. This approach has the advantage that it is based on observed field experience. Thus, when applied in similar situations, these methods can produce reliable results. In recent years, direct CPTU based design methods have also been developed for other applications, such as design of shallow foundations, liquefaction assessment, and for quality assurance in geotechnical works like embankment construction and ground improvement.

The direct methods have a particular advantage in sands, where use of intermediate parameters like relative density can produce misleading results. However, in areas where little design experience exists, it becomes necessary to use the indirect approach.

This chapter presents guidance for the application of SCPTU data to geotechnical design.

9.2 CPT- SPT Correlations

Much geotechnical practice relies on design experience based on local SPT correlations. Consequently, when first using SCPTU data for design, engineers may find it useful to convert the CPT data to equivalent SPT N values so that they may continue to design using methods based on their local experience. Section 6.2.2.7 of this manual provides a basis for the required CPT-SPT correlation. It should be noted that the q_t/N ratios shown in Figure 6-10 were derived based on SPT N values obtained with an average energy ratio of about 55% to 60% and those given by Equation 6.7 are for 60% of theoretically available potential energy. If local design correlations have been developed based on SPT data obtained using alternative procedures with different average energy levels, the N-values derived from q_t should be adjusted accordingly. Jefferies and Davies (1993) suggested that Equation 6-7 provided a more reliable method of obtaining representative SPT N-values, than actual field SPT measurements. This is because of the many sources of uncertainty in SPT testing (e.g. ASTM D6066 1996).

Recent work by Idriss and Boulanger (2004) has suggested that the q_t/N ratios above may not apply in very loose saturated clean sands.

9.3 Shallow foundations

In routine design of shallow foundations, it is necessary to first check that there is sufficient margin of safety against a bearing capacity failure. It is then necessary to check that that the anticipated settlements are tolerable and, in many cases, it is the estimated foundation settlements at working load that govern design. SCPTU data can be used for estimating shear strength parameters for input to bearing capacity analysis and to provide estimates of stiffness for deformation analyses.

9.3.1 Design of Shallow Foundations on Sand using CPT

9.3.1.1 Bearing capacity

For narrow footings, bearing capacity may govern design. Values of friction angle may be estimated using cone data from Figure 7-16 for input to bearing capacity analyses. However, the values in Figure 7-16 are the peak friction angles that would be obtained from triaxial compression testing and may not be applicable to a bearing capacity analysis as the mobilized friction angle along a slip surface will vary depending on the amount of dilation that occurs. Consequently, the ϕ' estimated from the CPT data needs to be modified to reflect the applied bearing stress and the foundation size. Jamiolkowski et al. (2001) recommend using an iterative process to calculate the ultimate bearing capacity. To begin, they suggest selecting the operational friction angle, $\phi'_{op} = (\phi'_p + \phi'_{cv})/2$ for input to the bearing capacity analysis to obtain, q_{ult}, where ϕ'_p is estimated by the methods in 7.4.1. Once the initial value of bearing pressure is calculated, a new ϕ'_p can be calculated based on an operational confining stress given by the expression (De Beer 1965):

$$\sigma'_{mf} \approx \frac{(q_{ult} + 3\sigma'_{vo})}{4}\left(1 - \sin\phi'_{op}\right) \tag{9.1}$$

and the bearing capacity can be recalculated.

Bearing capacity analyses are also inherently uncertain due to the assumptions of the theoretical approach used to develop the equations. Consequently, it may be advantageous to derive the ultimate bearing capacity, q_{ult}, directly from q_t as originally proposed by Meyerhof (1956). In recent years, Briaud and Jeanjean (1994), Tand et al. (1995), Eslaamizaad and Robertson (1996a) and Lee and Salgado (2005) have proposed relationships to allow direct estimates of q_{ult} from q_t data. The relationships are of the form:

$$q_{ult} = \beta q_{t(ave)} \tag{9.2}$$

where β is a correlation factor and $q_{t(ave)}$ is the average cone penetration resistance from the base of the footing to a depth below the footing base equal to the footing diameter, B. The definition of q_{ult} varies but is typically taken to be the bearing pressure at a particular value of normalized settlement ratio, ρ/B, where ρ is the settlement. The value of ρ/B taken to represent q_{ult} ranges from 0.05 (Tand et al., 1995) to 0.2 (Lee and Salgado, 2005). Figure 9-1 from Lee and Salgado (2005) presents results obtained from finite element analysis of circular footings using a soil model which incorporates realistic treatment of both pre- and post-peak behaviour of silica sand. The same soil model has been used with some success to model cone penetration in chamber tests (Salgado et al. 1997). The figure shows how β varies with B for a range of relative densities, assuming ρ/B=0.2 represents failure. Eslaamizaad and Robertson (1996a) suggested that a value of β=0.16 will provide a reasonably conservative estimate of the ultimate capacity of shallow foundations on sands with any shape and for a wide range of soil density. They defined failure to be at ρ/B=0.1. Briaud and Gibbens (1999) observed the relationship q_{ult}=0.23q_t for ρ/B=0.1 based on full scale loading tests on square footings with B ranging from 1 to 3m on medium dense sand.

Based on the above, β=0.2 is considered to provide a reasonable basis for preliminary assessment of the ultimate capacity of square or circular shallow footings on sand. This value is not appropriate for foundation design on heavily cemented sands.

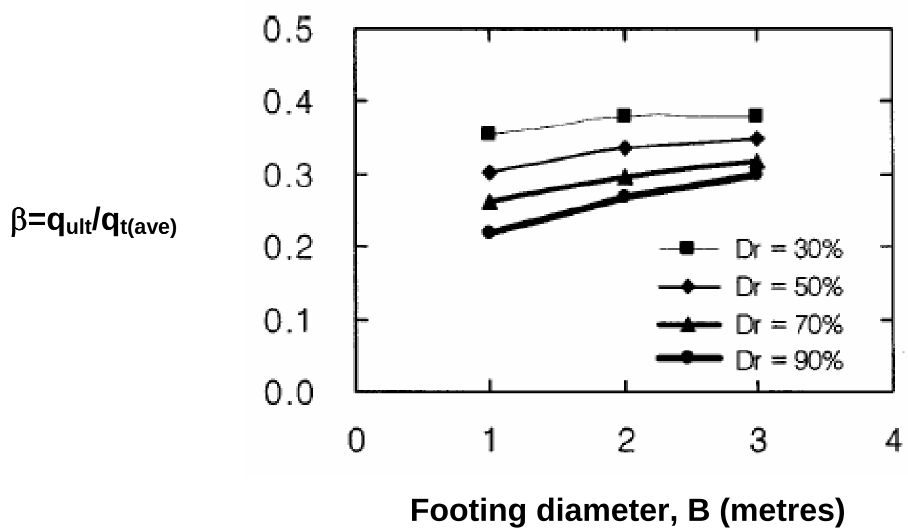

Figure 9-1 Normalized limit unit bearing capacity versus footing diameter (adapted from Lee and Salgado (2005)

9.3.1.2 Settlement

Most approaches to settlement analysis on sands model the soil as a linear elastic material and are based on an equation of the general form:

$$\rho = \frac{\Delta p B I}{E_s} \tag{9.3}$$

where ρ=foundation settlement, Δp is the increase in stress at foundation level, B=foundation width, E_s=equivalent elastic soil modulus and I=displacement influence factor. The influence factor, I, is obtained by integrating the vertical strains over the zone of influence of the footing.

Schmertmann (1970) suggested that for practical purposes, the distribution of vertical strain within the soil below a footing could be described by the equation:

$$\varepsilon_z = \frac{\Delta p}{E} I_z \tag{9.4}$$

where Δq is the intensity of the uniformly distributed load, E is the Young's modulus and I_z is a strain influence factor. He proposed a distribution of I_z with depth. Based on experience with the original method, Schmertmann et al. (1978) revised their proposed distribution of I_z for square and strip footings to those shown in Figure 9-2 and introduced factors to account for the depth of footing (C_1), and for time effects (C_2). In Figure 9-2, Δp is the increase in pressure at foundation depth, D. The depth of influence (2B for square footings and 4B for strip foundations) is divided into depth increments Δz and the total vertical settlement is given by the expression:

$$\rho = C_1 C_2 \Delta p \sum_{1}^{n} \frac{I_z}{E} \Delta z\,. \tag{9.5}$$

where $C_1 = 1 - 0.5(p'_o/\Delta p)$

$C_2 = 1 + 0.2 \log(10\, t_{yr})$

where t_{yr} is the design of the foundation in years.

Schmertmann proposed the direct use of CPT data in determining stiffness using the equation:

$$E = \alpha q_t \tag{9.6}$$

The α values suggested by Schmertmann et. Al (1978) were as follows:

α = 2.5 for square and 3.5 for strip footings for first loading on recent N.C. silica sand fills (age <100 years);

α = 5.0 for square and 7.0 for strip footings on O.C. or compacted sands.

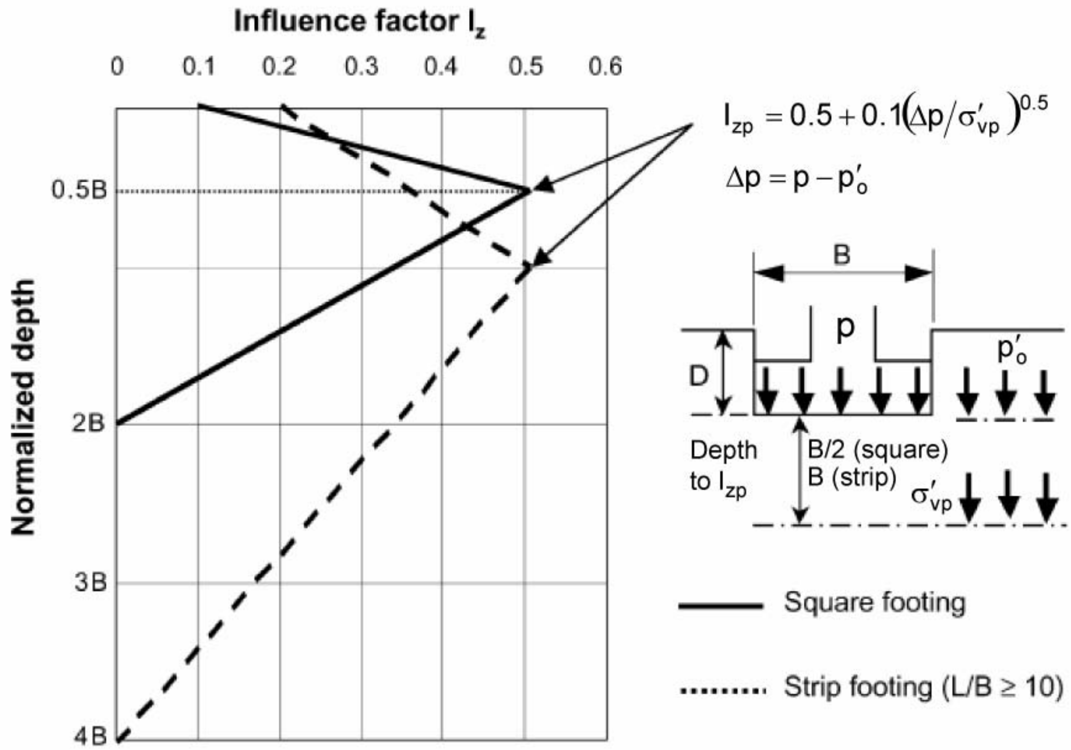

Figure 9-2 Influence factor I_z vs. depth (adapted from Schmertmann et al. 1978)

The different α values for square and strip footings reflect the different geometrical constraints on deformation. Caution should be exercised before increasing α appreciably for overconsolidated sands because of the uncertainty in estimating OCR in sand. More details are given in the Worked Examples.

Mayne and Poulos (1999) noted that many solutions have been proposed for a variety of initial assumptions and this has led to a profusion of charts in the geotechnical literature that may be used to derive influence factors for input to settlement calculations. They introduced an approximate spreadsheet integration technique suitable for deriving displacement influence factors for a variety of initial conditions which allows Schmertmann's method to be extended to other initial assumptions, including consideration of a range of degrees of loading (Mayne and Poulos 2001). Their method compares favourably with available published and analytical and numerical solutions for isolated circular and rectangular footings but is not applicable to strip foundations.

The key to the success of these elasticity-based methods lies in the appropriate choice of soil modulus (Poulos et al. 2002). Estimates of stiffness can be made either through correlations to q_t or from direct measurement of small strain modulus adjusted to account for the anticipated degree of loading or shear strain level.

Stroud (1988) analyzed data for model footing tests on normally consolidated sand at a range of densities and obtained the relationship shown in Figure 9-3. It shows degree of loading, q/q_{ult} plotted against ρ/B, where q is the applied bearing pressure and q_{ult} is the ultimate bearing capacity As discussed in 9.3.1.3, q_{ult} was defined to be the bearing pressure at $\rho/B=0.2$ or 20%. The normalization results in a single curve. Such normalized relationships between degree of loading and settlement are useful in interpretation of load tests (Briaud and Gibbens 1999) and in foundation design. For example, a typical acceptable footing settlement of 25 mm, represents $\rho/B=2.5\%$ for B=1 m and 0.63% for B=4 m. Consequently, to meet settlement criteria, the permissible degree of loading, q/q_{ult}, would be much greater for a narrow footing than for a larger footing (0.2 for B=1 and 0.05 for B=4 m).

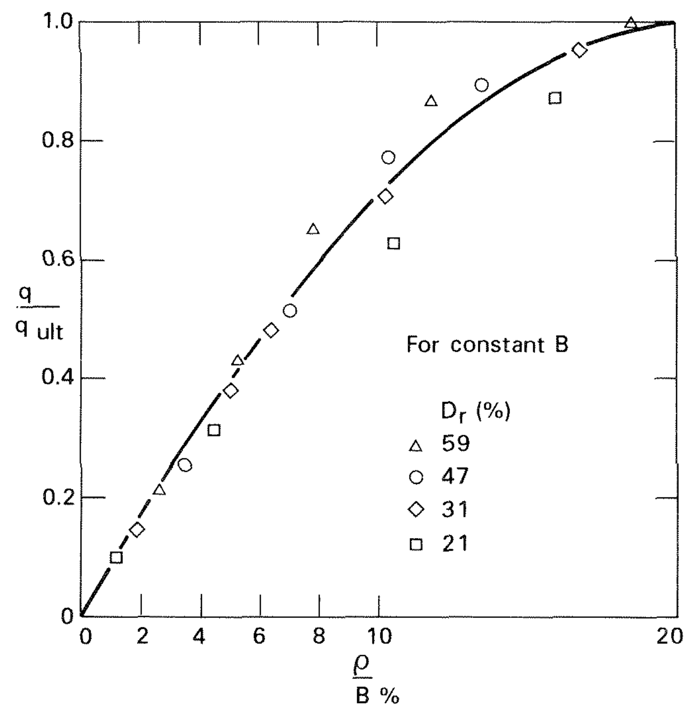

Figure 9-3 Normalized plot of settlement against bearing stress (Vesic 1973, Stroud 1988)

Robertson (1991a) adapted Stroud's concept to develop charts that allow estimates of E'/q_t for a range of degrees of loading. He obtained the curves shown in Figures 9-4(a), (b) and (c) for OC , aged NC and Young NC silica sand, respectively. E' is the equivalent Young's modulus appropriate for input to settlement calculations by elasticity based methods for spread footings. If G_o is available from V_s, Figures 7-7 and 7-8 can be used for guidance as to which chart in Figure 9-4 is applicable. Figure 9-4(c) will give the most conservative equivalent stiffnesses.

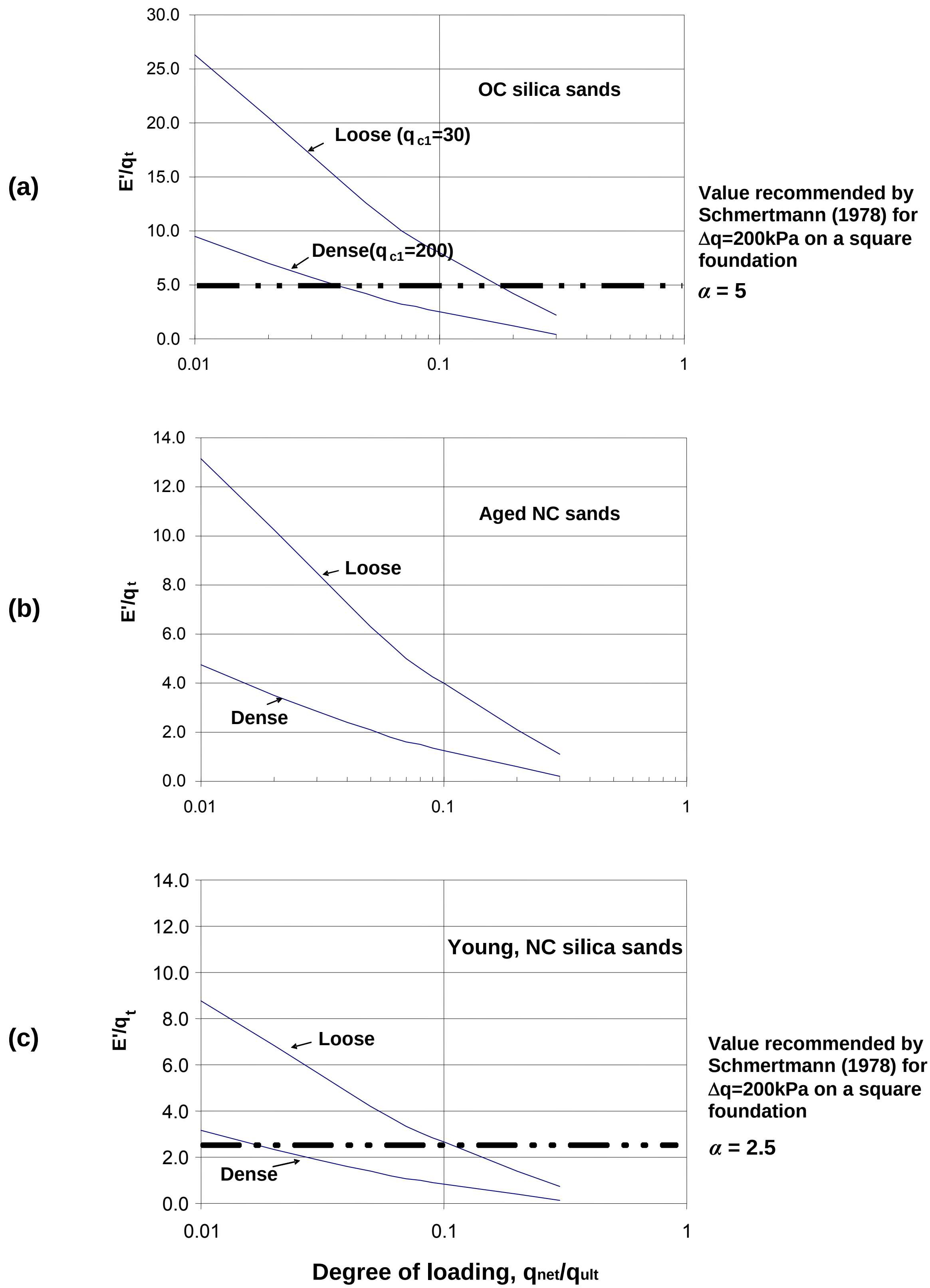

Figure 9-4 Variation of E'/q_t with degree of loading (adapted from Robertson 1991)

Schmertmann's E'/q_t recommendations are shown on Figures 9-4(a) and (c) for comparison. These values indicate that the degree of loading would be much less in dense sand than in loose. Schmertmann's method is applicable for a loading range from 100 to 300 kPa, and so it is logical that a stress increase, Δq= 200 kPa, would represent a higher value of q_{net}/q_{ult} for loose sands than for dense.

Values of soil stiffness may also be derived from the shear modulus, G, and an appropriate value of Poisson's ratio, ν', using the expression:

$$E = 2(1 + \nu')G\,. \tag{9.6}$$

ν' varies with strain level but is normally between 0.1 and 0.2 for sands for strains applicable to well designed foundations (Mayne and Poulos 1999). The appropriate value of G may be obtained from G_o, making appropriate allowance for the degree of loading as shown in Figure 7-21. Care should be exercised when using these methods for cemented or compressible sands as the assumed modulus attenuation curve may not be applicable.

9.3.2 Shallow Foundations on Clay

The two main calculations for shallow foundations on clay are related to stability and settlement.

9.3.2.1 Bearing Capacity

On saturated fine-grained soils, short term stability is assessed from bearing capacity calculations using the undrained shear strength, s_u, in the bearing capacity equation:

$$q_{ult} = N_c s_u + \sigma_{vo} \tag{9.7}$$

where N_c is a bearing capacity factor appropriate for undrained conditions (Skempton 1951). The undrained shear strength can be estimated from q_t or pore pressure data as discussed in Section 7.4.2. As noted earlier, s_u varies with the mode of shear. It is now considered that $(s_u)_{DSS}$ is the applicable shear strength to use in stability calculations (Ladd 1991). If the correlation used to estimate s_u from q_t is based on field vane shear measurements then it will be necessary to correct $(s_u)_{FV}$ to $(s_u)_{DSS}$ by applying the Bjerrum correction factors based on Plasticity Index shown in Figure 9-5 using the equation:

$$(s_u)_{DSS} = \mu (s_u)_{FV} \tag{9.8}$$

As the shear strength will increase as the soil consolidates under the foundation load, the long term stability should be higher than the short term. Ladd (1991) argues that the long term stability should be calculated using an undrained strength analysis based on the long term undrained strength (i.e. after completion of consolidation under the maintained bearing pressure).

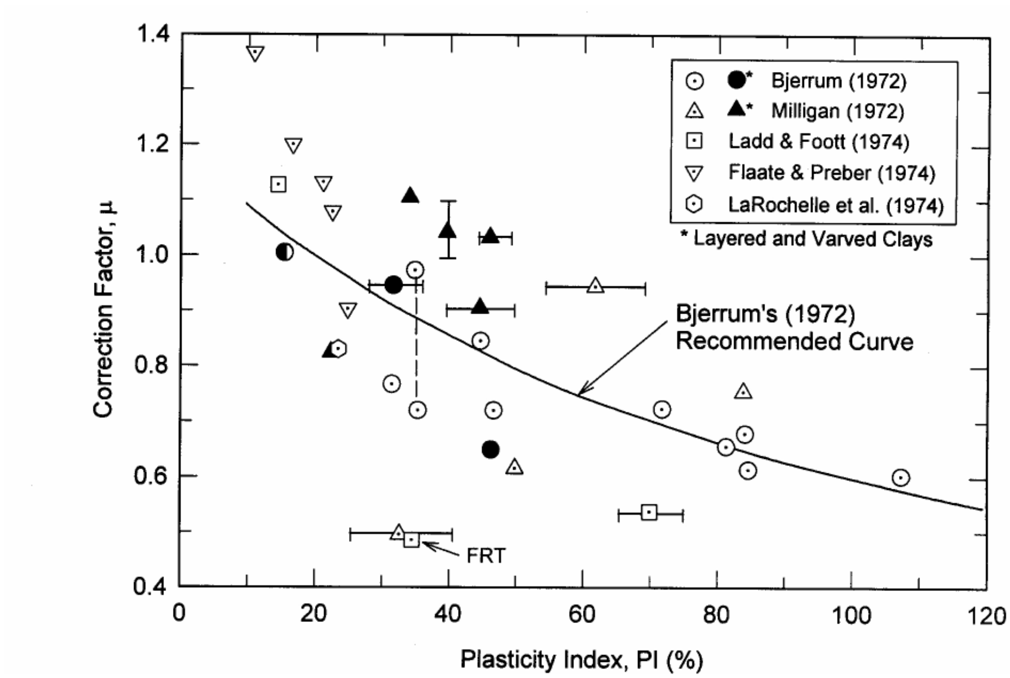

Figure 9-5 Field vane correction factor vs plasticity index derived from embankment failures (After Ladd et al. 1977)

9.3.2.2 Settlement

For saturated fine-grained soils, settlements include both immediate settlement, due to distortion of the clay that occurs immediately upon loading, and long term settlement that depends on the clay's compressibility. The initial settlement may be estimated using elasticity-based methods as for sands but using undrained soil moduli. Both drained and undrained Young's moduli may be estimated from G_o obtained from V_s measurements or from CPT correlations using an appropriate value of Poisson's ratio and equation 9.6. For saturated soils, ν_u=0.5. The modulus must be selected with due consideration for anticipated shear strain levels or degree of loading as discussed in Section 7.4.3.3.

Most published values of modulus reduction with strain level have been developed for cyclic loading. Fahey (1998) indicated that modulus degradation may occur more rapidly for cases of static loading than for dynamic loading and suggested the alternative approach to modulus degradation discussed in 7.4.3.1. G is assumed to vary with mobilised shear stress ratio, τ/τ_f, which for undrained deformation in clays, is often expressed as τ/s_u. For shallow foundation design, τ/τ_f may be assumed to be equal to (Factor of safety)$^{-1}$.

Alternatively, an estimate of E_u/s_u may be made from Figure 9-6 which shows secant Young's moduli normalized by undrained shear strength plotted against the applied shear stress ratio, $\tau_h/(s_u)_{DSS}$. The data comes from CK_oU DSS tests on 9 soils. The soils have similar trends in E_u/s_u with $\tau_h/(s_u)$ but the absolute values vary considerably. Ladd et al. (1977) found that the observed deformations during construction of embankments on five of the deposits used to develop Figure 9-6 were in general agreement with the relative magnitudes of E_u/s_u shown in the figure. It is important to note that these trends cannot be taken to apply to quick clays or naturally cemented soils.

9.3.2.3 Consolidation Settlement

Calculation of consolidation settlements requires:

- Determination of the yield stress (σ'_p) profile within the zone of influence of the foundation
- A settlement calculation using soil properties such as the constrained modulus M, the coefficient of volume compressibility, m_v, or the coefficient of compressibility (C_c) as input.

CPTU based methods of estimating yield stress, σ'_p, were described in Section 7.3.2. Once the yield stress profile has been established, then the final stress imposed by the foundation loading should be calculated and compared to the yield stress. If the yield stress exceeds the final applied stress, then settlement will likely be small and will occur relatively rapidly. In this case, final settlement may be estimated using elasticity methods and an estimate of the drained modulus or using an estimate of m_v or constrained modulus, $M=1/m_v$ as discussed in 7.4.3.4.

Where the final estimated effective stress exceeds the yield stress, settlements are likely to be larger and may occur over a greater time period depending on the consolidation characteristics of the clay. For this calculation, an estimate of the soil compressibility will be required. Unfortunately, the compressibility of clay is not reliably estimated from cone data without local correlation or experience. However, a variety of crude empirical methods are discussed in Section 7.4.3.4. Methods based on the suggested parameters allow only a first approximation of the likely settlement. For a more accurate prediction of compressibility, it remains necessary to obtain samples and perform laboratory consolidation tests. For any particular clay, however, the methods can be adjusted based on local experience and on field settlement observations (see Crawford and Campanella 1991).

The CPTU also offers the potential to estimate the rate of consolidation, as discussed in Section 7.4.4. The rate of pore pressure dissipation, during a pause in the penetration, provides a measure of the coefficient of horizontal consolidation, c_h (Robertson et al. 1992a). However, the theories related to these measurements make many simplifying assumptions and Leroueil and Hight (2003) note that the coefficient of consolidation remains one of the most difficult geotechnical parameters

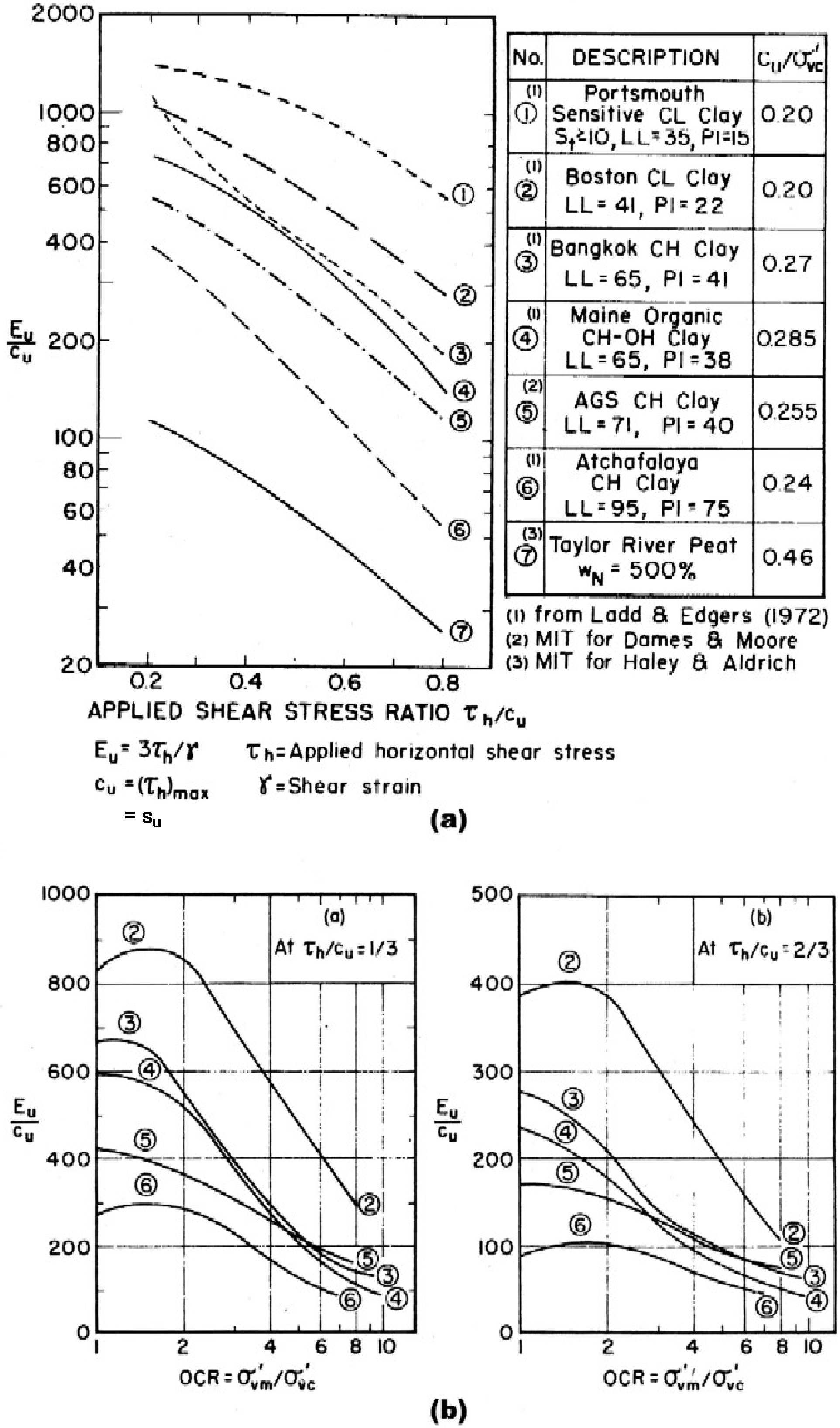

Figure 9-6 Selection of soil stiffness ratio for clays (adapted from Ladd et al., 1977)

to determine. For any particular clay, the method therefore *requires local adjustment* by an adequate number of field settlement observations.

It should be made clear that because the CPTU provides continuous profiles of soil variability, judgement and experience should be applied to adequately account for the soil variability. The continuous nature of the CPTU in-situ data provides a good basis for such judgement.

9.4 Deep foundations

As installation of piles changes the soil properties of the zone that will provide resistance to applied loads, the final capacity is very sensitive to the details of the installation process, and the complexity of the changes in soil conditions immediately adjacent to the pile means that most practical design relies on empirical correlations (O'Neil 2001). The problem of estimating pile capacity is further complicated by the large variety of pile types and installation procedures available, as well as the wide variation in soil types.

CPT profiles are ideal for use in pile design as they provide a detailed picture of the soil stratigraphy in which the piles will be founded and the cone is in effect a small-diameter displacement pile. As a result, many empirical formulae have been developed relating cone parameters to pile capacity. A number of studies of CPT-based methods (Abu-Farsakh and Titi 2004; Briaud and Tucker 1988), including one at UBC (Robertson et al. 1988), have shown the LCPC method by Bustamante and Gianeselli (1982) to provide the best predictions of pile capacity. The method by de Ruiter and Beringen (1979) also performed well.

Conventionally, ultimate axial pile capacity, R_{ult}, is estimated as the sum of the ultimate shaft capacity, R_s, and the ultimate base capacity, R_b:

$$R_{ult}=R_s+R_b \tag{9.10}$$

The ultimate shaft capacity is given by:

$$R_s=\Sigma r_s C dz, \tag{9.11}$$

where r_s is the unit shaft resistance, C is the pile perimeter and dz is an increment of depth. The ultimate tip capacity is given by:

$$R_b=r_b A_b, \tag{9.12}$$

where r_b is the unit base resistance and A_b is the area of the pile base. CPT based methods are direct and use empirical factors to relate cone parameters (usually q_t) to r_s and r_b, with the factors varying depending on the soil type and the installation method. In most practical design methods, an upper limit is placed on the calculated values of r_s and r_b, the upper limits depending on soil and pile type.

It is also important to consider the displacement required to mobilize the end bearing resistance in comparison to the cone resistance. The scale effects for relating cone data to pile end bearing are complex, with large diameter piles reacting differently to soil stratigraphy than CPTs due to their larger zone of influence. It is thus necessary to average q_t over a number of pile diameters above and below the pile tip level. Each method includes rules for selection of appropriate average tip resistances. Because of the uncertainties that remain, pile design is empirical and should be confirmed by full scale load testing.

9.4.1 Pile Design in Sand

The limiting unit shaft capacity in sands is conventionally estimated using

$$r_s = \beta \sigma'_{vo} \tag{9.13}$$

where $\beta = K_s \tan\delta$, K_s is a lateral stress coefficient and δ is the soil-pile interface friction angle. Both K_s and δ depend on the pile type and installation method and on the soil. As it is based on effective stress, equation 9.13 is applicable to all soil types. Typical values of β for cohesionless soils are given in the Table 9-1.

Soil Type	Cast-in-place piles	Driven Piles
Silt	0.2-0.3	0.3-0.5
Loose sand	0.2-0.4	0.3-0.8
Medium sand	0.3-0.5	0.6-1.0
Dense sand	0.4-0.6	0.8-1.2
Gravel	0.4-0.7	0.8-1.5

Table 9-1 Range of β values (Canadian Foundation Engineering Manual 1992)

The ultimate unit base resistance is conventionally calculated using the expression:

$$r_b = N_t \sigma'_b \tag{9.14}$$

where N_t is a bearing capacity factor and σ'_b is the vertical effective stress at the pile base. Typical values of N_t are given in Table 9-2.

Soil Type	Cast-in-place piles	Driven Piles
Silt	10-30	20-40
Loose sand	20-30	30-80
Medium sand	30-60	50-120
Dense sand	50-100	100-120
Gravel	80-150	150-300

Table 9-2 Range of N_t values (Canadian Foundation Engineering Manual 1992)

A large portion of the working load capacity of driven piles in sand comes from end bearing. Complex installation phenomena such as vibratory loading of soil and residual pile stresses affect the available pile capacity.

9.4.2 Pile Design in Clays

Historically, the limiting shaft resistance, r_s, on the pile shaft has been expressed as a proportion of the in-situ undrained shear strength of the soil, s_u, as

$$r_s = \alpha s_u \tag{9.15}$$

where α typically varies from 0.5 to 1.0 depending on the shear strength ratio, s_u/σ'_v, of the soil. α also varies with pile embedment and the method of pile installation.

The effective stress approach can also be used for clays using Equation 9.13.

For clays Randolph (2003) notes that α and β are complex functions of soil parameters such as Yield Stress Ratio (OCR), PI, sensitivity etc. As q_t is also affected by these parameters, the CPT continues to be important in the development of new pile design methods (e.g. Lehane et al. 2000).

Similarly, the total stress approach to estimating the ultimate base resistance has been related to the undrained shear strength through the equation:

$$r_b = N_c s_u \tag{9.16}$$

where N_c is a bearing capacity factor that is typically 9 but may be as low as 6 for large diameter piles of limited penetration. Poulos et al. (2002) note that one of the key difficulties in using the total stress approach is the estimation of undrained shear strength. The CPT allows estimates of s_u to be made based on the methods in 7.4.2.1.

9.4.3 Non or low-displacement piles

Non-displacement piles include bored cast-in-situ piles, precast piles placed in a pre-bored hole, piles placed with the aid of jetting and piles constructed by pumping grout through the hollow stem of a continuous-flight auger, etc. With bored piles, horizontal stresses will decrease during installation rather than increase as they do with a displacement pile. With pre-bored or jetted piles, any stress increase will be less than for a driven parallel-sided pile, the reduction depending on the extent to which the pile is driven below the pre-bored or jetted depth. Stress increase may also be less with a pile which is vibrated into the ground or is cast within a vibrated open-ended casing. Hence, non-displacement piles should have lower shaft resistance than displacement piles of the same diameter considering this factor only. However, the soil/pile interface is much rougher for bored piles which compensates to some degree for the reduction in lateral stress. In bored piles, there may also be a reduction in end bearing capacity because of loosening of soil below pile tip level. These effects are included in the α and β factors in the tables above.

9.4.4 CPT Pile Design Methods

As noted above, the LCPC method by Bustamante and Gianeselli (1982) and the method by de Ruiter and Beringen (1979) have performed well. These have mostly been applied to design of driven piles. A summary of these two methods for using CPT data to predict axial pile capacity is given in the following sections. Generally, it is recommended that capacities be estimated by both methods and that the lower value of ultimate capacity should be adopted. A worked example for each is given in the Worked Examples Volume.

A new approach based on research at Imperial College also appears to have considerable merit and is gaining in popularity, particularly for offshore piles. The method is summarized in Tomlinson (2001) and full details are given in Jardine and Chow (1996).

Pile capacities of non-displacement piles can also be calculated by the CPT methods, but a higher factor of safety is often applied. The LCPC method was based on the results of 55 bored piles and is therefore the recommended CPT-based approach for bored piles. Because of the uncertainties concerning non-displacement piles, especially in sand, and the considerable effect that installation procedures can have on bearing capacity and settlement, it is recommended that pre-construction pile load tests should be performed. It may be feasible to dispense with these on very small projects where there is considerable local experience, but in such cases factors of safety may need to be increased by some 50 percent.

9.4.4.1 LCPC Method (Bustamante and Gianeselli, 1982)

The method developed at LCPC (France) is summarized in Tables 9-3, 9-4, and 9-5. The unit end bearing is calculated using an equivalent cone resistance at the pile tip, as shown in Figure 9-7.

The equivalent average cone resistance, q_{ca}, is calculated in three steps:

- The mean value of q_c over the depth interval $\pm a$ above and below the proposed pile tip depth, q'_{ca}, is calculated;
- Tip resistances greater than $1.3q'_{ca}$ or less than $0.7q_{ca}$, are then eliminated;
- The mean value of the remaining values is calculated to give q_{ca}.

	SAND AND CLAY
Unit Skin Friction f_p	$f_p = \frac{q_c}{\alpha}$ α = friction coefficient (Table 9-5)
Unit End q_p	q_p = $q_p = k_c \bullet q_{ca}$ q_{ca} = equivalent cone resistance at level of pile tip (Fig. 9-7) k_c = bearing capacity factor (Table 9-4)

Table 9-3 LCPT CPT Method (Bustamante and Gianeselli, 1982)

Nature of Soil	q_c (MPa)	Factors k_c	
		Group I	Group II
Compact to very compact sand and gravel	<1	0.4	0.5
Moderately compact clay	1 to 5	0.35	0.45
Silt and loose sand	≤ 5	0.4	0.5
Compact stiff clay and compact silt	>5	0.45	0.55
Soft chalk	≤ 5	0.2	0.3
Moderately compact sand and gravel	5 to 12	0.4	0.5
Weathered to fragmented chalk	> 5	0.2	0.4
Compact to very compact sand and gravel	>12	0.3	0.4

Group I:
- Plain bored piles
- Mud bored piles
- Micro piles (grouted under low pressure)
- Cased bored piles
- Hollow auger bored piles
- Piers
- Barrettes

Group II:
- Cast screwed piles
- Driven precast piles
- Prestressed tubular piles
- Driven cast piles
- Jacked metal piles
- Micropiles (smaller diameter piles grouted under high pressure with diameter < 250 mm)
- Driven grouted piles (low pressure grouting)
- Driven metal piles
- Driven rammed piles
- Jacked concrete piles
- High pressure grouted piles of large diameter

Table 9-4 Bearing Capacity Factor, k_c

Nature of Soil	q_c (MPa)	Coefficients, α				Maximum Limit of f_p (MPa)					
		Category									
		I		II		I		II		III	
		A	B	A	B	A	B	A	B	A	B
Soft clay & mud	<1	30	30	30	30	0.015	0.015	0.015	0.015	0.035	-
Moderately compact clay	1 to 5	40	80	40	80	0.035 (0.08)	0.035 (0.08)	0.035 (0.08)	0.035	0.08	≥0.12
Silt & loose sand	≤ 5	60	150	60	120	0.035	0.035	0.035	0.035	0.08	-
Compact to stiff clay & compact silt	>5	60	120	60	120	0.035 (0.08)	0.035 (0.08)	0.035 (0.08)	0.035	0.08	≥0.20
Soft chalk	≤ 5	100	120	100	120	0.035	0.035	0.035	0.035	0.08	-
Moderately compact sand & gravel	5 to 12	100	200	100	200	0.08 (0.12)	0.035 (0.08)	0.08 (0.12)	0.08	0.12	≥0.20
Weathered to fragmented chalk	>5	60	80	60	80	0.12 (0.15)	0.08 (0.12)	0.12 (0.15)	0.12	0.15	≥0.20
Compact to very compact sand & gravel	>12	150	300	150	200	0.12 (0.15)	0.08 (0.12)	0.12 (0.15)	0.12	0.15	≥0.20

CATEGORY:

IA - Plain bored piles
Mud bored piles
Hollow auger bored piles
Micropiles (grouted under low pressure)
Cast screwed piles
Piers
Barettes

IB - Cased bored piles
Driven cast piles

IIA - Driven precast piles
Prestressed tubular piles
Jacked concrete piles

IIIA - Driven grouted piles
Driven rammed piles

IIB - Driven metal piles
Jacked metal piles

IIIB - High pressure grouted piles diameter >250 mm
Micro piles grouted under high pressure

Note:

Maximum limit unit skin friction, f_p: bracket values apply to careful execution and minimum disturbance of soil due to construction.

Table 9-5 Friction Coefficient, α

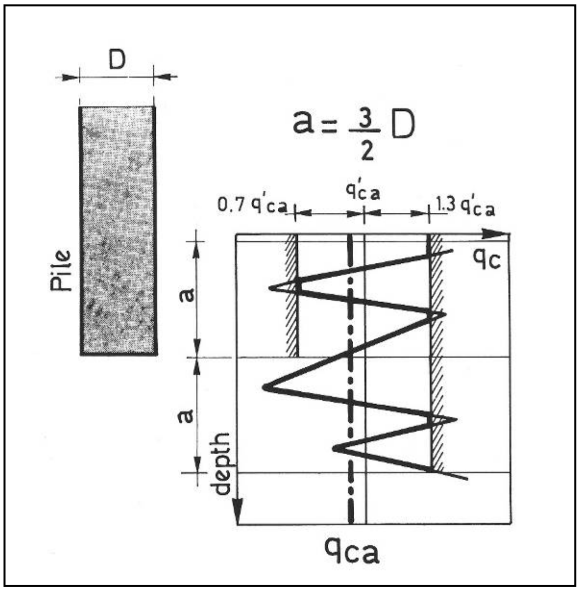

Figure 9-7 LCPC CPT Method to Determine Equivalent Cone Resistance at Pile Tip (After Bustamante and Gianeselli, 1982)

9.4.4.2 European Method (de Ruiter and Beringen, 1979)

The CPT method used in Europe and especially for design of piles in the North Sea is summarized in Table 9-6.

The unit end bearing for piles in sand is based on pile load test data and is governed by the q_c in a zone of between 0.7D to 4D (where D = pile diameter) below the pile tip and 8D above the pile tip, as shown in Figure 9-8. The base resistance is determined as an average value according to the relation below:

$$q_p = [(I+ II)/2 +(III)]/2 \tag{9.17}$$

where I, II and III are obtained as follows:

I: The average q_c is calculated from pile base to 0.7D below the base. This averaging is repeated for a range of depth intervals from the pile base up to a maximum of 4D. The minimum value is selected for input to Eq. 9.17.

II: The minimum q_c value over the depth range below the level of the pile base used for I.

III: Take the average q_c between the level of the pile base and 8 pile diameters above. Values that exceed q_c determined in II are to be disregarded.

Schmertmann (1978) also presented a CPT method, extensively used in North America, in which the design value of q_p was selected in a very similar way.

De Ruiter and Beringen (1979) noted that overconsolidated cohesionless soils tend to experience some strength reduction during driving and so recommended that q_p should be limited as shown in Figure 9-8. An upper limit of 15 MPa was recommended for all cohesionless soils. Full details are provided in the 1979 paper.

	SAND	CLAY
Unit Skin Friction, f_p	Minimum of: f_1 = 0.12 MPa f_2 = CPT sleeve friction, f_s $f_3 = q_c/300$ (compression) $f_4 = q_c/400$ (tension)	$f = \alpha\, s_u$ where: α = 1 for NC Clay = 0.5 for OC Clay
Unit End Bearing, q_p	Minimum: q_p from Fig. 9-8	$q_p = N_c \cdot s_u$ where: N_c = 9 $s_u = q_c/N_k$ N_k = 15 to 20

Table 9-6 European CPT Design Method (After de Ruiter and Beringen, 1979)

9.4.5 Factors of Safety

The choice of factor of safety to be applied to the calculated ultimate pile capacity depends on many factors, including reliability and sufficiency of the site investigation data, confidence in the method of calculation, previous experience with similar piles in similar ground conditions and whether or not pile load tests to failure are available. Different factors of safety are often applied to R_s and R_b.

Where there are appreciable differences in CPT profiles, a reasonable lower bound profile should be adopted or the site should be divided into similar regions. In cases where no specific estimate of settlement is to be made, the factor of safety may also be intended to limit settlements to reasonable values. In such cases, due allowance should be made for the type of loading, which may affect settlement; i.e., cyclic live loads will give larger settlements than single (or few) load applications, particularly if the live load is large compared with the dead load.

The recommended factors of safety for the above CPT methods are listed in Table 9-7.

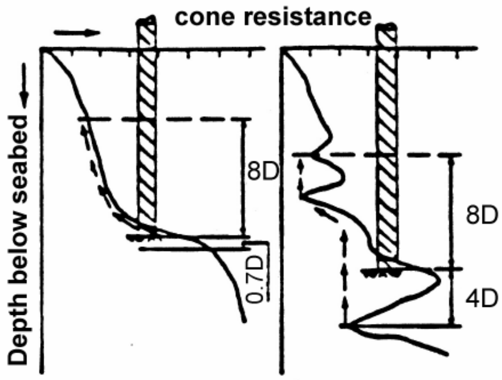

$$q_p = \frac{(I + II)/2 + III}{2}$$

Key

- D : Diameter of the pile
- I : Average cone resistance below the tip of the pile over a depth which may vary between 0.7D and 4D
- II : Minimum cone resistance recorded below the pile tip over the same depth of 0.7D to 4D
- III : Average of the envelope of minimum cone resistances recorded above the pile tip over a height which may vary between 6D and 8D. In determining this envelope, values above the minimum value selected under II are to be disregarded
- q_p : Ultimate unit point resistance of the pile

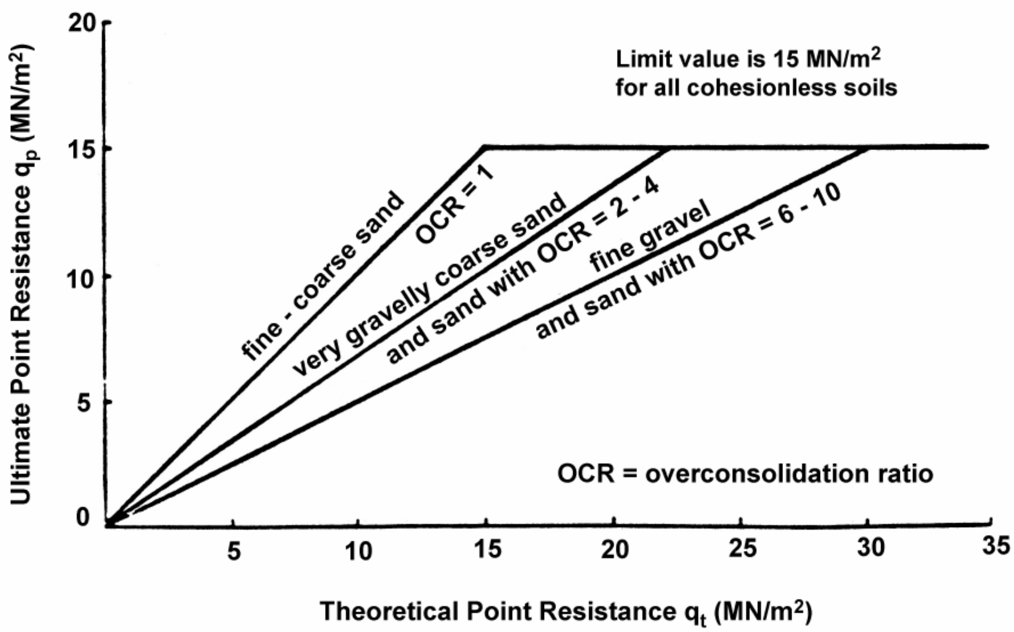

Figure 9-8 Application of CPT to Pile Design (After de Ruiter and Beringen, 1979)

Method	Load condition	Factors of safety
Bustamante and Gianeselli	R_s R_b	2.0 3.0
De Ruiter and Beringen (1979)	Static loads Static + Storm Loads	2.0 1.5

Table 9-7 Recommended factors of safety for CPT based design methods (adapted from Lunne et al. 1997)

9.4.6 Settlement of Piles

Tomlinson (2001) notes that safety factors in the range of 2-3 are usually capable of restricting settlements to acceptable values for piles up to about 600 mm diameter. For larger diameter piles and for pile groups, it is necessary to check the settlements at working load. Although installation of piles changes the deformation and compressibility characteristics of the soil mass governing the behaviour of single piles under load, this influence extends only a few pile diameters below the pile tip. Meyerhof (1974) therefore suggests that the total settlement of a group of driven or bored piles under a safe design load (not exceeding about one-third of the ultimate group capacity) can generally be estimated using the equivalent raft method in which the pile group is represented by an equivalent raft acting at some characteristic depth along the piles an equivalent foundation.

Poulos et al. (2002) found that the method was suitable for predicting the overall settlement of a group but was not suitable for predicting the detailed distributions of settlement and pile load within the group. For a group of friction piles, the equivalent foundation is assumed to act on the soil at an effective depth of two-thirds the pile embedment and the load is assumed to spread at 1H:4V. For a group of point-bearing piles the equivalent foundation is taken at the elevation of the pile points and no load spread is assumed. The settlement of the equivalent foundation can be estimated using the methods given in 9.3 for shallow foundations, although Van Impe (1991) and Poulos (1993) concluded that the equivalent raft method should not be used for pile groups in which the sum of the pile cross-sectional areas was less than 10% of the plan area of the group.

Fellenius (1989) suggests that all piles will, in the long term, be subjected to downdrag along their upper portions due to relative settlements of the surrounding soil. He suggests a unified approach to pile design incorporating downdrag.

9.4.7 Negative Shaft Friction (Downdrag)

Negative shaft friction and subsequent downdrag are rarely a problem of capacity but one of settlement. The magnitude of the downdrag generally has no influence on the bearing capacity of a pile, since the capacity of a pile is based on a plunging failure when the pile is assumed to be moving down relative to all the soil. Exceptions to this are end bearing piles driven into a very strong layer such as rock where large negative friction forces can cause damage to the piles. In general, a rigid, high capacity pile will experience a large drag load, but small settlements, whereas a less rigid, smaller capacity pile will experience a smaller drag load, but larger settlements. No pile will settle more than the ground surface nearest the pile. For further details, see Fellenius (1989), and Goudreault and Fellenius (1990).

9.5 Liquefaction assessment

9.5.1 Screening for liquefaction susceptibility

Due to the difficulties in obtaining and testing undisturbed samples from most potentially liquefiable soil materials, it is common for engineers to use empirical methods based on in-situ testing for a preliminary evaluation of the liquefaction susceptibility at a site. The ‘‘simplified procedure’’ was proposed by Seed and Idriss (1971) following disastrous earthquakes in Alaska and in Niigata, Japan in 1964. That procedure has been modified and improved periodically since that time with major reviews by an expert committee of the National Research Council (NRC) in 1985 and another by National Center for Earthquake Engineering Research (NCEER) in 1997 (Youd and Idriss 1997). The reviews examined the state-of-knowledge and the state-of-the-art for assessing liquefaction hazard due to earthquake loading. The results of the NCEER review have been summarized in Youd et al. (2001). The early “empirical method” was based largely on the use of in situ testing by SPT N-values but Youd et al. (2001) present detailed recommendations for the use of the CPT and V_s in liquefaction assessment. This has become the recognized guidance document for liquefaction assessment due to earthquake loading in North America.

Youd et al. (2001) recommend that the CPT is the preferred approach for site characterization where possible as CPT results are more consistent and repeatable than other in situ tests and the CPT provides a nearly continuous profile of penetration resistance available for stratigraphic interpretation. This allows a more detailed definition of soil layers than by other tools. They note that the SPT can completely miss thin (but potentially important) liquefiable strata between test depths and can fail to suitably characterize strata less than about 3 to 4 feet in thickness. They also note the disadvantage that the CPT provides no sample and so recommend that the CPT interpretation be confirmed by occasional drilling and sampling and that liquefaction susceptibility be assessed using a combination of q_t and $(N_1)_{60}$ from SPT testing. To identify sand and silts that may be liquefiable, use can be made of the soil behaviour type classification chart. Robertson and Wride (1998) presented a screening chart in terms of normalized cone parameters, shown in Figure 9-9.

Soils in Zone A are susceptible to cyclic liquefaction, depending on the size and duration of cyclic loading; and liquefaction is unlikely for soils in Zone B. Soils in Zone C may experience flow liquefaction and (or) cyclic liquefaction, depending on soil plasticity and sensitivity as well as size and duration of cyclic loading and should be sampled and tested. Youd et al. (2001) recommend that the liquefaction susceptibility of soils with Robertson I_c between 2.4 and 2.6 should be assessed by sampling and testing.

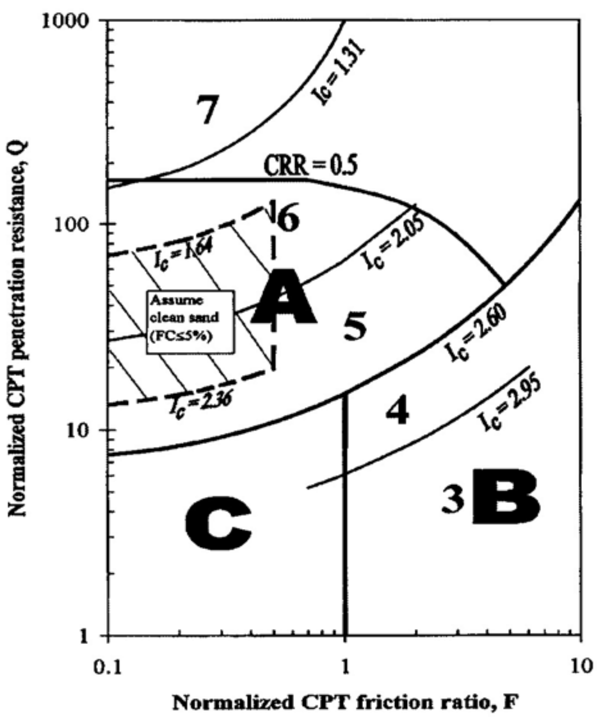

Figure 9-9 Summary of liquefaction potential on soil classification chart by Robertson and Wride (1998)

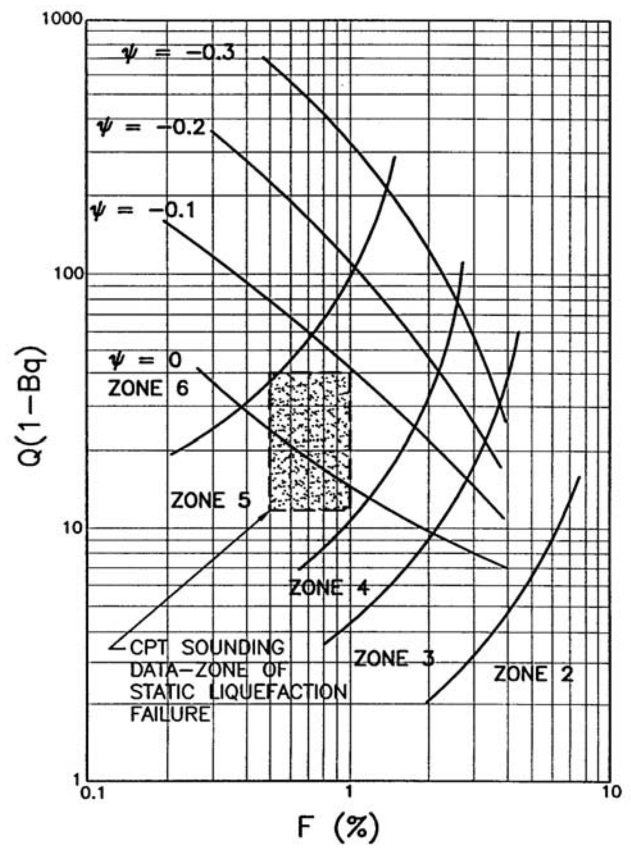

Figure 9-10 CPTU State Parameter Screening for Static Liquefaction (Davies 1999)

The chart by Plewes et al. (1992), presented as Figure 6-14, has been used successfully to identify tailings that are susceptible to static liquefaction. The contours of State Parameter suggest that soils in the lower left corner of the screening chart should be contractive during shear and so susceptible to liquefaction under undrained loading. Figure 9-10 (Davies 1999) shows data from a static liquefaction failure. Although plotted in terms of slightly different parameters, both charts are useful for screening of liquefaction susceptibility.

9.5.2 Liquefaction due to earthquake loading

The recommended procedure for liquefaction assessment involves three steps:

- Characterization of the dynamic effects of the earthquake – i.e. the demand on the soil or the Critical Stress Ratio (CSR) applied by the earthquake;
- Characterization of the resistance of the soil to the imposed cyclic loading, i.e. assessment of the capacity of the soil or the Cyclic Resistance Ratio (CRR).
- Assessment of the factor of safety against liquefaction, i.e. F.S. = CRR/CSR.

9.5.2.1 Characterization of the Earthquake

Seismic shear stresses play a major role in the development of liquefaction. Time histories of shear stresses are usually very non-uniform and are difficult to apply in empirical methods. Seed (1983) suggested replacing the irregular time history by an equivalent number of uniform cycles and normalizing to the shear stresses by dividing by the effective overburden stress. This is the cyclic stress ratio (CSR).

Seed and Idriss (1971) proposed that this uniform cyclic shear stress ratio (CSR) be determined by:

$$CSR = (\tau_{av}/\sigma'_{vo}) = 0.65\,(a_{max}/g)(\sigma_{vo}/\sigma'_{vo})r_d; \qquad (9.18)$$

where:

τ_{av} = equivalent average shear stress

σ_{vo} = total overburden stress

σ'_{vo} = effective overburden stress

a_{max} = maximum surface acceleration in units of g

g = acceleration due to gravity

r_d = a reduction factor to account for soil flexibility and depth.

The coefficient r_d provides an approximate correction for flexibility of the soil profile. Youd et al. (2001) recommended that for non-critical projects, the following equations may be used to estimate average values of r_d:

$$r_d = 1.0 - 0.00765\,z \qquad \text{for } z \le 9.15 \text{ m} \qquad (9.19a)$$

$$r_d = 1.174 - 0.0267\,z \qquad \text{for } 9.15 \text{ m} < z \le 23 \text{ m} \qquad (9.19b)$$

where z is depth below ground surface in metres.

9.5.2.2 Characterization of resistance to liquefaction

Seed and his colleagues developed correlations between the SPT $(N_1)_{60}$-value and the cyclic stress ratio (CSR) to cause liquefaction during earthquakes of magnitude M=7.5. The SPT was considered to be a useful index because it was available for most sites and it was considered that the same factors that affected liquefaction susceptibility affected the SPT blow count. The assessment of whether or not a site had liquefied was based on observation of surface features of liquefaction, such as sand boils or ground fissures. Lower bound curves separating liquefied from non-liquefied sites were developed and these are used to screen sites for liquefaction susceptibility.

Since the original curves were developed based on $(N_1)_{60}$ values, a large database of CPT data has been accumulated. Figure 9-11 shows a similar chart for liquefaction assessment developed in terms of normalized CPT tip resistance, q_{c1N}. The CPT recommendations are based on the contribution to the NCEER workshop by Robertson and Wride (1998), subsequently published in the Canadian Geotechnical Journal (Robertson and Wride, 1998).

The recommended procedure is as follows:

- Classify soil to determine liquefiable strata
- Determine CRR from Figure 9-11 based on q_{c1N} given by:

$$q_{c1N}=C_Q(q_c/P_{a2}) \qquad (9.20)$$

where $C_Q=(P_a/\sigma'_v)^n \leq 1.7$

P_a = 100 kPa or approximately one atmosphere of pressure in the same units used for σ'_v

P_{a2}= 100 kPa or approximately one atmosphere of pressure in the same units used for q_c

The value of the exponent, n, is dependent on grain characteristics of the soil and ranges from 0.5 for clean sands to 1.0 for clays (Olsen 1997).

The general conditions for the case history data presented in this chart are as follows:

- The charts apply to Holocene sands
- The average q_c in liquefied layers is plotted
- All sites evaluated were on level or gently sloping ground
- The effective overburden pressure for all cases does not exceed 96 kPa.
- The magnitude of the earthquakes in all cases was about 7.5.

Screening charts have also been developed using shear wave velocity.

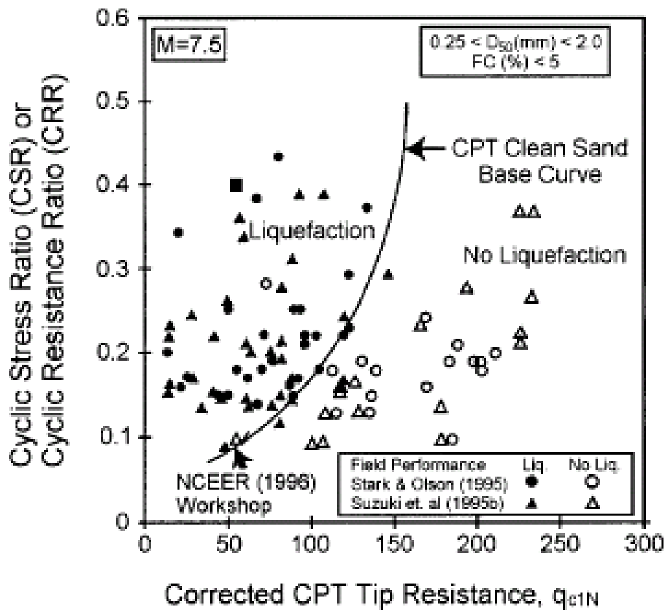

Figure 9-11 Curve Recommended for Calculation of CRR from CPT Data along with Empirical Liquefaction Data from Compiled Case Histories (Reproduced from Robertson and Wride 1998)

9.5.2.3 Effects of fines

The presence of fines has an effect on the cyclic resistance. Youd et al. (2001) recommend that for silty sands, q_{c1N} should be converted to an equivalent value that would be applicable to clean sand $(q_{c1N})_{cs}$ given by:

$$(q_{c1N})_{cs} = K_c \, q_{c1N} \tag{9.21}$$

where K_c is a correction factor based on grain characteristics. However, Seed et al. (2003) have presented additional data that indicate that this approach may be unconservative for soils with fines content. This lends support to the recommendation by Youd et al. (2001) that the liquefaction susceptibility of soils with a Robertson I_c between 2.4 and 2.6 should be assessed by sampling and testing and suggests that the above approach should be used with caution for sand containing fines.

The type of fines (e.g. clay or non-plastic silt) is also important. In clayey soils, the assessment of liquefaction susceptibility is based on the so-called Chinese Criterion (Seed and Idriss 1982). In such soils, this criterion states that liquefaction can only occur if the following conditions are met:

- The clay content (particles smaller than 5 microns) is less than 15% by mass
- The natural moisture content is greater than 0.9 times the liquid limit.

- The natural moisture content is less than 35%.

Recent publications have discredited the use of the Chinese Criterion. (e.g. Bray et al. 2004).

9.5.2.4 Corrections for different earthquake magnitudes and stress levels

For conditions differing from the above, some correction factors are applicable. The corrected CRR is calculated as follows:

$$CRR = CRR_{7.5}.K_M.K_\sigma \tag{9.22}$$

where K_M is the correction factor for earthquake magnitudes other than 7.5 and K_σ is a correction factor for use where effective overburden stresses are greater than 96 kPa. No K_σ correction is required for effective overburden stresses less than 96 kPa.

The above procedure should only be used for LEVEL GROUND conditions. Sloping ground presents additional challenges requiring additional correction factors. Youd et al. (2001) should be consulted for details.

9.5.2.5 Use of q_c/N relationships

The original Cyclic Resistance curves developed for liquefaction assessment based on CPT data by Robertson and Campanella (1985) were based on conversion of the original Seed et al. (1985) SPT-based CRR curves using q_c/N relationships. The new CRR curve based on CPT case histories is close to the Robertson and Campanella (1985) curve for clean sand. It is still common in engineering practice for engineers to convert q_c values to equivalent N-values before carrying out a liquefaction assessment using the $(N_1)_{60}$ correlations to CRR. There is now no need to carry out this conversion.

9.5.3 Liquefaction assessment based on V_s

It has also been suggested (Andrus and Stokoe 1997; 2000) that shear wave velocity obtained by Seismic CPTU can be used for screening for liquefaction susceptibility and this approach has been endorsed by MCEER (Youd et al. 2001). They state that:

> "the use of V_s as a field index of liquefaction resistance is soundly based because both V_s and CRR are similarly, but not proportionally, influenced by void ratio, effective confining stresses, stress history, and geologic age."

This means, however, that the V_s approach to liquefaction assessment can <u>only</u> be used for uncemented, normally consolidated, clean sands which are unaged.

However, seismic wave velocity measurements are made at small strains, whereas pore-water pressure build-up and the onset of liquefaction are medium- to high-strain phenomena. Consequently, V_s should not be relied upon as the sole indicator of resistance to liquefaction. Other tests are needed to detect liquefiable weakly cemented soils that may have high V_s values due to high small-strain shear stiffness.

Figure 9-12 shows the proposed relationship between normalized shear wave velocity, V_{s1} and CRR recommended by Youd et al. (2001). V_{s1} is given by the expression:

$$V_{s1} = V_s \left(\frac{P_a}{\sigma'_{vo}} \right)^{0.25} \tag{9.23}$$

where V_{s1} = overburden-stress corrected shear wave velocity; P_a = atmospheric pressure approximated by 100 kPa; and σ'_{vo}= initial effective vertical stress in the same units as P_a. Equation 9.23 implicitly assumes a constant coefficient of earth pressure, K_o, which is approximately 0.5 for sites susceptible to liquefaction.

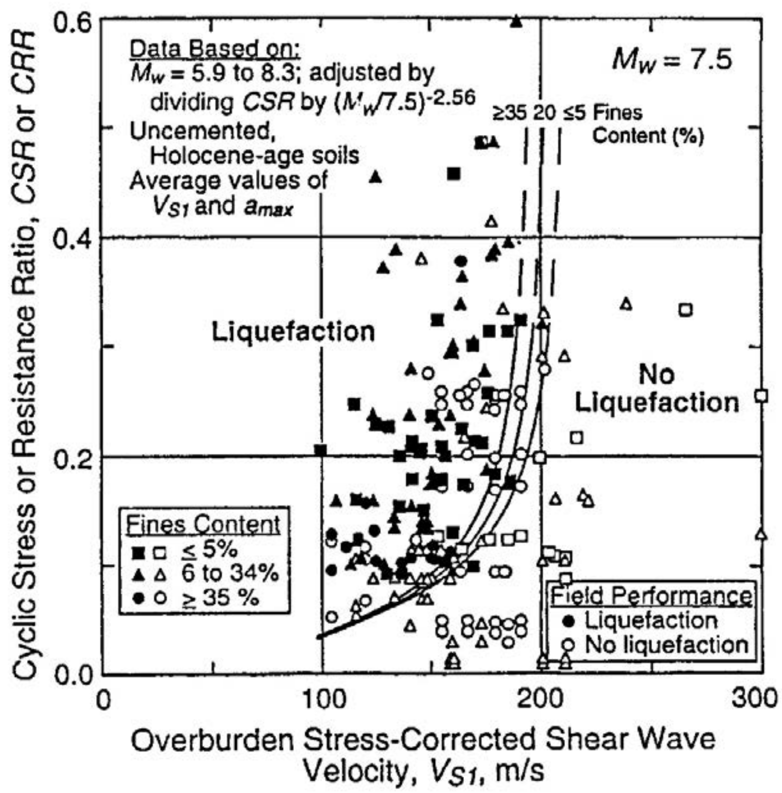

Figure 9-12 Liquefaction relationship recommended for clean, uncemented soils with liquefaction data from compiled case histories (Reproduced from Andrus and Stokoe 2000) (Youd et al. 2001)

Application of Equation 9.23 also implicitly assumes that V_s is measured with both the directions of particle motion and wave propagation polarized along principal stress directions and that one of those directions is vertical (Stokoe et al. 1985).

The curves in Figure 9-12 were recommended by Andrus and Stokoe (2000) and are applicable to magnitude 7.5 earthquakes in uncemented Holocene-age soils. The presence of cementation may be detected using G_o/q_t and Figure 7-7.

The recommended curves shown in Figure 9-12 are dashed above CRR of 0.35 to indicate that field-performance data are limited in that range. Also, they do not extend much below 100 m/s, because there are no field data to support extending them to the origin.

9.5.4 Conclusion on liquefaction assessment

The topic of liquefaction assessment under earthquake loading by the above approach is an area of active research and of frequent revision to the applicable factors as new information becomes available (Cetin et al. 2004; Idriss and Boulanger 2004; Seed et al. 2003). The reader is cautioned that the details of the above approach may be superseded by the time of reading this manual.

9.6 Specification and quality control of ground improvement

9.6.1 Introduction

Ground improvement is a design option where the strength and stiffness of foundation soils are inadequate. The most applicable method of improvement depends primarily on the soil conditions. Volume decrease by consolidation works well in fine-grained material, whereas vibratory compaction is more efficient for granular soils.

9.6.2 Specification of compaction

The optimum ground improvement method for a site requires compatibility between the improvement process and the soil conditions. It must be possible to achieve the desired performance by the process selected. After completion of the treatment, the engineer must be able to verify that the desired performance under design loading conditions has been achieved.

The CPT is an ideal tool for evaluating both the need for ground improvement and for quality management of the ground improvement process. Figure 9-13 shows zones on a CPT classification chart that are considered “compactable” and “marginally compactable” by Massarsch (1991).

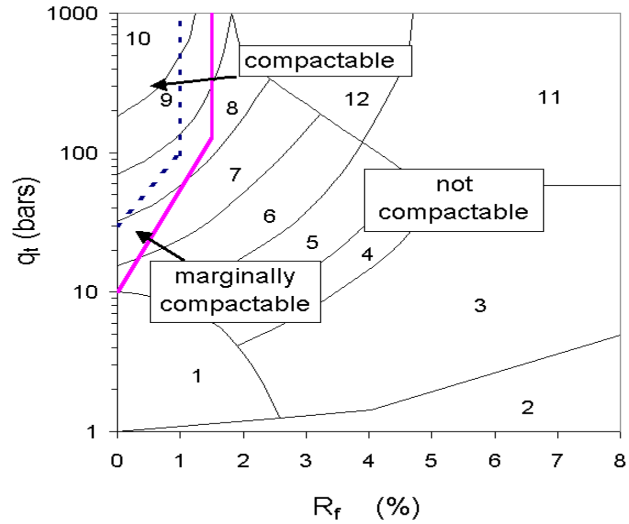

Figure 9-13 CPT based criteria for compactability (adapted from Massarsch 1991)

The significant factors that influence CPT data are the same parameters that are changed by the ground improvement process. These are in-situ vertical and horizontal effective stress, stress history, density, and cementation. Consequently, care should be taken to ensure that correlations used to establish target CPT parameters to be achieved by ground improvement are applicable to the post-improvement ground conditions. For example, a number of investigators (Gohl et al. 1998; Mitchell and Solymar 1984) have noted a decrease in q_c immediately after ground improvement by blasting, despite the occurrence of large settlements indicating an increase in density. In such cases, correlations to Relative Density based on chamber testing would suggest that the improvement process had decreased the density. In the case of explosive compaction, correlations based on chamber testing in unaged, normally consolidated sands are likely more applicable to post-treatment CPT testing than to the assessment of pre-treatment D_r.

This illustrates a common problem in applying CPT data in sands. Relative density is a poor parameter to represent the behaviour characteristics of sands. It is also a very difficult parameter to measure in-situ since no unique relationship exists between cone resistance and relative density for all sands. The relationships are influenced significantly by soil compressibility and in-situ horizontal stress. The final application for many problems in sand relate to the shear strength. Thus, it is often more logical to investigate the shear strength or friction angle, ϕ, of a sand, rather than relative density. The friction angle correlations are much less influenced by soil compressibility and in-situ stress.

In many cases the interpretation of CPT data to estimate intermediate parameters, such as, density or friction angle, is unnecessary if the cone data are affected in the same manner as the soil characteristic being investigated. A good example of this approach is the assessment of liquefaction resistance in sands using cone penetration resistance. The liquefaction resistance and cone resistance both increase with increasing soil density, K_o, aging and prior seismic history. Often the CPT data can be correlated directly to the soil characteristic required.

9.6.3 Compaction Control

CPT data has been found to be extremely useful for evaluation of deep compaction techniques such as, vibroflotation, dynamic compaction, compaction by vibratory rollers and vibrocompaction (stone columns). However, as mentioned above, cone resistance is influenced by soil density and in-situ stresses. Most of the deep compaction techniques induce significant changes in the horizontal stresses. As the ultimate aim of most compaction techniques is usually to improve the soil strength or resistance to some loading condition or to improve the soil compressibility characteristics, CPT data can be used directly to monitor changes in these behaviour characteristics. Sometimes this may involve the use of the term "apparent relative density", since the real relative density is not known or required but the apparent change in relative density is of more importance.

Recent studies have also shown the importance of time effects after deep compaction techniques. Cone resistance values have been observed to increase several weeks after compaction of clean sands (Mitchell 1986; Schmertmann et al. 1986). This behaviour appears to be more pronounced after deep compaction by blasting than for dynamic compaction and vibro-densification and appears to be related to the structure and cementation of the sand.

9.6.4 Ground improvement by preloading or staged construction

The stability of slopes and embankments depends upon the shear strength of the foundation soil. In ground improvement by preloading or staged construction, the required ground improvement is usually an increase in strength of the foundation soils or precompression to reduce post-construction settlements, both achieved by consolidation to a higher effective stress state. Ladd (1991) notes that this approach carries the risk of a stability failure during construction or of excessive long-term settlement due to uncertainties in the initial soil conditions, soil compressibility and subsequent gain in strength, in the rates of loading and consolidation and in the methods of stability and settlement analysis. Careful site characterisation using the detailed soil profiling capability of the CPTU can minimize these risks. Of prime importance is the pre-construction in situ state of stress and yield stress profile. The estimation of yield stress profile from CPTU data is discussed in Section 7.3.2.

For embankments placed on soft, low permeability soils (clays, silts, etc.), the stability is usually assessed using an undrained strength analysis. Thus, the key parameter for design is the relevant undrained shear strength at the current effective stresses. The estimation of the pre-construction undrained strength profile from CPTU data is discussed in Section 7.4.2. Critical areas, defined by the CPTU, may require selective testing (field shear vane test) or sampling and laboratory testing.

The CPTU can also be used to monitor the improvement in properties of foundation soils during staged construction but this should be done with care. The significant factors that influence CPT data in clays (in-situ stresses, stress history, and shear strength) are the same parameters that are changed by the ground improvement process. For example, the appropriate value of N_{kt} for estimation of shear strength varies with stress history and so it will be difficult to determine a reliable estimate of shear strength from q_t *during* construction. It is possible to determine profiles of equilibrium pore pressures during construction from CPTU dissipation tests where piezometers are unavailable.

For monitoring of stability during construction, Ladd (1991) notes that measurements of horizontal displacements generally give the clearest evidence of instability since they directly reflect deformations caused by undrained shear and are less affected by consolidation than settlement data.

A full discussion on the design of embankments is given in Ladd (1991) and useful additional comments are given in Ladd and deGroot (2003).

9.6.5 Other Applications

Other applications of CPT data include:

1) checking the adequacy and uniformity of placed fill
2) locating bedrock
3) checking the amount of undesirable material for excavation
4) locating cavities in soft rocks, e.g. chalk
5) locating permafrost
6) pipeline investigations.

9.7 Summary

9.7.1 General

Figure 9-14 summarizes the basic approaches that may be followed when using SCPTU data for geotechnical design. The primary use of the SCPTU is for delineation of site stratigraphy. Once the stratigraphy has been determined, the data can also be used for estimation of soil properties for each of the layers. Soil properties may then be used for foundation design. This is termed the "indirect" approach to design. Care should be taken to ensure that the estimated design

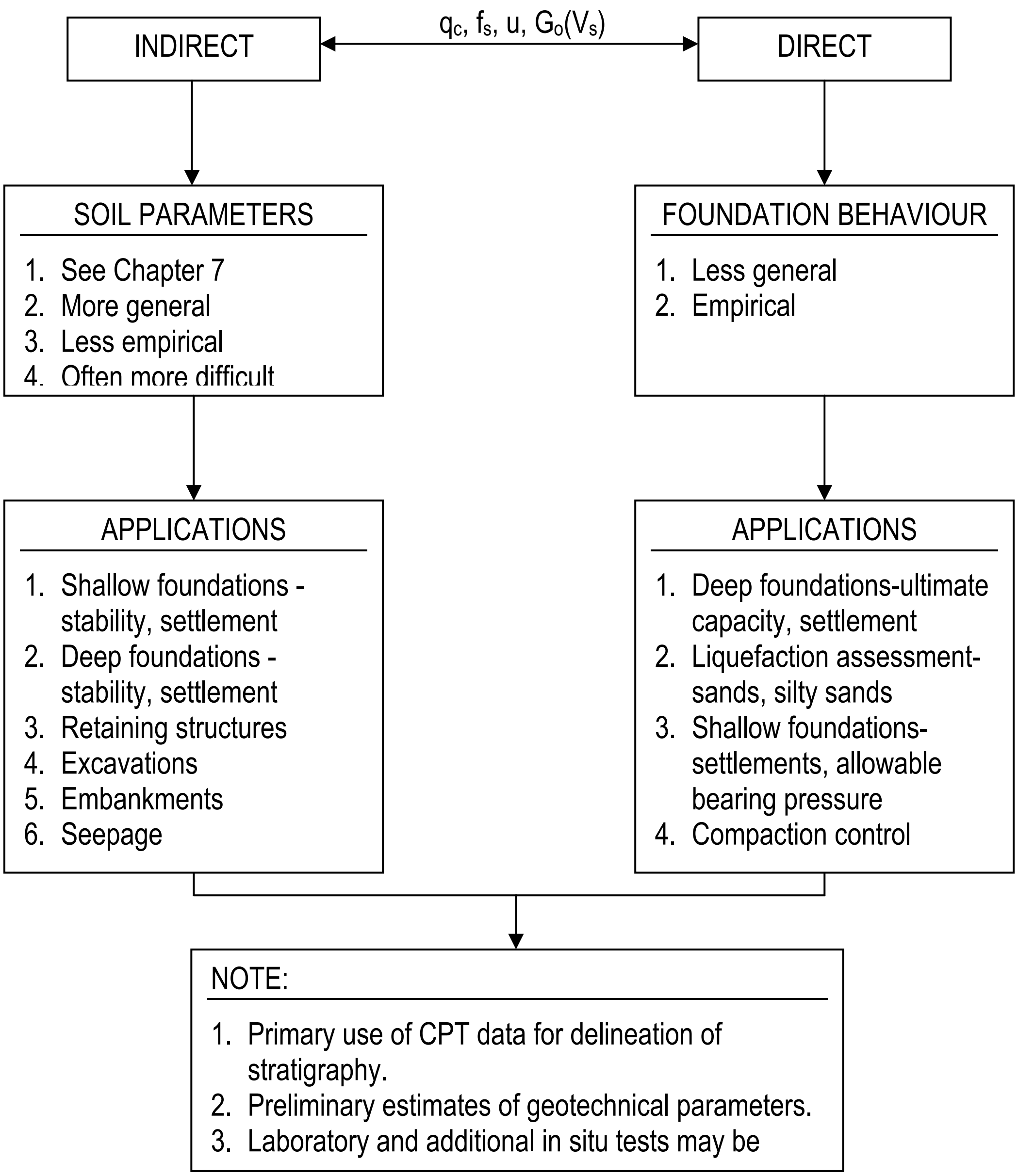

Figure 9-14 Geotechnical Design from CPT Data

parameters are compatible with the design approach being used as many existing design methods rely on compensating errors for their success.

Alternatively, the SCPTU parameters may be used “directly” in design methods developed using SCPTU data. The most common “direct” applications for SCPTU data are pile design and liquefaction assessment.

For both approaches, the engineer should ensure the applicability of the proposed design approach by developing local correlations to SCPTU data.

The SCPTU is a valuable tool for site characterization but should not be used in isolation from other techniques. Figure 9-15 illustrates how in situ testing can fit within a risk based approach to site characterization (Lacasse et al. 2001).

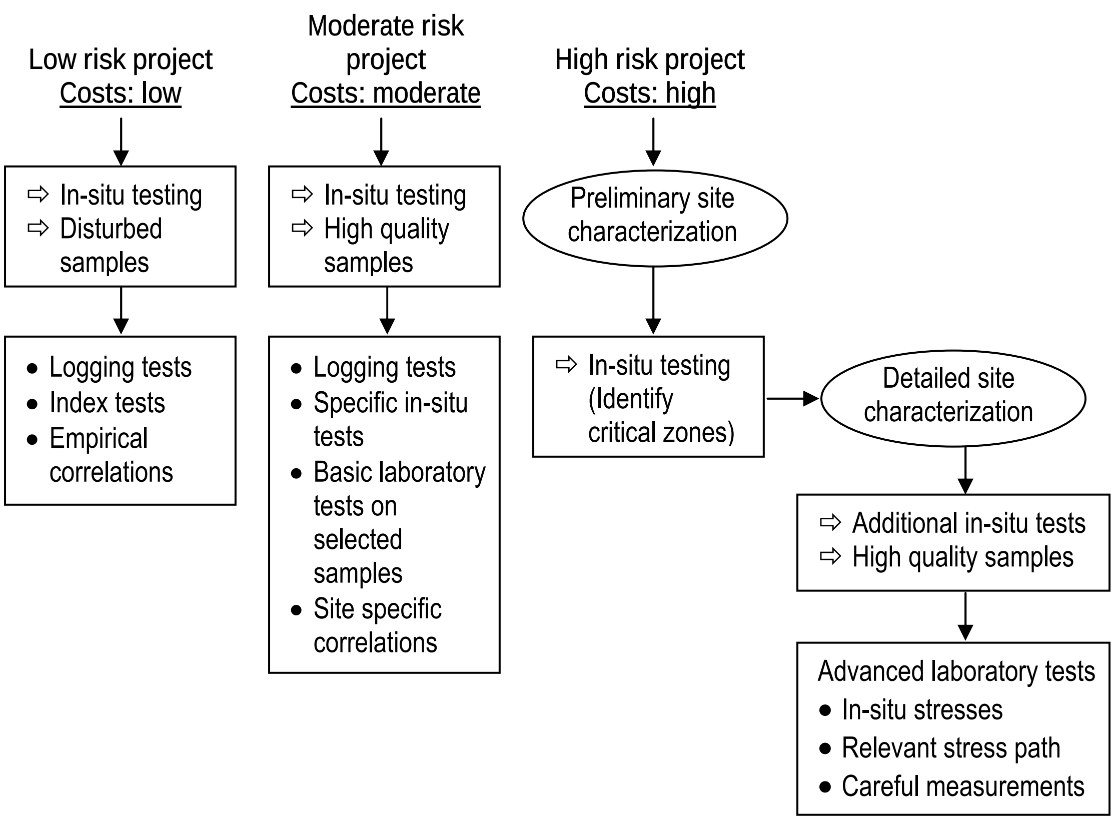

Figure 9-15 Risk-based soil investigation (Lacasse and Nadim 1998; Robertson 1998)

REFERENCES

Abu-Farsakh, M.Y., and Titi, H.H. 2004. Assessment of direct cone penetration test methods for predicting the ultimate capacity of friction driven piles. Journal of Geotechnical and Geoenvironmental Engineering, **130**(9), September 2004.

Ahmadi, M.M. 2000. Analysis of cone tip resistance in sand. Ph.D. Thesis, Department of Civil Engineering, The University of British Columbia, Vancouver, B.C.

Andrus, R.D., and Stokoe, K.H., II 1997. Liquefaction resistance based on shear wave velocity. *In* Proceedings of NCEER Workshop on Evaluation of Liquefaction Resistance of Soils. Nat. Ctr. for Earthquake Engrg. Res., State Univ. of New York at Buffalo, pp. 89-128.

Andrus, R.D., and Stokoe, K.H., II 2000. Liquefaction resistance of soils from shear-wave velocity. Journal of Geotechnical and Geoenvironmental Engineering, ASCE, **126**(11), 1015-1025.

ASTM D5778-95(2000). Standard Test Method for Performing Electronic Friction Cone and Piezocone Penetration Testing of Soils, ASTM International. www.astm.org.

ASTM D6066(2004). Standard Practice for Determining the Normalized Penetration Resistance of Sands for Evaluation of Liquefaction Potential, ASTM International, www.astm.org.

Atkinson, J.H. 2000. Non-linear soil stiffness in routine design. Geotechnique, **50**(5): 487-508.

Atkinson, J.H., and Sallfors, G. 1991. Experimental determination of soil properties. General Report to Session 1. *In* Proceedings of the 10th ECSMFE. Florence, Vol.3, pp. 915-956.

Baldi, G., Bellotti, R., Ghionna, V., Jamiolkowski, M., and Pasqualini, E. 1981. Cone resistance of a dry medium sand. *In* Proceedings of the 10th International Conference on Soil Mechanics and Foundation Engineering. Stockholm, Vol.2, pp. 427-432.

Baldi, G., Bellotti, R., Ghionna, V., Jamiolkowski, M., and Pasqualini, E. 1982. Design parameters for sands from CPT. *In* Proceedings of the 2nd European Symposium on Penetration Testing, ESOPT II. Amsterdam. May 1982, Vol.2, pp. 425-438.

Baldi, G., Bellotti, R., Ghionna, V., Jamiolkowski, M., and Pasqualini, E. 1986. Interpretation of CPT's and CPTU's, 2nd part: drained penetration of sands. *In* Proceedings of 4th Int. Geotechnical Seminar. Nanyang Technological Institute, Singapore, Field Inst. & In Situ Measurements, pp. 143-162.

Baldi, G., Bellotti, R., Ghionna, V.N., Jamiolkowski, M., and Lo Presti, D.F.C. 1989. Modulus of sands from CPTs and DMTs. *In* Proceedings of the 12th International Conference on Soil Mechanics and Foundation Engineering. Rio de Janeiro. Balkema Pub., Rotterdam, Vol.1, pp. 165-170.

Baligh, M.M., and Levadoux, J.N. 1980. Pore pressure dissipation after cone penetration, Massachusetts Institute of Technology, Department of Civil Engineering, Construction Facilities Division, Cambridge, Massachusetts 02139.

Baligh, M.M., and Levadoux, J.N. 1986. Consolidation after undrained piezocone penetration. II: Interpretation. Journal of Geotechnical Engineering, ASCE, 112(7): 727-745.

Baligh, M.M., Vivatrat, V., and Ladd, C.C. 1980. Cone penetration in soil profiling. ASCE, Journal of Geotechnical Engineering Division, 106(GT4): 447-461, April 1980.

Baligh, M.M., Azzouz, A.S., Wissa, A.Z.E., Martin, R.T., and Morrison, M.J. 1981. The piezocone penetrometer. *In* Proceedings of Symposium on Cone Penetration Testing and Experience, ASCE, Geotechnical Division. St. Louis, pp. 247-263.

Battaglio, M., and Maniscalco, R. 1983. I1 Piezocone. Esecuzione ed Interpretazione. Scienza delle Costryzioni Politecnico di Torino(607).

Battaglio, M., Jamiolkowski, M., Lancellotta, R., and Maniscalco, R. 1981. Piezometer Probe Test in cohesive deposits. *In* Proceedings of Symposium on Cone Penetration Testing and Experience, ASCE, Geotechnical Division, pp. 264-302.

Battaglio, M., Bruzzi, D., Jamiolkowski, M., and Lancellotta, R. 1986. Interpretation of CPT's and CPTU's - undrained penetration of saturated clays. *In* Proceedings of the 4th Int. Geot. Sem. Singapore.

Been, K., and Jefferies, M.G. 1985. A state parameter for sands. Geotechnique, 35(2): 99-112, June 1985.

Bellotti, R., Ghionna, V.N., Jamiolkowski, M., and Robertson, P.K. 1989. Design parameters of cohesionless soils from in-situ tests. *In* Proceedings of Transportation Research Board Conference. Washington. January 1989.

Bjerrum, L. 1973. Problems of soil mechanics and construction on soft clays. *In* Proceedings of the 8th International Conference on Soil Mechanics and Foundation Engineering. Moscow, U.S.S.R., Vol.3, pp. 111-159.

Bolton, M.D. 1986. The strength and dilatancy of sands. Geotechnique, 36(1): 65-78.

Boulanger, R.W. 2003. High overburden stress effects in liquefaction analyses. Journal of Geotechnical and Geoenvironmental Engineering ASCE: 1071-1082, December.

Bray, J.D., Sancio, R.B., Riemer, M.F., and Durgunoglu, T. 2004. Liquefaction susceptibility of fine-grained soils. *In* Proceedings of the 11th Int. Conf. on Soil Dynamics and Earthquake Engineering and the 3rd Int. Conf. on Earthquake Geotechnical Engineering. Berkeley, CA. Jan. 7-6. *Edited by* Doolin, Kammerer, Nogami, Seed, and Towhata, Vol.1, pp. 655-662.

Briaud, J.-L., and Tucker, L.M. 1988. Measured and predicted axial response of 98 piles. Journal of Geotechnical Engineering, ASCE, 114(9): 984-1001.

Briaud, J.-L., and Jeanjean, P. 1994. Load settlement curve method for spread footings on sand. Settlement '94, Vertical and Horizontal Deformations of Foundations and Embankments. *In* Proceedings of a Prediction Symposium Sponsored by the Federal Highway Administration at the occasion of the Settlement '94 ASCE Conference at Texas A & M University, College Station. *Edited by* A. Jean-Louis Briaud, New York. Texas Geotechnical Special Publication No. 41, Vol.2, pp. 1774-1804.

Briaud, J.-L., and Gibbens, R. 1999. Behavior of five large spread footings in sand. Journal of Geotechnical and Geoenvironmental Engineering, ASCE, 125(9): 787-796.

Burns, S.E., and Mayne, P.W. 1998. Penetrometers for soil permeability and chemical detection, Report No. GIT-CEEGEO-98-1, Georgia Institute of Technology.

Bustamante, M., and Gianeselli, L. 1982. Pile bearing capacity prediction by means of static penetrometer CPT. *In* Proceedings of the 2nd European Symposium on Penetration Testing. Amsterdam. May 1982, pp. 493-500.

Campanella, R.G. 1999. Geo-environmental site characterization of soils using in-situ testing methods. *In* Proceedings of Asia Institute of Technology 40th Year Conference, New Frontiers and Challenges. November 1999.

Campanella, R.G., and Robertson, P.K. 1981. Applied cone research. *In* Proceedings of Symposium on Cone Penetration Testing and Experience, Geotechnical Engineering Division, ASCE. October 1981, pp. 343-362.

Campanella, R.G., and Robertson, P.K. 1982. State of the art in In-situ testing of soils: developments since 1978. *In* Proceedings of Engineering Foundation Conference on Updating Subsurface Sampling of Soils and Rocks and Their In-situ Testing. Santa Barbara, California. January 1982, pp. 245-267.

Campanella, R.G., and Robertson, P.K. 1984. A seismic cone penetrometer to measure engineering properties of soil. *In* Proceedings of the 54th Annual International Meeting and Exposition of the Society of Exporation Geophysics. Atlanta, Georgia. December 1984.

Campanella, R.G., and Robertson, P.K. 1988. Current status of the piezocone test. *In* Proceedings of First International Conference on Penetration Testing, ISOPT-1. Invited Lecture. Disney World. March 1988. A.A. Balkema, pp. 93-116.

Campanella, R.G., and Weemees, I. 1990. Development and use of an electrical resistivity cone for groundwater contamination studies. Canadian Geotechnical Journal, 27(5): 557-567.

Campanella, R.G., and Stewart, W.P. 1992. Seismic cone analysis using digital signal Processing for Dynamic Site Characterization. Canadian Geotechnical Journal, 29(3): 477-486.

Campanella, R.G., and Davies, M.P. 1997. In-situ testing for the geo-environmental characterization of mine tailings. *In* Proceedings of XIV International Conference on SM&GE. Hamburg, Vol.1, p. 43.

Campanella, R.G., Gillespie, D., and Robertson, P.K. 1982. Pore pressures during cone penetration testing. *In* Proceedings of the 2nd European Symposium on Penetration Testing, ESOPT II. Amsterdam. A.A. Balkema, pp. 507-512.

Campanella, R.G., Robertson, P.K., and Gillespie, D. 1983. Cone penetration testing in deltaic soils. Canadian Geotechnical Journal, 20(1): 23-35, February 1983.

Campanella, R.G., Robertson, P.K., Gillespie, D., and Greig, J. 1985. Recent developments in in-situ testing of soils. *In* Proceedings of XI ICSMFG. San Francisco, Vol.2, pp. 849-854.

Cetin, K.O., Seed, R.B., Der Kiureghian, A., Tokimatsu, K., Harder Jr., L.F., Kayen, R.E., and Moss, R.E.S. 2004. Standard penetration test-based probabilistic and deterministic assessment of seismic soil liquefaction potential. Journal of Geotechnical and Geoenvironmental Engineering, 130(12): 1314-1340.

Chen, B.S.-Y., and Mayne, P.W. 1996. Statistical relationships between piezocone measurements and stress history of clays. Canadian Geotechnical Journal, 33(3): 488-498.

Crawford, C.B., and Campanella, R.G. 1991. Comparison of field consolidation with laboratory and in-situ tests. Canadian Geotechnical Journal, 28(1): 103-112.

Dahlberg, R. 1974. Penetration, pressuremeter and screw plate tests in a preloaded natural sand deposit. *In* Proceedings of European Symposium on Penetration Testing, ESOPT I. Stockholm, Vol.2.2.

Daniel, C.R., Campanella, R.G., Howie, J.A., and Giacheti, H.L. 2002. Specific depth resistivity cone measurements to determine soil engineering properties. Journal of Environmental and Engineering Geophysics, 8(1).

Danziger, F.A.B., Almeida, M.S.S., and Sills, G.C. 1997. The significance of the strain path analysis in the interpretation of piezocone dissipation data. Geotechnique, 47(5): 901-914.

Davies, M.P. 1999. Piezocone technology for the geoenvironmental characterization of mine tailings. Ph.D. Thesis, Department of Civil Engineering, The University of British Columbia, Vancouver, B.C.

De Beer, E.E. 1965. Bearing capacity and settlement of shallow foundations on sand. *In* Proceedings of Bearing Capacity and Settlement of Foundation Symp. Duke University, Durham, N.C., pp. 15-34.

De Ruiter, J. 1971. Electric penetrometer for site investigations. Journal of Soil Mechanics and Foundation Engineering, ASCE, 97(2): 457-472, February 1971.

De Ruiter, J. 1982. The static cone penetration test state-of-the-art report. *In* Proceedings of the 2nd European Symposium on Penetration Testing, ESOPT II. Amsterdam. May 1982, Vol.2, pp. 289-405.

De Ruiter, J., and Beringen, F.L. 1979. Pile foundations for large North Sea structures. Marine Geotechnology, **3**(3): 267-314.

Demers, D., and Leroueil, S. 2002. Evaluation of preconsolidation pressure and the overconsolidation ratio from piezocone tests of clay deposits in Quebec. Canadian Geotechnical Journal, **39**: 174-192.

Douglas, B.J., and Olsen, R.S. 1981. Soil classification using electric cone penetrometer. *In* Proceedings of Symposium on Cone Penetration Testing and Experience, Geotechnical Engineering Division, ASCE. St. Louis. October 1981, pp. 209-227.

Douglas, B.J., Strutynsky, A.I., Mahar, L.J., and Weaver, J. 1985. Soil strength determinations from the cone penetration test. *In* Proceedings of Civil Engineering in the Arctic Offshore. San Francisco.

Dunnicliff, J. 1988. Geotechnical Instrmentation for Monitoring Field Performance. John Wiley & Sons, Inc., New York, NY.

Durgunoglu, H.T., and Mitchell, J.K. 1975. Static penetration resistance of soils: I-ANALYSIS. *In* Proceedings of ASCE Specialty Conference on In-Situ Measurement of Soil Parameters. Raleigh, Vol.1.

Eslaamizaad, S., and Robertson, P.K. 1996a. Cone penetration test to evaluate bearing capacity of foundation in sands. *In* Proceedings of the 49th Canadian Geotechnical Conference. St. John's, Newfoundland. September, pp. 429-438.

Eslaamizaad, S., and Robertson, P.K. 1996b. Estimation of in-situ lateral stress and stress history in sands. *In* Proceedings of the 49th Canadian Geotechnical Conference. St. John's, Newfoundland, pp. 439-448.

Fahey, M. 1998. Deformation and in situ stress measurement. Invited Theme Lecture, Geotechnical Site Characterization: Proc. 1st International Conference on Site Characterization (ISC '98), Altanta, Georgia, Balkema, Rotterdam, Vol.1, pp. 49-68.

Fahey, M., Lehane, B.M., and Stewart, D. 2003. Soil stiffness for shallow foundation design in the Perth CBD. Australian Geomechanics, **38**(3): 61-89.

Fellenius, B.H. 1989. Unified Design of Piles and Pile Groups, TRB Reord 1169, Transportation Research Board, Washington, pp.75-82.

Gillespie, D.G. 1981. The Piezometer Cone Penetration Test. M.A.Sc. Thesis, Department of Civil Engineering, The University of British Columbia.

Gillespie, D.G. 1990. Evaluating shear wave velocity and pore pressure data from the seismic cone penetration test. Ph.D. Dissertation, Department of Civil Engineering, The University of British Columbia, Vancouver, Canada.

Gillespie, D.G., and Campanella, R.G. 1981. Consolidation characteristics from pore pressure dissipation after piezometer cone penetration, Soil Mechanics Series No. 47, Department of Civil Engineering, The University of British Columbia.

Gohl, W.B., Tsujino, S., Wu, G., Yoshida, N., Howie, J.A., and Everard, J. 1998. Field applications of explosive compaction in silty soils and numerical analysis, Geotechnical Earthquake Engineering and Soil Dynamics III. *In* Proceedings of ASCE Specialty Conference. Seattle, Washington. Geotechnical Special Publication No. 75, pp. 654-665.

Goudreault, P.A., and Fellenius, B.H. 1990. UNIPILE - A Program for Design According to the Fellenius Unified Method for Design of Piles and Pile Groups Considering Bearing Capacity, Settlement and Negative Skin Friction, Beng & Fellenius Consultants Inc.

Hardin, B.O., and Drnevich, V.P. 1972. Shear modulus and damping in soils: design equations and curves. *In* Proceedings of ASCE, Journal of the Soil Mechanics and Foundation Division, Vol.98, SM7, pp. 667-692.

Holden, J.C. 1971. Laboratory Research on Static Cone Penetrometers, Internal Report, CE-SM-71-1, Department of Civil Engineering, University of Florida, Gainsville.

Huang, A.B., and Hsu, H.H. 2004. Advanced calibration chambers for cone penetration testing in cohesionless soils. *In* Proceedings of ISC-2 on Geotechnical and Geophysical Site Charaterization. Rotterdam. *Edited by* V.d.F. Mayne, pp. 147-166.

Idriss, I.M., and Boulanger, R.W. 2004. Semi-empirical procedures for evaluating liquefaction potential during earthquakes. *In* Proceedings of the 11th International Conference on Soil Dynamics and Earthquake Engineering and the 3rd International Conference on Earthquake Geotechnical Engineering. University of California, Berkeley, CA.

Jamiolkowski, M., Lancellotta, R., and Wolski, W. 1983. Recompression and speeding up consolidation, S.O.A. and General Report, VIII European Conf. SMFE, Helsinki, May 1983.

Jamiolkowski, M., Lo Presti, D.F.C., and Manassero, M. 2001. Evaluation of relative density and shear strength of sands from CPT and DMT. Soil Behaviour and Soft Ground Construction: proceedings of the symposium October 5-6, 2001, Cambridge, Massachusetts, sponsored by The Geo-Institute of the American Society of Civil Engineers.

Jamiolkowski, M., Ladd, C.C., Germaine, J.T., and Lancellotta, R. 1985. New developments in field and laboratory testing of soils. *In* Proceedings of the 11th International Conference on Soil Mechanics and Foundation Engineering. San Francisco. August 1985, Vol.1, pp. 57-153.

Jamiolkowski, M., Ghionna, V.N., Lancellotta, R., and Pasqualini, E. 1988. New correlations of penetration test for design practice. Invited Lecture, ISOPT-1, Balkema Publ., Disney World, March 1988, pp. 263-196.

Janbu, N., and Senneset, K. 1974. Effective stress interpretation of in-situ static penetration tests. *In* Proceedings of the European Symposium on Penetration Testing, ESOPT I. Stockholm, Sweden, Vol.2.2, pp. 181-193.

Jardine, R.I., and Chow, F.C. 1996. New design methods for offshore piles. MTD Publication 96/103. London: Marine Technology Directorate.

Jefferies, M.G., and Funegard, E. 1983. Cone penetration testing in the Beaufort Sea. *In* Proceedings of ASCE Specialty Conference, Geotechnical Practice in Offshore Engineering. Austin, Texas, pp. 220-243.

Jefferies, M.G., and Davies, M.P. 1993. Use of CPTU to estimate equivalent SPT N_{60}. Geotechnical Testing Journal, ASTM, 16(4): 458-468.

Jones, G.A., and Rust, E.A. 1982. Piezometer penetration testing CPTU. *In* Proceedings of the 2nd European Symposium on Penetration Testing, ESOPT II. Amsterdam, Vol.2, pp. 607-613.

Joustra, K., and de Gijt, J.G. 1982. Results and interpretation of cone penetration tests in soils of different mineralogic composition. *In* Proceedings of the European Symposium on Penetration Testing, ESOPT II. Amsterdam, Vol.2, pp. 615-626.

Keaveny, J.M., and Mitchell, J.K. 1986. Strength of fine-grained soils using the piezocone. *In* Proceedings of In Situ 86, Specialty Conference sponsored by ASCE, Geotech. Sp. Publication No. 6. Blacksburg, Virginia. June 1986. *Edited by* S. Clemence, pp. 668-685.

Kroezen, M. 1981. Measurement of in-situ density in sandy/silty soil. Canadian Geotechnical Society Newsletter, September 1981, Vol.18, No.4.

Kulhawy, F.H., and Mayne, P.H. 1990. Manual on estimating soil properties for foundation design, Electric Power Research Institute, EPRI, August 1990.

Lacasse, S., and Nadim, F. 1998. Risk and reliability in geotechnical engineering. State-of-the-Art paper. *In* Proceedings of 4th International Conference on Case Histories in Geotechnical Engineering. St. Louis, Missouri, Paper No. 50.A.-S.

Lacasse, S., Hermann, S., Jensen, T.G., and Kveldsvik, V. 2001. Improved engineering solutions because of improved site characterization. Soil Behaviour and Soft Ground Construction: proceedings of the symposium October 5-6, 2001, Cambridge, Massachusetts, sponsored by The Geo-Institute of the American Society of Civil Engineers, pp. 239-254.

Ladd, C.C. 1991. Stability evaluation during staged construction (22nd Terzaghi Lecture). Journal of Geotechnical Engineering, 117(4): 540-615.

Ladd, C.C., and Foott, R. 1974. New design procedure for stability of soft clays. Journal of Geotechnical Engineering Division, ASCE, 100(GT7): 763-786.

Ladd, C.C., and DeGroot, D.J. 2003. Recommended practice for soft ground site characterization. *In* Proceedings of 12th Panamerican Conference on Soil Mechanics and Geotechnical Engineering and 39th U.S. Rock Mechanics Symposium, Arthur Casagrande Lecture. Cambridge, Massachusetts, Vol.1, pp. 3-57.

Ladd, C.C., Foott, R., Ishihara, K., Schlosser, F., and Poulos, H.G. 1977. Stress-deformation and strength characteristics. *In* Proceedings of 9th International Conference on Soil Mechanics and Foundation Engineering. Tokyo, Japan, Vol.2, pp. 421-494.

Laing, N. 1985. Sources and Receivers with the CPT. M.A.Sc. Thesis, Department of Civil Engineering, The University of British Columbia, Vancouver, Canada.

Lee, J., and Salgado, R. 2005. Estimation of bearing capacity of circular footings on sands based on cone penetration test. Journal of Geotechnical and Geoenvironmental Engineering, ASCE, 131(4): 442-452, April 2005.

Lehane, B.M., Chow, F.C., McCabe, B.A., and Jardine, R.J. 2000. Relationships between shaft capacity of driven piles and CPT end resistance. *In* Proceedings of Institution of Civil Engineers, Geotechnical Engineering. April, pp. 93-101.

Leroueil, S., and Hight, D.W. 2003. Behaviour and properties of natural soils and soft rocks. *In* Characterisation and Engineering Properties of Natural Soils. *Edited by* Tan et al. Swets & Zeitlinger, Lisse. pp. 29-254.

Lunne, T., Christoffersen, H.P., and Tjelta, T.I. 1985. Engineering use of piezocone data in North Sea clays. *In* Proceedings of the 11th International Conference on Soil Mechanics and Foundation Engineering. San Francisco. Balkema Pub., Rotterdam, Vol.2, pp. 907-912.

Lunne, T., Robertson, P.K., and Powell, J.J.M. 1997. Cone penetration testing in geotechnical practice. Blackie Academic & Professional.

Lunne, T., Eidsmoen, T., Gillespie, D., and Howland, J.D. 1986. Laboratory and field evaluation of cone penetrometers. *In* Proceedings of In Situ 86, ASCE Specialty Conference, Use of In Situ Tests in Geotechnical Engineering. Blacksburg, Virginia. June 1986.

Mair, R.J. 1993. Developments in geotechnical engineering research: applications to tunnels and deep excavations. Unwin Memorial Lecture 1992. *In* Proceedings of Instn. Civ. Engrs. Civ. Engng, Vol.3, pp. 27-41.

Marr, L.S. 1981. Offshore application of the cone penetrometer. *In* Proceedings of ASCE Symposium on Cone Penetration Testing and Experience. October 1981, pp. 456-476.

Massarsch, K.R. 1991. Deep soil compaction using vibratory probes, ASTM Special Technical Publication, STP 1089, Philadelphia, pp.297-319.

Massarsch, K.R., and Broms, B.B. 1981. Pile driving in clay slopes. *In* Proceedings of ICSMFE. Stockholm.

Mayne, P.W. 1991. Determination of OCR in clays by piezocone tests using cavity expansion and critical state concepts. Soils and Foundations, 31(2): 65-76.

Mayne, P.W. 2001. Stress-strain-strength-flow parameters from enhances in-situ tests. *In* Proceedings of International Conference on In-Situ Measurement of Soil Properties & Case Histories. Bali, Indonesia. May 21-24, 2001, pp. 27-48.

Mayne, P.W., and Kulhawy, F.H. 1982. K_o-OCR relationships in soil. Journal of Geotechnical Engineering, 108(GT6): 851-872.

Mayne, P.W., and Poulos, H.G. 1999. Approximate displacement influence factors for elastic shallow foundations. Journal of Geotechnical and Geoenvironmental Engineering, 125(6): 453.

Mayne, P.W., and Poulos, H.G. 2001. Approximate displacement influence factors for elastic shallow foundations. Closure to discussion. Journal of Geotechnical and Geoenvironmental Engineering, ASCE, 127(1): 101-102.

Meyerhof, G.G. 1956. Penetration tests and bearing capacity of cohesionless soils. Journal of the Soil Mechanics and Foundations Division, ASCE, 82(SM1): 1-19.

Meyerhof, G.G. 1974. State of the art penetration testing in countries outside Europe. *In* Proceedings of the European Symposium on Penetration Testing. Stockholm, Vol.2.1, pp. 40-48.

Mitchell, J.K. 1986. Practical problems from surprising soil behaviour. 12th Terzaghi Lecture, Journal of Geotechnical Div., Vol.112, No.4, pp. 1259-1289.

Mitchell, J.K., and Gardner, W.S. 1975. In-situ measurement of volume change characteristics. *In* Proceedings of the Conference on In-Situ Measurement of Soil Properties, Specialty Conference of the Geotechnical Division. North Carolina State University, Raleigh, Vol.II.

Mitchell, J.K., and Solymar, Z.V. 1984. Time-dependent strength gain in freshly deposited or densified sand. Journal of Geotechnical Engineering, ASCE, 110: 1559-1576.

Mitchell, J.K., and Keaveny, J.M. 1986. Determining sand strength by cone penetrometer. *In* Proceedings of In Situ 86, ASCE Specialty Conference, Use of In Situ Tests in Geotechnical Engineering. Blacksburg, Virginia. June 1986, pp. 823-839.

Mitchell, J.K., Guzikowski, F., and Villet, W.C.B. 1978. The measurement of properties in-situ, Report prepared for U.S. Department of Energy Contract W-7405-ENG-48, Lawrence Berkeley Laboratory, University of California, Berkeley, CA 94720, March 1978.

Olsen, R.S. 1984. Liquefaction analysis using the cone penetration test. *In* Proceedings of the 8th World Conference on Earthquake Engineering. San Francisco.

Olsen, R.S. 1997. Cyclic liquefaction based on the cone penetration test. *In* Proceedings of NCEER Workshop on Evaluation of Liquefaction Resistance of Soils. Nat. Ctr. for Earthquake Engrg. Res., State Univ. of New York at Buffalo, pp. 225-276.

Olsen, R.S., and Malone, P.G. 1988. Soil classification and site characterization using the cone penetrometer test. Penetration Testing 1988, ISOPT-1, Edited by De Ruiter, Balkema, Rotterdam, Vol.2, pp. 887-893.

O'Neil, M.W. 2001. Side resistance in piles and drilled shafts. Journal of Geotechnical and Geoenvironmental Engineering, 127(1): 3-16, January 2001.

Parkin, A.K., and Lunne, T. 1982. Boundary effects in the laboratory calibration of a cone penetrometer in sand. *In* Proceedings of the Second European Symposium on Penetration Testing, ESOPT II. Amsterdam. May 1982, Vol.2, pp. 761-768.

Plewes, H.D., Davies, M.P., and Jefferies, M.G. 1992. CPT based screening procedure for evaluating liquefaction susceptibility. *In* Proceedings of the 45th Canadian Geotechnical Conference, pp. 41-49.

Potts, D.M. 2003. Numerical analysis: a virtual dream or practical reality? Geotechnique, 53(6): 535-573.

Poulos, H.G. 1993. Settlement of bored pile groups. *In* Proceedings of B.A.P. II. Ghent, Balkema, Rotterdam, pp. 103-117.

Poulos, H.G., Carter, J.P., and Small, J.C. 2002. Foundations and retaining structures - research and practice. *In* Proceedings of ICSSMFE 2002. Istanbul, pp. 2527-2606.

Powell, J.J.M., and Quaterman, R.S.T. 1988. The interpretation of CPT in clays with particular reference to rate effects. *In* Proceedings of ISOPT-1. Balkema Publ., Vol.2, pp. 903-910.

Pullan, S.E., and MacAulay, H.A. 1987. An inhole shotgun source for engineering seismic surveys. Geophysics, 52(7), July.

Randolph, M.F. 2003. Science and empiricism in pile foundation design. Geotechnique, 53(10): 847-875.

Randolph, M.F., and Wroth, C.P. 1979. An analytical solution for the consolidation around a driven pile. International Journal for Numerical and Analytical Methods in Geomechanics, **3**: 217-229.

Robertson, P.K. 1986. In-situ testing and its application to foundation engineering. 1985 Canadian Geot. Colloquium, Canadian Geot. Journal, **23**(23, No. 4): 573-594.

Robertson, P.K. 1990. Soil classification using the cone penetration test. Canadian Geotechnical Journal, **27**(1): 151-158.

Robertson, P.K. 1991a. Estimation of foundation settlements in sand from CPT. *In* Proceedings of ASCE Geotechnical Engineering Congress. Boulder.

Robertson, P.K. 1991b. Soil classification using the cone penetration test: Reply. Canadian Geotechnical Journal, **28**(1): 176-178.

Robertson, P.K. 1998. Risk-based site investigation. Geotechnical News: 45-47, September 1998.

Robertson, P.K. 2004. Evaluating soil liquefaction and post-earthquake deformations using the CPT. *In* Proceedings of ISC-2 on Geotechnical and Geophyscial Site Characterization. *Edited by* Viana da Fonseca and Mayne. Millpress, Rotterdam, pp. 233-249.

Robertson, P.K., and Campanella, R.G. 1983a. Interpretation of cone penetration tests - Part I (sand). Canadian Geotechnical Journal, **20**(4): 718-733.

Robertson, P.K., and Campanella, R.G. 1983b. Interpretation of cone penetration tests - Part II (clay). Canadian Geotechnical Journal, **20**(4): 734-745.

Robertson, P.K., and Campanella, R.G. 1984. Guidelines for use, interpretation and application of the CPT and CPTU, Soil Mechanics Series No. 105, Civil Eng. Dept., The University of British Columbia, Vancouver, B.C., Canada.

Robertson, P.K., and Campanella, R.G. 1985. Evaluation of liquefaction potential of sands using the CPT. Journal of Geotechnical Engineering Division, ASCE, **III**(4): 384-407, March 1985.

Robertson, P.K., and Campanella, R.G. 1989. Guidelines for geotechnical design using CPT and CPTU, Soil Mechanics Series No. 120, Department of Civil Engineering, The University of British Columbia, Vancouver, B.C., November 1989.

Robertson, P.K., and Wride, C.E. 1998. Evaluating cyclic liquefaction potential using the cone penetration test. Canadian Geotechnical Journal, Ottawa, **35**(3): 442-459.

Robertson, P.K., Campanella, R.G., Gillespie, D., and Rice, A. 1986. Seismic CPT to measure in-situ shear wave velocity. Journal of Geotechnical Engineering Division, ASCE, **112**(8): 791-803.

Robertson, P.K., Campanella, R.G., Gillespie, D., and Greig, J. 1986a. Use of piezometer cone data. *In* Proceedings of In Situ 86, ASCE Specialty Conference, Use of In Situ Tests in Geotechnical Engineering. Blacksburg, Virginia. June 1986.

Robertson, P.K., Campanella, R.G., Brown, P.T., and Robinson, K.E. 1988. Prediction of wick drain performance using piezometer cone data. Canadian Geotechnical Journal, **25**(1), February 1988.

Robertson, P.K., Fear, C.E., Woeller, D.J., and Weemees, I. 1995. Estimation of sand compressibility from seismic CPT. *In* Proceedings of 48th Canadian Geotechnical Conference. Vancouver, B.C. September, 1995, Vol.1, pp. 441-448.

Robertson, P.K., Sully, J.P., Woeller, D.J., Lunne, T., Powell, J.J.M., and Gillespie, D.G. 1992a. Estimating coefficient of consolidation from piezocone tests. Canadian Geotechnical Journal, **29**(4): 539-550, August, 1992.

Salgado, R., Mitchell, J.K., and Jamiolkowski, M. 1998. Calibration chamber size effects on penetration resistance in sand. Journal of Geotechnical and Geoenvironmental Engineering, ASCE, **124**(9): 878-888.

Sanglerat, G. 1972. The Penetrometer and Soil Exploration. Elsevier.

Schaap, L.H.J., and Zuidberg, H.M. 1982. Mechanical and electrical aspects of the electric cone penetration tip. *In* Proceedings of the Second European Symposium on Penetration Testing, ESOPT II. Amsterdam. A.A. Balkema, Vol.2, pp. 841-851.

Schmertmann, J.H. 1970. Static cone to compute static settlement over sand. Journal of Geotechnical Engineering Division, ASCE, **96**(SM3): 1011-1043.

Schmertmann, J.H. 1975. Measurement of in-situ shear strength. *In* Proceedings of the Specialty Conference on In-Situ Measurement of Soil Properties, ASCE. Raleigh, Vol.2, pp. 57-138.

Schmertmann, J.H. 1976b. Study of feasibility of using Wissa-type piezometer probe to identify liquefaction potential of saturated sands, Report S-78-2, U.S. Army Engineer Waterways Experiment Station.

Schmertmann, J.H. 1978. Guidelines for cone penetration test, performance and design, Report FHWA-TS-787-209, Federal Highway Administration, Washington, July 1978.

Schmertmann, J.H., Hartman, J.P., and Brown, P.R. 1978. Improved strain influence factor diagrams. Journal of Geotechnical Engineering Division, ASCE, **104**(GT8): 1131-1135, August 1978.

Schmertmann, J.H., Baker, W., Gupta, R., and Kessler, K. 1986. CPT/DMT QC of ground modification at a power plant. *In* Proceedings of In Situ 86, ASCE Specialty Conference, Use of In Situ Tests in Geotechnical Engineering. Blacksburg, Virginia. June 1986, pp. 985-1001.

Schnaid, F., Lehane, B.M., and Fahey, M. 2004. In situ test characterization of unusual geomaterials. *In* Proceedings of ISC-2 on Geotechnical and Geophysical Site Charaterization. Rotterdam. *Edited by* Viana da Fonseca and Mayne, pp. 49-74.

Seed, H.B. 1983. Earthquake-resistant design of earth dams. *In* Proceedings of Symp. Seismic Des. of Earth Dams and Caverns, ASCE. New York, pp. 41-64.

Seed, H.B., and Idriss, I.M. 1970. Soil moduli and damping factors for dynamics response analysis, Report No. EERC 70-10, University of California, Berkeley, December 1970.

Seed, H.B., and Idriss, I.M. 1971. Simplified procedure for evaluating soil liquefaction potential. Journal of Soil Mechanics and Foundation Engineering, ASCE, 97(SM9), September 1971.

Seed, H.B., and Idriss, I.M. 1982. Ground motions and soil liquefaction during earthquakes, Earthquake Engineering Research Institute Monograph, Oakland, Calif.

Seed, H.B., Tokimatsu, K., Harder, L.F., and Chung, R.M. 1985. Influence of SPT procedures in soil liquefaction resistance evaluations. Journal of Geotechnical Engineering Division, ASCE, III(12): 1425-1448.

Seed, R.B., Cetin, K.O., Moss, R.E.S., Kammerer, A.M., Wu, J., Pestana, J.M., Riemer, M.F., Sancio, R.B., Bray, J.D., Kayen, R.E., and Faris, A. 2003. Recent advances in soil liquefaction engineering: a unified and consistent framework. 26th Annual ASCE Los Angeles Geotechnical Spring Seminar, Keynote Presentation, H.M.S. Queen Mary, Long Beach, California, April 30, 2003.

Senneset, K., and Janbu, N. 1984. Shear strength parameters obtained from static cone penetration tests. *In* Proceedings of ASTM STP 883, Symposium. San Diego.

Senneset, K., Janbu, N., and Svanø, G. 1982. Strength and deformation parameters from cone penetration tests. *In* Proceedings of the European Symposium on Penetration Testing, ESOPT II. Amsterdam. May 1982, pp. 863-870.

Smits, F.P. 1982. Penetration pore pressure measured with piezometer cones. *In* Proceedings of the Second European Symposium on Penetration Testing, ESOPT II. Amsterdam, Vol.2, pp. 877-881.

Stokoe , K.H., II, Lee, S.H.H., and Knox, D.P. 1985. Shear moduli measurements under true triaxial stresses. *In* Advances in the Art of Testing under Cyclic Conditions. ASCE, New York. pp. 166-185.

Stroud, M.A. 1988. The Standard Penetration Test - its application and interpretation. *In* Proceedings of conference, Institution of Civil Engineers. UK. Thomas Telford, London, pp. 29-49.

Sully, J.P., Campanella, R.G., and Robertson, P.K. 1988. Interpretation of penetration pore pressures to evaluate stress history in clays. *In* Proceedings of ISOPT-1. Balkema Publ., Vol.2, pp. 993-999.

Sully, J.P., Robertson, P.K., Campanella, R.G., and Woeller, D.J. 1999. An approach to evaluation of field CPTU dissipation data in overconsolidated fine-grained soils. Canadian Geotechnical Journal, **36**: 369-381.

Tand, K.E., Funegard, E.G., and Wardeb, P.E. 1995. Predicted/measured bearing capacity of shallow foundations. *In* Proceedings of Proceedings of International Symposium on Cone Penetration Testing, CPT'95. Linkoping, Sweden, pp. 589-594.

Tavenas, F., Leroueil, S., and Roy, M. 1982. The piezocone test in clays: use and limitations. *In* Proceedings of the Second European Symposium on Penetration Testing, ESOPT II. Amsterdam, pp. 889-894.

Teh, C.I., and Houlsby, G.T. 1991. An analytical study of the cone penetration test in clay. Geotechnique, **41**(1): 17-34.

Tomlinson, M.J. 2001. Foundation Design and Construction. Pearson Education Ltd., Essex.

Torstensson, B.-A. 1975. Pore pressure sounding instrument. *In* Proceedings of ASCE Specialty Conference on In-Situ Measurement of Soil Properties. Raleigh, N.C., Vol.II, pp. 48-54.

Torstensson, B.-A. 1982. A combined pore and point resistance probe. *In* Proceedings of the Second European Symposium on Penetration Testing, ESOPT II. Amsterdam, Vol.2, pp. 903-908.

Treadwell, D.D. 1975. The influence of gravity, prestress, compressibility, and layering on soil resistance to static penetration. Ph.D. Dissertation, Graduate Division of the University of California, Berkeley.

Trevor, F.A., and Mayne, P.W. 2004. Undrained shear strength and OCR of marine clays from piezocone test results. *In* Proceedings of ISC-2 on Geotechnical and Geophysical Site Characterization. *Edited by* Viana da Fonseca and Mayne. Millpress, Rotterdam, pp. 391-398.

Tumay, M.T., and Kurup, P.U. 2001. Development of a continuous intrusion miniature cone penetration test system for subsurface explorations. Soils and Foundations, **41**(6): 129-138.

van de Graaf, H.C., and Jekel, J.W.A. 1982. New guidelines for the use of the inclinometer with the cone penetration test. *In* Proceedings of the Second European Symposium on Penetration Testing. Amsterdam. May 1982, Vol.2.

Van Impe, W.F. 1991. Deformations of deep foundations. *In* Proceedings of Proceedings of the 10th European Conference on Soil Mechanics and Foundation Engineering. Florence, Vol.3, pp. 1031-1062.

Vesic, A.S. 1963. Bearing capacity of deep foundations in sand, Highway Research Report 39, Highway Research Board, National Research Council, Washington, D.C.

Vesic, A.S. 1972. Expansion of cavities in infinite soil masses. Journal of Soil Mechanics and Foundation Engineering, ASCE, 98(SM3): 265-290.

Villet, W.C.B., and Mitchell, J.K. 1981. Cone resistance, relative density and friction angle. *In* Proceedings of Symposium on Cone Penetration Testing and Experience, Geotechnical Engineering Division, ASCE. October 1981, pp. 178-208.

Vucetic, M., and Dobry, R. 1991. Effect of soil plasticity on cyclic response. Journal of Geotechnical Engineering, 117(1): 89-107.

Wissa, A.E.Z., Martin, R.T., and Garlanger, J.E. 1975. The piezometer probe. *In* Proceedings of ASCE Specialty Conference on In-Situ Measurement of Soil Properties. Raleigh, N.C., Vol.1, pp. 536-545.

Wroth, C.P. 1984. The interpretation of in-situ soil tests. Rankine Lecture, Geotechnique(4).

Youd, T.L., and Idriss, I.M., eds. 1997. Proc., NCEER Workshop on Evaluation of Liquefaction Resistance of Soils. Nat. Ctr. for Earthquake Engrg. Res., State University of New York at Buffalo.

Youd, T.L., Idriss, I.M., Andrus, R.D., Arango, I., Castro, G., Christian, J.T., Dobry, R., Liam Finn, W.D., Harder Jr., L.F., Hynes, M.E., Ishihara, K., Koester, J.P., Liao, S.S.C., Marcuson III, W.F., Martin, G.R., Mitchell, J.K., Moriwaki, Y., Power, M.S., Robertson, P.K., Seed, H.B., and Stokoe, K.H., II 2001. Liquefaction resistance of soils: summary report from the 1996 NCEER and 1998 NCEER/NSF Workshops on Evaluation of Liquefaction Resistance of Soils. Journal of Geotechnical and Geoenvironmental Engineering, ASCE, 127(10): 817-833.

Yu, H.S. 2004. In situ soil testing: from mechanics to interpretation. *In* Proceedings of ISC-2 on Geotechnical and Geophysical Site Charaterization. Rotterdam. *Edited by* Viana da Fonseca and Mayne, pp. 3-38.

Yu, H.S., and Mitchell, J.K. 1998. Analysis of cone resistance: review of methods. Journal of Geotechnical and Environmental Engineering: 140-149, February.

APPENDIX A

International Reference Test Procedure for the Cone Penetration Test (CPT) and the Cone Penetration Test with pore pressure (CPTU)

International Society for Soil Mechanics
and Geotechnical Engineering (ISSMGE)

International Society for Soil Mechanics
and Geotechnical Engineering (ISSMGE)

International Reference Test Procedure for the Cone Penetration Test (CPT) and the Cone Penetration Test with pore pressure (CPTU)

Report of the ISSMGE
Technical Committee 16
on
Ground Property Characterisation from In-situ Testing

1999 (corrected 2001)

BRE

Soil Characterisation by In Situ Tests:
International Reference Test Procedure for CPT/CPTU

This report contains the International Reference Test Procedure (IRTP) for the Cone Penetration Test (CPT) and the Cone Penetration Test with pore pressure (CPTU). The report was prepared by a working Group of ISSMGE Technical Committee 16, 'Ground Characterisation from In Situ Testing'. The following persons from the working group compiled the document:

Tom Lunne, Norwegian Geotechnical Institute (NGI), Norway
John Powell, Building Research Establishment (BRE), UK
Joek Peuchen, Fugro, Holland
Rolf Sandven, NTNU, Norway
Martin van Staveren, Delft Geotechnics, Holland

Several other members of the working group contributed by commenting on the document.

ABSTRACT: The Cone Penetration Test (CPT) consists of pushing a cone penetrometer using a series of push rods into the soil at a constant rate of penetration. During penetration, measurements of cone resistance and sleeve friction are recorded. The piezocone penetration test (CPTU) also includes the measurement of pore pressures at or close to the cone. The test results may be used for interpretation of stratification, classification of soil type and evaluation of engineering soil parameters. This report presents the recommended guidelines for test equipment, field procedures and presentation of test results. In addition, recommendations for required accuracy, calibration routines and maintenance procedures are outlined. The recommendations are meant to replace international reference test procedures (IRTP) recommended by the International Society for Soil Mechanics and Foundation Engineering (ISSMFE) in 1989 for the electrical CPT/CPTU. This is not a standard but a set of recommendations for good practice. These are meant to form the basis of future efforts for national/international standardisation. For the mechanical CPT the 1989 version will still be valid.

CONTENTS

1 INTRODUCTION

Two categories of the cone penetration test are considered.

1. The electric cone penetration test (CPT) which includes measurement of cone resistance and sleeve friction.
2. The piezocone test (CPTU) which is a cone penetration test with the additional measurement of pore pressure.

Note: This document may also be used for CPT/CPTU without measurement of sleeve friction.

The CPT is performed with a cylindrical penetrometer with a conical tip, or cone, penetrating into the ground at a constant rate of penetration. During penetration, the forces on the cone and the friction sleeve are measured.

The CPTU is performed as the CPT but with the additional measurement of the pore pressure at one or several locations on the penetrometer surface.

Note: Usually, the measurements are carried out using electronic transfer and data logging, with a measurement frequency that can secure detailed information about the soil conditions.

The results from a cone penetration test can in principle be used to evaluate:

- stratification
- soil type
- soil density and in situ stress conditions
- mechanical soil properties
  - shear strength parameters
  - deformation and consolidation characteristics

Note: The results from cone penetration tests may also be used directly in design e.g. pile foundations, liquefaction potential (e.g. Lunne et al. 1997).

Cone penetration testing with pore pressure measurements (CPTU) gives a more reliable determination of stratification and soil type than standard CPT. In addition, CPTU gives a better basis for interpretation of the results in terms of mechanical soil properties.

The purpose of this reference test procedure is to establish definitions and requirements for equipment and test method, which will lead the users to employ the same procedures on an international basis.

The reference test procedure is to a large extent based on testing procedures and guidelines given by the ISSMFE Technical Committee on Penetration Testing (1989) but is updated to include details on measurements of pore pressure i.e. the CPTU. This is not a standard but a set of recommendations for good practice. These are meant to form the basis of future efforts for national/international standardisation. For the mechanical CPT the 1989 version will still be valid.

Note: It is permitted to deviate from the requirements of this document if it can be demonstrated that the deviation(s) in results are not significantly different compared to results of the tests following the IRTP given herein.

2 DEFINITIONS

2.1 *Cone penetration test*

The pushing of a cone penetrometer at the end of a series of cylindrical push rods into the ground at a constant rate of penetration.

2.2 *Cone penetrometer*

The cone penetrometer is the assembly containing the cone, friction sleeve, any other sensors and measuring systems as well as the connection to the push rods. Figure 2.1 shows a section through an example of a cone penetrometer.

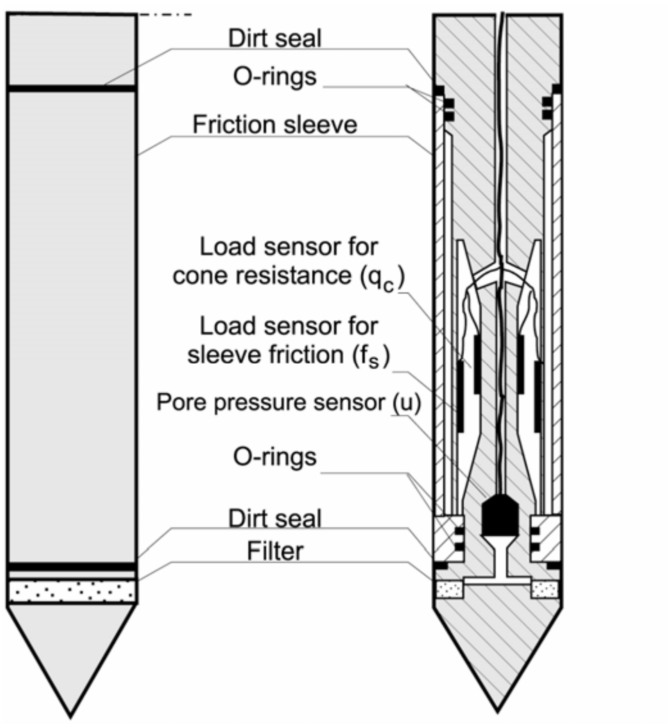

Figure 2.1 Section through an example of a cone penetrometer

The cone penetrometer includes internal load sensors for measurement of force against the cone (cone resistance), side friction against the friction sleeve (sleeve friction) and if applicable pore pressure at one or several locations on the surface of the cone penetrometer. An internal inclinometer is included for measurement of the penetrometer inclination to meet the requirements of the accuracy classes 1, 2 and 3 as given in Table 5.2.

Note: Other sensors can be included in the cone penetrometer.

2.3 *Cone*

The cone has an apex angle of 60° and forms the bottom part of the cone penetrometer. When pushing the penetrometer into the ground, the cone resistance is transferred through the cone to the load sensor.

Note: In this document it is assumed that the cone is rigid, so that its relative deformation when loaded is very small compared to other parts of the cone penetrometer.

2.4 *Friction sleeve*

The friction sleeve is the section of the cone penetrometer upon which the sleeve friction is measured.

2.5 *Filter element*

The filter element is the porous element inserted into the cone penetrometer to allow transmission of the pore pressure to the pore pressure sensor, while maintaining the correct geometry of the cone penetrometer.

2.6 *Measuring system*

The measuring system includes all sensors and ancillary parts which are used to transfer and/or store the electrical signals which are generated during the cone penetration test. The measuring system normally includes components for measuring force (cone resistance, friction), pressure (pore pressure) and depth.

2.7 *Push rods*

The push rods are a string of rods for transfer of compressive and tensile forces to the cone penetrometer.

Note: The push rods can also be used for supporting and/or protecting parts of the measuring system. With acoustic transfer of sounding results the rods are also used for transmission of data.

2.8 *Thrust machine*

The thrust machine is the equipment which pushes the cone penetrometer and rods into the ground along a vertical axis at a constant rate of penetration.

Note: Required reaction for the thrust machine may be supplied by dead weights and/or soil anchors.

2.9 *Penetration depth and length*

Penetration depth: Depth of the base of the cone, relative to a fixed horizontal plane (Figure 2.2).
Penetration length: Sum of the length of the push rods and the cone penetrometer, reduced by the height of the conical part, relative to a fixed horizontal plane (Figure 2.2).

Note: The fixed horizontal plane usually corresponds with a horizontal plane through the (underwater) ground surface at the location of the test.

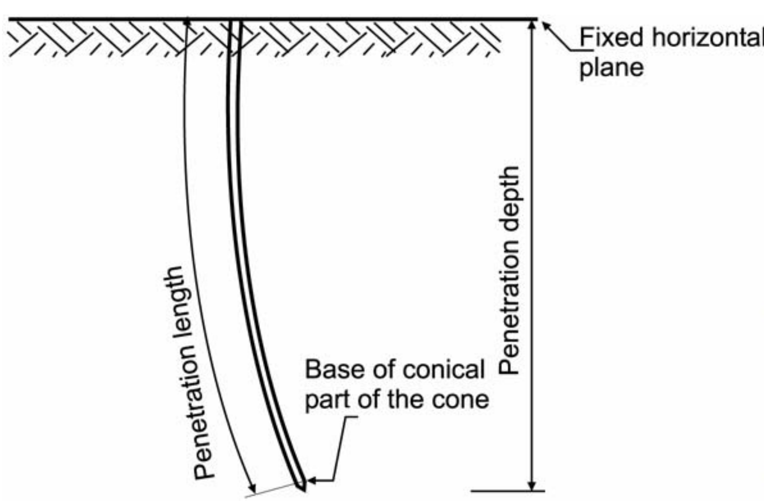

Figure 2.2 Penetration length and penetration depth

2.10 *Friction reducer*

A friction reducer consists of a local and symmetrical enlargement of the diameter of a push rod to obtain a reduction of the friction along the push rods.

2.11 *Cone resistance, q_c*

Measured cone resistance, q_c, is found by dividing the measured force on the cone, Q_c, by the cross-sectional area, A_c:

$$q_c = Q_c/A_c$$

2.12 *Sleeve friction, f_s*

Measured sleeve friction, f_s, is found by dividing the measured force acting on the friction sleeve, F_s, by the area of the sleeve, A_s:

$$f_s = F_s/A_s$$

2.13 *Pore pressure, u*

The pore pressure, u, is the fluid pressure measured during penetration and dissipation testing. The pore pressure can be measured at several locations as shown in Figure 2.3.

The following notation is used:

u_1: Pore pressure measured on the cone face
u_2: Pore pressure measured at the cylindrical extension of the cone
u_3: Pore pressure measured immediately behind the friction sleeve

Note: The measured pore pressure varies with soil type, in situ pore pressure and filter location on the surface of the cone penetrometer. The pore pressure consists of two components, the original in situ pore pressure and the additional or excess pore pressure caused by the penetration of the cone penetrometer into the ground.

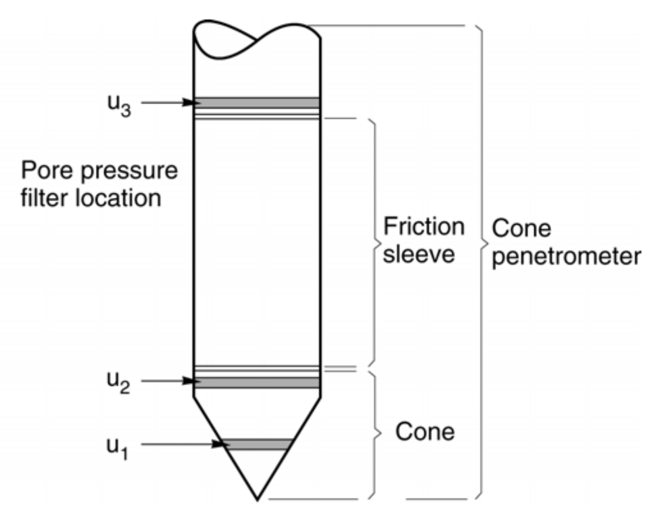

Figure 2.3 Locations of measured pore pressures

2.14 *Excess pore pressure, Δu*

The excess pore pressure is $\Delta u = u - u_o$, where u_o is the in situ pore pressure existing in the ground at the level of the cone before the penetration starts.

Note: Δu_1, Δu_2 or Δu_3 should be used according to the location at which the pore pressure is measured; see Figure 2.3.

2.15 *Net area ratio, a*

The ratio of the cross-sectional area of the load cell or shaft of the cone penetrometer above the cone at the location of the gap or groove where pore pressure can act, to the nominal cross-sectional area of the base of the cone.

Note: See section 5.11 and Figure 5.1 for details.

2.16 *Corrected cone resistance, q_t*

The corrected cone resistance, q_t, is the measured cone resistance, q_c, corrected for pore pressure effects, and is found from:

$$q_t = q_c + (1-a) \cdot u_2$$

Note: Section 5.11 gives more details on this correction.

2.17 *Friction ratio, R_f*

The ratio, expressed as a percentage, of the sleeve friction to the cone resistance both measured at the same depth.

Note: In some cases the inverse of the friction ratio, called the friction index, is used. Whenever possible the corrected cone resistance q_t should be used in calculating R_f.

2.18 *Pore pressure ratio, Bq*

The pore pressure ratio B_q is defined as:

$$B_q = \Delta u_2/(q_t-\sigma_{vo})$$

where σ_{vo} is the total vertical stress existing in the ground at the level of the cone before the penetration starts.

2.19 *Zero reading, reference reading and zero drift*

Zero reading: The output of a measuring system when there is zero load on the sensor, i.e. the measured parameter has a value of zero, any auxiliary power supply required to operate the measuring system being switched on.

Reference reading: the reading of a sensor just before the penetrometer is pushed into the soil e.g. in the offshore case the reading taken at the sea bottom - water pressure acting.

Zero drift: Absolute difference of the zero reading or reference reading of a measuring system between the start and completion of the cone penetration test.

2.20 *Accuracy, precision and resolution*

Accuracy is the closeness of a measurement to the true value of the quantity being measured. It is the accuracy of the measuring system as a whole that is ultimately important not the individual parts.

Precision is the closeness of each set of measurements to each other. It is synonymous with repeatability and can be expressed as a value with say a standard deviation indicating the scatter.

Note: In terms of calibration then if a measurement system shows, for example, a repeatable but non-linear calibration, then the use of a linear approximation for the calibration would immediately result in a loss of accuracy, however the results may still be repeatable and precise. The loss of accuracy would be related to the difference between the true and assumed calibration lines. The use of any incorrect calibration could result in repeatable (precise) results which would have a systematic error and would be inaccurate. Precision or repeatability is not a guarantee of accuracy.

The most desirable situation is to have an instrument that is accurate and precise. This is a prerequisite to obtaining accurate and precise readings in the field where it is then important to record all information such as temperature, wear etc, during the field testing that could influence the accuracy of the final deduced readings.

The resolution of a measuring system is the minimum size of the change in the value of a quantity that it can detect. It will influence the accuracy and precision of a measurement.

2.21 *Dissipation test*

In a dissipation test the pore pressure change is obtained by recording the values of the pore pressure with time during a pause in pushing and whilst the cone penetrometer is held stationary.

3 METHODOLOGY

The following reference conditions shall be determined:

a) the type of cone penetration test, according to Table 5.1

Note: Filter element location u_1, u_2 or u_3 should be decided upon.

b) the Accuracy Class, according to Table 5.2
c) the required penetration length or penetration depth

Note: The required penetration length or penetration depth depends on the soil conditions, the allowable penetration force, the allowable forces on the push rods and push rod connectors and the application of a friction reducer and/or push rod casing and the measuring range of the cone penetrometer.

d) the elevation of the ground surface or the underwater ground surface at the location of the cone penetration test with reference to a Datum
e) the location of the cone penetration test relative to a fixed location reference point
f) if applicable, the method of back filling of the hole in the soil resulting from the cone penetration test
g) if applicable, the depths and duration of the pore pressure dissipation tests.

Note: The required depth and minimum duration of a dissipation test depends on the soil conditions and the purpose of the measurement. A maximum duration is also a common reference condition for avoiding inappropriately long interruptions.

Note: If the drainage- and/or consolidation characteristics of the soil are to be evaluated, dissipation tests can be carried out at preselected depths in the deposit. In a dissipation test, the pore pressure decay is obtained, by recording the values of pore pressure with time. In fine grained, low permeability soil, the pore pressure record is used to evaluate the coefficient of consolidation, c. In well-draining soils, a dissipation test can additionally be used to evaluate the in situ pore pressure.

The determination of the cone resistance of the soil, the CPT length and, if applicable, the sleeve friction and/or pore pressure of soil and the inclination of the cone penetrometer relative to the vertical axis, shall be according to Section 5, taking into account the Accuracy Class according to Table 5.2, the required depth and the maximum allowable inclination of the cone penetrometer relative to the vertical axis.

The apparatus required to undertake the work shall meet the requirements of Section 4.

4 EQUIPMENT

4.1 *Geometry of the cone penetrometer*

The axis of all parts of the cone penetrometer shall be coincident.

Note: Cone penetrometer design should aim for a high net area ratio and also the end area of the top end of the friction sleeve should preferably be equal or slightly greater than the cross sectional area of the lower end.

4.2 *Cone*

The cone consists of a conical part and a cylindrical extension. The cone shall have a nominal apex angle of 60°. The cross-sectional area of the cone shall nominally be 1000 mm^2, which corresponds to a diameter of 35.7 mm.

Note: Cones with a diameter between 25 mm (A_c = 500 mm^2) and 50 mm (A_c = 2000 mm^2) are permitted for special purposes, without the application of correction factors. The recommended geometry and tolerances should be adjusted proportionately to the diameter.

The diameter of the cylindrical part shall be within the tolerance requirement as shown in Figure 4.1:

$$35.3 \text{ mm} \leq d_c \leq 36.0 \text{ mm}.$$

The length of the cylindrical extension shall be within the tolerance requirement:

$$7.0 \text{ mm} \leq h_e \leq 10.0 \text{ mm}$$

The height of the cone shall be within the following tolerance requirement:

$$24.0 \text{ mm} \leq h_c \leq 31.2 \text{ mm}$$

Note: If a u_2 position filter is included the diameter of the filter element itself may be larger than the steel dimensions given above. See also Sections 4.3 and 4.4.

The face of the cone should be smooth.

Note: The surface roughness, R_a, should typically be less than 5 μm. This is defined as the average deviation between the real surface of the probe and a medium reference plane placed along the surface of the probe. See also note in Section 4.3.

The cone shall not be used if it is asymmetrically worn, even if it otherwise fulfils the tolerance requirements.

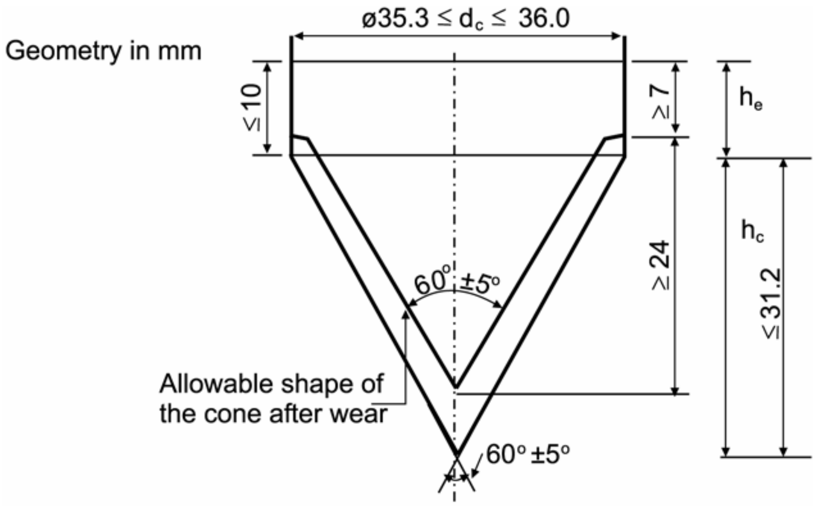

Figure 4.1 Tolerance requirements for use of cone penetrometer

4.3 *Friction sleeve*

The friction sleeve shall be placed just above the cone. The maximum distance due to gaps and soil seals shall be 5.0 mm.

The nominal surface area shall be 15000 mm^2. Tolerance requirements are shown in Figure 4.2.

Note: Friction sleeves with an external diameter between 25 mm and 50 mm are permitted for special purposes when used with cones of the corresponding diameter without the application of correction factors. The recommended geometry and tolerances should be adjusted proportionally to the diameter of the base of the cone. The preferred ratio of the length of the friction sleeve and the diameter of the base of the cone is 3.75, but values between 3.5 and 4.0 are permissible.

Note: Conical wear affects the measurement of sleeve friction. It should be taken into account for accuracy of the sleeve friction measurements.

The diameter of the friction sleeve shall be equal to the maximum diameter of the cone, with a tolerance requirement of 0 to +0.35 mm.

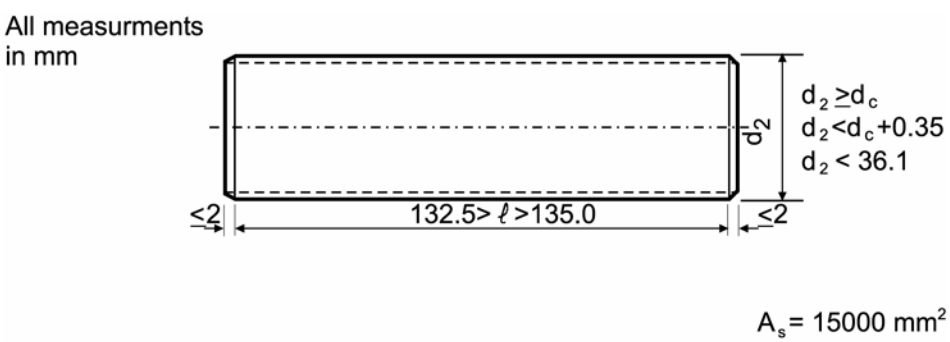

Figure 4.2 Geometry and tolerances of friction sleeve

The friction sleeve shall have a surface roughness of 0.4 µm ± 0.25 µm, measured in the longitudinal direction.

Note: The surface roughness refers to average roughness R_a determined by a surface profile comparator according to ISO 8503 (1988) or equivalent. Average roughness is "the arithmetic average of the absolute distances for the actual profile to the centreline" and applies to a specified test length (typically in the range 2.0 mm to 4.0 mm, depending on the applied standard). The intention of the surface roughness requirement is to prevent the use of an "unusually smooth" and "unusually rough" friction sleeve. Steel, including hardened steel, is subject to wear in soil (in particular sands) and the friction sleeve develops its own roughness with use. It is therefore important that the roughness at manufacture approaches the roughness acquired upon use. It is believed that the surface roughness requirement will usually be met in practice for common types of steel used for penetrometer manufacture and for common ground conditions (sand and clay). The effort required for metrological confirmation may thus be limited in practice. The use of the R_a parameter may be reasonable for geotechnical applications, but the use of the parameter R_y is possibly more relevant. The surface roughness R_y is the distance between the highest peak and deepest trough within one cut-off length, taken as the maximum of a series of cut-off lengths within a test length. Further research is necessary to define adequate parameters for the effects of geometry on sleeve friction accuracy.

4.4 *Filter element*

A filter position in or just behind the cylindrical extension of the cone is recommended, but other filter locations can be accepted, see Figure 2.3.

Note: Filter locations in addition to the recommended one can give valuable information about the soil conditions.

Pore pressure u_2:
The filter element shall be placed in or just behind the cylindrical part of the cone. The diameter of the filter shall correspond to the diameter of the cone and the friction sleeve, with a tolerance limit 0.0 to +0.2 mm. The filter can be larger, but never smaller than the diameter of the cone. The filter shall not have a larger diameter than the friction sleeve.

Note: The following relation applies:

$$d_{friction\ sleeve} \geq d_{filter} \geq d_{cone}$$

Note: This filter position also gives more consistent results for classification and interpretation purposes.

Note: For correction of cone resistance for pore pressure effects, the best location of the filter element would be in the groove between the cone and the friction sleeve. A location in the cylindrical part of the cone is recommended for obtaining and maintaining saturation of the pore pressure system.

Pore pressure u_1:
The diameter of the filter shall correspond to the diameter of the cone with a tolerance limit 0.0 -0.2 mm. The shape of the filter should fit to the shape of the cone, i.e. the diameter of the filter shall be equal to but not larger than the diameter of the conical part in the position of the filter.

Note: It is recommended to place the filter element within the middle third of the conical part.

Pore pressure u_3:
The diameter of the filter shall correspond to the diameter of the friction sleeve with a tolerance limit 0.0 - 0.2 mm, i.e. the diameter of the filter can be equal to but not larger than the diameter of the friction sleeve.

Note: It is recommended to place the filter element immediately above the groove between the friction sleeve and the shaft of the cone penetrometer.

The filter shall be saturated at the start of the test.

Note: It is important that the filter remains saturated even when the cone penetrometer is penetrating an upper unsaturated layer.

Note: Porous filters should have a pore size between 2 and 20 μm, corresponding to a permeability between 10^{-4} and 10^{-5} m/sec. Filter materials that get clogged by fine particles should be avoided.

Note: The following types of material have been used with good experience in soft normally consolidated clay: sintered stainless steel or bronze, carborundum, ceramics, porous PVC and HDPE.

The cone penetrometer shall be designed in such a way that it is easy to replace the filter and that the liquid chamber is easy to saturate (see Section 5.3.).

Note: With regard to the choice of saturating liquid, saturation of pore pressure measurement system, and use of slot filters, see Section 5.4.

4.5 *Gaps and soil seals*

The gap between the different parts of the cone penetrometer shall not exceed 5 mm. The gap shall be protected by a soil seal so that soil particles do not move into it.

Note: The soil seal must be easy to deform relative to the load cell and other elements in the penetrometer, so that no significant forces can be transferred through the gap.

4.6 *Push rods*

Deviation from a straight line through the ends of 1 m long rod shall be within permissible limits. A check of rod straightness shall follow the criteria given below:

- Each of the 5 lower rods shall have a maximum deviation from the centreline of 1 mm.
- Two connected rods (of the lower 5) shall at a maximum have a deviation of 4 mm.

The other rods shall have a maximum deviation of 2 mm. Two connected rods (of the rest) shall have a maximum deviation of 8 mm.

Note: The above requirements are valid for 1m long rods. If other lengths of rod are used for special purposes then the requirements should be adjusted accordingly.

Note: The straightness of the push rods can be checked by holding the rod vertically and rotating it. If the rod appears to wobble, the straightness is not acceptable.

Note: Friction along the push rods can be reduced by a local increase in the rod diameter (friction reducer). The friction could also be reduced by lubrication of the push rods, for instance by mud injection during the test.

Note: Above the ground level the push rods should be guided by rollers, a casing or similar device to reduce the risk of buckling. The push rods may also be guided by a casing in water or soft strata to avoid buckling.

Note: The push rods should be chosen with respect to the required penetration force and the data signal transmission system chosen.

4.7 *Measuring system*

The resolution of the measuring system shall be better than one-third of the accuracy applicable to the required accuracy class given in Table 5.2.

Note: An electric cable can be used to transfer signals from the sensors to a recording unit at ground level, or alternatively acoustic transmission through the rods, or electronic transmission to a memory unit in the cone penetrometer.

Sensors for cone resistance and sleeve friction

The load sensor shall be compensated for possible eccentricity of axial forces. The sensor for recording the side friction force shall be constructed so that it measures the friction along the sleeve, and not the earth pressure against it.

Note: Normally strain gauged load cells are used for recording cone resistance and sleeve friction.

Sensor for pore pressure

The sensor shall show insignificant deformation during loading. The sensor communicates with a porous filter on the surface of the cone penetrometer via a liquid chamber.

Note: The pore pressure sensor is normally a pressure transducer of the membrane type.

Note: This system measures the pore pressure in the surrounding soil during penetration.

Sensor for inclination

The inclinometer should have a measuring range of at least 20^{o} relative to the vertical axis.

Measuring system for penetration length.

The measuring system shall include a depth sensor for registration of the penetration length.

Note: If relevant, the measurement system for depth should also include a procedure for correction of measurements if upward movements of the push rods occur relative to the depth sensor, caused by a decrease in force on the push rods.

4.8 *Thrust machine*

The equipment shall be able to penetrate the cone penetrometer at a standard speed of 20 mm/s ±5 mm/s, and it shall be loaded or anchored such that it limits movements relative to ground level while the penetration occurs.

Note: Hammering or rotation of the penetration rods during measurements shall not be used.

Note: The pushing equipment should give a stroke of at least 1000 mm. Other stroke lengths may be acceptable in special circumstances.

5 PROCEDURES

5.1 *Selection of cone penetrometer*

Select a cone penetrometer to fulfil the requirements of the penetration test according to Table 5.1.

Table 5.1 Types of cone penetration tests

Type of cone penetration test	Measured parameter
A	Cone resistance
B	Cone resistance and sleeve friction
C	Cone resistance and pore pressure
D	Cone resistance, sleeve friction and pore pressure

Note: Cone penetration tests with measurements of pore pressures at more than 1 location are variants of types C or D.

5.2 *Selection of equipment and procedures according to required accuracy class*

Equipment and procedures to be used shall be selected according to the required accuracy class given in Table 5.2.

If all possible sources of errors are added, the accuracy of the recordings shall be better than the largest of the values given in Table 5.2.

Note: The errors may include internal friction, errors in the data acquisition, eccentric loading and temperature effects.

Table 5.2 Accuracy classes

Accuracy class	**Measured parameter**	**Allowable minimum accuracy***	**Maximum length between measurements**
1	Cone resistance Sleeve friction Pore pressure Inclination Penetration depth	50 kPa or 3% 10 kPa or 10% 5 kPa or 2% 2° 0.1 m or 1%	20 mm
2	Cone resistance Sleeve friction Pore pressure Inclination Penetration depth	200 kPa or 3% 25 kPa or 15% 25 kPa or 3% 2° 0.2 m or 2%	20 mm
3	Cone resistance Sleeve friction Pore pressure Inclination Penetration depth	400 kPa or 5% 50 kPa or 15% 50 kPa or 5% 5° 0.2 m or 2%	50 mm
4	Cone resistance Sleeve friction Penetration length	500 kPa or 5% 50 kPa or 20% 0.1 m or 1%	100 mm

* See definitions in Section 2.20

Note: The allowable minimum accuracy of the measured parameter is the larger value of the two quoted. The relative or % accuracy applies to the measurement rather than the measuring range or capacity.

Note: See Appendix B regarding calculation of penetration depth from penetration length and measured inclination.

Note: Class 1 is meant for situations where the results will be used for precise evaluation of stratification and soil type as well as parameter interpretation in profiles including soft or loose soils. For Classes 3 and 4, the results should only be used for stratification and for parameter evaluation in stiff or dense soils. Class 2 may be considered more appropriate for stiff clays and sands.

Note: At extreme air temperatures, the probe should be stored so that its temperature is in the range 0 - 25^{o}C. During the sounding, zero readings should be carried out with the probe temperature as close as possible to the ground temperature, and all sensors and other electronic components in the data acquisition system should be temperature stabilised.

Note: Current thinking is that for Class 1 testing (see Table 5.2) the temperature sensitivity of the probe transducers should be better than:

2.0 kPa/^{o}C	for cone resistance
0.1 kPa/^{o}C	for sleeve friction
0.05-0.1 kPa/^{o}C	for pore pressure (measuring range 1-2 MPa)

These stability requirements are valid for probes with a load capacity of 5 tonnes. For probes with different capacities, the presented requirements can be changed proportionally with due consideration to the effects on the accuracy of the measured value.

Note: For all classes the temperature sensitivity should be an integral part of the CPT Accuracy Classes given in Table 5.2.

Metrological confirmation applicable to a cone penetration test shall be according to ISO 10012-1; 1992 (E).

5.3 *Position and level of thrust machine*

Position the thrust machine at a distance of at least 1 m from a previous cone penetration test, or at a distance of at least 20 times the borehole diameter of a previous borehole.

Note: Smaller distances may affect the measurements.

The thrust machine shall push the push rods so that the axis of the pushing force is as close to vertical as possible. The deviation from the vertical axis should be less than 2°. The axis of the penetrometer shall correspond to the loading axis at the start of the penetration.

5.4 *Preparation of the cone penetrometer*

The actual cross-sectional area of the base of the cone and, if applicable, the actual external cylindrical surface area of the friction sleeve shall be determined and recorded as required to achieve the Accuracy Class of Table 5.2.

For cone penetrometers with measurement of pore pressure the filter element and other parts of the pore pressure system shall be saturated with a liquid before field use.

Note: Usually, de-aired, distilled water is used when testing is carried out in saturated soils. When performing penetration tests in unsaturated soils, dry crust and dilative soils (e.g. dense sands), the filter should be saturated with glycerine or similar, which makes it easier to maintain saturation throughout the test. When deaired water is used, the filters should be boiled for at least 15 minutes. The filter should be cooled in the water, before being stored in a sealed container. A larger volume of de-aired water should also be prepared. This water is necessary when mounting before use.

Boiling of filters may not be acceptable for some types of filters (e.g. HDPE). If glycerine (or silicone oil) is used, the dry filters are placed directly in the liquid and treated with vacuum for approximately 24 hours. A larger volume of liquid should be treated similarly and stored in a sealed container. The transducer chamber is usually saturated with the same fluid as used for the filter. This can be done by direct injection of fluid into the chamber, or by treatment of the dismantled probe in a vacuum chamber. The vacuum should be applied until no air bubbles escape from the probe (approx. 15-30 mins). The final mounting of filter and seals should be carried out with the penetrometer submerged in the saturation fluid. After mounting, the fitting of the filter should be checked. The height of the filter should be sufficient so that the filter is not loose, but small enough so that the filter can be rotated by the finger tips. This prevents excessive stresses in the joint around the filter, and also reduces any influence on the measurements. After mounting the filter, it is good practice to cover the filter element with a rubber membrane, which will burst when the penetrometer comes into contact with the soil. Other alternatives are also possible. If clogging is suspected then a new filter should be mounted for each test.

<u>Note</u>: During saturation and mounting of the rubber membrane, the penetrometer will be subjected to small stresses, so that the sensors can show values different from zero.

<u>Note</u>: *Slot filter*

In this system, the pore pressure is measured by an open system with a 0.3 mm slot immediately behind the conical part (e.g. Larsson, 1995). Hence the porous filter element between the soil and the pressure chamber becomes redundant. The slot communicates with the pressure chamber through several channels. The pressure chamber is saturated by de-aired water, antifreeze liquid or other liquid, whereas the channels are saturated with gelatine, silicone grease or similar. Both gelatine and silicone grease are well-suited for field use. When silicone grease is used, this is injected into the channels directly from a tube. This can cause insufficient saturation of the pore pressure system, since air bubbles may be entrapped in the grease. This is avoided by using gelatine, but some more time is needed for preparation using this saturation medium.

The use of a slot filter may reduce the time required for preparation of the probe. In addition, this pore pressure system also maintains its saturation better when passing through unsaturated zones in the soil. The pressure changes in the saturated system are recorded by a pressure sensor, similar to conventional porous filter piezocones. As for other cone penetrometers, the requirements for sufficient saturation are the same, so that adequate pore pressure response is obtained during penetration.

<u>Note</u>: *Predrilling*

When penetrating coarse materials, predrilling may be used in parts of the profile if the penetration stops in dense, coarse or stone-rich layers. Predrilling may be used in coarse top layers, sometimes in combination with casings to avoid collapse of the borehole. In soft or loose soils, predrilling should be used through the crust down to the groundwater table. The predrilled hole should be filled with water if the pore pressure shall be measured by a water-saturated system. If the ground water table is located at large depths, the pore pressure system should be saturated with glycerine. In some cases, the predrilling can be carried out by ramming a dummy-rod of 45 - 50 mm diameter through the dense layer to provide an opening hole and reduce the penetration resistance.

<u>Note</u>: *Temperature stabilisation*

Before commencing testing, zero readings of all sensors should be taken with the cone penetrometer unloaded and temperature-stabilised ideally at ground temperature.

When the cone penetrometer is lowered into the ground, small temperature gradients will occur if the air temperature is different from the ground temperature. This will influence the sensors, and it is

therefore important that the penetrometer is left to come to equilibrium so that the temperature gradients can be reduced to zero before the penetration starts. Usually, the largest gradients will occur after 2 - 3 minutes. The cone penetrometer will usually be completely temperature-stabilised after 10 - 15 minutes.
See Table 5.2 for required accuracies and Appendix A for calibration procedures.

The zero readings of the cone resistance and the penetration length and, if applicable, the sleeve friction and pore pressure and the inclination of the cone penetrometer relative to the vertical axis shall be recorded.

Note: Whenever possible the zero readings should be taken when the cone penetrometer is at or near the temperature of the ground.

Note: The reference readings for underwater cone penetration tests are those applicable immediately above the underwater ground surface.

5.5 *Pushing of the cone penetrometer*

During the penetration test, the probe shall be pushed into the ground at a constant rate of penetration 20 ± 5 mm/s. The rate shall be checked by recording time.

Note: The penetration is regarded as continuous even if the penetration is stopped regularly for a new stroke or mounting of a new push rod. Some thrust machines can carry out true continuous penetration without any stops and this can be an advantage, particularly in layered silt- and clay deposits.

Note: The penetration is regarded as discontinuous if larger stops are introduced, such as dissipation tests (see Section 2.21) or due to unforeseen malfunctions of the equipment.

5.6 *Use of friction reducer*

The use of a friction reducer (see definition Section 2) is permissible. The cone penetrometer and if relevant the push rod shall have the same diameter for at least 400 mm before the introduction of the friction reducer if applicable.

5.7 *Frequency of logging parameters*

The minimum logging frequency of parameters shall be in accordance with Table 5.2. Logging shall include (clock)time for Accuracy Classes 1 & 2 of Table 5.2.

Note: The logging interval for the various measured values can also be chosen from a consideration of the detail required in the profile, i.e. detection of thin layers. Usually the same reading interval is used for registration of cone resistance, sleeve friction and pore pressure.

Note: The average measured value over the 20 mm interval may be used, even if the values are measured more frequently. The maximum logging interval should be according to Table 5.2.

5.8 *Registration of penetration depth*

The level of the cone base shall be determined according to Table 5.2, relative to the ground level or another fixed reference system (not the thrust machine). The resolution of the depth sensor shall be at least 0.01 m.

The penetration length shall also be measured and recorded at least every 5 m for tests according to Accuracy Class 1 of Table 5.2, not using the depth sensor.

The penetration of the cone penetrometer and the push rods shall be terminated when the required penetration length or penetration depth according to Section 3 has been reached, or when the inclination of the cone penetrometer relative to the vertical axis has reached 20^o. The penetration length shall be measured and recorded not using the depth sensor.

<u>Note</u>: The measured parameters for a cone penetrometer with a large inclination can deviate from the values that would have been measured if the cone penetrometer was vertical. Appendix B gives guidelines on how to calculate penetration depth from penetration length and inclination measurements.

<u>Note</u>: During the cone penetration test, particulars or deviations from this standard should be recorded, which can affect the results of the measurements and the corresponding penetration length.

5.9 *Dissipation test*

Pore pressure and cone resistance shall be measured with time. It is particularly important to take frequent readings at the beginning of the dissipation test.

<u>Note</u>: The logging frequency should be at least 2 Hz for the initial 1st min of the dissipation test, 1 Hz between 1 min and 10 min, 0.5 Hz between 10 min and 100 min and 0.2 Hz thereafter, as applicable.

<u>Note</u>: The duration of the dissipation test should normally correspond to at least the time needed for 50 % pore pressure dissipation (t_{50} -> $u_t = u_o + 0.5\ \ u_i$), since t_{50} is the time used in most interpretation methods.

<u>Note</u>: The procedure for interruption of penetration should aim for constant cone resistance during the dissipation test. Variation in cone resistance is unavoidable in practice and will depend on factors such as type of equipment and soil conditions.

5.10 *Test completion*

The zero readings of the measured parameters shall be measured and recorded after extraction of the cone penetrometer from the soil and, if necessary after cleaning of the cone penetrometer. The zero drift of the measured parameters shall be within the allowable minimum accuracy according to the required accuracy class of Table 5.2.

The cone penetrometer shall be inspected and any excessive wear or damage noted.

5.11 *Correction of measurements*

Recorded values that are not representative due to penetration interruption shall be corrected for. Correction of measured parameters for zero drift shall be done if appropriate for meeting the requirements of the Accuracy Classes according to Table 5.2.

When the probe is subjected to an all-round water pressure, this will influence the cone resistance and sleeve friction. This is explained by the effect of the water pressure in the grooves between the cone and the friction sleeve, and in the groove above the friction sleeve. This effect shall be accounted for cone penetrometer types C and D of Table 5.1 and where the filter element is at the cylindrical extension of the cone (u_2) by using the following correction formula (e.g. Campanella et al., 1982):

Cone resistance:

$$q_t = q_c + u_2 \cdot (1 - a)$$

where:

q_t = corrected cone resistance
q_c = cone resistance
u_2 = pore water pressure in the cylindrical part of extension of the cone (assumed equal to

the pore pressure in the gap between the cone and the sleeve)

a = net area ratio = A_n/A_c (see Figure 5.1)

A_c = projected area of the cone

A_n = area of load cell or shaft

Note: It is recommended to only carry out this correction if u_2 is measured. Approximate calculation procedures are available in some soil types for the determination of q_t for filter element positions other than the u_2 location (Lunne et al. 1997).

Note: The net area ratio 'a' varies between 0.3 and 0.9 for commonly used cone penetrometers. The area ratio cannot be determined from geometrical considerations alone, but should be determined by tests in a pressure chamber or similar.

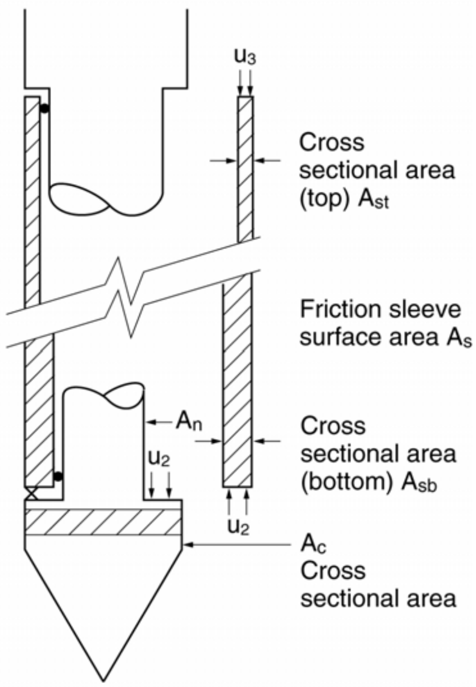

Figure 5.1 Correction of cone resistance and sleeve friction due to the unequal end area effect.

Note: The measured sleeve friction is influenced by a similar effect. However, since it is not usual to measure the pore pressure above the friction sleeve, the uncorrected sleeve friction, f_s, is commonly used. A possible correction method for the recorded sleeve friction is however given below, see Figure 5.1:

Sleeve friction:

$$f_t = f_s - \frac{(u_2.A_{sb} - u_3.A_{st})}{A_s}$$

where:
f_t = corrected sleeve friction
f_s = sleeve friction
A_s = area of friction sleeve
A_{sb}= cross sectional area of the bottom of the friction sleeve
A_{st}= cross sectional area of the top of the friction sleeve
u_2 = pore pressure measured between the friction sleeve and the cone
u_3 = pore pressure measured above the friction sleeve

This correction should only be carried out if both u_2 and u_3 are measured.

Note: These corrections are most important in fine-grained soils where the excess pore pressure during penetration can be significant. It is recommended to use corrected values of the test results for interpretation and classification purposes.

Correction for inclination, i.e. calculation of penetration depth from penetration length, should also be carried out according to the procedure given in Appendix B to meet the requirements of Accuracy Classes 1, 2 and 3 (see Table 5.2).

Note: Various other corrections may be required to meet the requirements of the Accuracy Classes, e.g. temperature effects, cross sectional area of cone, compression of the push rods, rebound of the thrust machine etc.

6 REPORTING OF TEST RESULTS

6.1 *General reporting and presentation of test results*

The following information shall be reported from a (piezo)cone penetration test (selected information marked with * shall be included on every plot from the test):

- Cone penetrometer type, geometry and dimensions, filter location, net area ratio.

  Note: The actual dimensions of the cone and friction sleeve should be used whenever possible.

- Type of thrust machine used, pushing capacity, associated jacking and anchoring systems
- Use of soil anchors (number and type) if applicable
- Date of test *
- Identification of the test *
- Co-ordinates and altitude of the cone penetration test *
- Reference altitude
- Depth to the groundwater table (if recorded)
- In situ pore pressure measurements (if recorded)
- Depth of predrilling
  - Note: when possible also the type of materials encountered
- If trenching is carried out: trenching depth
  - Note: when possible also type of materials encountered
- Depth of the start of penetration
- Saturation fluid used in pore pressure system (if piezocone)
- Depth and possible causes of any stops in the penetration (e.g. dissipation tests)
- Zero readings of cone resistance and, if applicable sleeve friction and pore pressure before and after the test and zero drift (in engineering units)
- Stop criteria applied, i.e. target depth, maximum penetration force, etc
- Corrections applied during data processing (e.g. zero drifts)
- Reference to this IRTP or other standard
- Test type (Table 5.1) and Accuracy Class (Table 5.2)

- If applicable, the inclination of the cone penetrometer to the vertical axis, for a maximum penetration depth spacing of 1m

Note: In the presentation of test results, the information should be easily accessible, for example in tables or as a standard archive scheme.

Note: In addition to the above it is desirable that the following information is given:
- Manufacturer of cone penetrometer
- Observations done in the test, for example the presence of stones, noise from the pushing rods, incidents, buckled rods, abnormal wear or changes in zero / reference readings
- Identification number of the penetrometer, and measuring ranges of the transducers
- Date of last calibration of sensors

6.2 *Choice of axis scaling*

In the graphical presentation of test results the following axis scaling shall be used when required:

- Penetration depth z:	1 cm = 1 m
- Cone resistance q_c, q_t:	1 cm = 2 MPa
- Sleeve friction f_s, f_t:	1 cm = 0.05 MPa = 50 kPa
- Pore pressure u:	1 cm = 0.2 MPa = 200 kPa
- Friction ratio R_f:	1 cm = 2 %
- Pore pressure ratio B_q:	1 cm = 0.5

Note: A different scaling may be used in the presentation if the recommended scaling is used in an additional plot. The recommended scaling can for example be used for general presentation, whereas selected parts may be presented for detailed studies, using a different scaling. In clays, and where the test results are to be used for interpretation of soil parameters (Accuracy Classes 1 and 2, see Table 5.2), it is particularly important to use enlarged scaling in the presentation of test results.

The axis scaling for dissipation test results (cone resistance q_c, pore pressure u and time t) shall suit the measured values.

Note: A common presentation format is to use linear scales for q_c and u and a logarithmic scale for t.

6.3 *Presentation of test results*

The test results shall be presented as continuous profiles of:

- Cone resistance - depth	q_c (MPa) - z (m)
- Sleeve friction - depth	f_s, (MPa) - z (m)
- Pore pressure - depth	u_2 (MPa) - z (m)
- Other pore pressures - depth	u (MPa) - z (m)

(location of pore pressure measurement should be given)

The depth here shall be according to Table 5.2 corrected when necessary for the measured inclination.

Presentation of the results of cone penetration tests according to Accuracy Classes 1 and 2 shall, if required, include tabular data according to Section 6.1. Tabular data per penetration length spacing according to Table 5.2 shall include the time t in s, penetration depth z in 0.01 m, cone resistance q_c in 0.01 MPa and, if applicable, sleeve friction in 1 kPa, pore pressure in 1 kPa, friction ratio R_f in 0.1%, corrected cone resistance q_t in 0.01 MPa, inclination of the cone penetrometer in ^{o}.

If relevant corrected values of cone resistance (q_t) and sleeve friction (f_t) should be plotted in addition, and should preferably be used in further processing of the data. An exception is made for testing of coarse-grained materials, where the effect of the end area correction is negligible.

Note: In situ pore pressure can be estimated from the location of the groundwater table, or preferably by local pore pressure measurements. It can also be evaluated from the test results by performing dissipation tests in permeable layers. The total overburden stress profile can be determined from density measurements in situ or from undisturbed samples in the laboratory. If adequate information is lacking, an estimate of the density may be obtained by use of a classification chart based on the results from the cone penetration test and local experience.

Note: Further processing of the measured data can be carried out based on the following relationships:

- Excess pore pressure	$\Delta u = u - u_o$
- Net cone resistance	$q_n = q_t - \sigma_{vo}$
- Friction ratio	$R_f = (f_s/q_c)x100$ %
- Pore pressure ratio	$B_q = (u_2 - u_o)/(q_t - \sigma_{vo}) = \Delta u_2/q_n$
- Normalised excess pore pressure	$U = (u_t - u_o)/(u_i - u_o)$ where u_t is the pore pressure at time t in a dissipation test and u_i is the pore pressure at the start of the dissipation test

Note: In addition the following parameters can be computed for effective stress interpretation:

- Cone resistance number $N_m = q_n/(\sigma_{vo}' + a)$ (a = attraction)

Note: Information of the following parameters is needed in the processing of the test results:

- In situ, initial pore pressure - depth	u_o (MPa) - z (m)
- Total overburden stress - depth	σ_{vo} (MPa) - z (m)
- Effective overburden stress - depth	$\sigma_{vo}' = \sigma_{vo} - u_o$

Note: These parameters, or additional derived and normalised values, can be used for both identification of strata and classification of soil types, and as basic input values for interpretation of engineering parameters.

7 REFERENCES

Campanella, R.G., Gillespie, D. and Robertson, P.K. 1982 Pore pressure during cone penetration testing. *Proc ESOPT II*, Vol. II: 507-512. Rotterdam: Balkema.

ISO 1988. Preparation of steel substrates before application of paints and related products – Surface roughness characteristics of blast-clean steel substrates. ISO 8503 (1988).

ISO 1992. Quality Assurance Requirements for Measuring Equipment - Part 1: Metrological Confirmation System for Measuring Equipment, ISO 10012-1:1992(E).

ISSMFE Technical Committee on Penetration Testing (1989) *Report on Reference Test Procedures, TC 16.* Swedish Geotechnical Society (SGF), Information No.7.

Larsson, R. 1995. Use of a thin slot as filter in piezocone test. *Proc CPT'95*, 2: 35-40.

Lunne, T., Robertson, P.K. and Powell, J.J.M. 1997. *Cone Penetration Testing in Geotechnical Practice*. London: E & FN Spon, an imprint of Routledge,

APPENDICES:

APPENDIX A- MAINTENANCE, CHECKS AND CALIBRATION

A1 MAINTENANCE AND CHECKS

A1.1 *General*

This Appendix contains informative guidance on maintenance, checks and calibrations. The guidance notes are meant to represent good practice.

A1.2 *Linearity of push rods*

Before the test is carried out, the linearity of the push rods shall be checked. A rough impression of the linearity may be obtained by rolling the rods on a plane surface. If any indications of bending appear, the linearity should be checked according to the procedures outlined in Section 4.6.

A1.3 *Wear of the cone*

The wear of the cone and the friction sleeve shall be checked regularly to ensure that the geometry satisfied the tolerances. A standard geometrical pattern similar to a new or unused probe may be used in this control.

A1.4 *Gaps and seals*

The seals and gaps between the different parts of the probe shall be checked regularly. In particular, the seals should be checked for intruding soil particles and cleaned.

A1.5 *Pore pressure measuring system*

If pore pressure measurements are carried out, the filter should have sufficient permeability for satisfactory response. The filter should be kept saturated between the tests. The pore pressure system should be completely saturated before the penetration starts, and this saturation should be maintained until the cone penetrometer reaches the groundwater surface or saturated soil.

A1.6 *Maintenance procedures*

When maintenance and calibration of the equipment is carried out, the check scheme in Table A1.1 may be used, along with the producer’s manual for the particular equipment.

Table A1.1 Control scheme for recommended maintenance routines

Checking Routine	Start of project	Start of test	End of test	Every 3.rd month
Verticality of thrust machine		x		
Penetration rate		x		
Depth sensor				x
Safety functions	x			x
Push rods	x	x		
Wear	x	x	x	
Gaps and seals	x	x	x	
Filter	x	x	x	
Zero drift		x	x	
Calibration	x			x*
Function control	x			x

* and at intervals during long term testing

A2 CALIBRATIONS

A2.1 *General procedures*

A new cone penetrometer has to be calibrated with respect to:

- the net area ratios, used for correction of measured cone resistance and sleeve friction
- influence of internal friction – restriction to movement of the individual parts.
- possible interference effects (electrical cross talk etc).
- transient temperature effects

The calibrations and checks are specific to each cone penetrometer. They will show variations during a penetrometer's life caused by small changes in the function and geometry of the cone penetrometer. In such cases, a re-calibration of the probe should be carried out. Calibration of the data acquisition system should be carried out regularly, according to the criteria listed below:

- at least every 3 months with the cone penetrometer in continuous use, or after approximately 100 soundings (approximately 3000 m)
- a new calibration should be carried out after soundings under difficult conditions, where the probe has been loaded close to its maximum capacity.

The calibrations should be carried out using the same data acquisition system, including cables, as in the field test, representing a check of possible inherent errors of the system. During the fieldwork, regular function controls of the equipment shall be carried out. These should be carried out at least once per location and/or once per day. Furthermore, a function control and possibly also a re-calibration should be carried out if the operator suspects overloading of the load sensors (loss of calibration).

In general the requirements presented in ISO 10012-1:1992(E) should be followed.

A2.2 *Calibration of cone resistance and sleeve friction*

The calibration of cone resistance and sleeve friction are performed by incrementally loading and unloading axially the cone and the friction sleeve. When loading the friction sleeve alone, the cone is substituted by a specially adapted calibration unit. This unit is designed so that the axial forces are transferred to the lower end area of the friction sleeve. The calibrations of cone resistance and sleeve friction are carried out separately, but the other sensors are checked to ensure that they are not influenced by the applied load. The calibration is carried out for various measuring ranges, with special emphasis on those ranges relevant for the forthcoming tests. When a new probe is calibrated, the sensors should be subjected to 15-20 repeated loading cycles up to the maximum load, before the actual calibration is carried out. The requirement for separate calibration procedures for cone and friction sleeve is not usually required for subtractive cone penetrometers.

The influence of non axial loading on the cone penetrometer and its effect on the measured parameters should be checked.

A2.3 *Calibration of pore pressure and net area ratio*

The calibration of the pore pressure measuring system shall be done in a pressure chamber. For pore pressure effects on the cone resistance and sleeve friction, the calibration of the net area ratio a shall be carried out in a specially designed pressure chamber (e.g. Figure A1), constructed so that the lower part of the penetrometer can be mounted in the chamber and be sealed above the friction sleeve. The enclosed part of the probe is then subjected to an incrementally increasing chamber pressure, and cone resistance, sleeve friction and pore pressure are recorded. In this way a calibration curve for the pore pressure transducer is obtained and the net area ratio can be determined from the response curves for cone resistance and sleeve friction. The pressure chamber is also well suited to check the response of the pore pressure sensor to cyclic pressure variations.

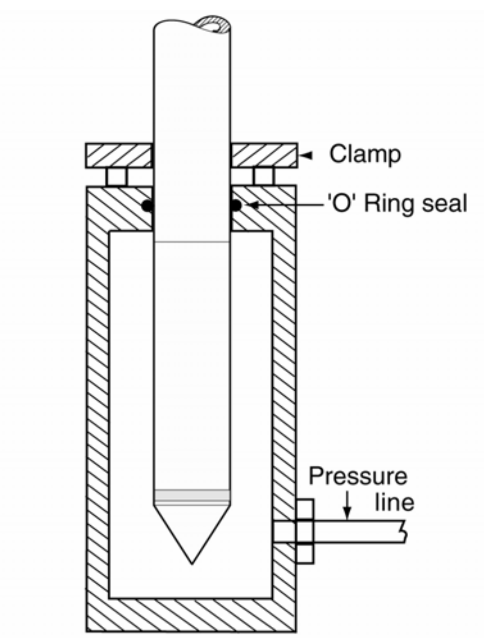

Figure A1 Pressure chamber for determination of the end area ratios a and b (from Lunne et al., 1997)

A2.4 *Calibration of temperature effects*

The cone penetrometer shall also be calibrated for temperature effects at various temperature levels, for example by lowering the cone penetrometer into water reservoirs at different temperatures. The sensor signals are recorded until the values stabilise. From these results a measure for changes in zero readings per ^{o}C is obtained and an impression is gained of the time needed for temperature stabilisation in the field performance. This is important information for a proper preparation of the test equipment before the penetration test starts.

The above applies to ambient temperatures only and not to transient temperatures.

A2.5 *Calibration of depth sensor*

The depth sensor calibration should be calibrated at least every 3rd month or after repair.

APPENDIX B - CALCULATION OF PENETRATION DEPTH

CORRECTION FOR PENETRATION DEPTH DUE TO INCLINATION

The depth of cone penetration tests according to Accuracy Classes 1, 2 and 3 of Table 5.2 can be corrected for inclination by the equation:

$$z = \int_{o}^{l} C_h \cdot dl$$

where:

z is the penetration depth, in m;
l is the penetration length, in m;
C_h is a correction factor for the effect of the inclination of the cone penetrometer relative to the vertical axis

Equations for the calculation of the correction factor C_h for the influence of the inclination of the cone penetrometer relative to the vertical axis, on the penetration depth:

a) for an now-directional inclinometer:

$$C_h = \cos\alpha$$

where:

α is the measured angle between the vertical axis and the axis of the cone penetrometer, in °

b) for a bi-axial inclinometer:

$$C_h = (1 + \tan^2\alpha + \tan^2\beta)^{-½}$$

where:

α is the angle between the vertical axis and the axis and the projection of the cone penetrometer on a fixed vertical plane, in°;
β is the angle between the vertical axis and the axis and the projection of the cone penetrometer on a vertical plane that is perpendicular to the plane of angle α, in°.

Note: It may be necessary to apply additional corrections to the CPT depth.

Note: The determination of the correction factor for the penetration depth should take account of a complex loading sequence. Additional factors include: bending and compression of the push rods and push rods connectors, vertical movements of the ground surface or the underwater ground surface and vertical movements of the depth sensor relative to the ground surface or the underwater ground surface. For some situations, such as penetration interruptions, it is possible to correct for bending and compressing of the push rods and push rod connectors by using a heave compensator.